Bearing Capacity of Footings Under Vertical and Inclined Loads on Layered Soils

by

ADEL M. HANNA

A Thesis Submitted to the

Faculty of Graduate Studies

in Partial Fulfillment of the Requirements

for the Degree of

DOCTOR OF PHILOSOPHY

Major Subject: Civil Engineering

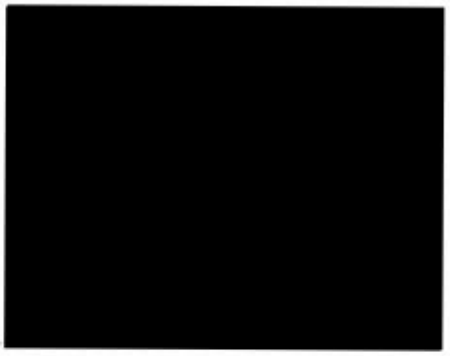

NOVA SCOTIA TECHNICAL COLLEGE

Halifax, Nova Scotia

1978

TABLE OF CONTENTS

LIST OF TABLES

List of Tables continued

List of Tables continued

List of Tables continued

LIST OF FIGURES

List of Figures continued

List of Figures continued

List of Figures continued

List of Figures continued

List of Figures continued

List of Figures continued

NOTATION

Symbol	Represents
A	Area of footing
B	Width or diameter of footing
C	Circumference of footing
C_a	Adhesion on the footing side
C_u	Undrained Shear strength
D	Depth of footing
D_{10}	Diameter at which 10% of the soil is finer
D_{60}	Diameter at which 60% of the soil is finer
D_r	Relative density of sand
d_q	Depth factor
E	Modulus of elasticity
e	Void ratio of the soil
e_{max}	Void ratio of the soil in loosest condition
e_{min}	Void ratio of the soil in densest condition
G	Specific gravity of soil
H	Thickness of upper layer
h	Thickness of upper layer below footing base
h_f, $h_{f\gamma}$, h_{fq}	Failure Depths
i'_γ i'_q	Inclination factors in the load direction
i_γ i_q	Vertical components of i'_γ i'_q respectively
K	Coefficient of earth pressure

NOTATION (continued)

Symbol	Represents
K_o	Coefficient of earth pressure at rest
$K_{p\gamma}$	Coefficient of passive earth pressure - Weight component
K_{pq}	Coefficient of passive earth pressure - Surcharge component
$K_{t\gamma}$	Coefficient of punching resistance - Weight component
K_{tq}	Coefficient of punching resistance - Surcharge component
L	Length
N_c, N_q, N_γ	Bearing capacity factors
$N_{\gamma q}$, N_{cq}	Bearing capacity factors
N'_q, N'_γ	Modified bearing capacity factors
$N_{\gamma 1}$, N_{q1}	Bearing capacity factors for the upper sand layer
$N_{\gamma 2}$, N_{q2}	Bearing capacity factors for the lower sand layer
P_1	Total passive earth pressure - Weight component
P_2	Total passive earth pressure - Surcharge component
Q	Ultimate load
q	Unconfined compressive strength of the soil
q_u	Ultimate bearing capacity
q_v	Vertical component of the ultimate bearing capacity
q_b	Ultimate bearing capacity of footing at the interface of two layer soil

NOTATION (continued)

Symbol	Represents
q_1	Ultimate bearing capacity of a surface strip footing on homogeneous upper layer soil
q_2	Ultimate bearing capacity of a surface strip footing on homogeneous lower layer soil
R_γ, R_q	Reduction factors
S	Footing settlement at failure
S_γ, S_q	Shape factors
$S_{\gamma q}$	Shape factor
U	Uniformity coefficient = $\frac{D_{60}}{D_{10}}$
X	Distance
Z	Depth of a point
γ	Bulk density of soil
γ_1	Bulk density of upper layer soil
γ_2	Bulk density of lower layer soil
α	Inclination angle
λ	Parameter
$\phi, \phi_\gamma, \phi_q$	Angle of internal friction of soil
δ_z	Locally mobilized angle of shearing resistance on the assumed failure planes
δ	The average mobilized angle of shearing resistance on the assumed failure planes
ε	Strain
$\sigma_1, \sigma_2, \sigma_3$	Principal stresses

NOTATION (continued)

Symbol	Represents
τ	Shear stress
η	Porosity of sand
C. Sand	Compact sand
D. Sand	Dense sand
L. Sand	Loose sand
D. Sand/L. Sand	Dense sand overlying loose sand
D. Sand/C. Sand	Dense sand overlying compact sand
D. Sand/Clay	Dense sand overlying clay
L. Sand/D. Sand	Loose sand overlying dense sand
C. Sand/D. Sand	Compact sand overlying dense sand

ACKNOWLEDGMENTS

I wish to express my sincere gratitude to Dr. G. G. Meyerhof, Professor and Head of Civil Engineering Department, under whose direct supervision and able guidance the present investigation has been carried out. The amount of consistent enthusiasm and constant encouragement received is gratefully acknowledged.

I am deeply indebted to Dr. J. D. Brown, Associate Professor, for many stimulating discussions during this research. Helpful comments received from Dr. H. G. Sherwood are acknowledged.

I am thankful to members of faculty and my colleagues for the discussions we shared, especially Mr. Alex Ritchie for his assistance with instrumentation.

Thanks go also to the laboratory technicians who have provided assistance in fabrication of equipment, particularly M. Theriault, C. Nickerson, and D. Yeadon, and A. Regala who did the typing of this thesis.

Thanks are due to the National Research Council of Canada for the financial assistance during the time of this work.

To the memory of my parents, who passed away during this program of study; without their encouragement, support, and happiness they gave, this work would not have been possible.

Finally I am indebted to my wife, Samia, for her support and constant encouragement and for her assistance in preparation of the drawings.

ABSTRACT

The bearing capacity of shallow foundations under axial vertical and inclined loads has been investigated for model strip and circular footings on layered soils. Two main cases have been considered, first, when the subsoil consists of a strong layer overlying a deep weak layer, and second, when a weak layer is overlying a deep strong layer.

Extensive theoretical and experimental studies have been found in the available literature on footings under vertical loads on a strong layer overlying a deep weak layer. Except for Meyerhof's theory (1974) for the case of footings under vertical loads on a weak layer overlying a strong layer, no other attempts have been made to develop a rational solution. Further, there does not appear to be any theoretical analysis or experimental data reported on footings on layered soils subjected to inclined loads.

In this investigation, the case of a strong layer overlying a weak layer was simulated in the laboratory by testing footings on a dense sand layer overlying loose sand, compact sand, and clay respectively. In the case of a weak layer overlying a strong layer, loose sand and compact sand overlying a dense sand were tested respectively. Homogeneous soils used in layer combinations were tested with the proposed footings under vertical and inclined loads. Results of these tests were verified according to established theories, and were used in the analyses of the test results of footings on layered systems. Further, these results provided an evaluation of the behaviour

of the test materials.

The ultimate bearing capacity of footings on the mentioned soil layers was noted to vary between the ultimate bearing capacities of the homogeneous upper and lower layers, Increasing the load inclination resulted in a decrease in this ultimate bearing capacity. New approaches for the analysis were developed by extending Meyerhof's theories (1974). The present test results, test results of other researchers, and the available data were found to be in reasonable agreement with proposed theories.

As a concluding part of the study, suitable design procedures are suggested for predicting the footing capacity in two layered soils and further research points on the subject are recommended.

Chapter 1

INTRODUCTION

1.1 General

Foundation problems necessitate two different studies: one dealing with the ultimate bearing capacity of the soil under the foundation, the second concerned with the limit of the soil deformation. The study of ultimate bearing capacity has the purpose of determining the load under which a foundation with given dimensions and depth sinks indefinitely into the soil; in other words, the study of the foundation failure in shear associated with plastic flow of the soil material underneath the foundation. The study of the limiting deformation has the purpose of determining the load causing such deformation of the soil. The corresponding total and differential settlements of the structure should not exceed the limits of the allowable deformation for stability, function and aspects of construction. These are the two independent foundation stability requirements which must be met simultaneously.

The ultimate bearing capacity problem may be solved by two different approaches: analytical solutions using such techniques as theory of plasticity, method of characteristics, and finite element method, or experimentally by conducting model and full-scale tests. A rational and satisfactory solution is found only when theoretical results agree with those obtained experimentally or from actual field data.

Analytical and experimental studies pertaining to bearing capacity of foundations resting on homogeneous soils are extensive and well documented. However, a literature survey on the subject showed that a study of the bearing capacity of shallow foundations, where the subsoil consists of two or more layers of soil having significantly different strength and deformation properties and with the emphasis on experimental research, would lead to results of interest to practicing foundation engineers. This may be explained from the fact that soil mechanics is the branch of applied mechanics which depends on the idealization of material properties, boundary conditions, loads, etc., for the formulation of theoretical solutions. However, the requirement of using a suitable stress-strain relationship for the soil imposes the greatest obstacle for obtaining an exact solution, especially in the case of layered soil with different shear strength properties which do not obey the Mohr-Coulomb failure criterion and do not fail simultaneously along a given failure surface. Therefore, the theories put forward depend, to a large extent, on the experimental results and observed modes of failure.

In addition, it is now generally accepted that the bearing capacity of a foundation depends not only on the properties of the soil but also on the dimensions, shape and depth of the foundation, as well as on the inclination and eccentricity of the foundation load.

1.2 Purpose and Scope

The main objectives of the present investigation are:

a. To review and discuss the existing bearing capacity theories suggested by various investigators for footings subjected to axial vertical or inclined loads and supported on a subsoil having two layers.

b. To develop a simple and rational procedure for the use of practicing foundation engineers for designing footings on two layers of soils with different shear strengths and subjected to axial vertical or inclined loads.

To achieve the above objectives, an experimental program has been organized especially to give answers to some of the field problems. The following parameters have been considered in the present investigation.

1.2.1 Thickness of the Upper Layer

Based on the fact that the influence of the lower layer will be felt by the footing for small thicknesses (H) of the upper layer, the bearing capacity was investigated for a series of increasing thicknesses of the upper layer, until no further change in the ultimate load was observed where the upper layer can theoretically accommodate a classical failure for uniform soil. It was assumed that the thickness of the lower layer would be such that it simulated the condition of a deep homogeneous thick layer. Based on theoretical considerations and available experimental data (Valsangker, 1977),

it was concluded that the soil below the footing base should have a minimum thickness of 4B for clay and 6B for sand, to avoid any boundary effect from the bottom of the experimental box.

1.2.2 Shape, Size and Embedment of Footing

The present investigation was restricted to the basic cases of strip and circular footings, as they represent the extremes of shapes for bearing capacity problems. Only footings with rough bases were considered. The experiments were conducted on strip and circular footings having dimensions of width and diameter (B) of two inches respectively. In order to study the variation of the ultimate bearing capacity with the embedment depth (D) the latter has been varied to give D/B ratios of 0.0, 0.5 and 1.0.

1.3 Organization of Thesis

A brief literature review of the subject of this thesis is presented in Chapter 2. The present investigation was basically experimental and a description of the various types of equipment, materials, test set-up and procedures are given in Chapter 3. The test results of strip and circular footings, each under vertical and inclined loads for the cases of a strong layer overlying a weak layer and a weak layer overlying a strong layer are summarized in Chapter 4. Typical load settlement curves are also included. The analysis and discussion of results for the two cases stated above are presented in Chapters 5 and 6 respectively. A design procedure is also given for each case in these chapters. Conclusions drawn from the present study and recommendations for future work are given in

Chapter 7.

Chapter 2

REVIEW OF PREVIOUS WORK

2.1 General

The ultimate bearing capacity problem of shallow foundations occupies a position of great importance in the field of soil mechanics. Although numerous studies have been reported by researchers, rational approaches are still needed for special problems such as footings on two-layered soils subjected to axial vertical or inclined loads.

From the earliest studies on the problem, knowledge of this behaviour has led to concentration of interest in 'ultimate' methods of analysis involving the use of some failure criterion for the soil. The most commonly used condition is that failure will occur at a point in a soil mass when the shear stress reaches a limiting value dependent on the normal stress (Coulomb, 1776). These solutions are usually based on failure surfaces, either assumed or derived from a hypothetical condition. Solutions of this type have been used to provide answers with acceptable accuracy to a great variety of bearing capacity analyses of homogeneous soils. Considerably less work has been published on shear failure in two layered soils. These studies are briefly discussed in this chapter.

2.2 Discussion of Results of Previous Studies

2.2.1 Footings Subjected to Vertical Loads

A significant contribution in this area is that of the problem of a two-layered clay which has been well documented by Meyerhof and Chaplin (1953), Brown (1967), and Brown and Meyerhof (1969). Some research work has been done on two-layered sands with different shear strengths (Meyerhof and Valsangkar, 1976) or a sand layer overlying a clay layer (Commisiong, 1968; Ho, 1973; Meyerhof, 1974). However, the available theories in this area are for vertical loads and include assumptions regarding the failure mechanism of nonhomogeneous subsoils. It is of interest to note that such theories have resulted in widely different answers.

The first work of direct interest to the subject were those of Taylor (1948) followed by Terzaghi and Peck (1948). They considered the case of footings founded at or near the surface of a strong layer overlying a weak layer. The solution was obtained by considering mainly the bearing capacity of the lower, weaker layer, as if it were a surface stratum. The upper layer serves principally to spread the load, and hence reduces its intensity on the lower layer. The empirical formulae presented in these analysis for both circular and strip footings depends mainly on the assumed load distribution through the upper layer. In fact, Taylor's solution seems to be conservative because he ignored the shearing resistance of the upper layer. In other words, the fact that some rupture surface must develop in the upper layer if it is to deform with the lower layer up to failure was ignored.

Tcheng (1956) developed a bearing capacity formula, based on test results on a long strip footing supported by a sand layer overlying a clay layer. He considered that the footing punches straight down without any lateral distribution of load, and he included the shearing resistance developed on the vertical planes through the top layer.

Yamaguchi (1963) attempted to improve Taylor's solution (1948) by considering the case of a sand layer resting on a soft clay layer, assuming that the load spreads with a slope having the ratio of two vertical to one horizontal from the footing level through the upper layer to the upper boundary of the clay layer. Then he considered a complete development of bearing capacity of the lower level as a surface stratum. He extended his solution to take into account the shearing resistance developed along the vertical planes in the upper layer at the end of Prandtl's sliplines. However, his choice of a shear plane was quite arbitrary, and it is difficult to establish the accuracy of this approximation.

It is notable that the works of Taylor, Tcheng and Yamaguchi were restricted to the case of a firm stratum overlying a soft stratum. In addition, these methods offer no assistance in assessing the case of the lower layer being the stronger. In this case the assumption of a 30 degree load spread is no longer correct.

Recently, Desai and Reese (1970) applied the finite element analysis technique for circular footings on layered clay with non-homogeneity and nonlinear stress-strain behaviour. It is of interest

to note that the computed bearing capacity values agreed well with the results of earlier researchers (Brown, 1967) with a maximum difference of 3%. It is hoped that further development of the ability to apply this technique to the case of two sand layers will allow a more accurate prediction of compressibility effects.

Myslivec (1971) proposed empirical formulae, based on his experimental results of model strip footing tests on various combinations of two-layered soil. His work may be considered as the first attempt to work on two sand layers, as well as consideration of the lower layer being the stronger. However, he failed to show any theoretical evidence for his formulae.

To aid in understanding the layer effect on bearing capacity, theoretical approaches have been proposed by assuming idealized conditions (Nagaoka, 1971 and Purshotamraj et al., 1973). The main difficulty with these solutions is that they depend mainly on some simplifying assumptions, which may not be valied in the field. However, it is of interest to note that a comparison between model test results (Bazan, 1976 and Sastry, 1976) and theoretical values proposed by Nagaoka (1971), shows that the theory leads to an over-estimation of the bearing capacity due to compressibility and other factors.

Meyerhof (1974) presented rational approaches to solve cases of circular or strip footings resting on subsoils consisting of two layers. These cases were dense sand on soft clay and loose

sand on stiff clay. The theoretical deductions were supported by experimental results and some field observations. The theory could be extended with equal validity to combinations of cohesionless layered materials with different shear strengths.

It is significant that while Taylor and Meyerhof have extended their solutions to square and circular footings, other workers deal only with long strip footings. However, there does not appear to be any justification in applying the shape factors used in the bearing capacity theories of homogeneous soils to the nonhomogeneous case.

2.2.2 Footings Subjected to Inclined Loads

It is often the case that the base of the footing is set in a foundation material consisting of two layers and the loads on these footings are frequently a combination of vertical and horizontal loads resulting in inclined resultant loads. Problems of this type have not yet been investigated and the available theories for estimating the ultimate bearing capacity of footings set in homogeneous soils cannot be applied.

Chapter 3

TEST APPARATUS, PROCEDURE AND MATERIALS

3.1 General

In the study of foundation engineering problems, full scale field tests are the ideal method for obtaining data. However, practical difficulties and economic considerations either eliminate or considerably restrict the field tests' scope. As an alternative to full scale field tests, carefully conducted model tests may be employed with advantage. Such model tests can provide useful qualitative and some quantitative data which could later be supplemented with some field tests. In addition, there are a number of variables which influence the behaviour of foundations and these can be isolated and studied in detail by means of model tests.

Shallow foundations, for example, are usually subjected to vertical as well as horizontal loads, the resultant of which is an inclined load with eccentricity acting on the footing base. However, it is generally accepted in the design of footings under eccentric load to consider the equivalent footing width (Meyerhof, 1953; Brinch-Hansen, 1970). This case is not included in the present investigation. The study of such problems, though quite complicated, can be simplified by conducting model tests to study the effect of load inclination separate from eccentricity effects.

In the present investigation, several attempts have been

made to determine the adaptability of suitable instrumentation to study the bearing capacity of model strip and circular footings located in two layers of sand under axial vertical or inclined loads.

3.2 Model Footings for Vertical Loads

The strip and circular model footings for testing under vertical loads were machined from aluminum sections. A threaded hole in the centre of the footing allowed rigid connection to a loading ram through which the loads were applied (Figure 3.1). The bases of the footings were roughened by cementing fine grain sandpaper onto them using epoxy resin glue. The vertical sides of the footing were left smooth.

Two strip footings were used in this investigation. The first one was a solid aluminum section 2 inches wide by 8 inches long and 1½ inches thick (Figures 3.1 and 3.2). To minimize friction at the interface of the footing and the glass sides of the testing box, a cut,0.25 inch thick, was made in the footing material and replaced with flexible foam. One side of the foam was glued to the footing, while the other side was covered with polyethylene.

The second footing was also fabricated from an aluminum section with the shape and dimensions given in Figures 3.3 and 3.4. The bottom of the footing was 8 inches long (the same as the inside width of the test box) to ensure plane strain conditions. The footing base was divided into three sections, where the loads were measured from the middle section to eliminate any increase of the measured loads due to

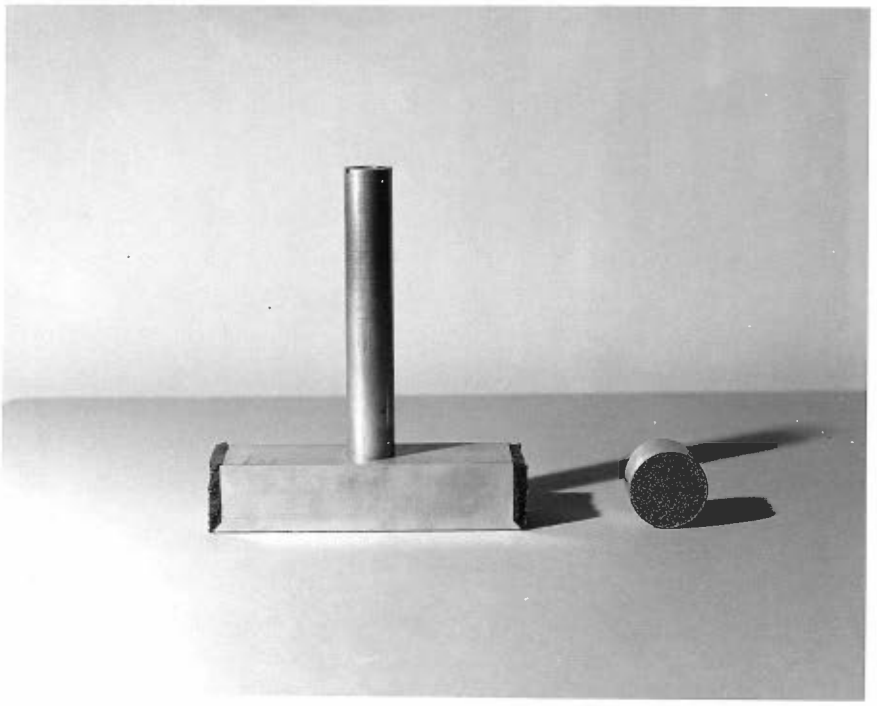

FIGURE 3.1 MODEL FOOTINGS FOR VERTICAL LOADS

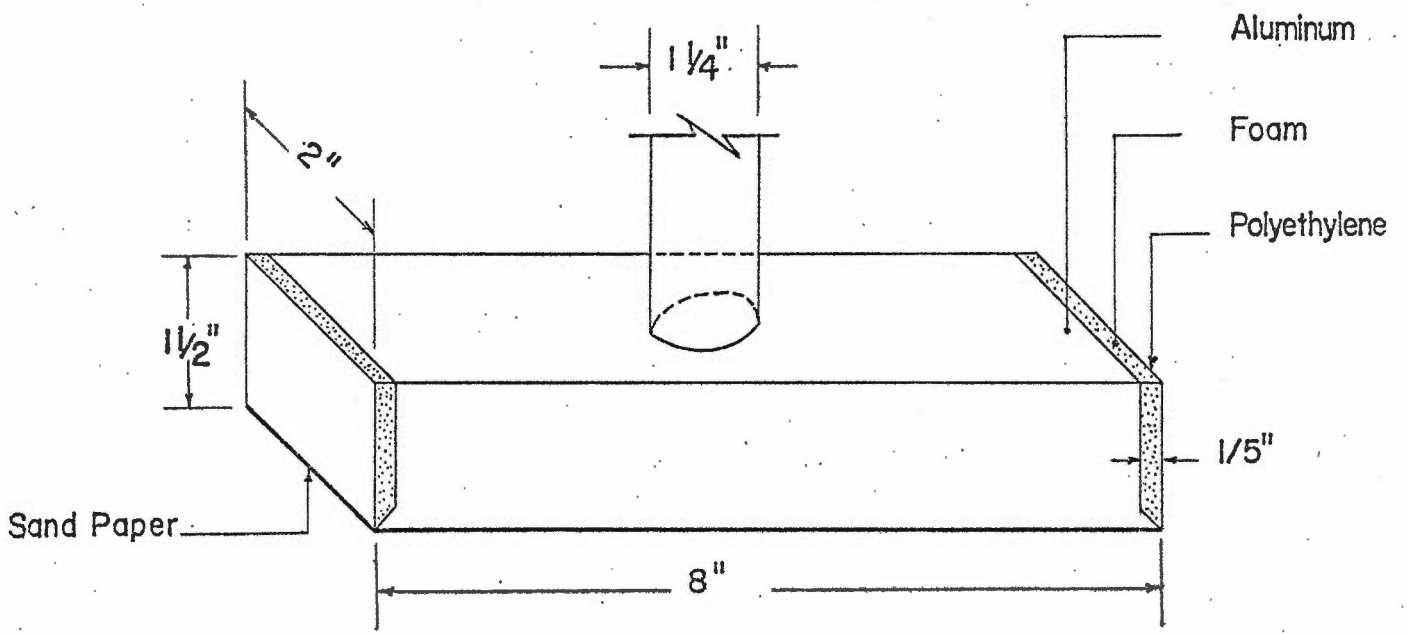

FIGURE 3·2 . MODEL STRIP FOOTING FOR VERTICAL LOADS

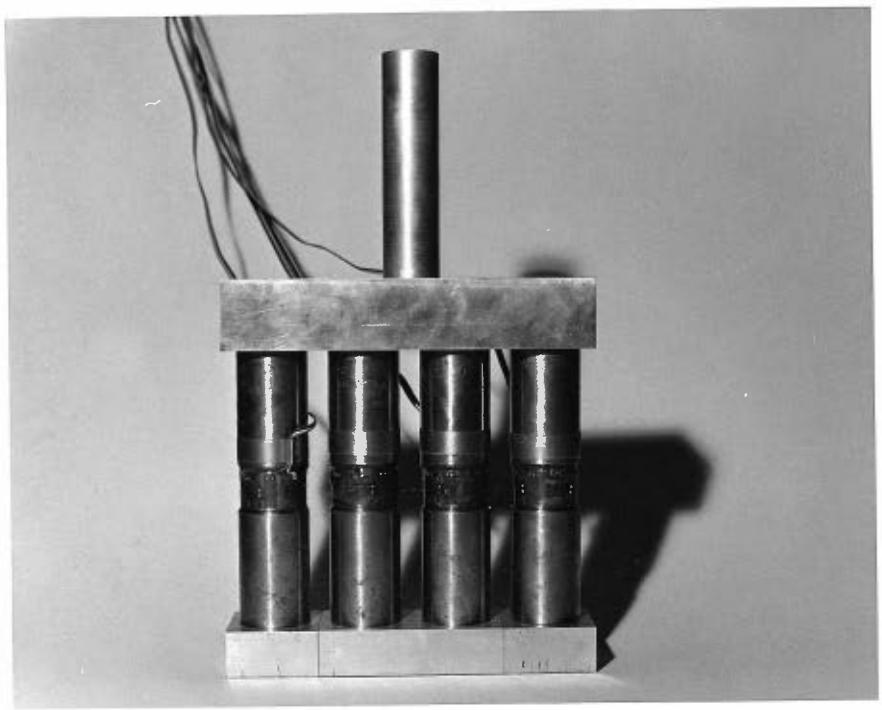

FIGURE 3.3 MODEL STRIP FOOTING FOR VERTICAL LOADS
(3 SECTION FOOTING)

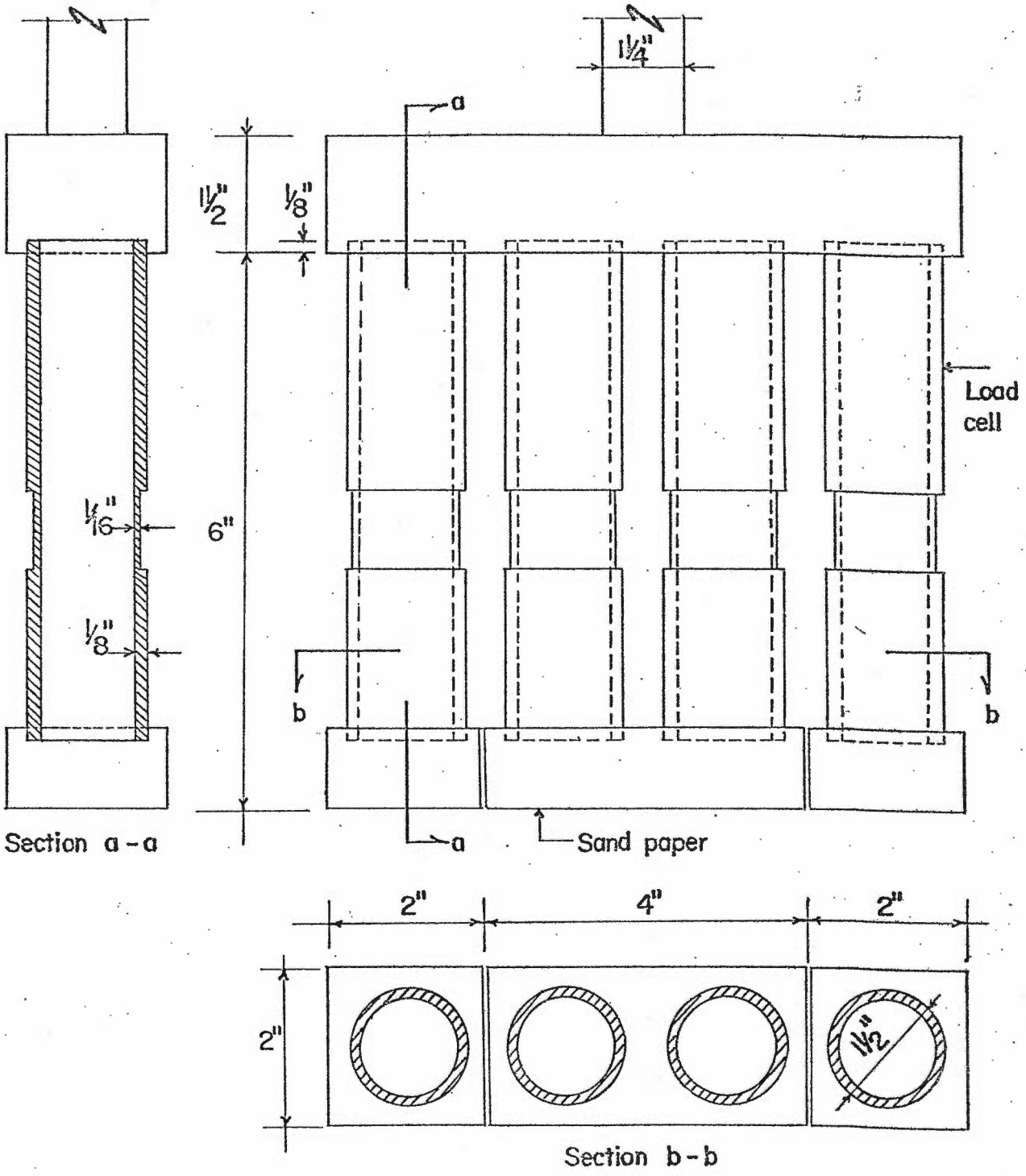

FIGURE 3·4 MODEL STRIP FOOTING - FOR VERTICAL LOADS (THREE PIECE FOOTING)

friction forces between the footings and the box sides. Footing calibration is given in Appendix II.

The model circular footing was an aluminum section with 2 inches diameter and one inch thick (Figure 3.1).

3.3 Model Footings for Inclined Loads

In order to maintain the line of action of the applied inclined loads at the centre of the footing base without using fixed connections between the loading rod and the footing, a steel ball was fixed to the footing base with different cones providing angles of inclination of 0, 10, 20 and 30 degrees (Figure 3.5).

The model strip footing was built-up of a U section made from ¼ inch thick aluminum plates with the dimensions shown in Figures 3.6 and 3.7. Six pressure transducers, 0 to 100 psi range, were installed to measure the stresses at predetermined locations on the footing boundary. The transducers were located such that they were not displaced nor did they significantly influence the stress conditions at the footing boundary. The transducers were connected to a stress indicator through a switch box, as shown in Figure 3.8. Due to the limitations of the apparatus and difficulty in placing footings buried to $D/B > 1$, only two transducers in the footings sides were used in addition to two transducers in the footing bottom.

The model circular footing for inclined loads consisted of a hollow aluminum cylinder, 5 inches in length and 2 inches in diameter, with a vertical cut 4½ inches long by one inch wide to

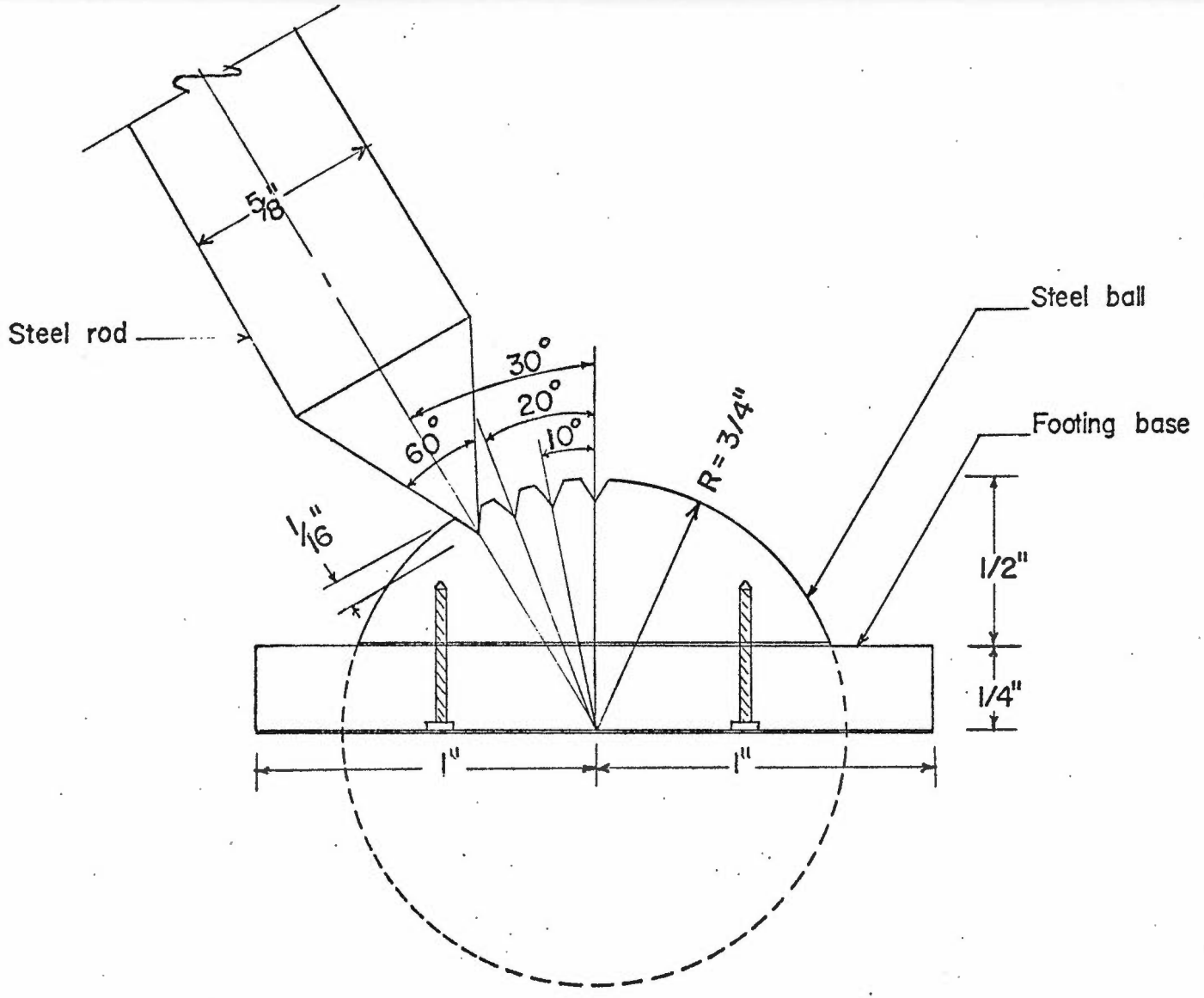

FIGURE 3·5 DETAILS OF INCLINED LOAD APPLICATION ON FOOTING BASE

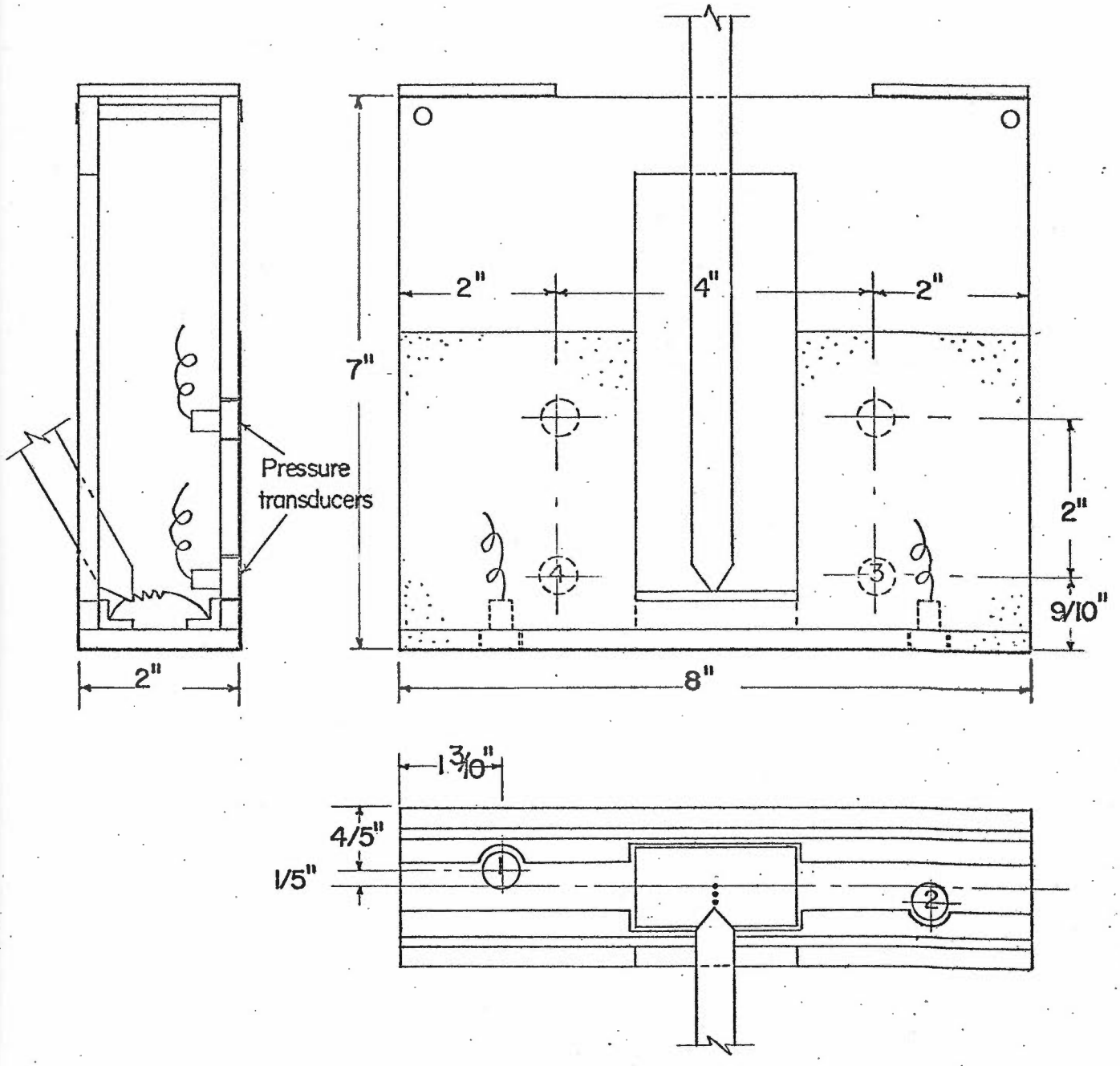

FIGURE 3·6 MODEL STRIP FOOTING FOR INCLINED LOADS

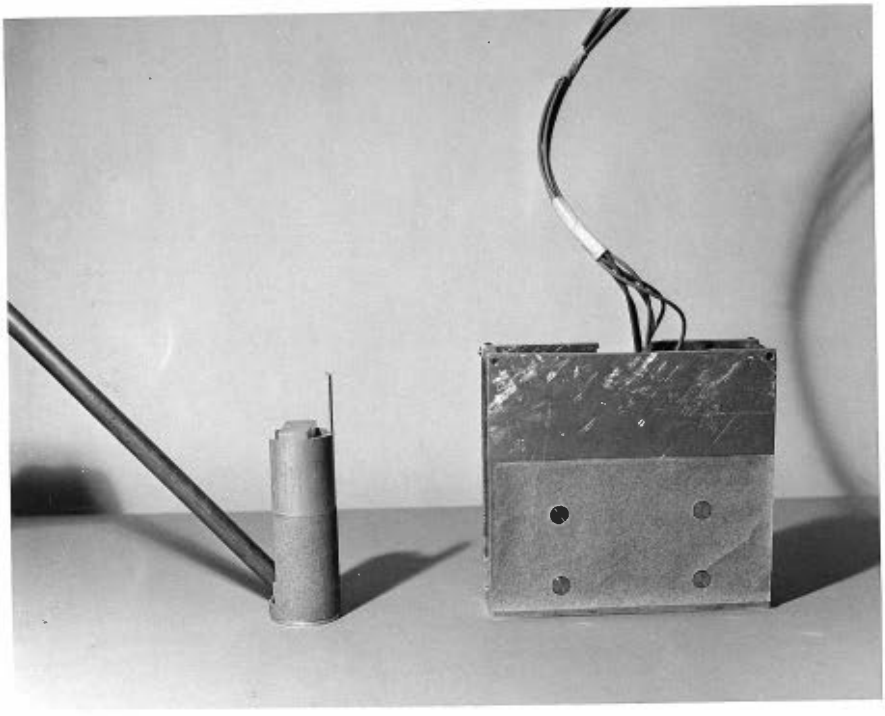

FIGURE 3.7 MODEL FOOTINGS FOR INCLINED LOADS

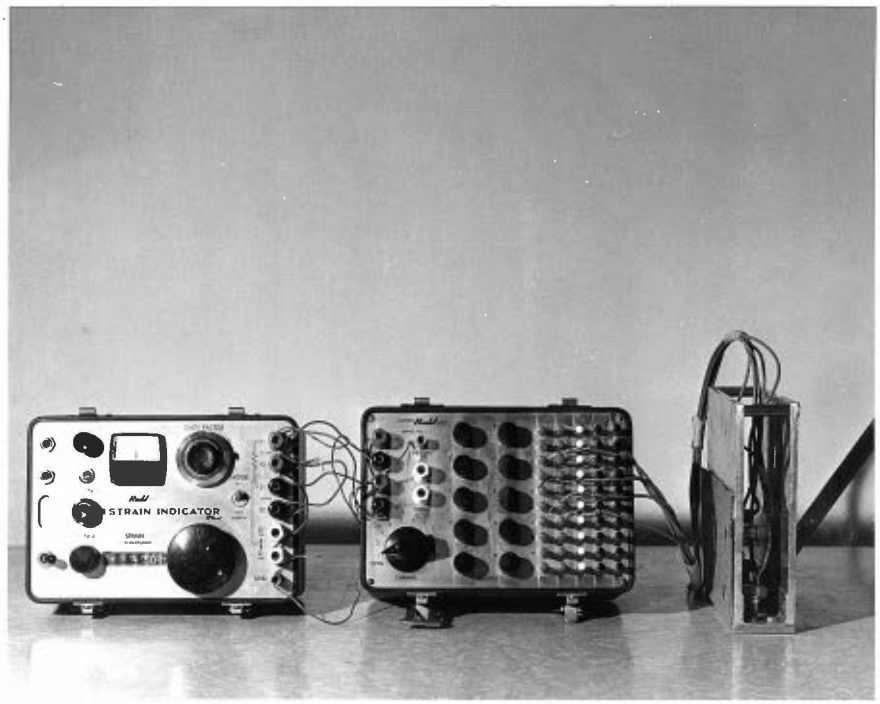

FIGURE 3.8 MODEL STRIP FOOTING AND INSTRUMENTATION FOR INCLINED LOADS

allow angular inclined loading. Both ends of the cylinder were capped with aluminum discs. The footing base and side were covered by sandpaper (Figure 3.7).

3.4 Model Test Boxes

Two main boxes were used in this investigation for both vertical and inclined load tests: rectangular for strip footing tests and circular for circular footing tests.

Plane-strain conditions were simulated by using a glass-sided soil box, similar to that used by Ko (1973) in his investigations. The basic concept used in the design and construction of the box was rigidity. The length, width and depth inside the box were 24, 8 and 20 inches, respectively. Each side wall was constructed of ½ inch thick plate glass. A cross-section through the box is shown in Figure 3.9 and the assembled box is shown in Figure 3.10. The glass walls were held securely by welded steel grids, each composed of two 1 x 1 x 24 inch steel runners with four ½ x 1½ x 22 inch steel bars used as vertical spacers at 8 inch centres. Inclined steel struts were placed at each vertical spacer to provide rigidity. The grids were bolted to the floor plate and turnbuckles were used on all eight of the vertical alignment of the glass walls and to provide additional rigidity. To provide a continuous bearing surface between the top of the grid and the glass walls, a plaster material was poured between the grid and the glass and allowed to harden. Four steel rods each ½ inch diameter were placed across the top of the box between the vertical spacers to prevent expansion.

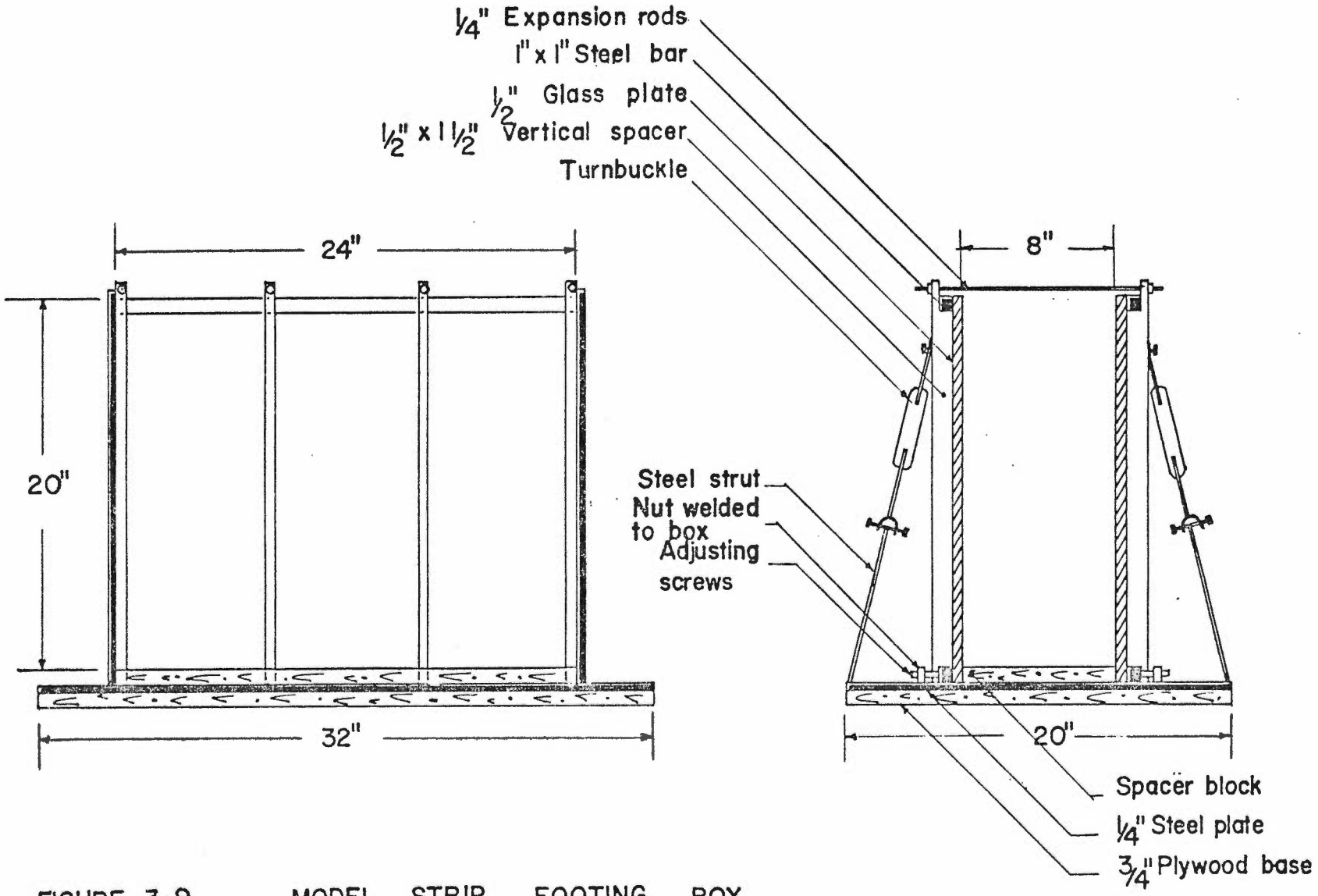

FIGURE 3·9 MODEL STRIP FOOTING BOX

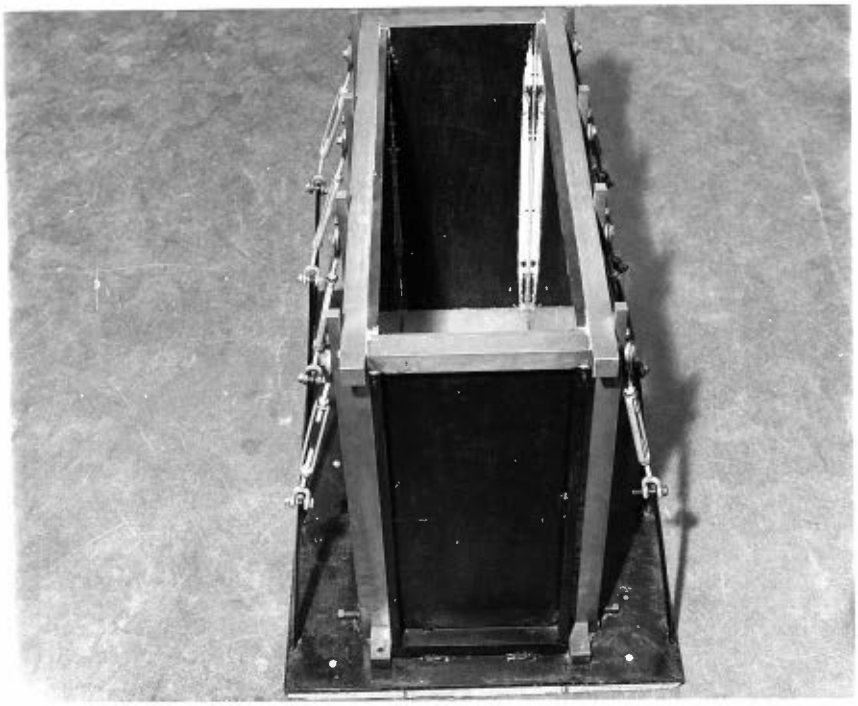

FIGURE 3.10 MODEL STRIP FOOTING BOX

The use of plate glass on the long sides of the strip footing box was based on the fact that the glass would define the intermediate principal stress plane along which soil movements would occur. The glass was relatively stiff and exhibited negligible friction; also, it enabled observations of relative movement along the intermediate principal stress plane during the test and inspection of rupture surfaces after failure.

The horizontal movement of the glass sides was measured at the mid-span points. The results showed that at the stress levels attained, the glass sides were inflexible. The friction between the sand and the glass sides was measured by means of a direct shear box test. In these tests the bottom half of the shear box was packed with dense sand, while the upper half consisted of a piece of glass attached to a block of wood, both having the same inner dimensions of the shear box. The results indicated that the angle of friction between the glass and the dense sand varied from 4.91 to 7.84 degrees for normal pressures of 9.58 psi and 3.26 psi respectively. Since the stress on the intermediate principal plane varies through the failure plane both in the vertical and horizontal directions, an accurate assessment of its frictional contribution to the ultimate bearing capacity is difficult. However, if we assume that the stress on the intermediate principal plane is about half way between the major and minor principal stresses (Shibata and Karube, 1965), an estimate of the stress component due to friction contribution would be small and negligible.

A steel drum was used for circular footing tests under axial vertical or inclined loads. The drum measured 19 inches in height and 20 inches in diameter (Figure 3.11).

3.5 Test Set-Up and Procedures

Every effort was made to prevent any vibration or other disturbances to the sand during the process of moving the sand box to the testing machine, in order that the sand density would not be affected. This was achieved by keeping the sand box at the same level of the platform of the testing machine during the sand-pouring process, and by means of rollers the box was pushed easily and smoothly to the loading system. This proved to be a relatively satisfactory technique. This is particularly important in the case of cohesionless soil.

3.5.1 Vertical Load Tests

In this series of tests a loading frame of a triaxial compression machine was used. In order to maintain the load in a vertical direction during the footing tests, the loading ram was passed through a lubricated ball bearing guide. Proving rings, each having a different sensitivity and maximum capacity, were used to measure the applied loads. In the case of the three-piece footing tests, the total load was measured using a proving ring and the load per cell was recorded by connecting the load cells to a Solartron Data Acquisition system, where the electronic signals were displayed and recorded by a printer (Figure 3.12). The proving rings and the load cells (individually and as a group) were calibrated prior to testing using an Instron Universal Testing Machine. Dial gauges, accurate to

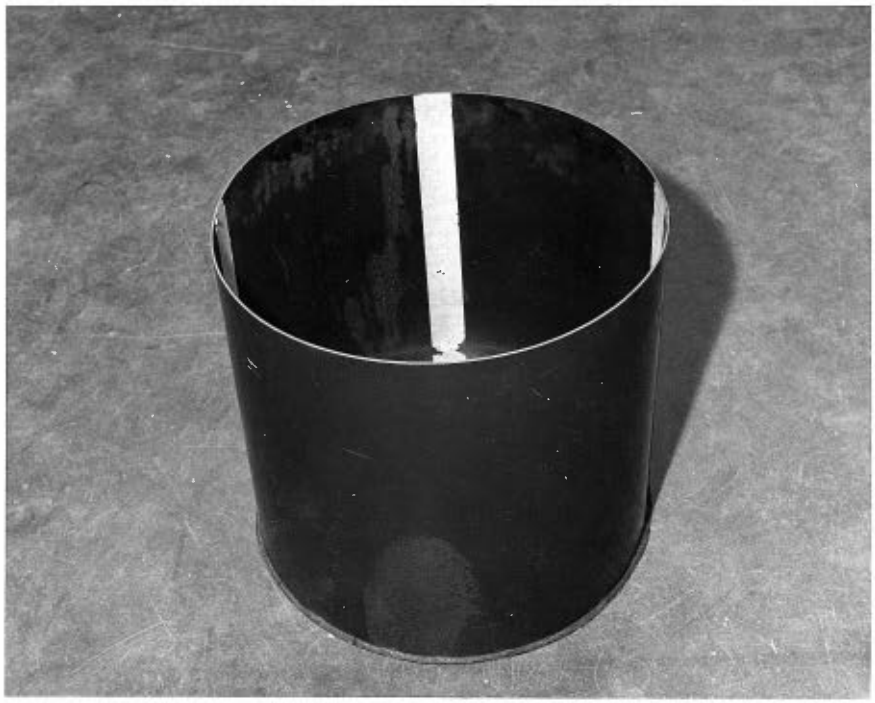

FIGURE 3.11 MODEL CIRCULAR FOOTING BOX

0.001 inch, were used to measure vertical displacement.

All tests were conducted at a nominal rate of feed of 0.01 inch/min. The load readings were recorded at predetermined strain values which were defined as the ratio (%) of settlement to the footing width or diameter (S/B)% in increments of S/B = 0.5%. Figure 3.13 shows a typical set-up.

3.5.2 Inclined Load Tests

For this series of tests a rigid steel reaction frame was used to support the loading system during the loading process. The frame was attached to the floor and a system of bracing was used on all sides to prevent any member buckling or swaying. The loading system consisted of a hydraulic jack, 4" travel, fixed upside down to the frame, connected to a priving ring to which was attached a 1/2 inch diameter steel rod with a pointed end (Figure 3.14). The pointed end of the steel rod fitted like a hinge into a set of cones drilled into the steel ball fixed to the footing base (Figure 3.5).

Two types of connections were used between the proving ring and the jack. The first type was a rigid connection, which allowed the rod to transmit to the proving ring, both axial load and bending moment. The latter was due to the horizontal displacement of the pointed end of the rod with the footing causing eccentricity of the axial load across the rod cross section. The moment value being a function of the rod length, soil uplift and angle of inclination or the horizontal movement. This fixed connection was used only in some tests with the circular footing for comparison purposes. The second type

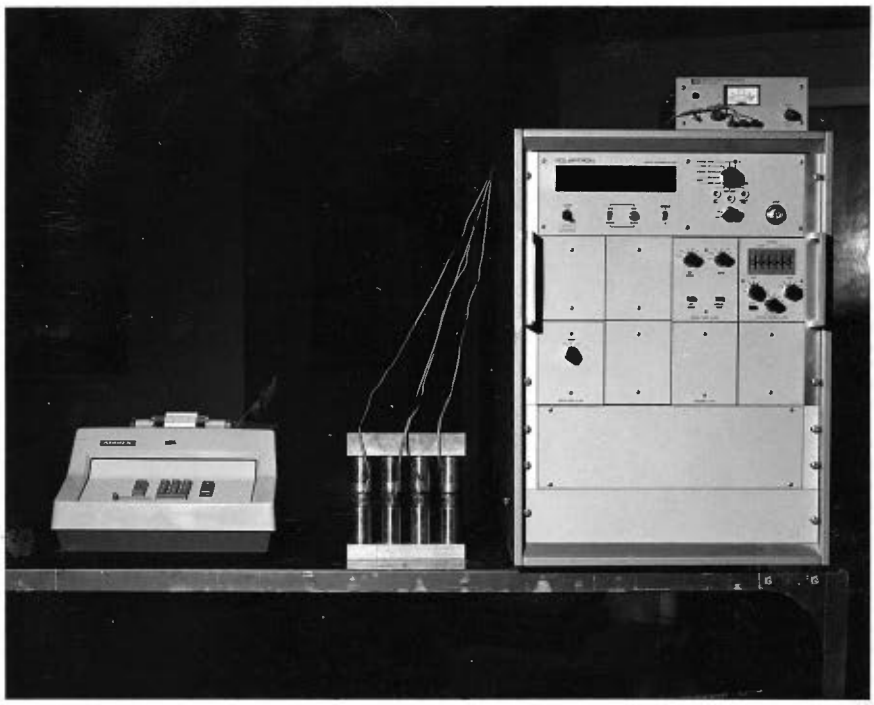

FIGURE 3.12 SOLARTRON DATA ACQUISITION SYSTEM

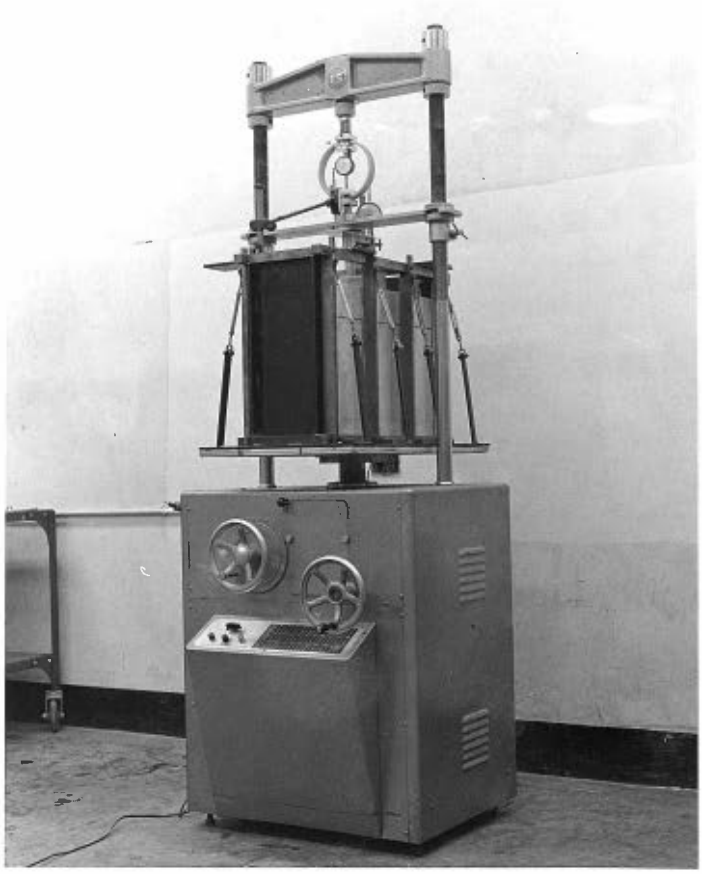

FIGURE 3.13 TYPICAL TEST SET-UP FOR VERTICAL LOADS

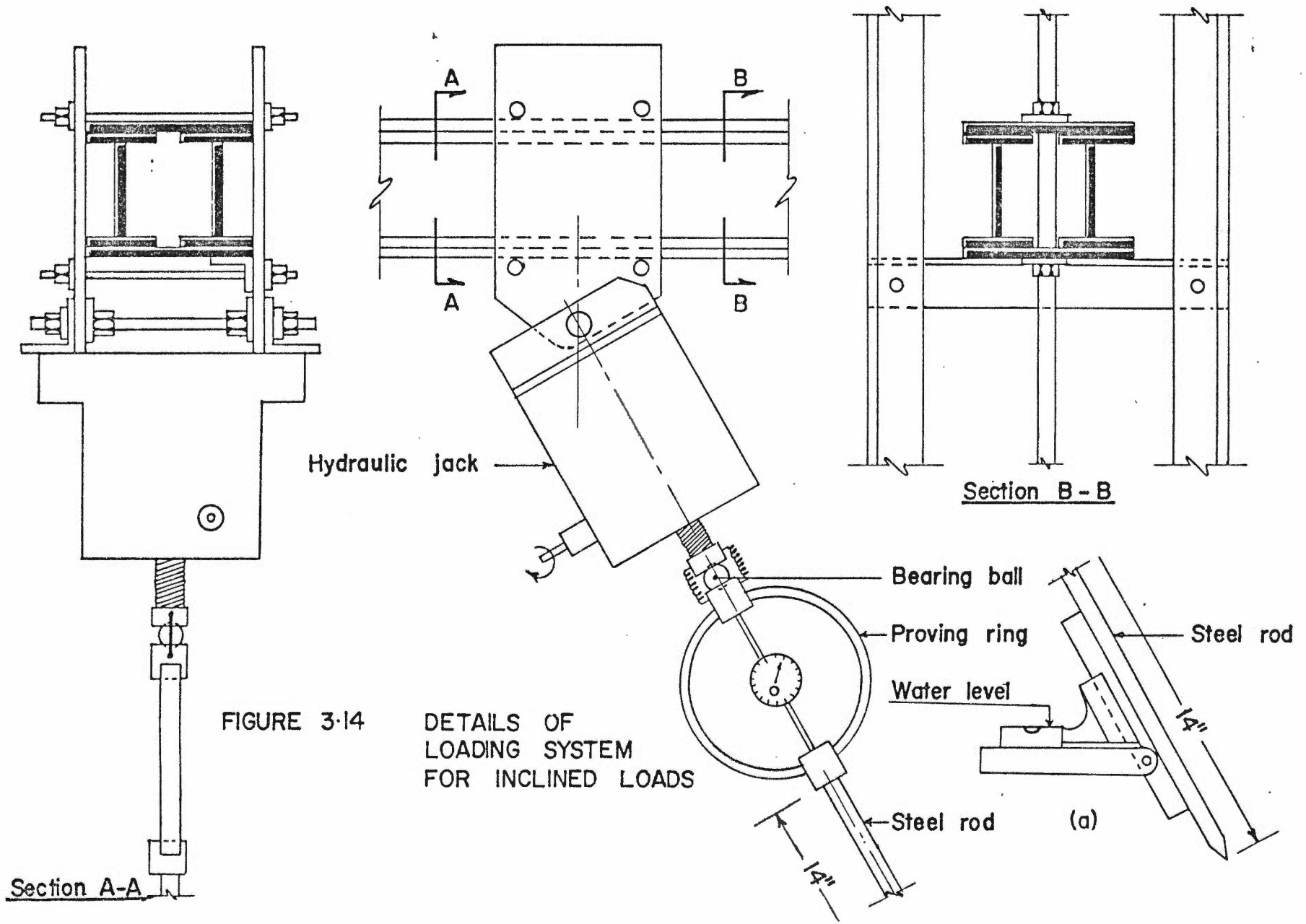

FIGURE 3·14 DETAILS OF LOADING SYSTEM FOR INCLINED LOADS

of connection was a hinged connection, used for both strip and circular footing tests, made by means of a ball bearing inserted between the jack and the proving ring (Figure 3.14). The hinged connection proved to be the ideal connection to test footings subjected to inclined loads without eccentricity because it provided a hinged condition which ensured that the rod was subjected only to axial compression. In fact, most of the field connections would lie between these two extremes.

The passive earth pressure exerted on the footing side and the normal stress distribution underneath the footing base were recorded periodically only for the case of buried strip footing tests (D/B = 1) by the system of transducers (Figure 3.6). The transducers were calibrated individually prior to testing by the following method: each transducer was fixed to a triaxial test apparatus and its wires were connected to the switch box (with maximum of 10 channels) using a full bridge connection. The switch box was connected to a stress indicator box. This connection utilized the actual testing system.

The vertical displacement was measured by means of one dial gauge in the case of circular footing tests and two dial gauges in the case of strip footing tests. The gauges were mounted directly on the footing top. The horizontal displacement was measured for both circular and strip footing tests by a horizontal dial gauge. Due to experimental difficulties of testing under the proposed inclination angles of 10, 20 and 30 degrees, the initial and final angles were measured (Figure 3.14.a) and recorded for each test. Approximately

the same rate of feed as used in the vertical load tests was used in the inclined load tests. A typical set-up is shown in Fugre 3.15.

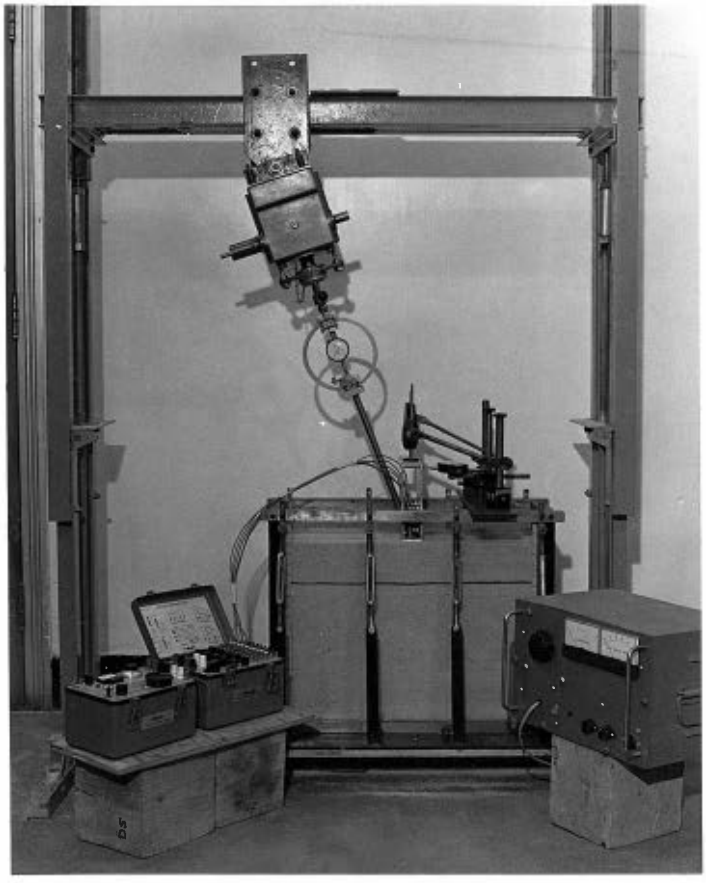

FIGURE 3.15 TYPICAL TEST SET-UP FOR INCLINED LOADS

3.6 Materials

The materials used in this investigation were sand and clay. The sand was air-dried, and composed of angular particles ranging in size from medium to coarse. The clay was obtained from Lantz, Nova Scotia, Canada, where it is used in brick manufacturing.

3.6.1 Sand Properties and Placing Technique

The predominant minerals of this sand were quartz and feldspar. The grain size distribution is represented in Figure 3.16 which shows a uniformity coefficient equal to 2.76. The specific gravity of the particles was found to be 2.64. Laboratory tests on this sand indicated maximum and minimum void ratios of 1.010 and 0.395 respectively, corresponding to maximum and minimum porosities of 0.502 and 0.283 respectively, and an effective size of 0.38 mm. The angle of internal friction ϕ has been determined from both triaxial test results (Sastry, 1976) and shear box test results (Bazan, 1976). A summary of these results is included in Appendix I.

In order to assure reproducibility of the sand density throughout the testing program, it was necessary that a sand placing technique be developed. After several trials with different methods, a definite procedure was developed by raining the sand from a certain height to give uniform and desired density. For the purpose of this investigation, the height of fall versus density relationship was established in the laboratory for the sand used (Figure 3.17). Dense packing was achieved by raining the sand from a height of 36 inches for each 3-inch layer by means of a metallic sieve, 18 inches in diameter; compact packing was

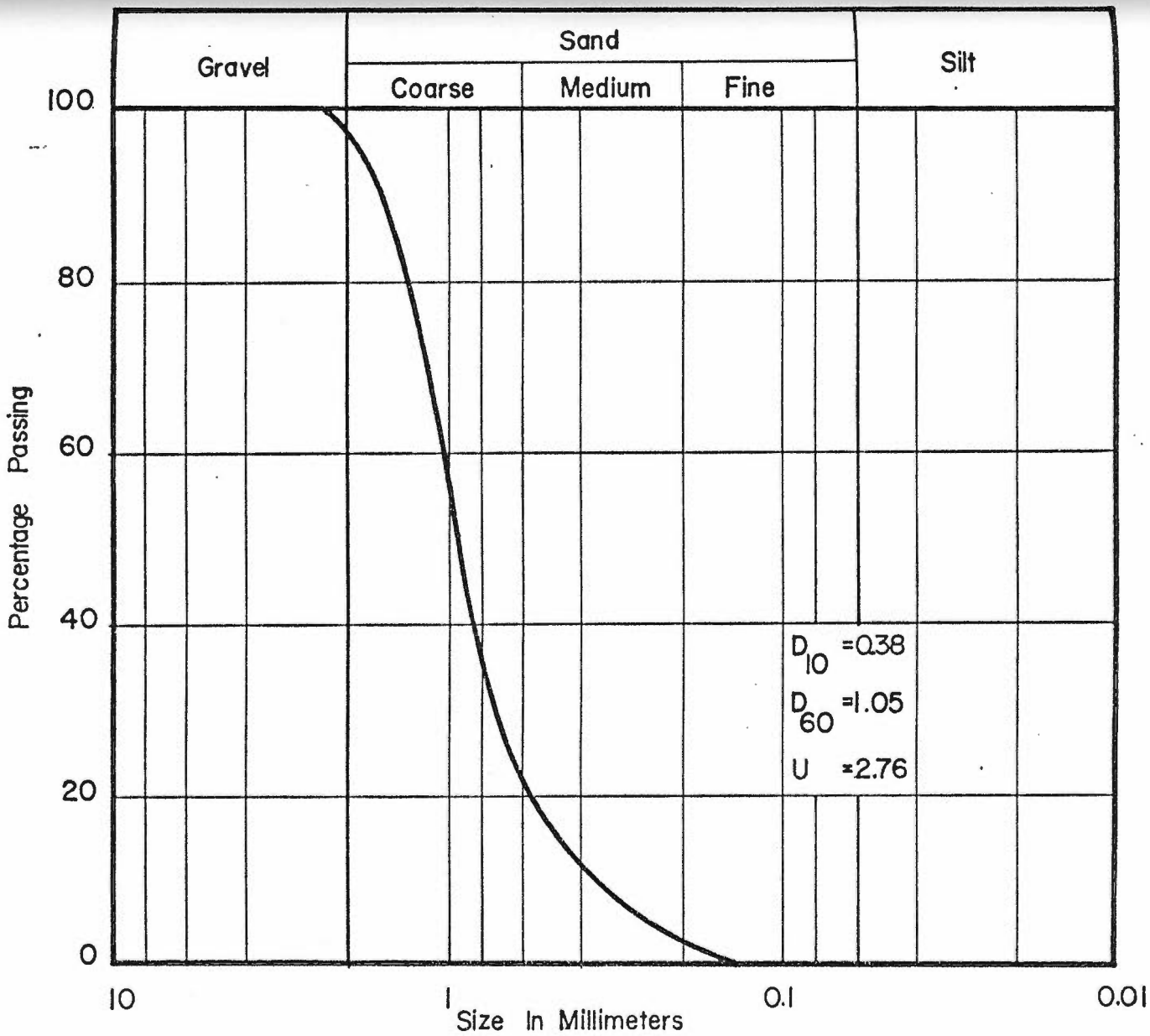

FIGURE 3·16 GRAIN SIZE DISTRIBUTION OF THE SAND

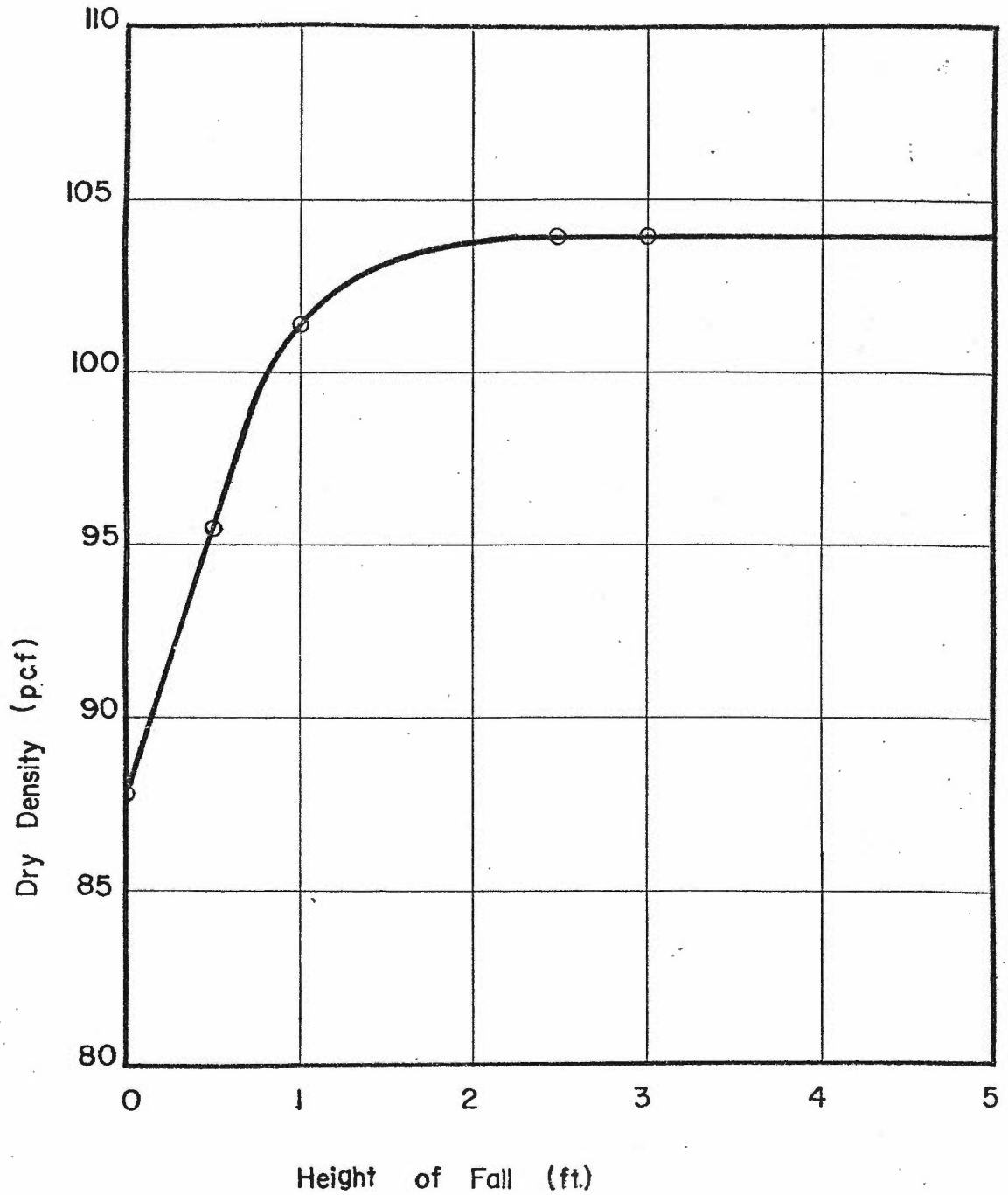

FIGURE 3·17 RELATIONSHIP BETWEEN SAND DENSITY AND HEIGHT OF FALL

achieved by raining the sand from a height of 6 inches for each one inch layer by means of a funnel with a rubber tube with an end sieve; and loose packing was obtained by pouring the sand slowly from a one-inch height for each one-inch layer, using the same funnel used for obtaining compact sand. The average dry density, porosity and relative density of the sand used in this investigation are given in Table 3.1 and Figure 3.18.

Since it was not feasible to check the sand density for every test, the density was checked after each 10 tests from the ratio of measured weight to volume of the sand to ensure that it was within the permitted range which was predetermined earlier. The observed densities were close to the values listed in Table 3.1 indicating the suitability of the filling techniques adopted. It should be pointed out that the terms "dense", "compact" and "loose" as described above are used to distinguish the state of the sand used in this investigation. It is of interest to note that the corresponding relative densities agreed well with the general definition of these terms.

Table 3.1

Properties of the Sands

State	Dry Density γ (pcf)	Porosity η (%)	Relative Density D_r
Dense	104.0	0.369	0.691
Compact	95.5	0.420	0.465
Loose	87.8	0.467	0.218

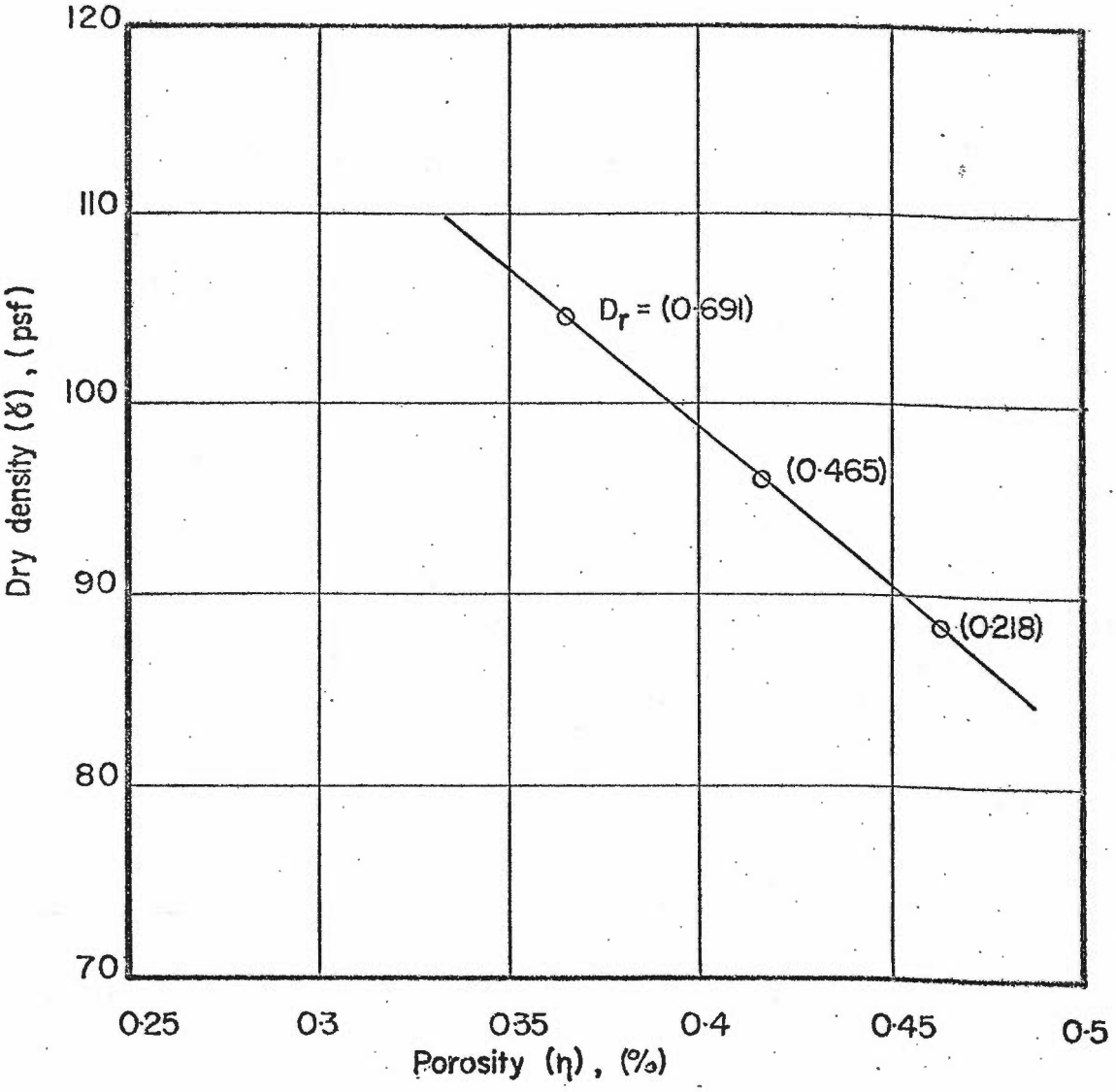

FIGURE 3·18 RELATIONSHIP BETWEEN DENSITY AND POROSITY FOR THE SAND

3.6.2 Properties and Placing of the Clay

The clay was obtained from Lantz, Nova Scotia, Canada. It was classified as an inorganic clay of medium plasticity, brown in colour, and the dominant clay mineral is illite with quartz and feldspar making up the non-clay minerals. The specific gravity was 2.74 and the water content varied from 25% to 30%. The liquid limit, plastic limit, and plasticity index were 43%, 23% and 20%, respectively. The clay, silt and sand fractions were 35%, 64% and 1% respectively.

In this investigation the clay was used as the lower weak layer where the upper strong layer was dense sand. The consistency of the clay was soft to medium. Since the failure strain of dense sand is less than of plastic clay, the simultaneous occurrence of shearing failure can hardly take place, rendering interpretation of the pressure at the lower clay layer surface at the point of the upper dense sand failure rather difficult and questionable.

Based on the study made on this clay (Kwaku, 1964; Brown, 1967), treatment of the clay with hydrated lime can reduce the plasticity index and decrease the deformation and volume change; in other words, stabilized specimens failed at low strain. Also, the shear strength increases with increasing lime content. In the present investigation 3% lime of the dry weight of the clay was added and a period 3 to 5 days was allowed for curing.

A Simpson 'Porto-Muller' mixer which stirred and kneaded the clay thoroughly was utilized to produce a uniform mix. Before

mixing, the initial water content of the stored raw clay was determined and the amount of the clay to be used was weighed, thus the required amount of lime and water were estimated to bring the mix up to 52% water content, taking into consideration the amount of water loss during the mixing and curing period. A 52% water content was chosen as giving the softest clay that could be conveniently worked in the mixer and suitable for packing the footing boxes.

The mixed clay was placed in the testing box by tamping molded balls in layers of about 2 inches thickness. Each layer was compacted (two cycles per layer) by means of a tamper with rectangular base of 1½ width and 8 inches length. The inside and seams of the footing test box were sealed with petroleum jelly to prevent loss of water and adhesion of the clay that was in contact with the box. After packing, the surface was covered with a double layer of saran wrap and the box was stored for curing. The procedure was determined in advance in order to maintain the clay strength within a limited range for all footing tests. The specific gravity of the mixed clay was 2.76, the bulk density as obtained in all tests varied 104.7 and 108.4 lb/ft^3, with water content of 48.9% and 56% respectively. The degree of saturation varied between 97.9% and 98.9%.

Since 98% saturation was achieved, the clay may be treated as fully saturated (Bishop, 1966); which meant that the shear strength was independent of the confining pressure, and the $\phi = 0$ concept applied to the analyses of results. Therefore, the shear strength was measured

by conducting unconfined compression tests on a sample 3 inches long and 1.5 inches diameter, trimmed from a block of clay cut from the box immediately after each footing test. At least two vertically-trimmed test samples were obtained for each footing test. The unconfined tests were conducted at a constant rate of 0.06 inch/min. The load was applied through a proving ring sensitive to 0.23 lb/division and deformations were measured to the nearest 0.001 inch. Typical stress-strain curves for the unconfined compression tests are illustrated in Figure 3.19.

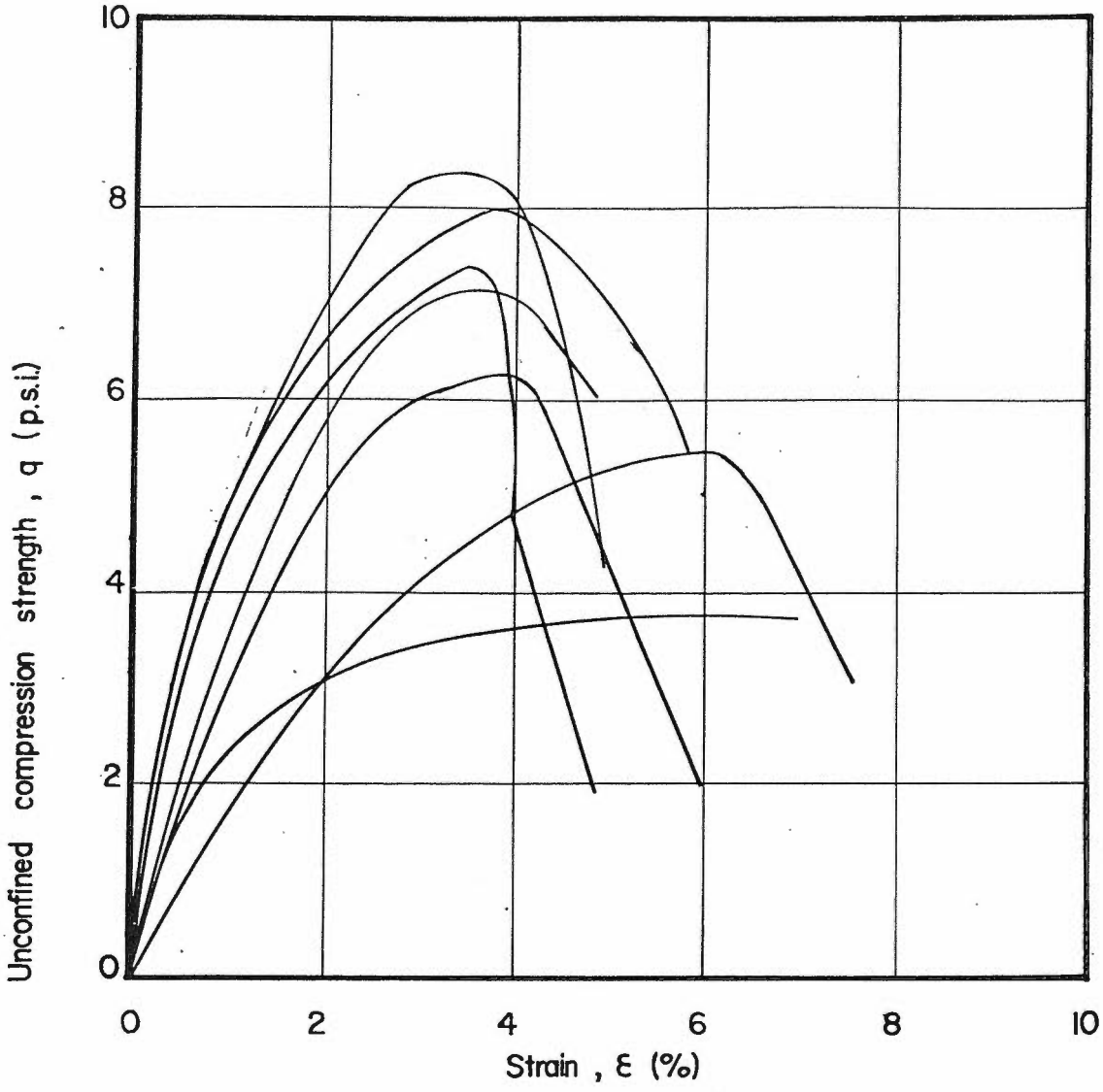

FIGURE 3·19 TYPICAL STRESS - STRAIN CURVES - UNCONFINED COMPRESSION TESTS

CHAPTER 4

TEST RESULTS

4.1 Scope

The testing program was conducted on different groups in which the effects of similar variables were studied. A testing schedule was selected for each group, such that each test would have a definite combination of the group variables (H and D in vertical load tests, and H, D and α in inclined load tests, see Figure 4.1) while the strengths of the upper and lower layers were kept constant. Each group was subdivided into a series of tests. In each series only one factor was varied in order to study its influence on the ultimate bearing capacity of the footing, while the other variables were kept constant. A summary of these groups is given in Tables 4.1.a and 4.1.b for vertical and inclined load tests respectively.

In this investigation, the depth of footing base from the soil interface (h) was varied from a minimum value of zero (footing at the interface) up to a maximum value, at which the influence of the lower layer was believed to be insignificant. The footing depth (D) in the upper layer was selected to give D/B ratios of 0, 0.5 and 1.0. The first of these ratios (D/B = 0) was used to study the effect of the upper layer depth; the other two ratios indicated the influence of surcharge strength on the ultimate bearing capacity. The inclination angle α was varied within the range of 0 to 30 degrees, this range may be of interest to practicing engineers.

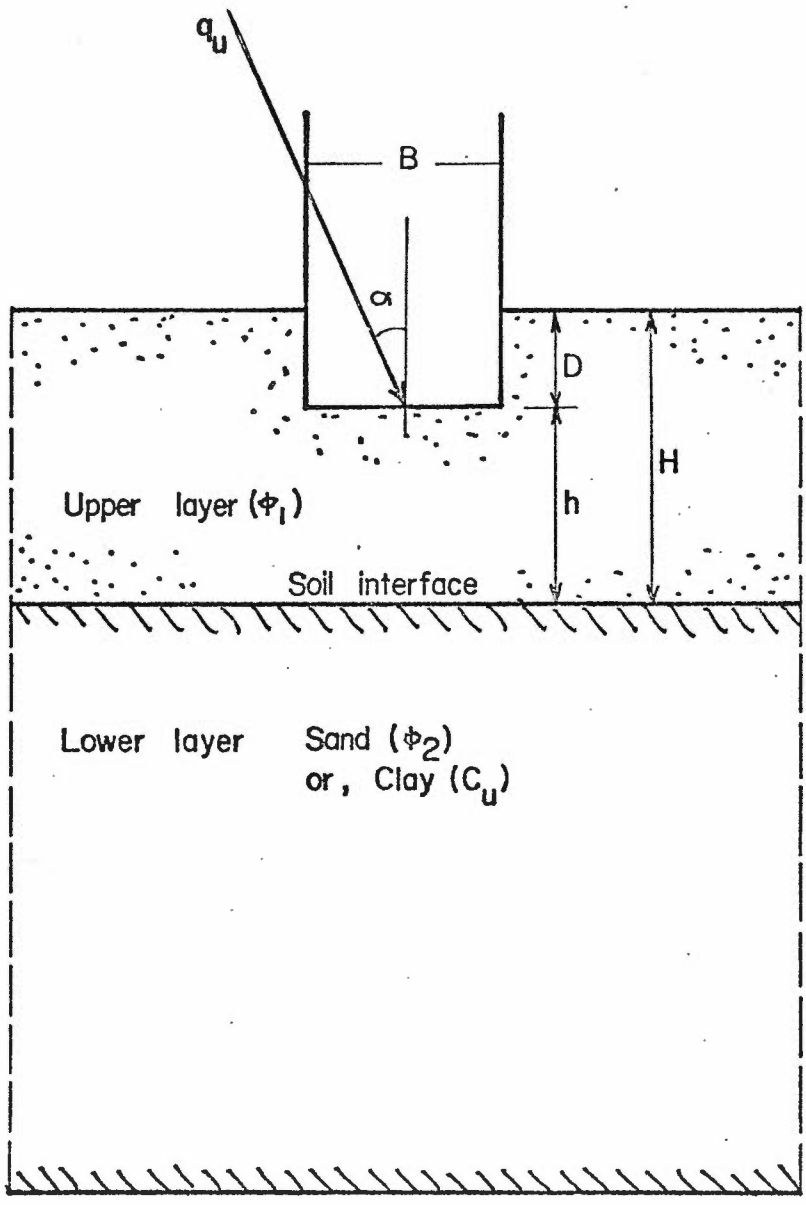

FIGURE 4·1 FOOTING IN A TWO LAYERED SOIL

Tests on footings under vertical loads were conducted in eight groups, designated A through H. In group A tests were performed in homogeneous soils which were later used in tests on layered systems. Groups B through H tests were performed on two-layered soils. In these groups the total load carried by the footing and its settlement were recorded for each test. The details of these groups (A to H) are presented in Tables 4.1.a and the corresponding results are given in Tables 4.2 to 4.9.

Tests on footings under inclined loads were conducted in five groups, designated I through M. Group I was for footing tests in homogeneous soils, and groups J through M were for footings in layered soils. In these groups, similar data were recorded as in the cases of footings under vertical loads; in addition, in the case of buried strip footing tests with D/B ratio equal to 1.0, the normal pressure on the footing base and the passive pressure on its side were measured by means of transducers Nos. 1, 2 and 3, 4 respectively. Also for inclined load tests, the initial and final inclination angles and the horizontal displacement of a point 6 inches above the footing base (strip and circular) were recorded. The details of these groups (I to M) are presented in Table 4.1.b and the corresponding results are given in Tables 4.10 through 4.14.

Whenever possible, an attempt was made to record the slip lines, and the deformation of the interface between the two layers by tracing from the glass face of the strip footing box, or by taking photographs at the end of each test.

Table 4.1.a

Summary of The Experimental Programme

For Footings Under Vertical Loads

Group No.	Type of Footing	Description		Results Table No.
A	strip	D. Sand	Homogeneous Soils	4.2
	circle	D. Sand		
	strip	L. Sand		
	circle	L. Sand		
	strip	C. Sand		
	strip	Clay		
B	strip	D. Sand/L. Sand	Strong Layer / Weak Layer	4.3
C	strip	D. Sand/C. Sand		4.4
D	strip	D. Sand/Clay		4.5
E	circle	D. Sand/L. Sand		4.6
F	strip	L. Sand/D. Sand	Weak Layer / Strong Layer	4.7
G	strip	C. Sand/D. Sand		4.8
H	circle	L. Sand/D. Sand		4.9

Table 4.1.b

Summary of the Experimental Programme

For Footings Under Inclined Loads

Group No.	Type of Footing	Description		Results Table No.
I	strip	D. Sand	Homogeneous Soils	4.10
	strip	L. Sand		
	strip	Clay		
	circle	D. Sand		
	circle	L. Sand		
J	strip	D. Sand/L. Sand	Strong Layer / Weak Layer	4.11
K	circle	D. Sand/L. Sand	Strong Layer / Weak Layer	4.12
L	strip	L. Sand/D. Sand	Weak Layer / Strong Layer	4.13
M	circle	L. Sand/D. Sand	Weak Layer / Strong Layer	4.14

Arrangements were made for taking time exposure photographs (2 minutes) of the strip footing box side for different sand layer combinations. The sand used for this purpose was the same sand used in the present investigation, 50% of this sand was coloured with green food colouring dye. These photographs were useful in understanding the sand motion beneath the footing. Some of these are included in Chapters 5 and 6.

4.2 Ultimate Bearing Capacity - (Failure Load)

The failure load is defined as the ultimate value of the average contact pressure, or load intensity transmitted by the footing base to the soil causing the soil mass to rupture or to fail in shear.

The failure load is usually determined from load-settlement curves similar in shape to a stress-strain curve. The shape of the load-settlement curve and consequently the mode of failure generally depends on the size and shape of the footing, the composition of the supporting soils, and character, rate and frequency of the loading. In addition, in the case of footings on two-layered soils, the mode of failure is influenced by the shear strength of the upper and lower layers, location of the weaker layer and upper layer thickness below the footing base. The three principal modes of shear failure under foundations have been described in the literature as general, local and punching shear failures (Caquot, 1934, Buisman, 1935, Terzaghi, 1943, DeBeer and Vesic, 1958 and Vesic, 1963a).

General shear failure is characterized by the existence of a well-defined failure pattern. Under stress-controlled conditions, footing failure is sudden and catastrophic, and in strain-controlled conditions, a visible decrease of load necessary to produce footing movement after failure may be observed. In this case, the strain prior to failure is relatively small and the load settlement curve exhibits a peak load which is defined as the ultimate bearing capacity.

In contrast with general shear failure, punching shear failure is characterized by a failure pattern which is not easy to observe. As the load increases, the footing sinks gradually. Continued penetration of the footing is made possible by vertical shear around the footing perimeter and there is practically no movement of the soil on the sides of the footing. In this case, the strain prior to failure is relatively large and the load-settlement curve does not exhibit a peak load. Finally, local shear failure truly represents a transitional mode. It retains some characteristics of both general and punching mode of failure.

In the case of general shear failure, there is no difficulty in determining the failure point, whereas for local and punching shear failures, it becomes less clearly defined and is often difficult to establish. In the latter cases, the ultimate load is selected arbitrarily, and different methods for selecting the ultimate load have been published, based on the author's experience. Terzaghi (1943) defined the ultimate load in these modes of failure as the point where the load settlement curve becomes relatively steep and straight. Brinch

Hansen (1963) has defined the failure point as the stress, for which the strain is twice the strain at a 10% smaller stress. Vesic (1963) defined the failure point as the point where the slope of the load-settlement curve first reaches zero or a steady, minimum value. Christiaens (DeBeer, 1967) found, by plotting the settlement against the load on a log-log scale, that the diagram consisted of an upper curved part and a lower part which is a straight line. The intersection of these two lines is considered as the rupture point. DeBeer (1970) reported that Christiaens' method was in close agreement with the criterion defined by Brinch Hansen.

In the present investigation both Terzaghi and Christiaens' criteria were used extensively to determine the failure point in cases of local and punching shear failure of footings. However, from a practical point of view, it may be preferrable to establish some other criterion, such as critical settlement. Such a criterion is no doubt justified by the basic philosophy of foundation design, which considers excessive settlement as failure of the foundation. It is of interest to note that in the present investigation the magnitude of settlement of surface footings on loose sand based on the previous criterion to mobilize the ultimate load is 30% of the footing width; in the case of the same footing on dense sand, the settlement was 9%.

4.3 Typical Test Results

In this section typical results of loading tests on footings are illustrated by load-settlement curves. Representative curves from each group are given in Figures 4.2 to 4.14 to show the general trend of the test groups. The failure loads for individual tests in each group and the observed settlement at failure are given in Tables 4.2 to 4.14.

Based on the observations in footing tests and from Figures 4.2 to 4.14, distinct features were observed and the salient trends were drawn for all test groups, which are summarized in the following items.

(i) For all footings in homogeneous and layered soils, the settlement at failure decreased with increasing load inclination, α. Also the settlement at failure for the strip footing was slightly higher than for the circular footing.

(ii) For footings in a strong layer overlying a weak layer under vertical loads, the load settlement curves were found to possess a peak value at higher h/B ratios where the mode of failure was general shear. The degree of curvature of the load settlement curves decreased with a decrease of the h/B ratio while the mode of failure changed to local shear failure.

For footings in a weak layer overlying a strong layer under vertical loads, for high h/B ratios the load-settlement

curves did not exhibit a peak load and the mode of failure was local shear. The degree of curvature of the load-settlement curve increased with decreasing h/B ratio, where a peak load could be found.

(iii) For footings under inclined loads in homogeneous or layered soils, whenever the mode of failure was defined by general shear, the failure was usually accompanied by continuous footing sliding. On the other hand in cases of local shear failure, failure was accompanied by footing rotation. These observations and by means of dial gauge and transducer readings (see Chapter 3) provided the criteria for determining the failure load of footings under inclined loads. It should be noted that the method of evaluating the failure load varied with the general behaviour of the layered system, the h/B ratio, and the inclination angle, α.

Table 4.2

Group A

Test Results: Footings in Homogeneous Soils Under Vertical Loads

Type of Footing	Type of Soil	Test No.	Footing Depth D / Footing Width B	Ultimate Load q_u (psi)	Settlement at Failure (S/B)%
Strip	D.Sand	1	0.0	34.32	9.0
	ϕ = 47.7	2	0.5	47.77	14.0
		3	1.0	59.59	15.5
Circular	D.Sand	4	0.0	15.66	8.0
		5	0.5	27.10	10.0
		6	1.0	40.42	12.0
Strip	L.Sand	7	0.0	2.60	30.0
	ϕ = 34.0	8	0.5	3.51	31.0
		9	1.0	4.47	32.5
Circular	L.Sand	10	0.0	2.21	25.0
		11	0.5	3.16	26.5
		12	1.0	4.06	29.0
Strip	C.Sand	13	0.0	11.15	14.5
	ϕ = 42.4	14	0.5	16.42	16.0
		15	1.0	20.67	18.0
Strip	Clay*	16	0.0	14.76	16.5

*Undrained shear strength C_u = 2.77 psi

Table 4.3

Group B

Test Results: Strip Footing in Dense Sand* Overlying Loose Sand Under Vertical Loads**

Series No.	Test No.	$\frac{H}{B}$	$\frac{D}{B}$	$\frac{h}{B}$	Ultimate Load q_u (psi)	Settlement At Failure (S/B)%	Footing Location
1	17	0.25	0.0	0.25	2.93	30.0	SURFACE FOOTING
	18	0.5	0.0	0.5	3.69	28.0	
	19	1.0	0.0	1.0	5.32	26.0	
	20	2.0	0.0	2.0	10.55	24.5	
	21	3.0	0.0	3.0	17.54	21.5	
	22	4.5	0.0	4.5	33.61	17.0	
	23	5.0	0.0	5.0	34.50	16.0	
2	24	0.5	0.5	0.0	4.06	31.0	BURIED FOOTING
	25	1.0	0.5	0.5	5.26	28.5	
	26	2.5	0.5	2.0	14.71	26.0	
	27	3.5	0.5	3.0	24.66	24.5	
	28	5.0	0.5	4.5	44.01	20.5	
	29	5.5	0.5	5.0	46.97	19.0	
3	30	1.0	1.0	0.0	5.02	32.5	
	31	1.5	1.0	0.5	7.02	31.5	
	32	2.5	1.0	1.5	14.48	28.0	
	33	4.0	1.0	3.0	31.85	31.0	
	34	5.5	1.0	4.5	56.82	24.0	
	35	6.0	1.0	5.0	59.82	23.0	

* $\phi_1 = 47.7^\circ$ ** $\phi_2 = 34.0^\circ$

Table 4.4

Group C

Test Results: Surface Strip Footing on Dense Sand*

Overlying Compact Sand Under Vertical Loads**

Test No.	$\frac{H}{B}$	$\frac{h}{B}$	Ultimate Load q_u (psi)	Settlement at Failure (S/B) %
36	0.5	0.5	16.12	14.0
37	1.0	1.0	22.67	13.0
38	1.5	1.5	30.48	12.0
39	2.0	2.0	33.95	11.5

* $\phi_1 = 47.7^{\circ}$

** $\phi_2 = 42.4^{\circ}$

Table 4.5

Group D

Test Results: Surface Strip Footing on

Dense Sand Overlying Clay Under Vertical Loads

Test No.	$\frac{H}{B}$	$\frac{h}{B}$	Ultimate Load q_u (psi)	Settlement At Failure (S/B) %	C_u (clay) (psi)
40	1	1	8.28	18	1.28
41	1	1	11.90	16	1.80
42	2	2	29.01	13	3.09

* $\phi_1 = 47.7^{\circ}$

Table 4.6

Group E

Test Results: Circular Footing in Dense Sand*

Overlying Loose Sand Under Vertical Loads**

Series No.	Test No.	$\frac{H}{B}$	$\frac{D}{B}$	$\frac{h}{B}$	Ultimate Load q_u (psi)	Settlement At Failure (S/B)%	Footing Location
1	43	0.5	0.0	0.5	3.77	20.5	SURFACE FOOTING
	44	1.0	0.0	1.0	6.98	17.0	
	45	1.75	0.0	1.75	14.30	14.0	
	46	2.0	0.0	2.0	15.86	13.5	
2	47	0.5	0.5	0.0	4.12	25.5	BURIED FOOTING
	48	1.0	0.5	0.5	6.13	22.5	
	49	2.0	0.5	1.5	17.49	18.0	
	50	2.5	0.5	2.0	25.18	16.5	
	51	3.0	0.5	2.5	26.78	15.0	
3	52	1.0	1.0	0.0	6.05	26.5	
	53	2.0	1.0	1.0	15.24	23.0	
	54	2.5	1.0	1.5	23.95	22.0	
	55	3.0	1.0	2.0	34.16	21.5	
	56	3.5	1.0	2.5	40.64	18.0	

* $\phi_1 = 47.7^\circ$

** $\phi_2 = 34.0^\circ$

Table 4.7

Group F

Test Results: Strip Footing in Loose Sand*

Overlying Dense Sand Under Vertical Loads**

Series No.	Test No.	$\frac{H}{B}$	$\frac{D}{B}$	$\frac{h}{B}$	Ultimate Load q_u (psi)	Settlement At Failure (S/B)%	Footing Location
1	57	0.25	0.0	0.25	22.13	13.5	SURFACE FOOTING
	58	0.5	0.0	0.5	15.10	16.5	
	59	0.5	0.0	0.5	15.77	18.0	
	60	1.0	0.0	1.0	5.59	27.0	
	61	2.0	0.0	2.0	2.67	30.0	
2	62	0.5	0.5	0.0	45.54	15.0	BURIED FOOTING
	63	0.5	0.5	0.0	45.02	15.0	
	64	1.0	0.5	0.5	23.12	17.0	
	65	1.5	0.5	1.0	10.19	24.5	
	66	2.0	0.5	1.5	5.57	29.0	
	67	2.5	0.5	2.0	3.61	30.0	
3	68	1.0	1.0	0.0	57.10	16.0	
	69	1.5	1.0	0.5	31.68	19.0	
	70	2.0	1.0	1.0	16.23	29.0	
	71	2.5	1.0	1.5	8.30	30.0	
	72	3.0	1.0	2.0	4.85	31.0	

* $\phi_1 = 34.0^\circ$

** $\phi_2 = 47.7^\circ$

Table 4.8

Group G

Test Results: Strip Footing In Compact Sand

Overlying Dense Sand Under Vertical Loads

Series No.	Test No.	$\frac{H}{B}$	$\frac{D}{B}$	$\frac{h}{B}$	Ultimate Load q_u (psi)	Settlement At Failure (S/B) %	Footing Location
1	73	0.5	0.0	0.5	25.40	11.0	SURFACE FOOTING
	74	1.0	0.0	1.0	17.53	12.5	
	75	1.5	0.0	1.5	12.31	13.5	
2	76	0.5	0.5	0.0	46.48	13.5	BURIED FOOTING
	77	1.0	0.5	0.5	35.11	14.5	
	78	2.0	0.5	1.5	19.74	16.0	
3	79	1.0	1.0	0.0	58.23	16.0	
	80	2.0	1.0	1.0	30.51	17.5	
	81	2.5	1.0	1.5	26.35	18.5	
	82	3.5	1.0	2.5	21.33	19.0	

$\phi_1 = 42.4^\circ$

$\phi_2 = 47.7^\circ$

Table 4.9

Group H

Test Results: Circular Footing in Loose Sand

Overlying Dense Sand Under Vertical Loads

Series No.	Test No.	$\frac{H}{B}$	$\frac{D}{B}$	$\frac{h}{B}$	Ultimate Load q_u (psi)	Settlement At Failure (S/B) %	Footing Location
1	83	0.25	0.0	0.25	10.72	18.0	SURFACE FOOTING
	84	0.5	0.0	0.5	7.43	20.5	
	85	1.0	0.0	1.0	3.48	22.5	
	86	2.0	0.0	2.0	2.39	24.0	
2	87	0.5	0.5	0.0	22.74	10.0	BURIED FOOTING
	88	1.0	0.5	0.5	12.49	16.0	
	89	1.5	0.5	1.0	6.97	19.0	
3	90	1.0	1.0	0.0	32.50	10.0	
	-	1.0	1.0	0.0	32.81	11.0	
	91	1.5	1.0	0.5	17.75	16.5	
	92	2.0	1.0	1.0	11.02	24.5	

$\phi_1 = 34.0^\circ$

$\phi_2 = 47.7^\circ$

Table 4.10.a

Group I

Test Results: Strip Footing In Homogeneous Dense Sand Under Inclined Loads

Series No.	Test No.	$\frac{D}{B}$	Inclination Angle α		q_u (psi)	(S/B)%
			Initial (degrees)	Final (degrees)		
1	93	0.0	0.0	0.0	35.21	9.5
	94	0.0	8.5	9.0	18.50	8.0
	95	0.0	13.0	14.0	13.85	6.5
	96	0.0	20.0	21.0	7.45	3.5
	97	0.0	24.6	25.7	5.47	3.0
	98	0.0	29.5	30.6	3.20	2.5
2	99	0.5	9.5	10.0	29.11	8.5
	100	0.5	16.0	16.6	19.65	6.0
	101	0.5	20.0	20.5	15.48	5.5
	102	0.5	28.5	29.3	9.47	4.0
3	103	1.0	9.5	10.5	40.74	9.0
	104	1.0	17.0	18.0	29.00	8.0
	105	1.0	20.0	21.1	24.80	7.5
	106	1.0	25.4	25.6	20.27	5.5

Table 4.10.b

Group I

Test Results: Strip Footing In Homogeneous Loose Sand Under Inclined Loads

Series No.	Test No.	$\frac{D}{B}$	Inclination Angle α		$q_{u(psi)}$	(S/B)%
			Initial (degrees)	Final (degrees)		
1	107	0.0	9.0	10.0	1.24	27.0
	108	0.0	24.6	25.8	0.32	19.0
2	109	0.5	10.0	11.1	1.61	27.5
	110	0.5	18.0	19.3	0.89	23.0
3	111	1.0	9.0	10.1	2.55	29.0
	112	1.0	20.0	21.2	1.15	22.5
	113	1.0	27.0	28.4	0.56	18.0

Table 4.10.c

Group I

Test Results: Surface Strip Footing In Homogeneous Clay

Under Inclined Loads

Series No.	Test No.	Inclination Angle α		C_u (psi)	Ultimate Load q_u (psi)	Settlement At Failure (S/B)%
		Initial (degrees)	Final (degrees)			
1	114	0.0	0.0	3.75	20.30	15.5
	115	8.9	9.8	3.95	16.82	11.5
	116	20.0	21.1	3.82	11.70	8.0
	117	29.0	30.4	3.56	7.25	5.5

Table 4.10.d

Group I

Test Results: Circular Footing In Homogeneous Dense Sand Under Inclined Loads

Series No.	Test No.	$\frac{D}{B}$	Inclination Angle α		q_u (psi)	(S/B)%
			Initial (degrees)	Final (degrees)		
1	118	0.0	0.0	0.0	16.46	9.0
	119	0.0	8.0	8.6	9.81	8.0
	120	0.0	11.0	12.0	7.70	7.0
	121	0.0	24.0	25.0	3.70	2.5
	122	0.0	29.5	30.5	2.26	1.5
2	123	0.5	9.6	10.1	19.49	9.5
	124	0.5	18.0	18.5	14.21	6.0
	125	0.5	26.0	26.7	9.81	3.0
3	126	1.0	9.7	10.0	32.11	11.0
	127	1.0	20.0	20.7	24.44	8.0
	128	1.0	28.3	29.2	17.27	5.5

Table 4.10.e

Group I

Test Results: Circular Footing In Homogeneous Loose Sand Under Inclined Loads

Series No.	Test No.	$\frac{D}{B}$	Inclination Angle α		q_u (psi)	(S/B)%
			Initial (degrees)	Final (degrees)		
1	129	0.0	10.3	11.1	1.29	20.5
	130	0.0	19.2	20.2	0.51	16.5
	131	0.0	29.0	30.1	0.22	10.0
2	132	0.5	9.8	10.5	1.95	22.0
	133	0.5	19.5	20.4	0.99	18.5
3	134	1.0	9.1	9.6	2.83	23.5
	135	1.0	20.2	21.0	1.44	19.5
	136	1.0	29.4	30.5	0.86	13.0

Table 4.11

Group J

Test Results: Strip Footing in Dense Sand Overlying Loose Sand Under Inclined Loads

Series No.	Test No.	$\frac{H}{B}$	$\frac{D}{B}$	$\frac{h}{B}$	Inclination Angle α		Ultimate Load q_u (psi)	Settlement at Failure (S/B)%
					Initial (degrees)	Final (degrees)		
1	137	1.0	0.0	1.0	8.0	9.3	3.44	18.0
	138	1.0	0.0	1.0	19.4	20.8	1.70	12.5
	139	1.0	0.0	1.0	29.1	30.7	1.10	10.5
	140	2.0	0.0	2.0	10.0	11.2	6.81	13.0
	141	2.0	0.0	2.0	17.5	19.0	4.15	10.5
	142	2.0	0.0	2.0	23.0	24.5	2.82	7.5
	143	3.0	0.0	3.0	11.0	12.0	10.23	10.0
	144	3.0	0.0	3.0	18.0	19.2	7.51	8.5
	145	3.0	0.0	3.0	27.5	28.8	3.10	5.5
	146	5.0	0.0	5.0	10.0	10.8	16.11	7.5
	147	5.0	0.0	5.0	18.1	19.2	9.02	4.0
2	148	0.5	0.5	0.0	10.0	10.9	2.10	27.0
	149	0.5	0.5	0.0	19.8	20.9	1.00	24.0
	150	0.5	0.5	0.0	30.0	31.3	0.44	16.5
	151	2.5	0.5	2.0	9.6	10.5	9.55	16.5
	152	2.5	0.5	2.0	20.0	21.0	6.13	12.0
	153	2.5	0.5	2.0	29.7	30.9	4.33	9.0
	154	3.5	0.5	3.0	0.0	0.0	25.10	23.5
	155	3.5	0.5	3.0	10.1	11.1	15.81	14.5

Table 4.11 (cont'd)

Group J

Test Results: Strip Footing in Dense Sand

Overlying Loose Sand Under Inclined Loads

Series No.	Test No.	$\frac{H}{B}$	$\frac{D}{B}$	$\frac{h}{B}$	Inclination Angle α		Ultimate Load q_u (psi)	Settlement at Failure (S/B)%
					Initial (degrees)	Final (degrees)		
2	156	3.5	0.5	3.0	20.5	21.7	10.75	10.5
	157	3.5	0.5	3.0	29.5	30.8	7.84	8.0
	158	5.5	0.5	5.0	12.0	12.7	25.11	7.0
3	159	1.0	1.0	0.0	11.5	12.6	2.22	28.0
	160	1.0	1.0	0.0	20.0	21.3	1.39	25.0
	161	1.0	1.0	0.0	28.5	29.9	0.97	18.0
	162	2.5	1.0	1.5	12.0	12.6	8.70	22.0
	163	2.5	1.0	1.5	18.0	18.8	6.76	17.5
	164	2.5	1.0	1.5	29.0	30.0	3.49	12.5
	165	4.0	1.0	3.0	10.5	11.2	20.42	20.5
	166	4.0	1.0	3.0	16.6	17.3	16.77	17.0
	167	4.0	1.0	3.0	30.0	31.0	10.20	11.5
	168	5.0	1.0	4.0	9.6	10.1	32.10	17.0
	169	5.0	1.0	4.0	20.0	20.8	21.45	13.5
	170	5.0	1.0	4.0	29.2	30.3	15.71	9.5

$\phi_1 = 47.7^\circ$

$\phi_2 = 34.0^\circ$

Table 4.12

Group K

Test Results: Circular Footing In Dense Sand

Overlying Loose Sand Under Inclined Loads

Series No.	Test No.	$\frac{H}{B}$	$\frac{D}{B}$	$\frac{h}{B}$	Inclination Angle α		Ultimate Load q_u (psi)	Settlement At Failure (S/B)%
					Initial (degrees)	Final (degrees)		
1	171	1.0	0.0	1.0	9.9	10.6	4.89	12.5
	172	1.0	0.0	1.0	20.0	20.8	2.99	8.5
	173	1.0	0.0	1.0	29.5	30.5	1.70	4.0
	174	2.0	0.0	2.0	10.0	10.6	9.10	8.0
	175	2.0	0.0	2.0	19.7	20.4	4.52	5.5
	176	2.0	0.0	2.0	28.9	29.8	2.25	2.5
2	177	0.5	0.5	0.0	9.7	10.4	3.01	21.0
	178	0.5	0.5	0.0	20.0	20.9	1.85	16.5
	179	0.5	0.5	0.0	29.0	30.1	0.96	13.5
	180	1.5	0.5	1.0	10.0	10.6	7.88	15.5
	181	1.5	0.5	1.0	19.5	20.3	5.62	12.5
	182	1.5	0.5	1.0	29.5	30.5	3.90	8.0
	183	2.0	0.5	1.5	9.6	10.2	12.76	13.0
	184	2.0	0.5	1.5	20.0	20.7	9.11	8.0
	185	2.0	0.5	1.5	29.7	30.7	6.49	5.5
	186	2.5	0.5	2.0	10.1	10.7	17.55	10.5
	187	2.5	0.5	2.0	19.5	20.1	12.48	6.0

Table 4.12 (continued)

Group K

Test Results: Circular Footing in Dense Sand

Overlying Loose Sand Under Inclined Loads

Series No.	Test No.	$\frac{H}{B}$	$\frac{D}{B}$	$\frac{h}{B}$	Inclination Angle α		Ultimate Load q_u (psi)	Settlement At Failure (S/B)%
					Initial (degrees)	Final (degrees)		
3	188	1.0	1.0	0.0	9.4	10.1	4.74	23.5
	189	1.0	1.0	0.0	19.5	20.6	3.32	18.5
	190	1.0	1.0	0.0	28.9	30.1	1.85	14.5
	191	2.0	1.0	1.0	10.1	10.7	11.36	17.5
	192	2.0	1.0	1.0	20.0	20.9	8.27	13.5
	193	2.0	1.0	1.0	29.3	30.3	6.19	9.5
	194	2.5	1.0	1.5	10.0	10.6	18.01	15.0
	195	2.5	1.0	1.5	19.7	20.6	13.39	11.5
	196	2.5	1.0	1.5	28.5	29.4	10.20	7.5
	197	3.0	1.0	2.0	10.0	10.6	25.94	13.0
	198	3.0	1.0	2.0	20.1	20.9	19.68	9.5
	199	3.0	1.0	2.0	29.5	30.5	14.50	6.0
	200	3.5	1.0	2.5	16.1	16.9	28.51	9.5
	201	3.5	1.0	2.5	24.5	25.5	19.80	7.0

Table 4.13

Group L

Test Results: Strip Footing in Loose Sand Overlying Dense Sand Under Inclined Loads

Series No.	Test No.	$\frac{H}{B}$	$\frac{D}{B}$	$\frac{h}{B}$	Inclination Angle α		Ultimate Load q_u (psi)	Settlement At Failure (S/B)%
					initial (degrees)	final (degrees)		
1	202	0.5	0.0	0.5	9.0	9.7	9.36	13.0
	203	0.5	0.0	0.5	20.1	20.9	3.51	9.0
	204	0.5	0.0	0.5	29.0	30.0	1.43	5.5
	205	1.0	0.0	1.0	10.0	10.8	2.49	22.0
	206	1.0	0.0	1.0	19.3	20.1	1.35	16.0
	207	1.0	0.0	1.0	28.7	29.8	0.76	9.5
2	208	0.5	0.5	0.0	9.1	9.7	26.01	8.0
	209	0.5	0.5	0.0	19.6	20.2	12.16	5.0
	210	0.5	0.5	0.0	29.5	30.5	4.37	3.5
	211	1.0	0.5	0.5	9.9	10.5	14.42	12.5
	212	1.0	0.5	0.5	20.0	20.7	6.50	9.5
	213	1.0	0.5	0.5	29.2	30.1	3.09	7.5
	214	1.5	0.5	1.0	10.1	10.9	6.22	18.5
	215	1.5	0.5	1.0	19.4	20.3	3.48	14.0
	216	1.5	0.5	1.0	29.6	30.6	1.38	10.5

Table 4.13 (cont'd)

Group L

Test Results: Strip Footing in Loose Sand Overlying Dense Sand Under Inclined Loads

Series No.	Test No.	$\frac{H}{B}$	$\frac{D}{B}$	$\frac{h}{B}$	Inclination Angle α		Ultimate Load q_u (psi)	Settlement At Failure (S/B)%
					initial (degrees)	final (degrees)		
3	217	1.0	1.0	0.0	9.8	10.5	31.46	9.0
	218	1.0	1.0	0.0	20.2	21.0	15.39	6.5
	219	1.0	1.0	0.0	30.0	31.0	6.40	3.5
	220	1.5	1.0	0.5	10.0	10.7	18.25	14.5
	221	1.5	1.0	0.5	19.8	20.6	9.61	10.0
	222	1.5	1.0	0.5	29.7	30.7	4.74	7.0
	223	2.0	1.0	1.0	9.1	10.0	9.38	22.5
	224	2.0	1.0	1.0	19.7	20.6	5.52	16.0
	225	2.0	1.0	1.0	28.5	29.6	2.84	11.5

$\phi_1 = 34.0^\circ$

$\phi_2 = 47.7^\circ$

Table 4.14

Group M

Test Results: Circular Footing In Loose Sand

Overlying Dense Sand Under Inclined Loads

Series No.	Test No.	$\frac{H}{B}$	$\frac{D}{B}$	$\frac{h}{B}$	Inclination Angle α		Ultimate Load q_u (psi)	Settlement At Failure (S/B)%
					Initial (degrees)	Final (degrees)		
1	226	0.5	0.0	0.5	9.9	10.7	4.31	16.5
	227	0.5	0.0	0.5	19.0	20.0	2.52	13.5
	228	0.5	0.0	0.5	29.6	30.7	1.40	6.0
2	229	0.5	0.5	0.0	9.6	10.2	15.44	8.5
	230	0.5	0.5	0.0	19.6	20.4	10.76	6.0
	231	0.5	0.5	0.0	29.5	30.5	6.23	2.5
	232	1.0	0.5	0.5	10.0	10.7	8.98	13.0
	233	1.0	0.5	0.5	19.9	20.8	6.30	10.5
	234	1.0	0.5	0.5	30.0	31.1	4.11	8.5
	235	1.5	0.5	1.0	8.9	9.6	5.08	16.0
	236	1.5	0.5	1.0	20.0	20.9	3.35	14.0
	237	1.5	0.5	1.0	28.8	29.9	2.26	10.0
3	238	1.0	1.0	0.0	9.8	10.4	22.65	10.0
	239	1.0	1.0	0.0	20.1	20.9	16.19	8.0
	240	1.0	1.0	0.0	28.9	30.0	10.36	5.0
	241	1.5	1.0	0.5	9.9	10.6	13.77	14.0
	242	1.5	1.0	0.5	20.0	20.7	10.02	10.5

Table 4.14 (cont'd)

Group M

Test Results: Circular Footing in Loose Sand Overlying Dense Sand Under Inclined Loads

Series No.	Test No.	$\frac{H}{B}$	$\frac{D}{B}$	$\frac{h}{B}$	Inclination Angle α		Ultimate load q_u (psi)	Settlement At Failure (S/B)%
					Initial (degrees)	Final (degrees)		
3	243	1.5	1.0	0.5	29.6	30.7	6.98	7.5
	244	2.0	1.0	1.0	10.0	10.6	8.51	20.0
	245	2.0	1.0	1.0	19.8	20.6	6.45	17.0
	246	2.0	1.0	1.0	29.9	31.0	3.67	10.5

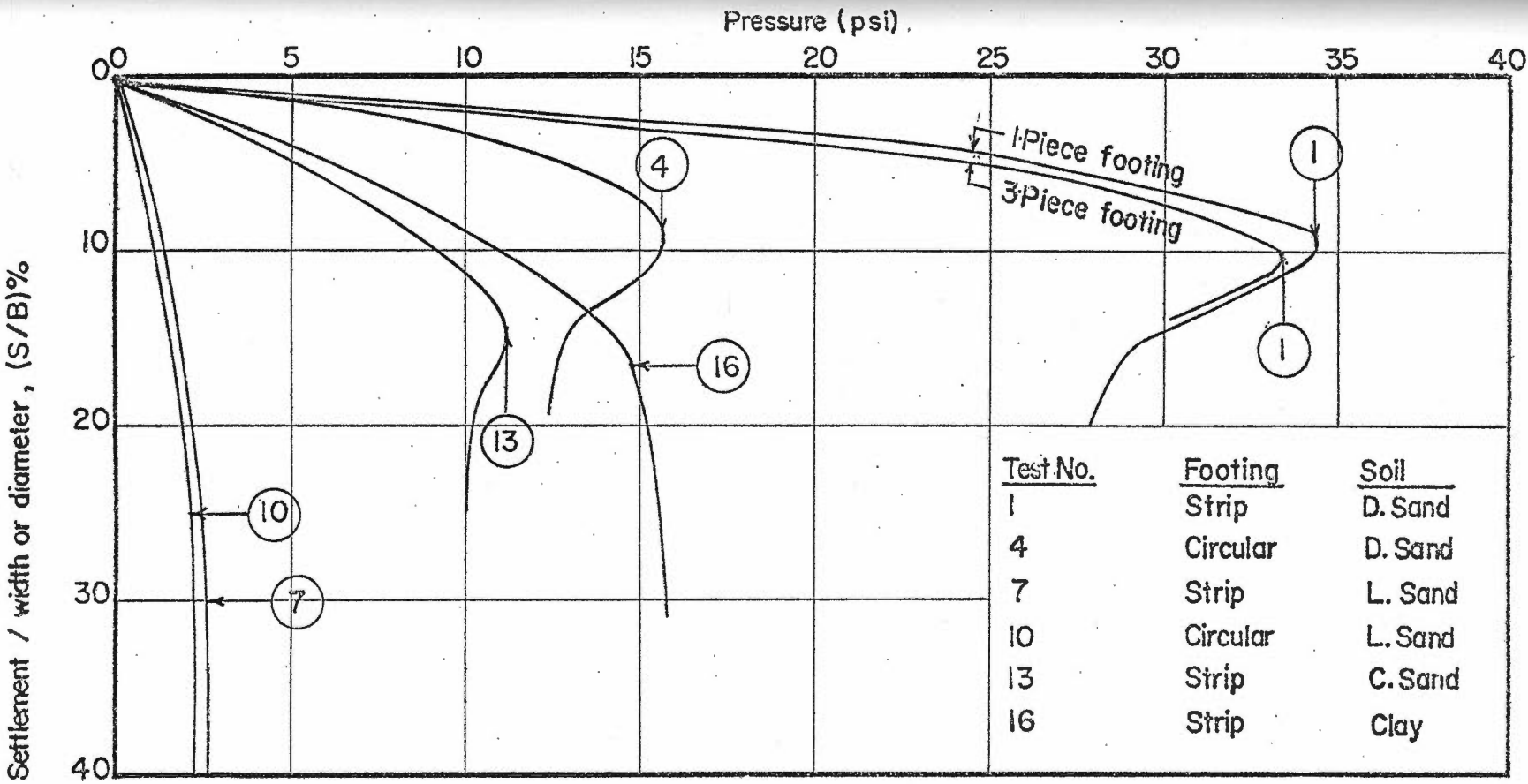

FIGURE 4·2 LOAD SETTLEMENT CURVES - SURFACE FOOTINGS IN HOMOGENEOUS SOILS - UNDER VERTICAL LOADS (GROUP A)

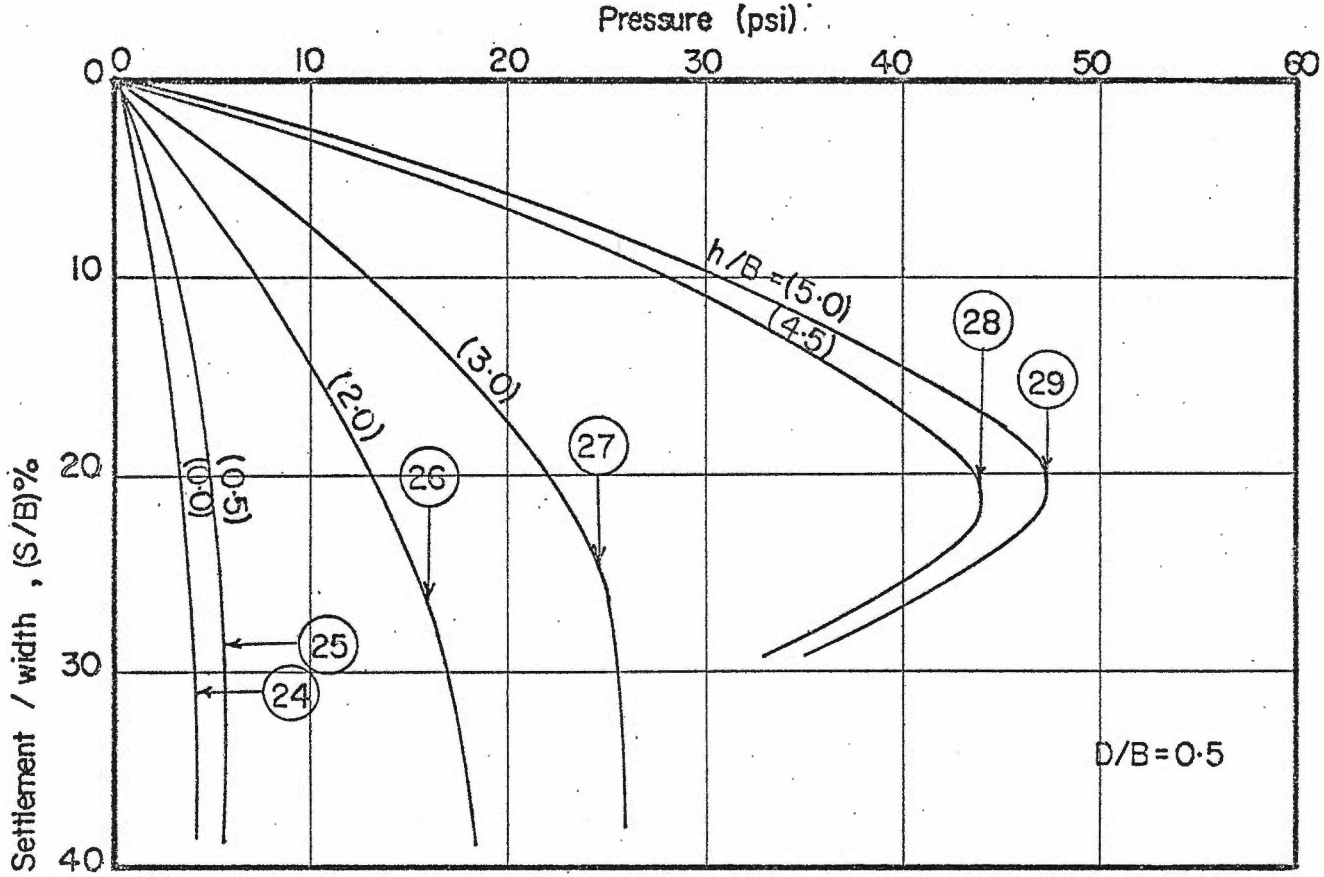

FIGURE 4·3 LOAD SETTLEMENT CURVES - BURIED STRIP FOOTING IN DENSE SAND OVERLYING LOOSE SAND - UNDER VERTICAL LOADS (GROUP B)

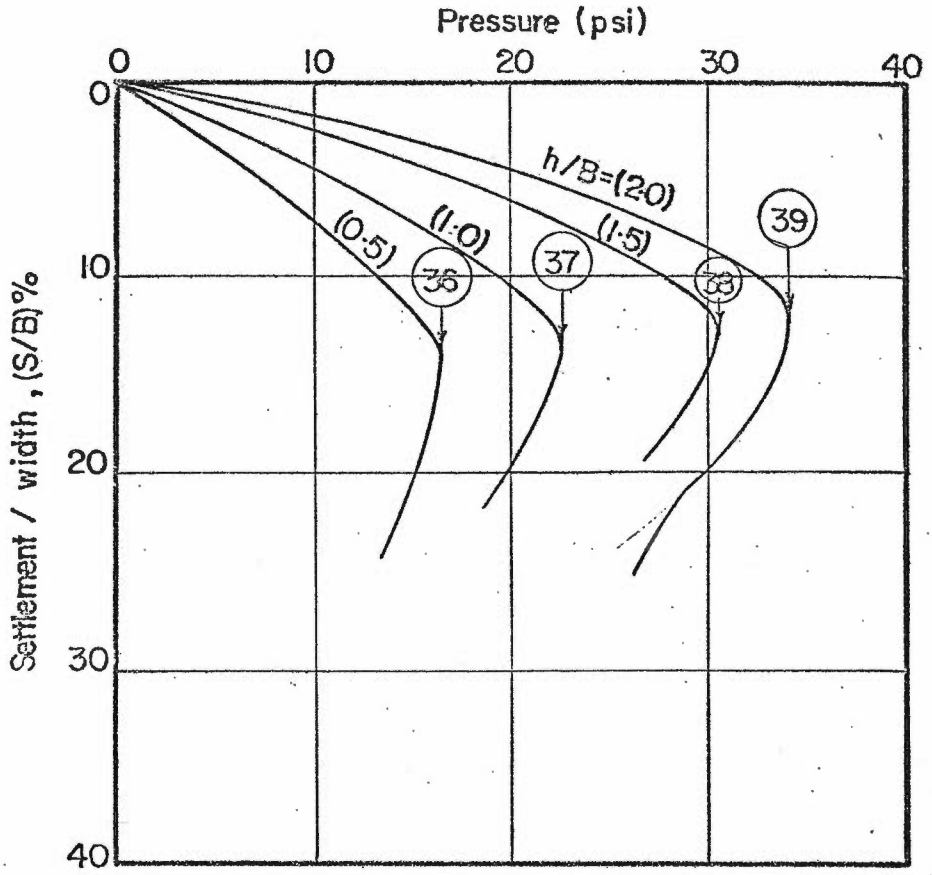

FIGURE 4·4 LOAD SETTLEMENT CURVES - SURFACE STRIP FOOTING ON DENSE SAND OVERLYING COMPACT SAND - UNDER VERTICAL LOADS (GROUP C)

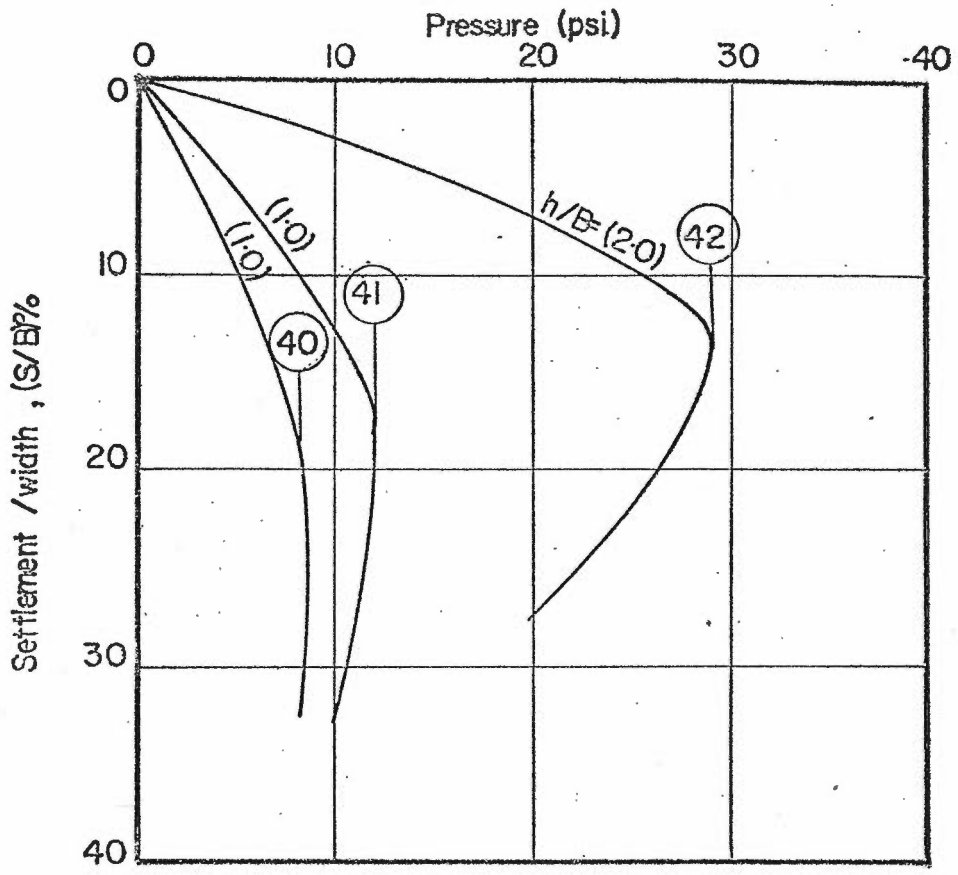

FIGURE 4·5 LOAD SETTLEMENT CURVES - SURFACE STRIP FOOTING ON DENSE SAND OVERLYING CLAY - UNDER VERTICAL LOADS (GROUP D)

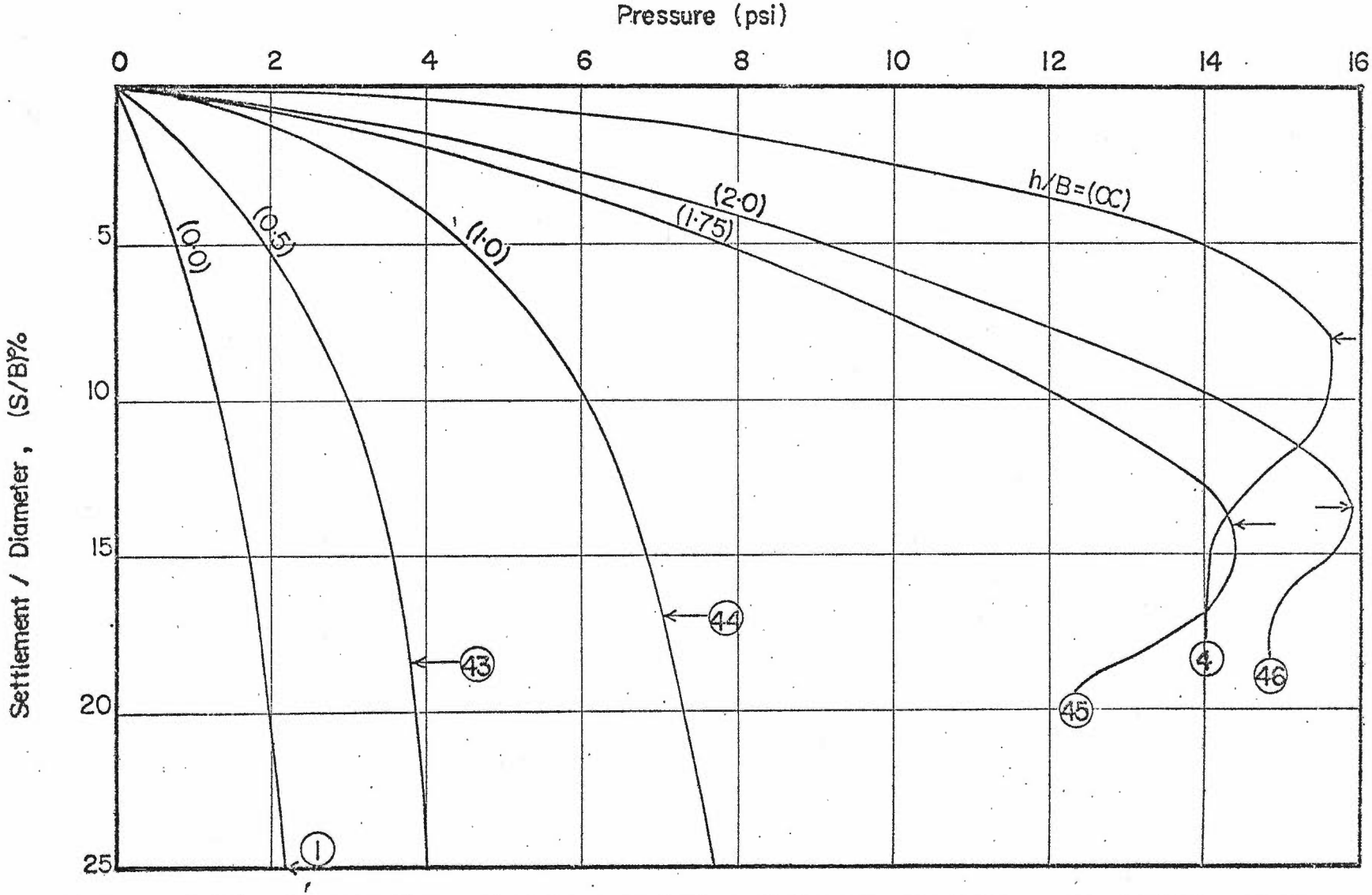

FIGURE 4·6 LOAD SETTLEMENT CURVES - SURFACE CIRCULAR FOOTING ON DENSE SAND OVERLYING LOOSE SAND UNDER VERTICAL LOADS (GROUP E)

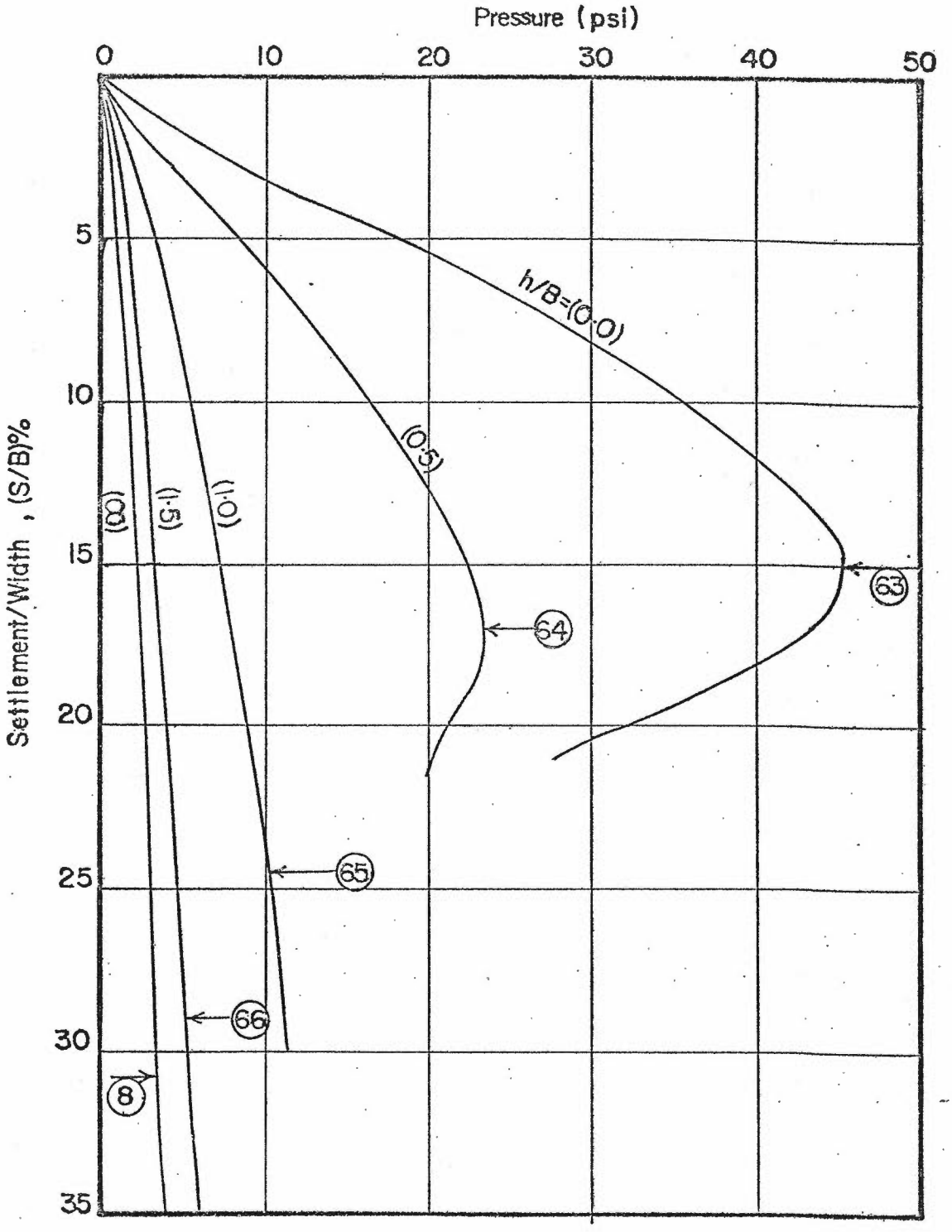

FIGURE 4·7 LOAD - SETTLEMENT CURVES - BURIED STRIP FOOTING IN LOOSE SAND OVERLYING DENSE SAND UNDER VERTICAL LOADS (GROUP F)

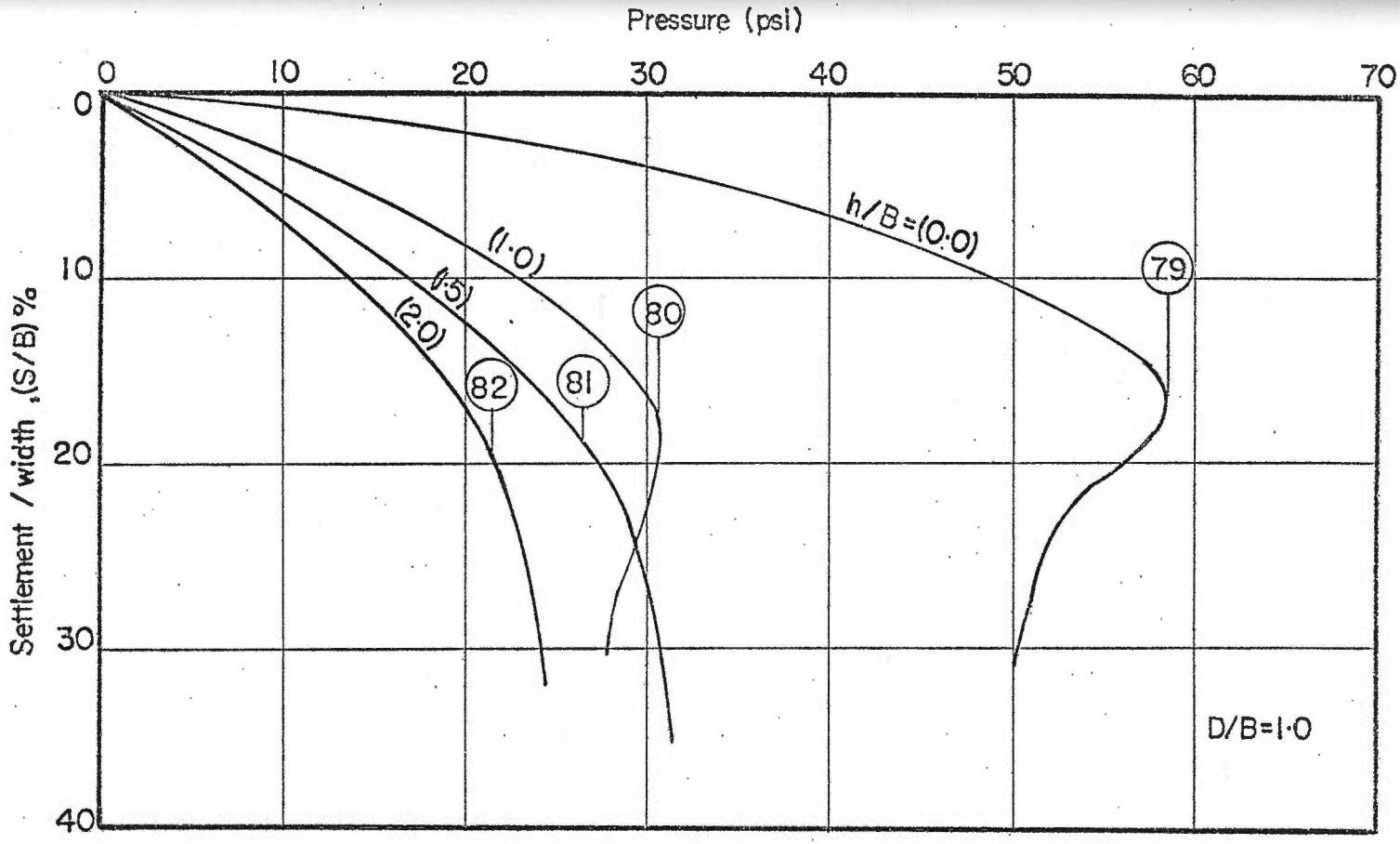

FIGURE 4·8 LOAD SETTLEMENT CURVES - BURIED STRIP FOOTING IN COMPACT SAND OVERLYING DENSE SAND - UNDER VERTICAL LOADS (GROUP G)

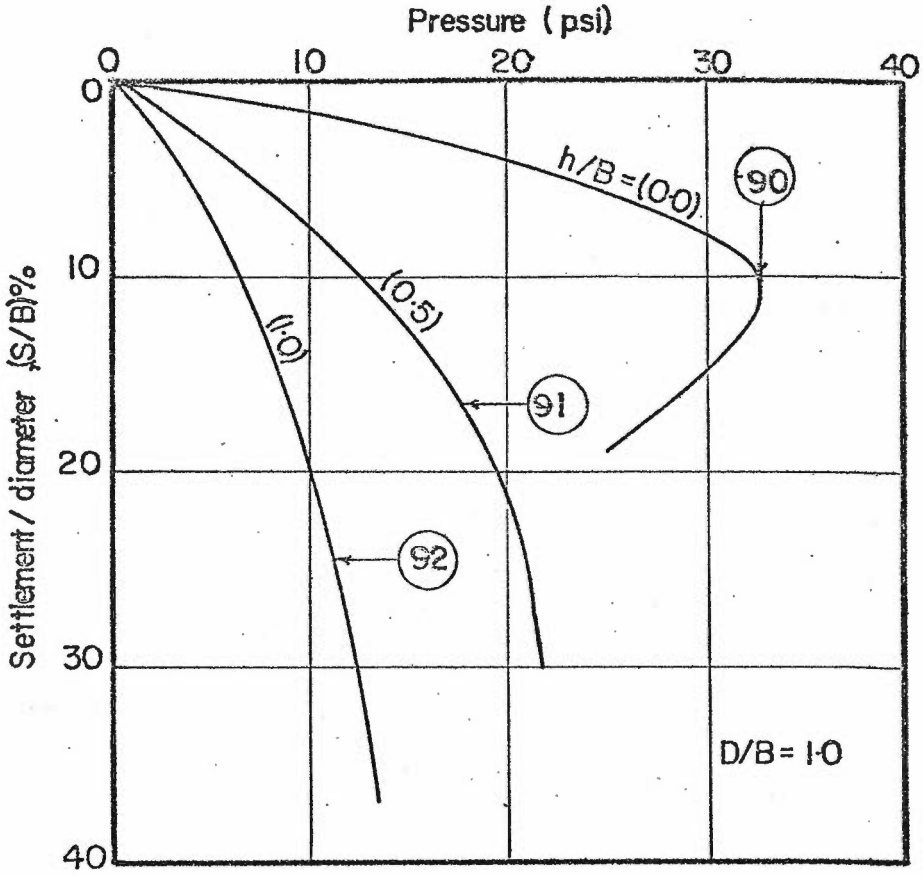

FIGURE 4·9 LOAD SETTLEMENT CURVES - BURIED CIRCULAR FOOTING IN LOOSE SAND OVERLYING DENSE SAND - UNDER VERTICAL LOADS (GROUP H)

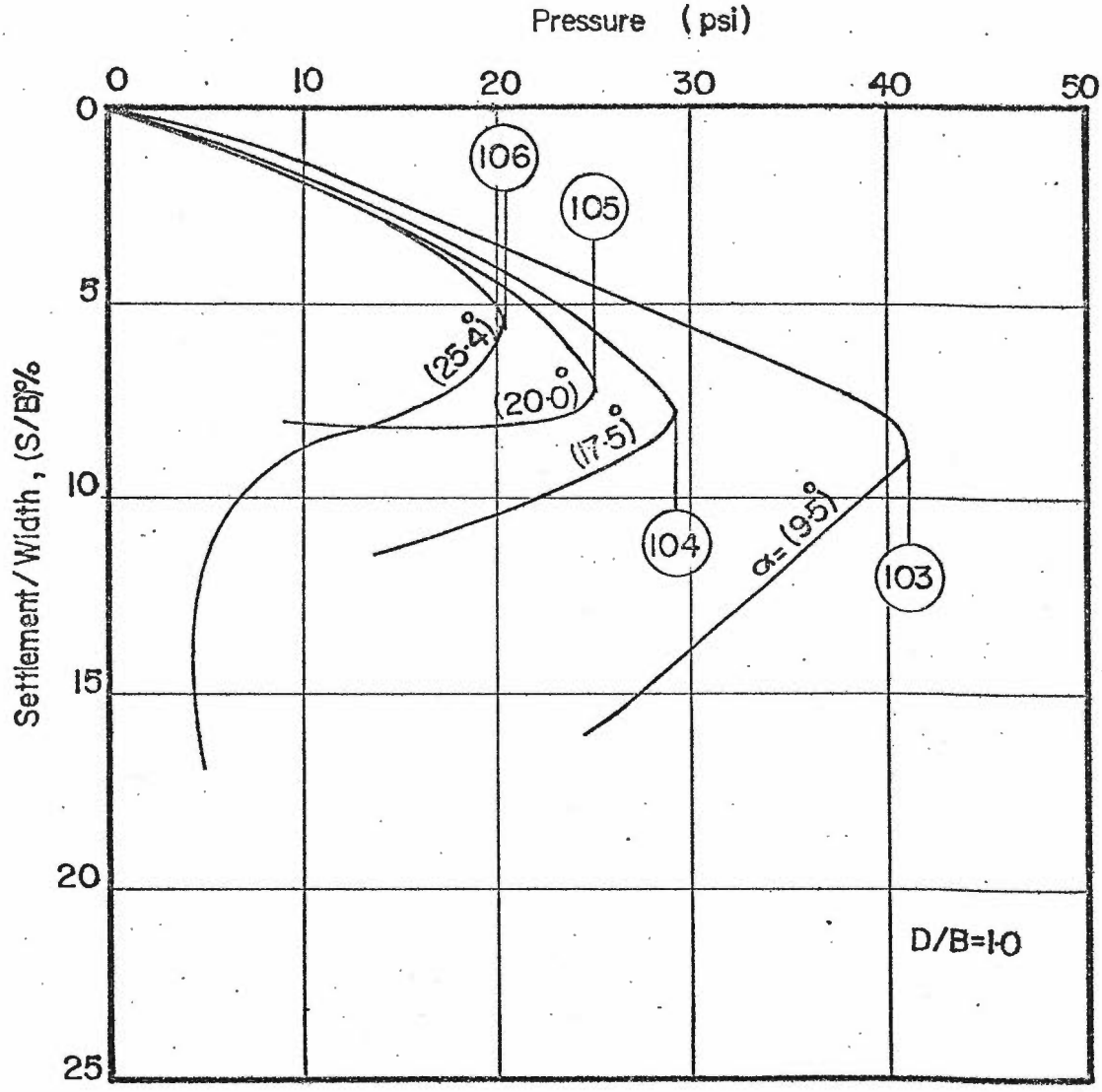

FIGURE 4·10 LOAD-SETTLEMENT CURVES - BURIED STRIP FOOTING IN DENSE SAND UNDER INCLINED LOADS (GROUP I)

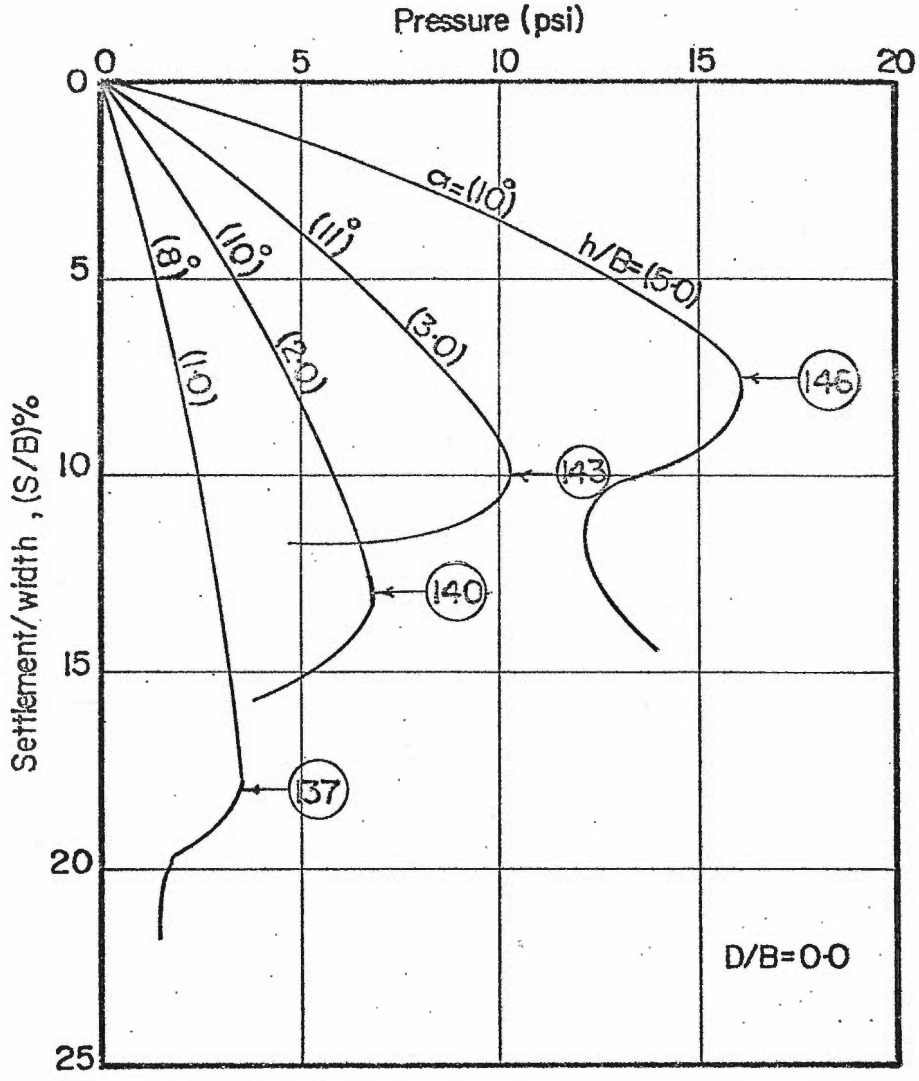

FIGURE 4.11 LOAD SETTLEMENT CURVES - SURFACE STRIP FOOTING ON DENSE SAND OVELYING LOOSE SAND -UNDER INCLINED LOADS (GROUP J)

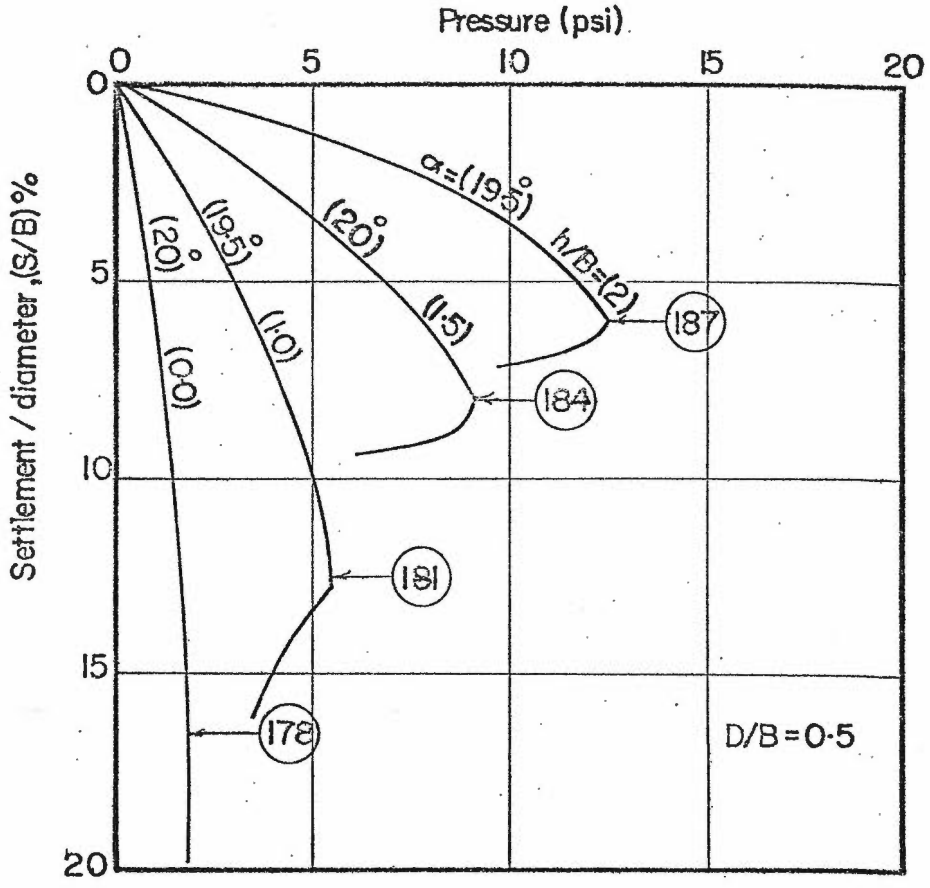

FIGURE 4-12 LOAD SETTLEMENT CURVES - BURIED CIRCULAR FOOTING IN DENSE SAND OVERLYING LOOSE SAND - UNDER INCLINED LOADS (GROUP K)

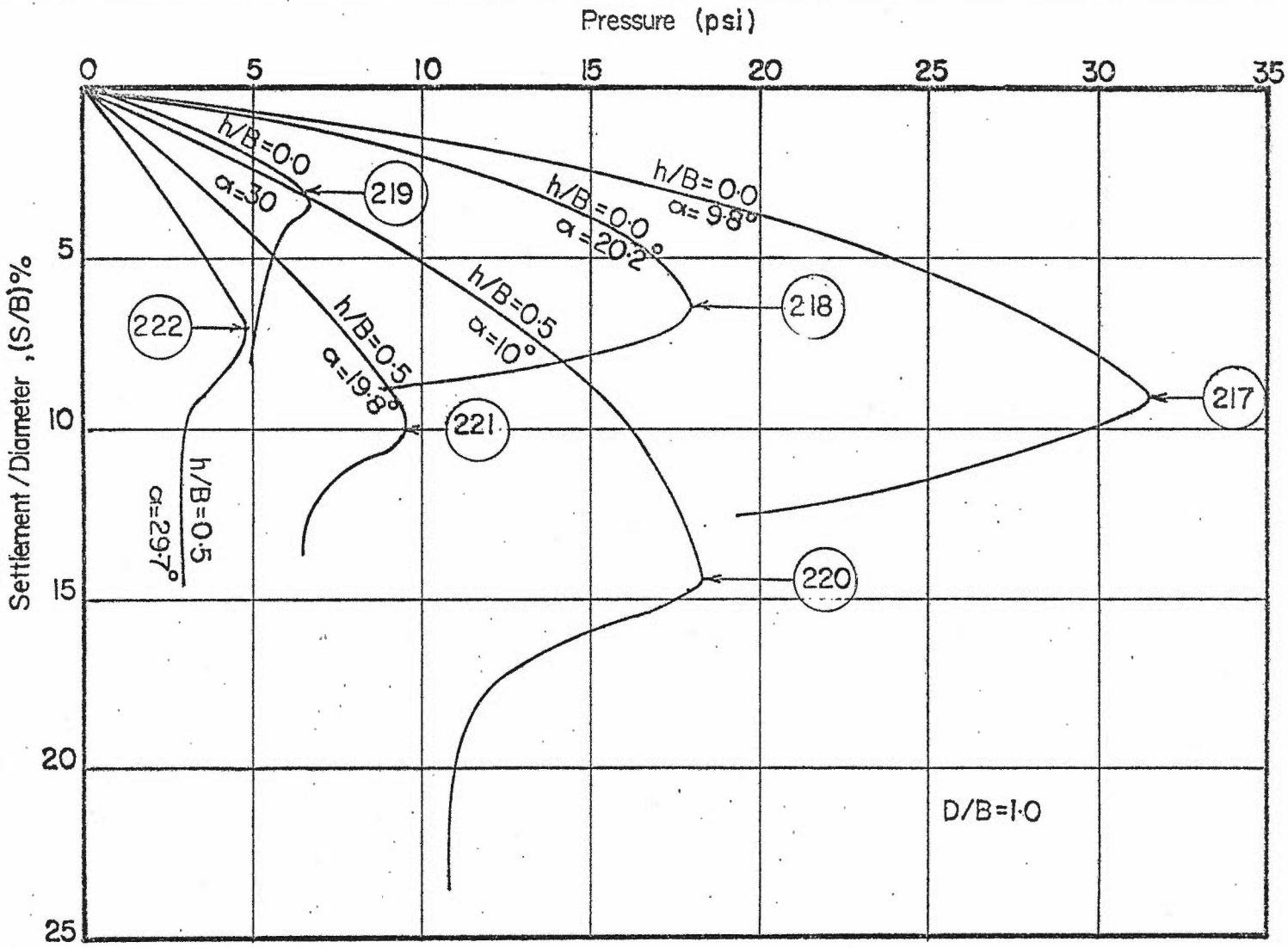

FIGURE 4·13 LOAD-SETTLEMENT CURVES - BURIED STRIP FOOTING IN LOOSE SAND OVERLYING DENSE SAND UNDER INCLINED LOADS (GROUP L)

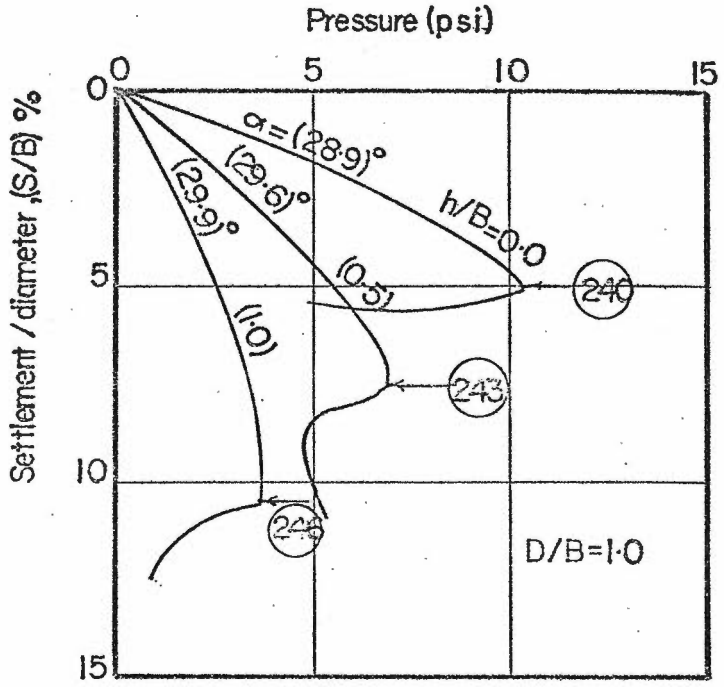

FIGURE 4·14 LOAD SETTLEMENT CURVES - BURIED CIRCULAR FOOTING IN LOOSE SAND OVERLYING DENSE SAND - UNDER INCLINED LOADS (GROUP M)

CHAPTER 5

ANALYSIS AND DISCUSSION OF TEST RESULTS ON A STRONG LAYER OVERLYING A WEAK LAYER

5.1 General

A number of theories, each based on different simplifying assumptions, have been developed for predicting the ultimate bearing capacity of shallow foundations under vertical loads and resting in stratified soils having a strong layer overlying a weak layer. A review of these methods is given in Chapter 2. However, prior to this study, no research had been reported on the problem of similar foundations subjected to inclined loads. This may be due to the large number of unknowns and to the mathematical complexities involved in the problem. Also, any theory for inclined loads should be applicable for vertical loads (i.e. when the inclination angle, α, is equal to zero). In view of the inherent complexities, this problem can only be solved by approximate methods based on certain simplifying assumptions.

Results from tests on homogeneous dense, compact, loose sands and clay are verified in this chapter according to established theories. These results were used in the analyses of the test results on the layered systems. They also served as a check of the performance of the apparatus and techniques used, and to give an evaluation on the behavior of the material used in these experiments. It is of interest to note that the test results for surface and buried circular footings on homogeneous dense and loose sands under inclined loads showed a

behavior which was not similar to those under vertical load. Thus, the foundation designer can no longer use the classic shape factors for circular footings under inclined loads.

In this chapter an analysis, based on observations of the upper layer deformation in the strip footing tests and on certain simplifying assumptions is presented for the cases of footings on dense sand over loose sand, dense sand over compact sand and dense sand over clay. Using the results of these analyses, in addition to the test results of previous researchers, a rational solution was developed for the ultimate bearing capacity of footings in a two-layered soil consisting of a strong layer overlying a weak layer under axial vertical or inclined loads.

Due to the restriction to one footing width or diameter (2 inches) in this investigation, it is admitted that the test results could not be precisely quantified, even though the influence of the different parameters on the footing behaviour was qualitatively established.

5.2 Footing Tests on Homogeneous Soils Under Vertical Loads

The test results of this group are summarized in Table 4.2, and presented in graphical form in Figure 5.1. It was found that the ultimate bearing capacity increased linearly with depth (D) for shallow depths. Equation 5.1 was used to evaluate the bearing capacity factors, N_γ and N_q, for strip footing tests, after adding the footing settlement at failure to the initial buried depth (D)

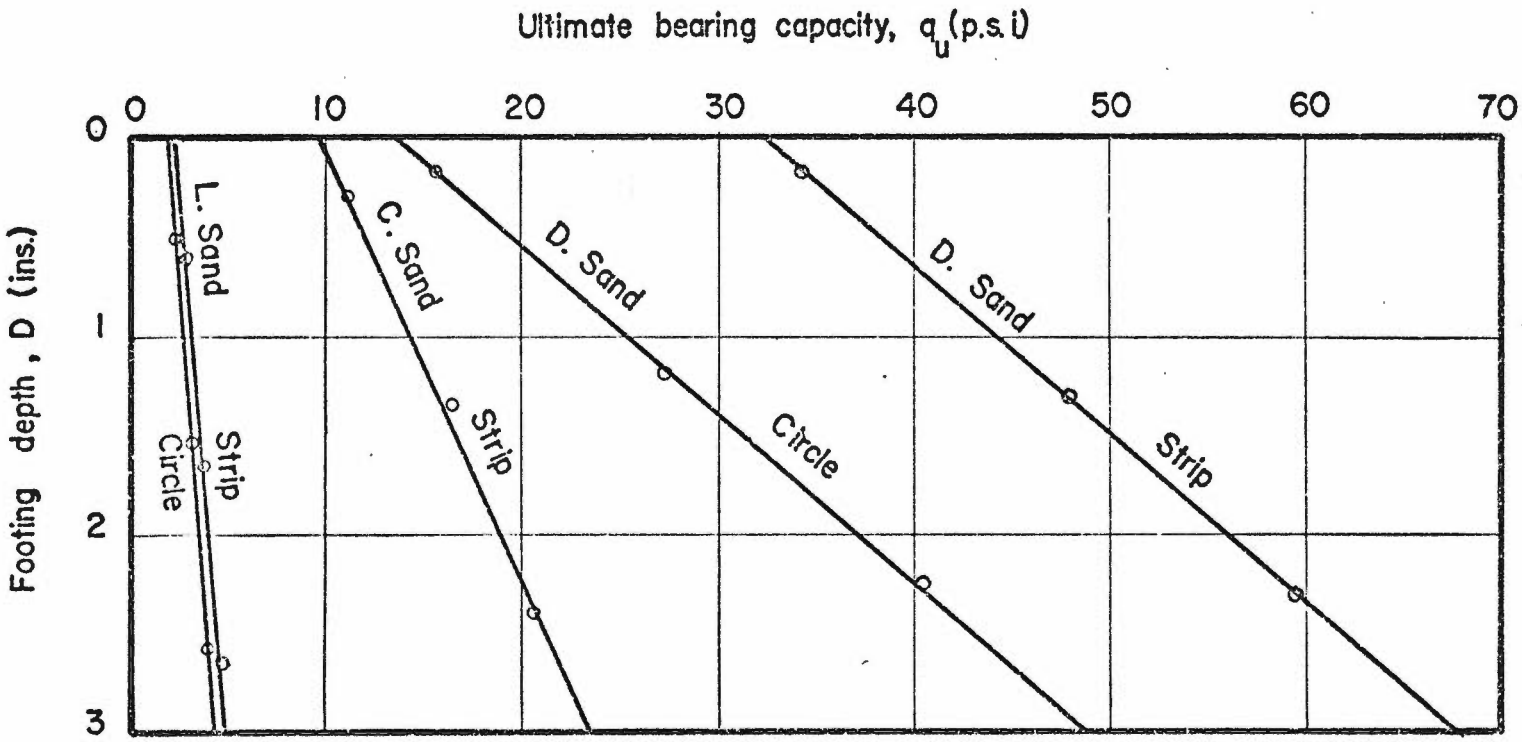

FIGURE 5·1 ULTIMATE BEARING CAPACITY VERSUS BURIED DEPTH HOMOGENEOUS SAND

$$q_u = \tfrac{1}{2} \gamma B N_\gamma + \gamma D N_q \qquad (5.1)$$

Tests No. (1), (2) and (3) on a strip footing on dense sand yielded bearing capacity factors of $N_\gamma = 535$ and $N_q = 199$. The corresponding angles of internal friction were $\phi_\gamma = 48.0^\circ$ and $\phi_q = 47.4^\circ$, respectively (Meyerhof, 1955), and an average value of $\phi = 47.7^\circ$ was used as the effective plane strain value. Tests No. (7), (8) and (9) on a strip footing on loose sand yielded bearing capacity factors of $N_\gamma = 41.5$ and $N_q = 16.0$. The corresponding angles of internal friction were $\phi_\gamma = 35.5^\circ$ and $\phi_q = 30.0^\circ$ or a weighted average value of 34.0°. It was remarkable that ϕ_q was less than ϕ_γ obtained from Meyerhof's curves. This difference was possibly due to the compressibility effect in the case of local shear failure. Tests No. (13), (14) and (15) on a strip footing on compact sand yielded average bearing capacity factors of $N_\gamma = 176.0$ and $N_q = 83.0$. The corresponding angles of internal friction were $\phi_\gamma = 42.8^\circ$ and $\phi_q = 42.0^\circ$ respectively (Meyerhof, 1955). An average value of $\phi = 42.4^\circ$ was used as the effective plane strain value. These values are summarized and compared with the values measured from direct shear tests (Bazan, 1976) and triaxial tests (Sastry, 1976) under a normal stress equal to one-tenth of the ultimate bearing capacity (Meyerhof, 1948) in Table 5.1. The difference in ϕ values for strip footing tests on dense sand was attributed to the plane strain effect, which leads to increased angles of shearing resistance, particularly in dense sand (Cornforth, 1964).

At the surface of homogeneous clay

$$q_u = C_u N_c \qquad (5.2)$$

Table 5.1

Comparison Between the Deduced and Experimental

Angle of Internal Friction

State	Deduced Angle of Internal Friction			Experimental Angle of Internal Friction	
	ϕ_γ (degrees)	ϕ_q (degrees)	Average (degrees)	Shear Box (degrees)	Triaxial (degrees)
Dense	48.0	47.4	47.7	48.5	46.0
Compact	42.8	42.0	42.4	--	42.5
Loose	35.5	30.0	34.0	--	34.0

which was used to evaluate the bearing capacity factor, N_c, for a surface strip footing. Test No. 16 yielded a bearing capacity factor, N_c, for a surface strip footing on homogeneous clay of 5.33. When compared with the theoretical value of 5.14, it was found to be 1.04 times greater (C_u = 2.77 psi).

It has been well established that the bearing capacity factor N_q in the case of deep foundations is greater than for shallow foundations (Terzaghi, 1943). The reason for this has been attributed to the depth effect, or to the effect of the shear strength of the soil above the footing level. However, for shallow foundations, the assumption of constant N_q values, which has its implication for engineering practice, is reasonable and confirmed by the test results of the present investigation (Figure 5.1).

Tests No. (4), (5) and (6) on a circular footing on dense sand yielded an average bearing capacity factor of $s_\gamma N_\gamma = 224$. The corresponding shape factor s_γ was found to be equal to 0.42 (less than the customary 0.6); this was probably due to the higher value of the angle of internal friction, ϕ, for this type of sand (Meyerhof, 1950; Bazan, 1976). Also, for $s_q N_q = 198$, the corresponding shape factor, s_q, was found to be equal to unity, (less than 1.7, according to De Beer, 1970). Tests No. (10), (11) and (12) on a circular footing on loose sand yielded average bearing capacity factors of $s_\gamma N_\gamma = 34.05$ and $s_q N_q = 16.0$. The corresponding shape factors were $s_\gamma = 0.82$ and $s_q = 1.0$.

This behavior of the dense, compact, and loose sands and

clay was sufficiently predictable to justify using the strength measured from footing tests in homogeneous soils as reference values in the layered foundations tests.

5.3 Footing Tests on Homogeneous Soils Under Inclined Loads

The test results of this group are summarized in Table 4.10 and presented in graphical form in Figures 5.2 to 5.6. As indicated by Meyerhof (1953), the ultimate bearing capacity of the footings decreases rapidly with increasing loading inclination angle, α.

For sand $$q_v = 0.5\ \gamma B\ N_{\gamma q} \qquad (5.3)$$

and for clay $$q_v = C_u\ N_{cq} \qquad (5.4)$$

Where: q_v is the vertical component of the ultimate bearing capacity,

i.e. $q_v = q_u \cos \alpha$,

α is the load inclination with the vertical,

and C_u is the undrained shear strength of the clay.

Equations 5.3 and 5.4 were used to determine the bearing capacity factors, $N_{\gamma q}$ and N_{cq}, for homogeneous sand and clay, respectively, for strip footing tests. The results are given in Tables 5.2 and 5.3.

In order to compare the experimental bearing capacity factors to the theoretical values proposed by Meyerhof (1953) and Brinch Hansen (1961), it was decided to superimpose them on the theoretical curves in Figures 5.7 and 5.8. These figures indicated that Meyerhof's theory (1953) gives a closer agreement with experimental results as compared to Brinch Hansen's theory (1961), except in the case of loose sand at D/B equal to 1.0 where the degree of compressibility of the material

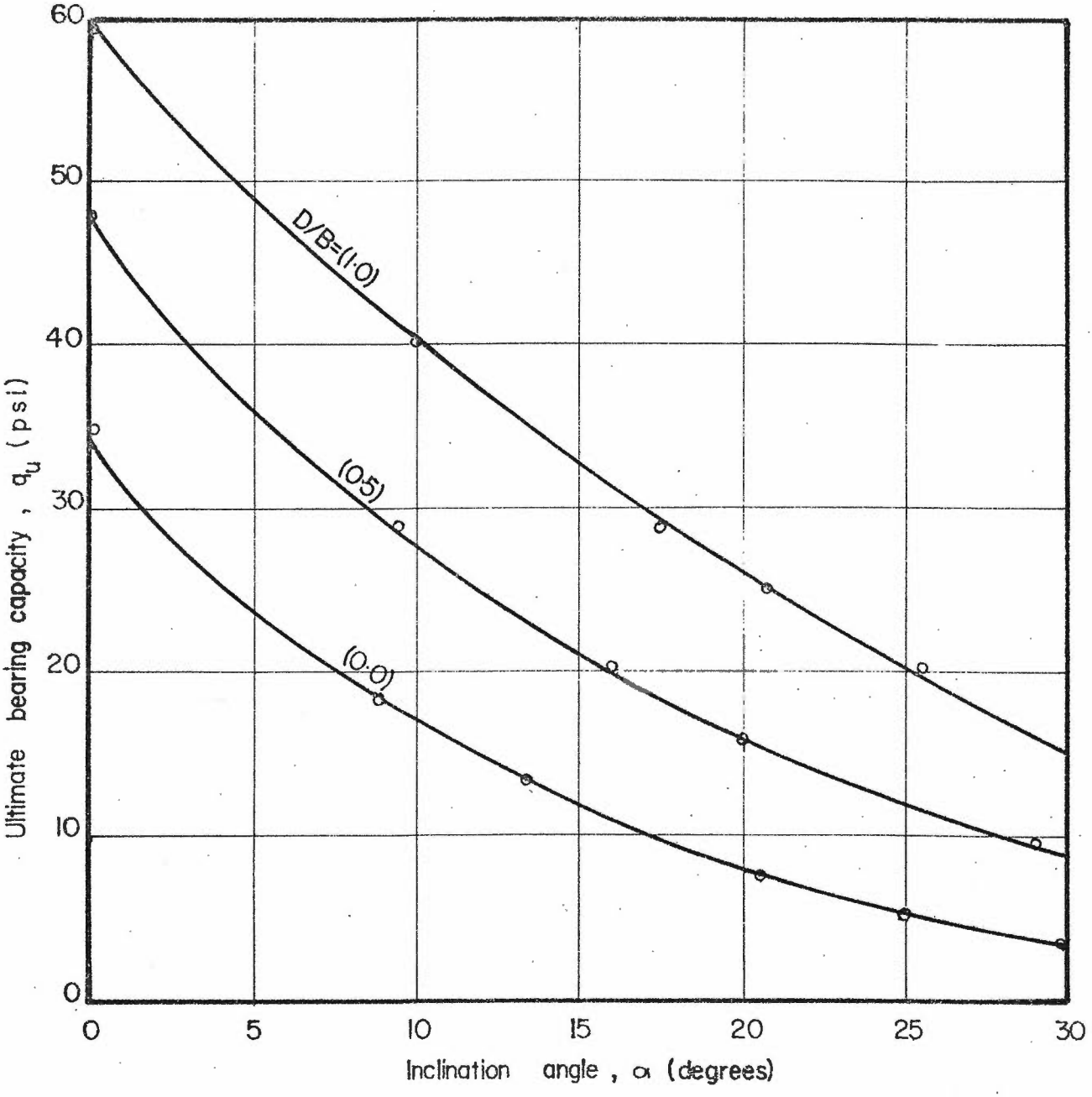

FIGURE 5·2 SUMMARY OF TEST RESULTS - STRIP FOOTING IN HOMOGENEOUS DENSE SAND

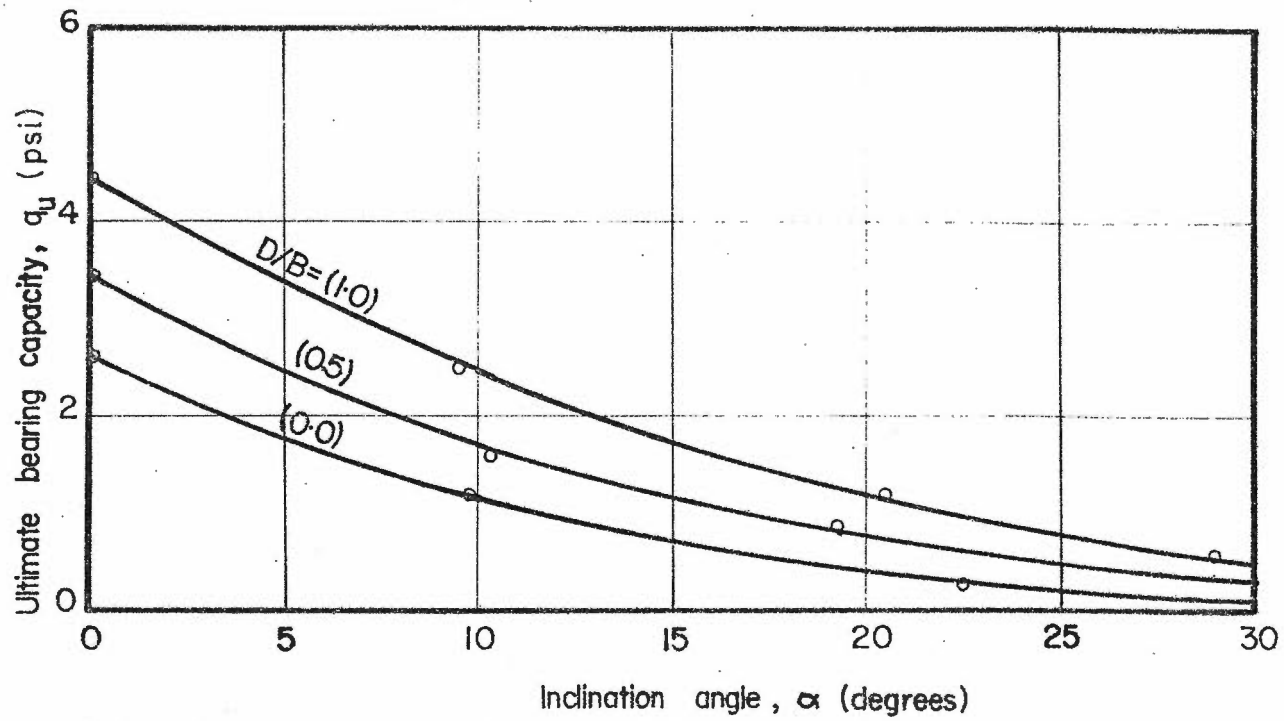

(a) Ultimate bearing capacity versus inclination angle

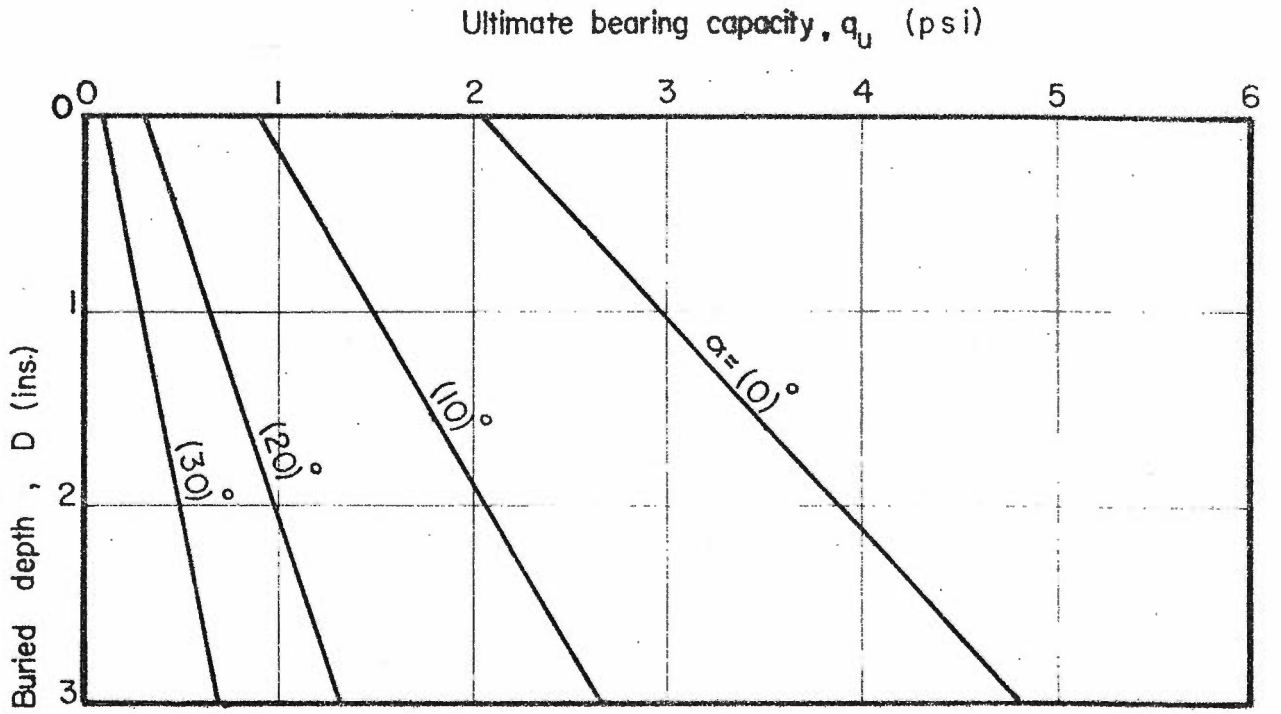

(b) Ultimate bearing capacity versus buried depth

FIGURE 5.3 SUMMARY OF TEST RESULTS - STRIP FOOTING IN HOMOGENEOUS LOOSE SAND

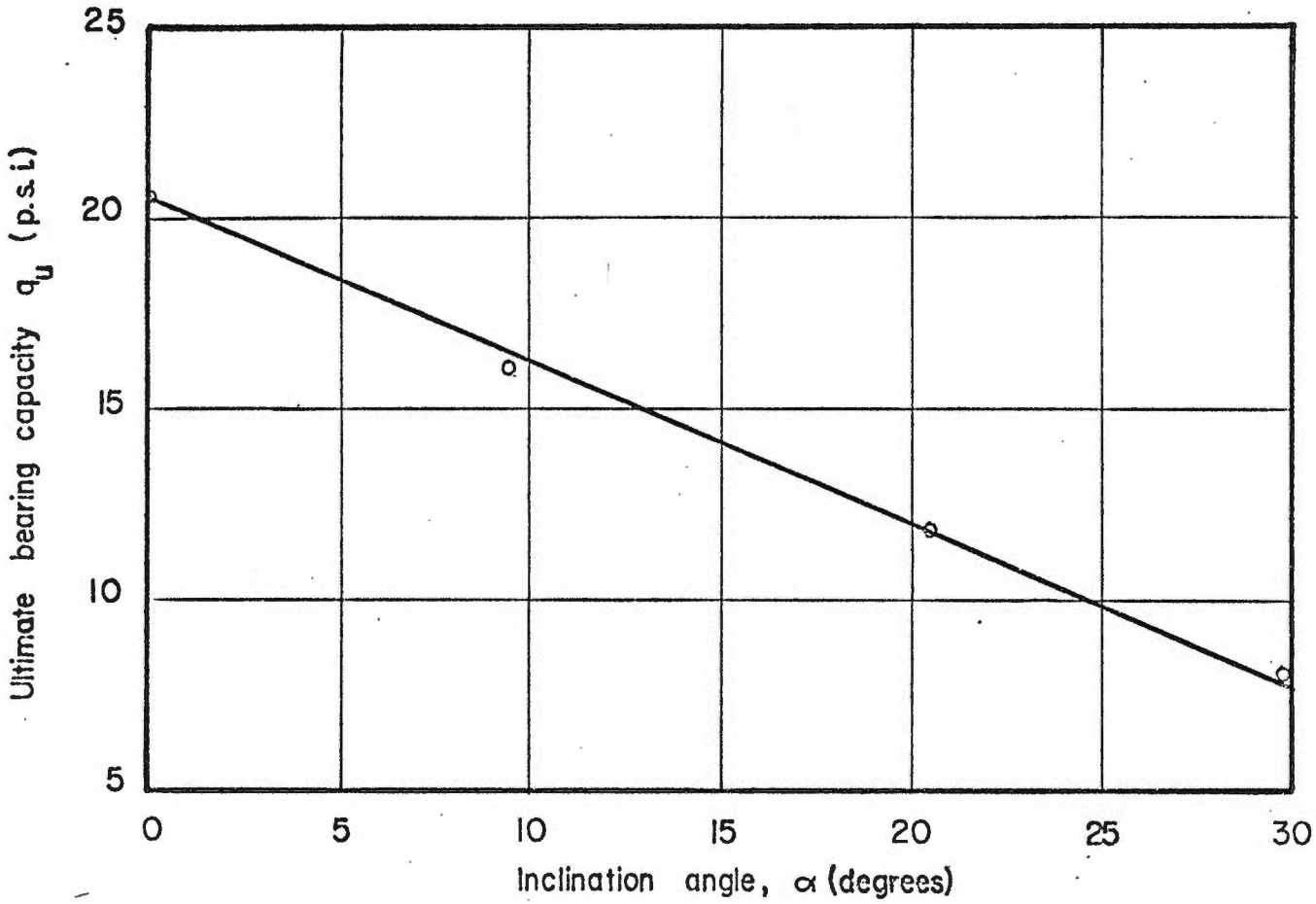

FIGURE 5·4 ULTIMATE BEARING CAPACITY VERSUS INCLINATION ANGLE — SURFACE STRIP FOOTING ON HOMOGENEOUS CLAY

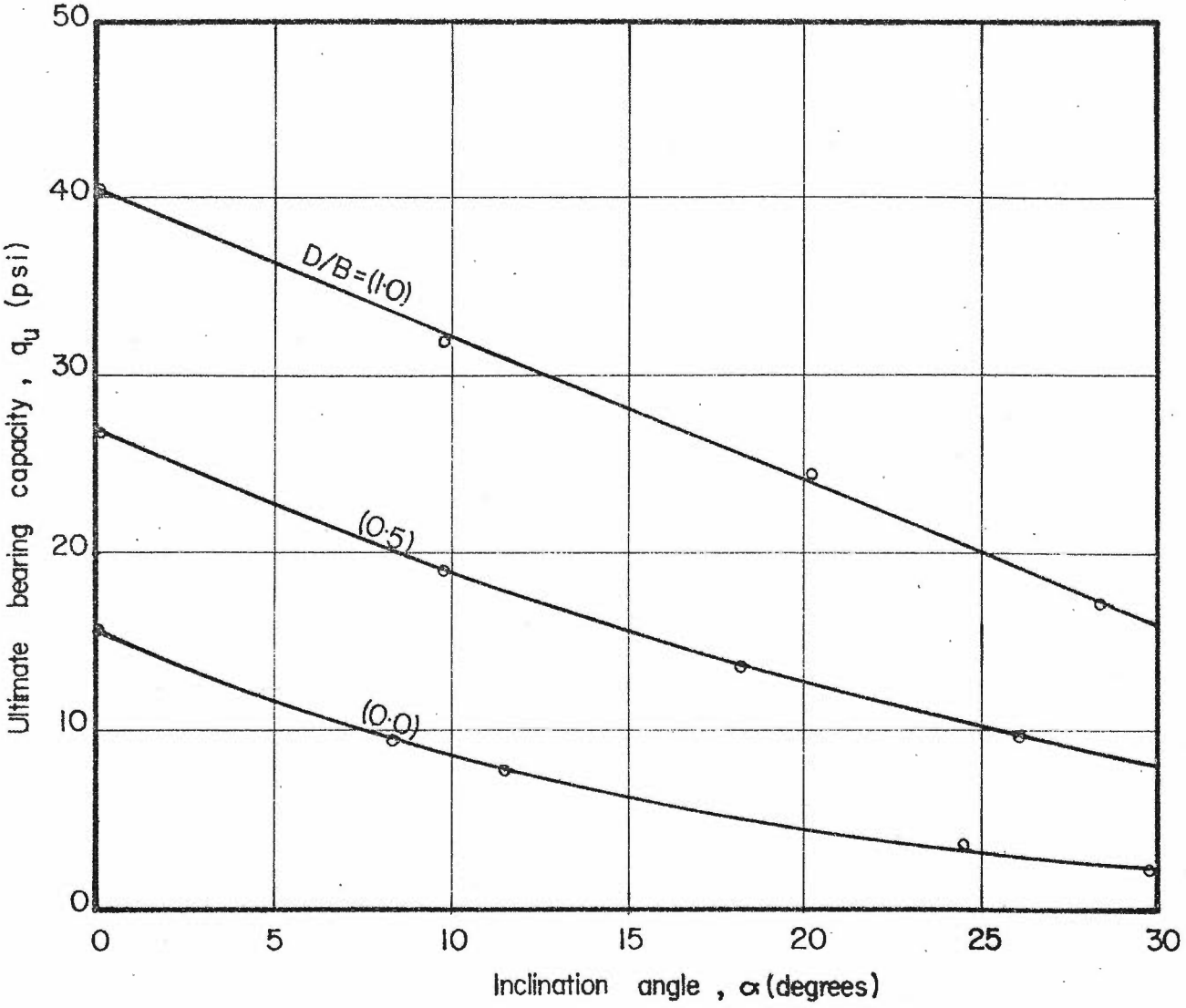

FIGURE 5·5 SUMMARY OF TEST RESULTS - CIRCULAR FOOTING IN HOMOGENEOUS DENSE SAND

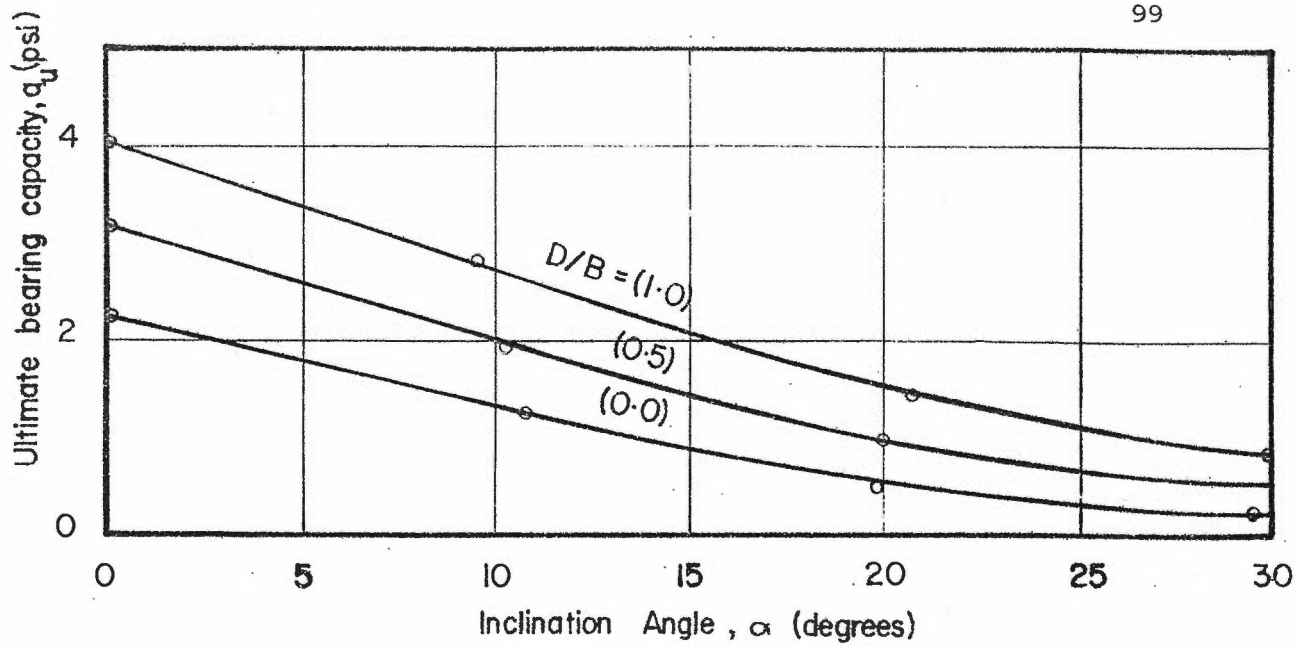

(a) ULTIMATE BEARING CAPACITY VERSUS INCLINATION ANGLE

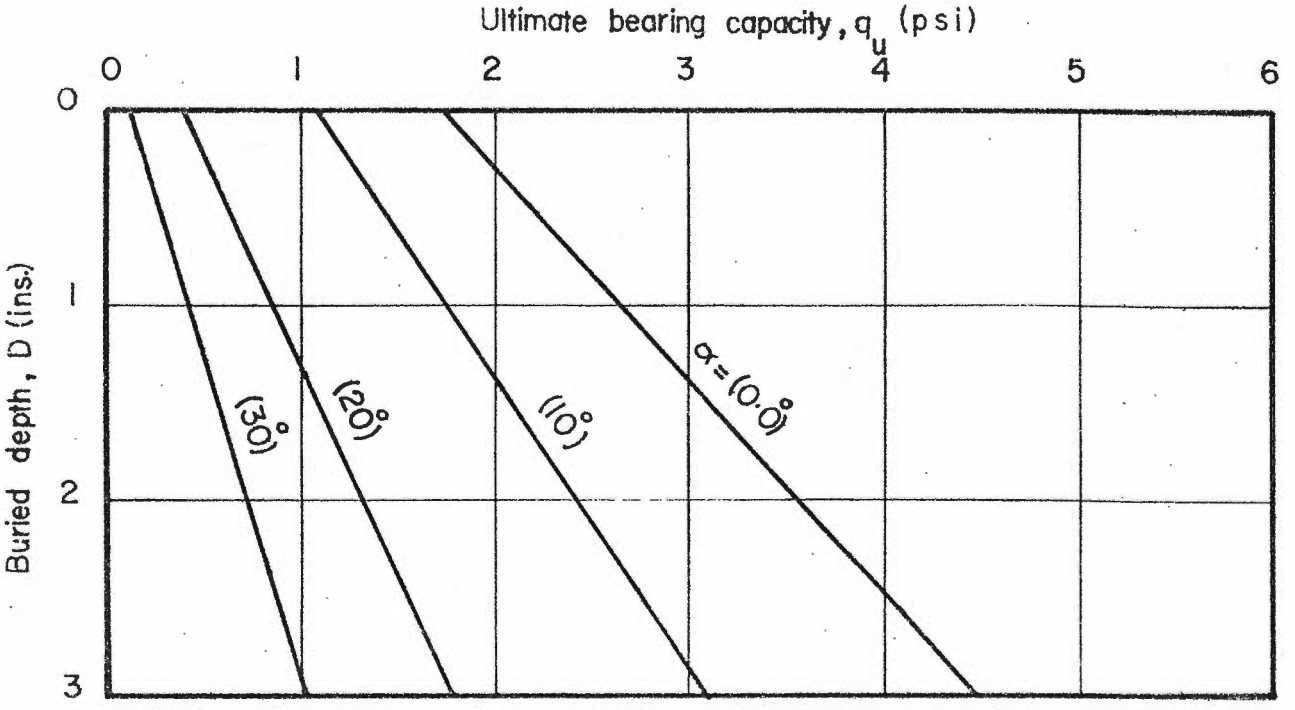

(b) ULTIMATE BEARING CAPACITY VERSUS BURIED DEPTH

FIGURE 5·6 SUMMARY OF TEST RESULTS - CIRCULAR FOOTING IN HOMOGENEOUS LOOSE SAND

Table 5.2

Bearing Capacity Factor - $N_{\gamma q}$

From Surface and Buried Strip Footing Tests In

Homogeneous Sand

Average α (degrees)	D/B	Dense Sand		Loose Sand	
		q_u (psi)	$N_{\gamma q}$	q_u (psi)	$N_{\gamma q}$
0	0.0	34.32	570	2.60	51.17
10	0.0	17.20	281	1.18	22.87
20	0.0	8.00	125	0.40	7.40
30	0.0	3.20	46	0.10	1.70
0	1.0	59.59	990	4.47	87.97
10	1.0	40.50	663	2.50	48.45
20	1.0	26.00	406	1.20	22.19
30	1.0	15.30	220	0.51	8.69

Table 5.3

Bearing Capacity Factor - N_{cq}

From Surface Strip Footing Tests on Homogeneous Clay*

Average α (degrees)	Ultimate Load q_u (psi)	Bearing Capacity Factor N_{cq}
0	20.55	5.33
10	16.25	4.15
20	12.00	2.92
30	7.75	1.74

* In this Table the ultimate bearing capacities (q_u) have been read from Figure 5.4, where the test points (Table 4.10.c) were plotted after correcting the ultimate loads for an undrained shear strength of 3.86 p.s.i.

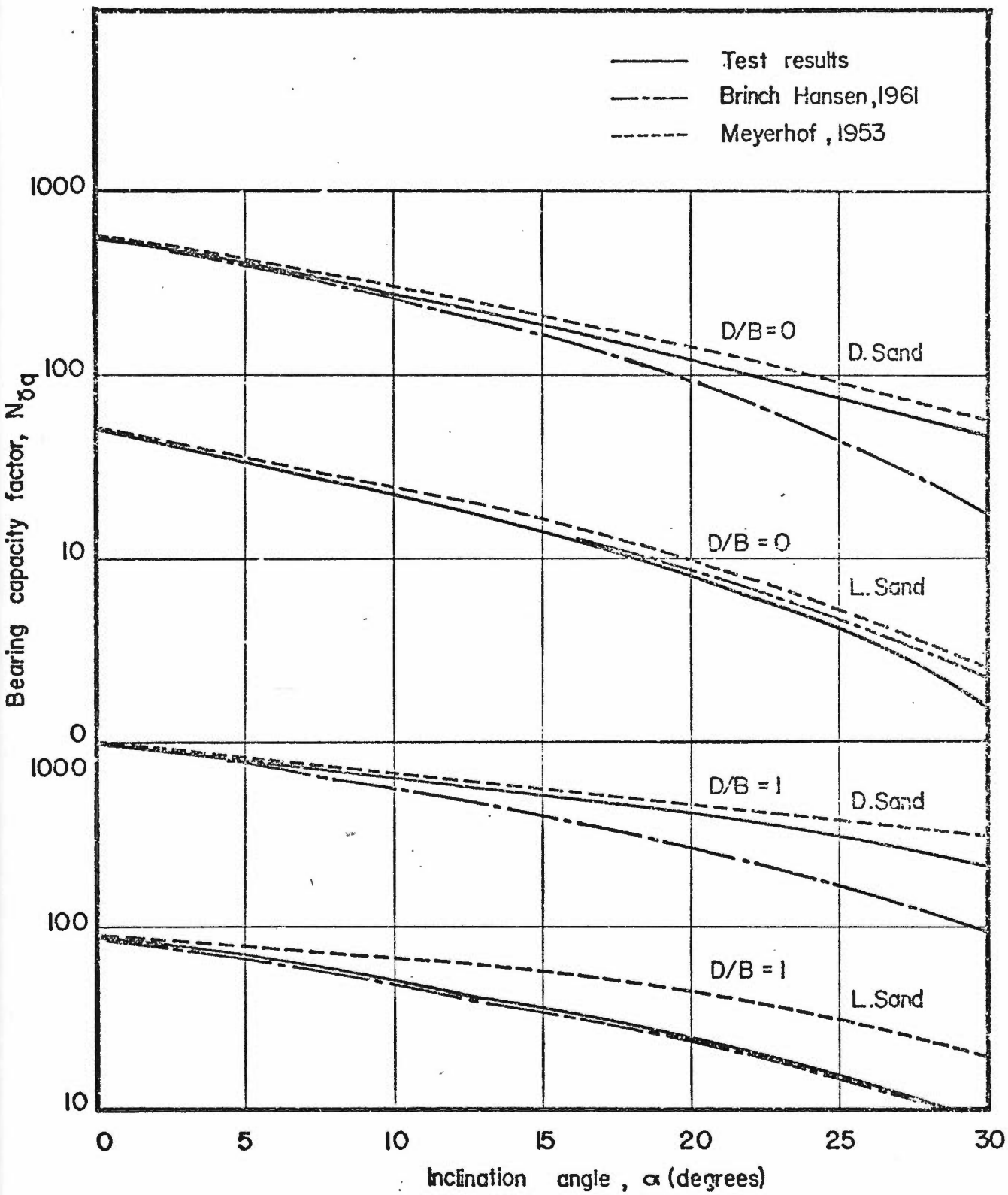

FIGURE 5·7 COMPARISON BETWEEN EXPERIMENTAL AND THEORETICAL VALUES OF $N_{\delta q}$

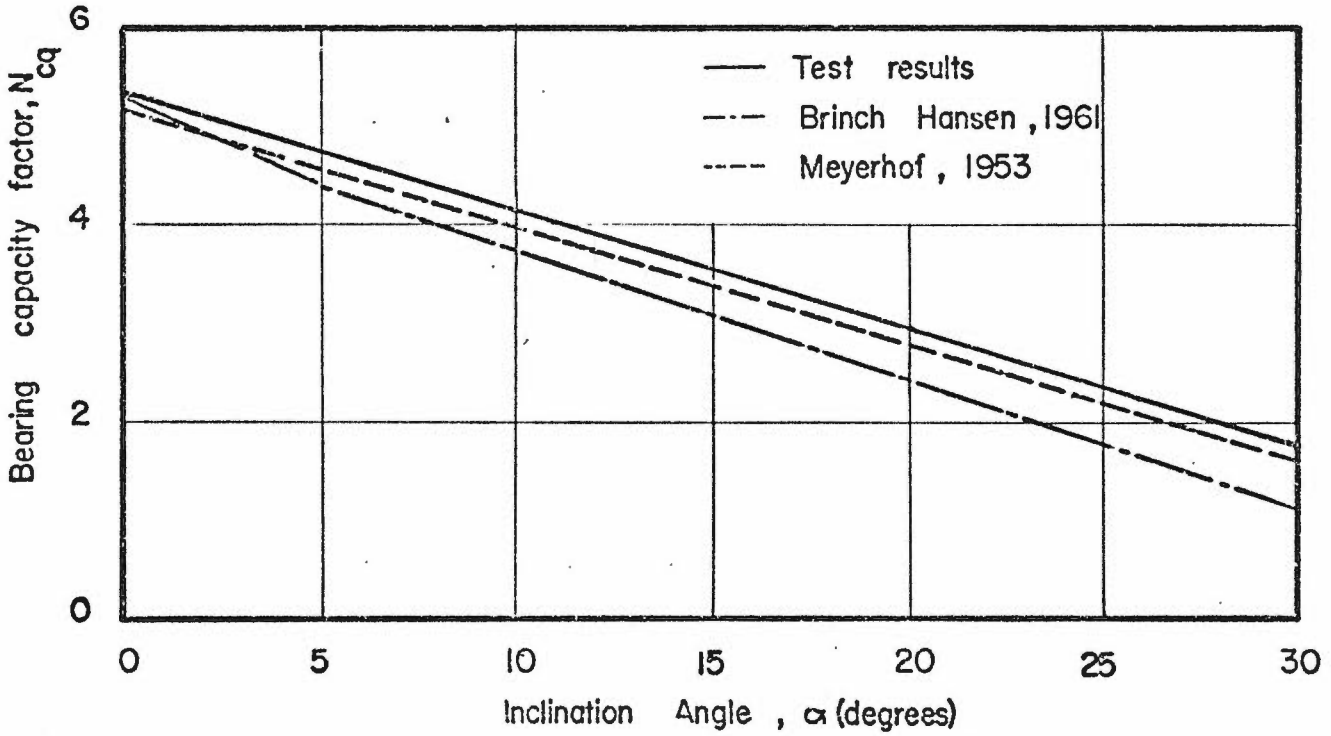

FIGURE 5·8· COMPARISON BETWEEN EXPERIMENTAL AND THEORETICAL VALUES OF N_{cq}

becomes of increasing importance, and it is not yet possible to estimate precisely the change in the ϕ value due to this compressibility.

As shown in Figures 5.5 and 5.6, the behavior of circular footings under inclined loads differs from that of strip footings. This is possibly due to higher passive pressures mobilized in circular footings as compared to strip footings. The ultimate bearing capacity of a circular footing is conventionally represented as a ratio of the ultimate bearing capacity of a strip footing under the same conditions. This ratio is called the shape factor. The test results of strip and circular footings in homogeneous dense or loose sands under inclined loads were analyzed to determine the shape factor. The following equations were used:

$$q_u = 0.5\ \gamma B\ S_\gamma\ N_\gamma + \gamma D\ S_q\ N_q \qquad (5.5)$$

$$q_v = 0.5\ \gamma B\ S_{\gamma q}\ N_{\gamma q} \qquad (5.6)$$

To employ equation (5.5), the ultimate bearing capacity from the test results of strip and circular footings in dense and loose sands were replotted against the buried depth after adding the settlement at failure to it, (Figure 5.3.b and 5.6.b for strip and circular footings, respectively, in loose sand). From these figures the average bearing capacity factors, N_γ, N_q and $S_\gamma\ N_\gamma$, $S_q\ N_q$ were computed for inclination angles of 0, 10, 20 and 30 degrees (Table 5.4). These values were used in the analysis of the layered system. For footings under vertical loads ($\alpha = 0^o$), these bearing capacity factors are the same as those given by Meyerhof (1955). As the inclination angle, α, increases,

Table 5.4.a

Bearing Capacity Factors - N_γ, N_q and $S_\gamma N_\gamma$, $S_q N_q$

From Footing Tests in Homogeneous Dense Sand

α Degrees	Strip Footing		Circular Footing		Shape Factors	
	N_γ	N_q	$S_\gamma N_\gamma$	$S_q N_q$	S_γ	S_q
0	535	199	224	198	0.42	1.00
10	258	179	116	174	0.45	0.98
20	125	135	61	141	0.49	1.05
30	55	88	30	105	0.54	1.19

Table 5.4.b

Bearing Capacity Factors - N_γ, N_q and $S_\gamma N_\gamma$, $S_q N_q$

From Footing Tests in Homogeneous Loose Sand

α Degrees	Strip Footing		Circular Footing		Shape Factors	
	N_γ	N_q	$S_\gamma N_\gamma$	$S_q N_q$	S_γ	S_q
0	41.50	16.00	34.05	16.00	0.82	1.00
10	17.52	11.51	21.26	12.99	1.21	1.13
20	5.90	6.69	7.87	8.86	1.33	1.32
30	1.57	4.03	2.26	6.00	1.44	1.49

Table 5.5.a

Deduced Shape Factor - $S_{\gamma q}$

From Circular Footing Tests in Homogeneous Dense Sand

Average α (degrees)	D/B	q_u (psi) Circle	q_u (psi) Strip	Shape Factor $S_{\gamma q}$
0	0.0	15.66	34.32	0.45
10	0.0	8.65	17.25	0.50
20	0.0	4.50	8.10	0.55
30	0.0	2.15	3.60	0.59
0	0.5	27.10	47.77	0.56
10	0.5	18.75	28.00	0.67
20	0.5	13.00	15.75	0.82
30	0.5	8.50	9.00	0.94
0	1.0	40.42	59.59	0.67
10	1.0	31.70	40.50	0.78
20	1.0	24.50	26.00	0.94
30	1.0	15.90	15.30	1.03

Table 5.5.b

Deduced Shape Factor - $S_{\gamma q}$

From Circular Footing Tests in Homogeneous Loose Sand

Average α (degrees)	D/B	q_u (psi) Circle	q_u (psi) Strip	Shape Factor $S_{\gamma q}$
0	0.0	2.41	2.60	0.93
10	0.0	1.35	1.18	1.14
20	0.0	0.53	0.40	1.32
30	0.0	0.21	0.14	1.50
0	0.5	3.26	3.51	0.92
10	0.5	2.05	1.75	1.17
20	0.5	0.98	0.75	1.30
30	0.5	0.53	0.35	1.51
0	1.0	4.06	4.47	0.91
10	1.0	2.75	2.50	1.10
20	1.0	1.55	1.20	1.29
30	1.0	0.83	0.55	1.50

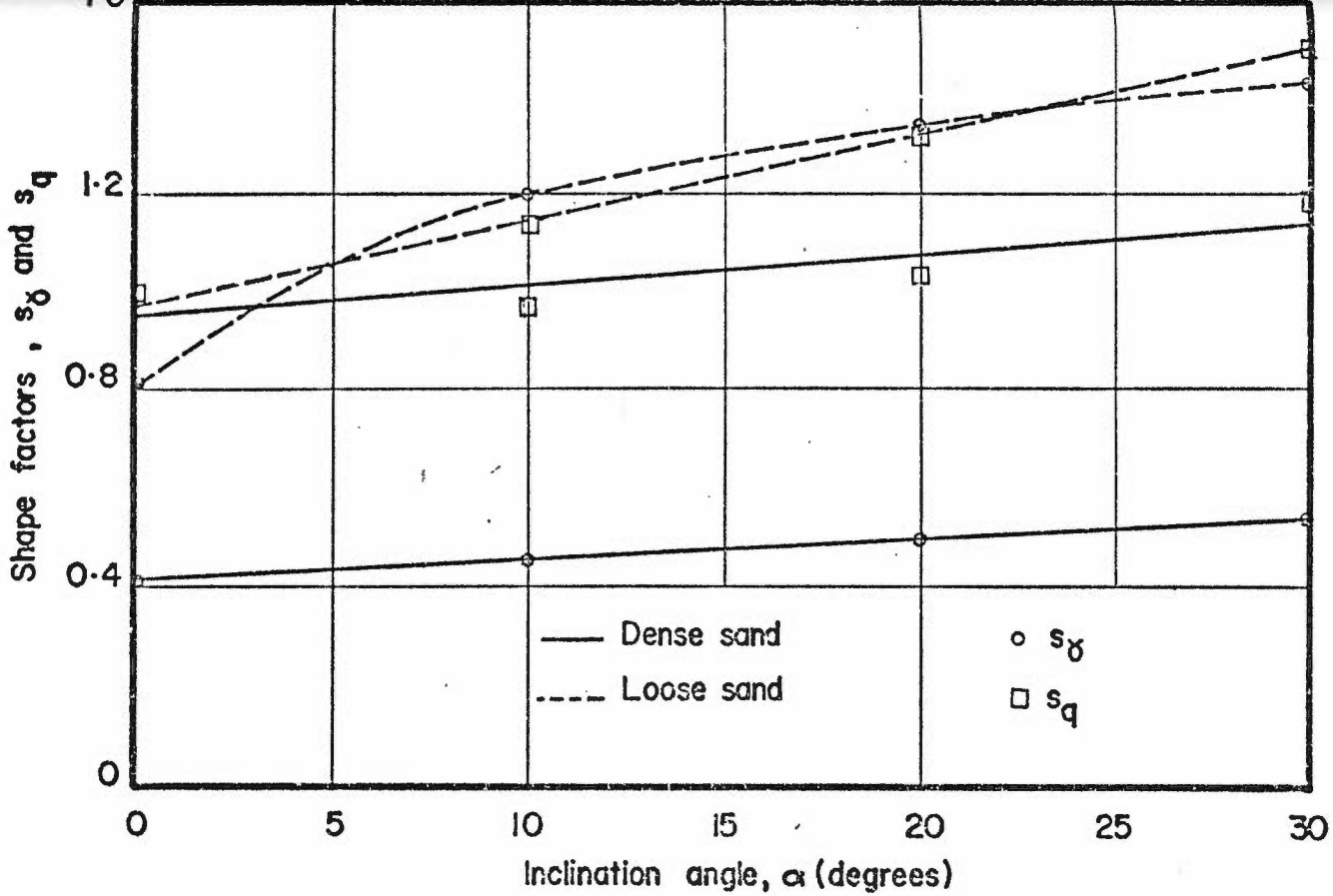

FIGURE 5·9·a EXPERIMENTAL SHAPE FACTORS , S_γ AND S_q

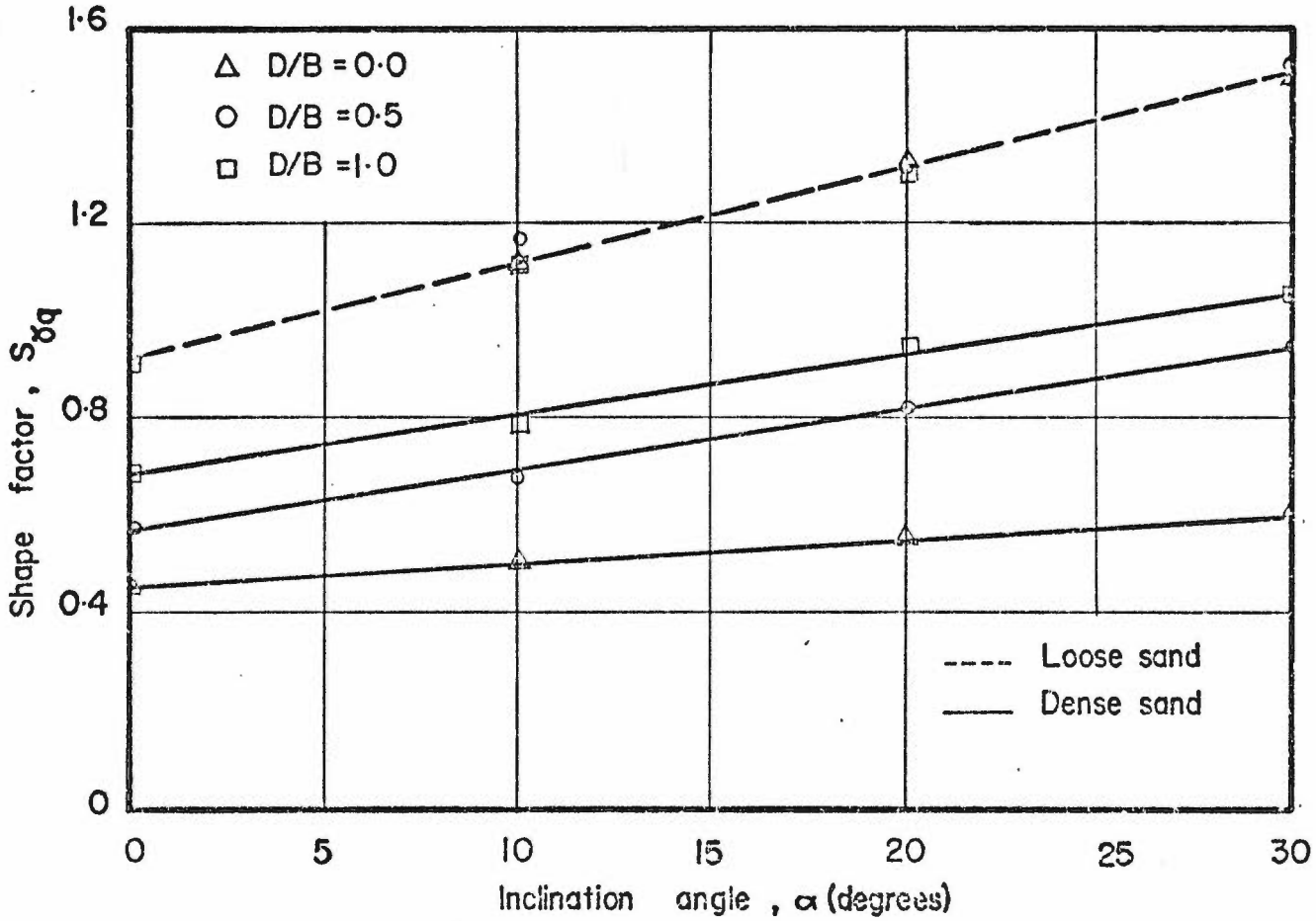

FIGURE 5·9·b EXPERIMENTAL SHAPE FACTOR , $S_{\sigma q}$

N_γ, N_q and $S_\gamma N_\gamma$, $S_q N_q$ decreased rapidly. The deduced shape factors S_γ and S_q are given in Tables 5.4.a and 5.4.b respectively for dense and loose sand and shown graphically in Figure 5.9.a. It should be noted that these values were computed in the load direction.

The deduced shape factors, $S_{\gamma q}$, from equation (5.6) are given in Table 5.5 and shown graphically in Figure 5.9.b. It can be seen that the shape factors, $S_{\gamma q}$, increased with the buried depth, D, and increased with an increase in the inclination angle, α. This can be explained by the fact that the mobilized passive pressure increased with horizontal movement of the footing, which in turn increased with increasing inclination angle, α, (Meyerhof, 1972). It should be noted that the ultimate bearing capacity at inclination angles of 10, 20 and 30 degrees were read from Figures 5.2, 5.3, 5.5, and 5.6; also the settlement at failure at these inclination angles were interpolated between the test points.

5.4 Footing Tests on Two-Layered Systems

The test results of these series are summarized in Tables 4.3 to 4.6 and 4.11 to 4.12 for vertical and inclined load tests, respectively, and they are presented in graphical form in this chapter. For vertical load tests, Figures 5.10 to 5.12 show the variation of the ultimate bearing capacity with the ratio of the initial upper layer thickness below the footing base to the footing width or diameter, h/B; for inclined load tests, Figures 5.13 to 5.18 show the variation of the ultimate bearing capacity with the average inclination angle, α, for different ratios of h/B. For convenience, Figures 5.19 to 5.24 are presented for comparing

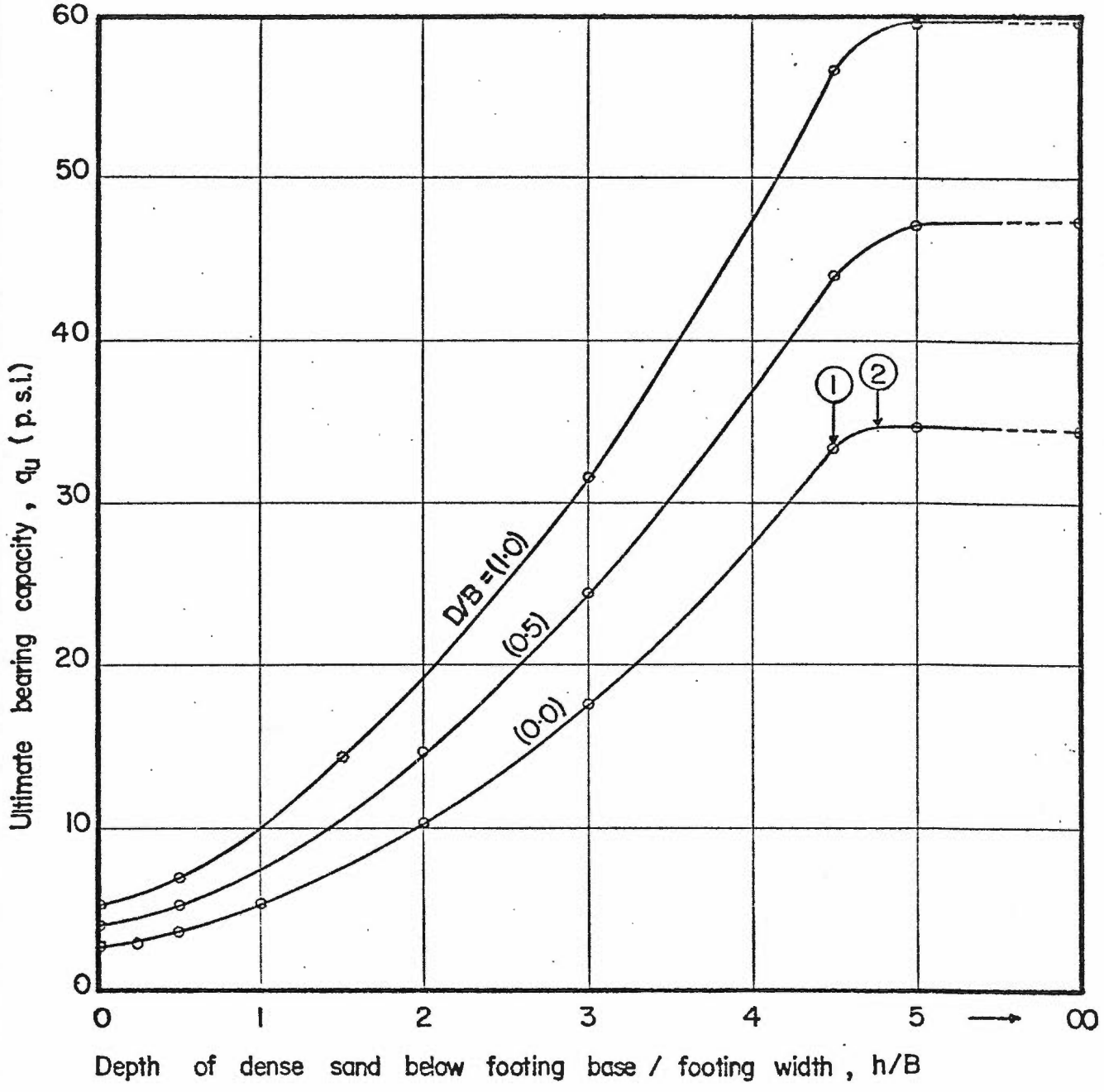

FIGURE 5·10 SUMMARY OF TEST RESULTS - STRIP FOOTING IN DENSE SAND OVERLYING LOOSE SAND ($\alpha = 0^{\circ}$)

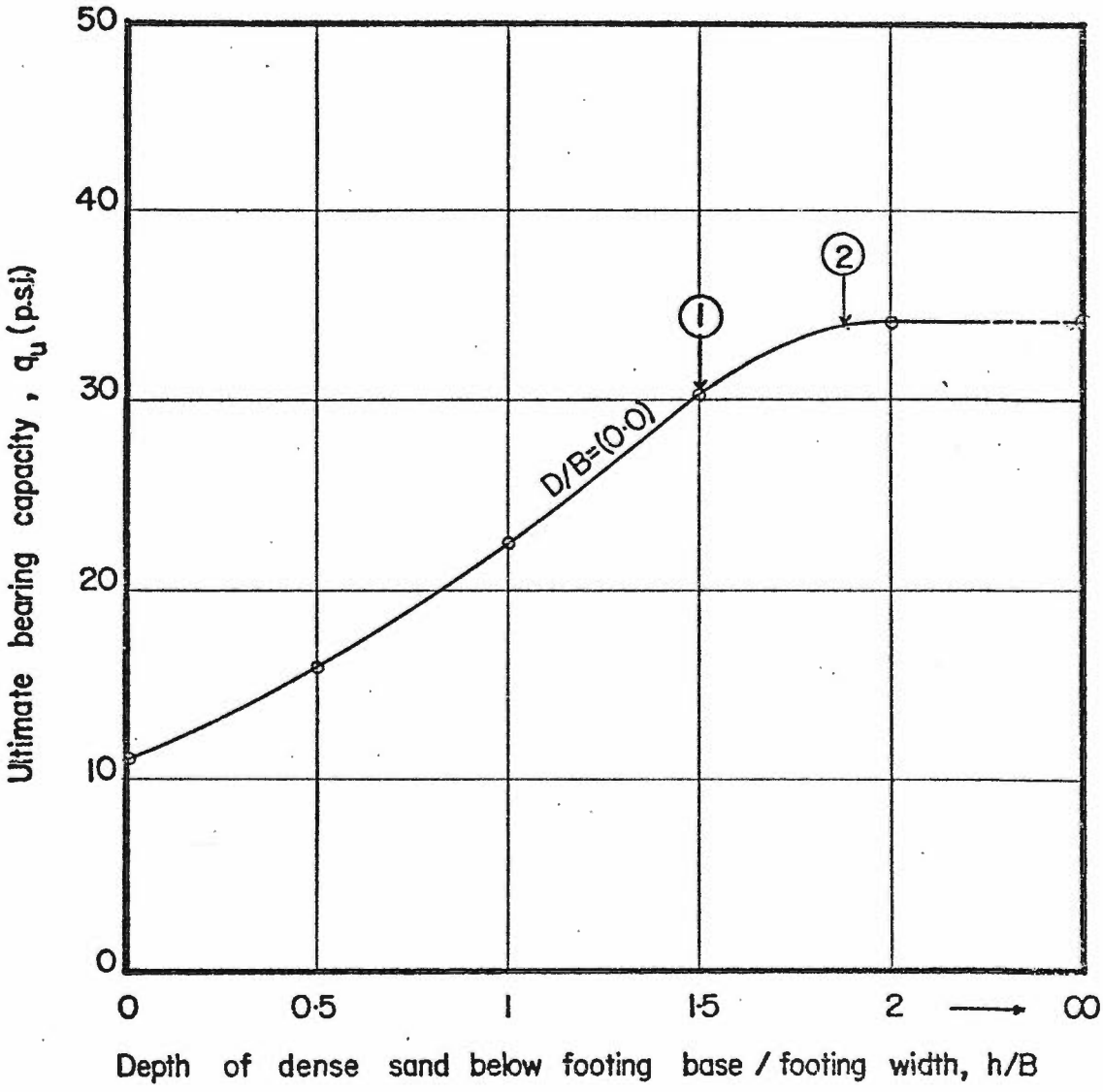

FIGURE 5·11 SUMMARY OF TEST RESULTS - STRIP FOOTING ON DENSE SAND OVERLYING COMPACT SAND ($\alpha = 0^{\circ}$)

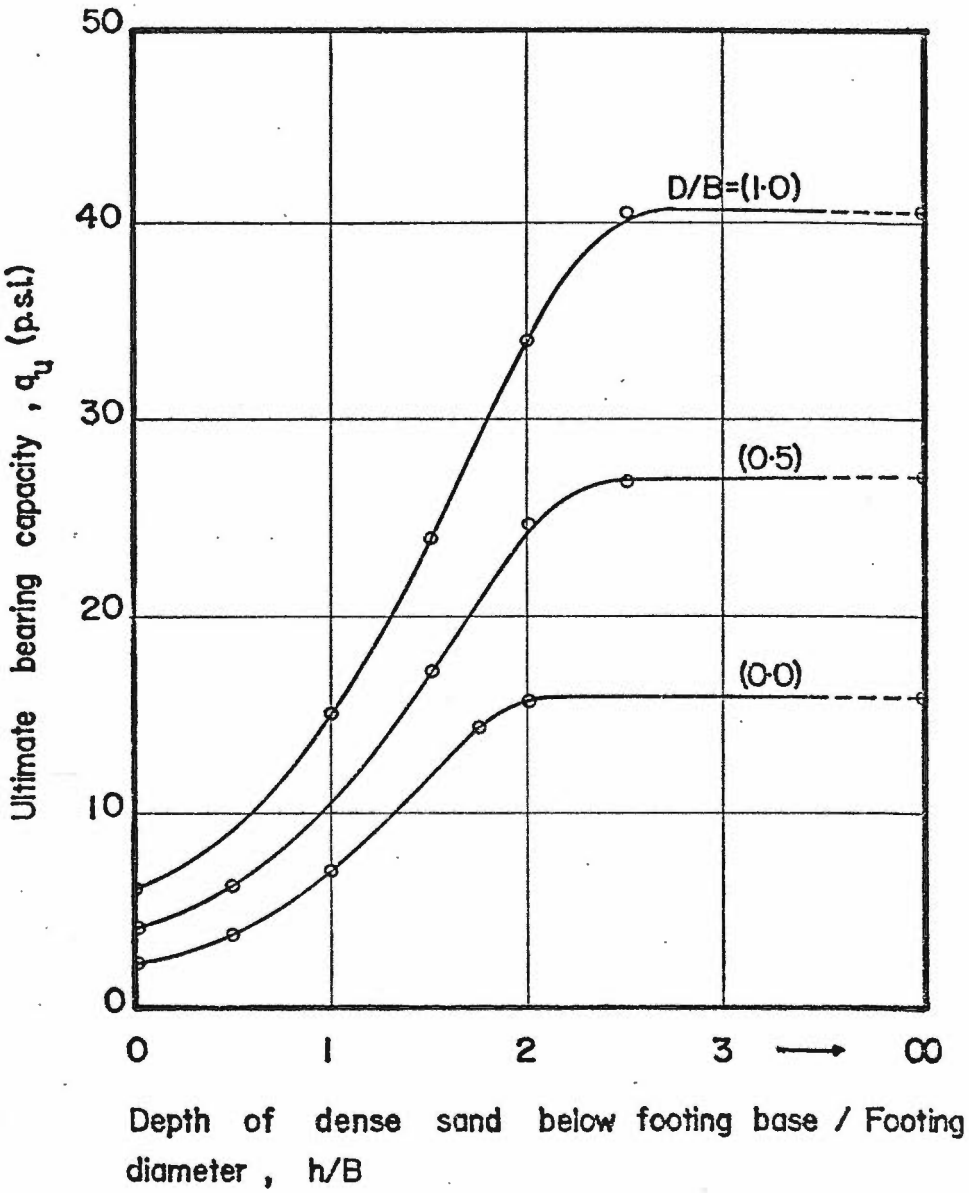

FIGURE 5·12 SUMMARY OF TEST RESULTS - CIRCULAR FOOTING IN DENSE SAND OVERLYING LOOSE SAND ($\alpha = 0^{\circ}$)

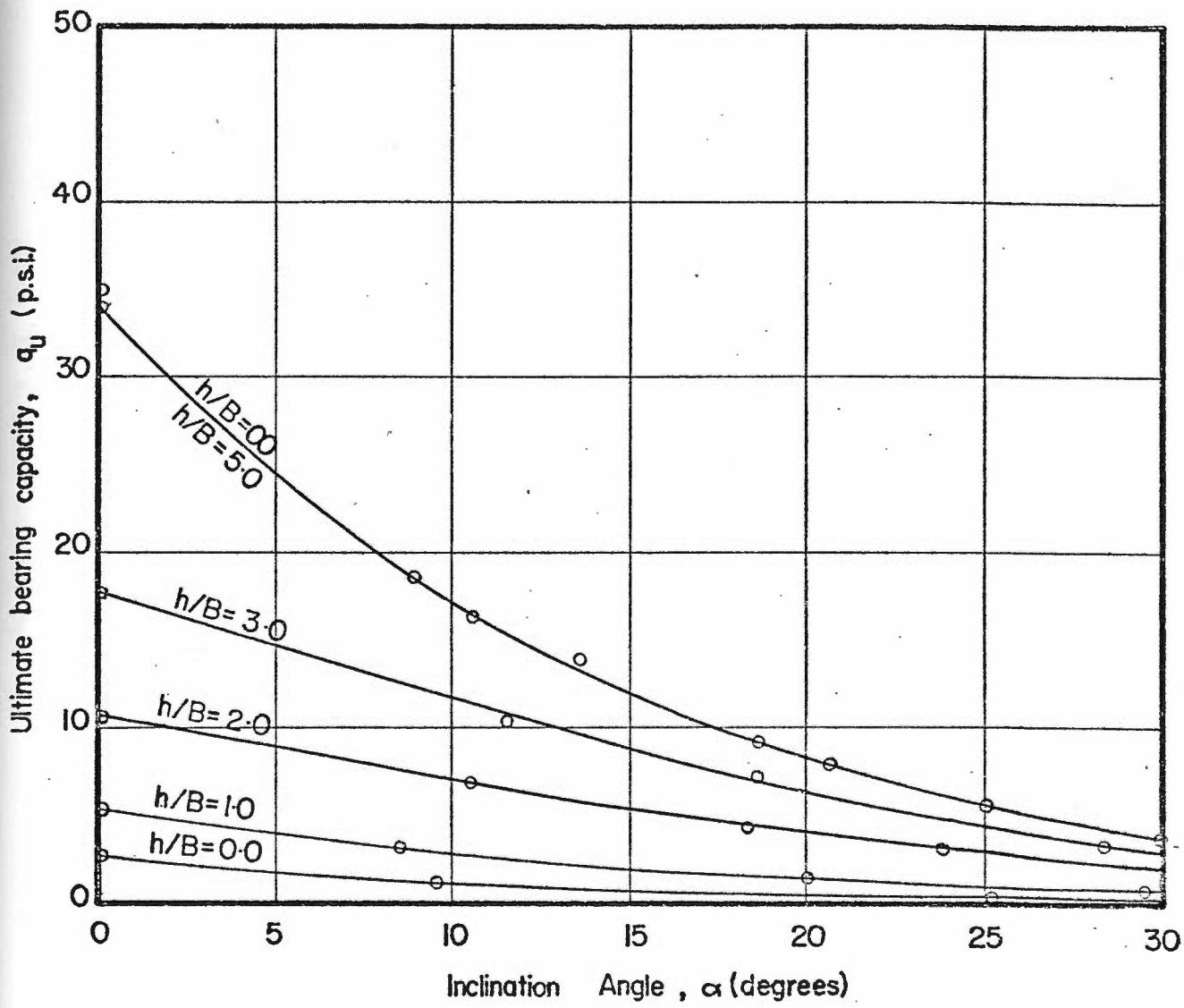

FIGURE 5.13 SUMMARY OF TEST RESULTS - SURFACE STRIP FOOTING ON DENSE SAND OVERLYING LOOSE SAND (D/B=0)

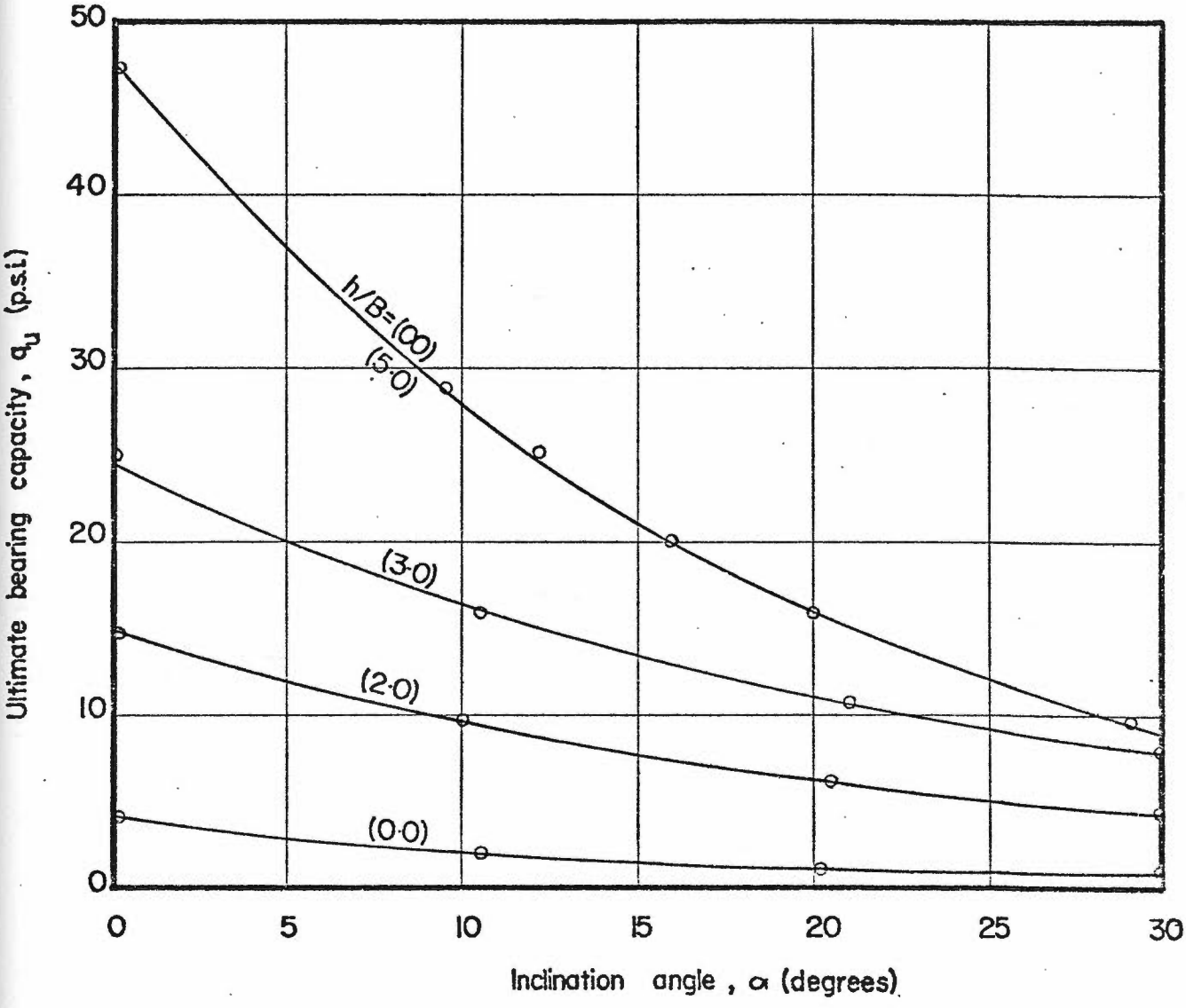

FIGURE 5·14 SUMMARY OF TEST RESULTS - BURIED STRIP FOOTING IN DENSE SAND OVERLYING LOOSE SAND, (D/B=0·5)

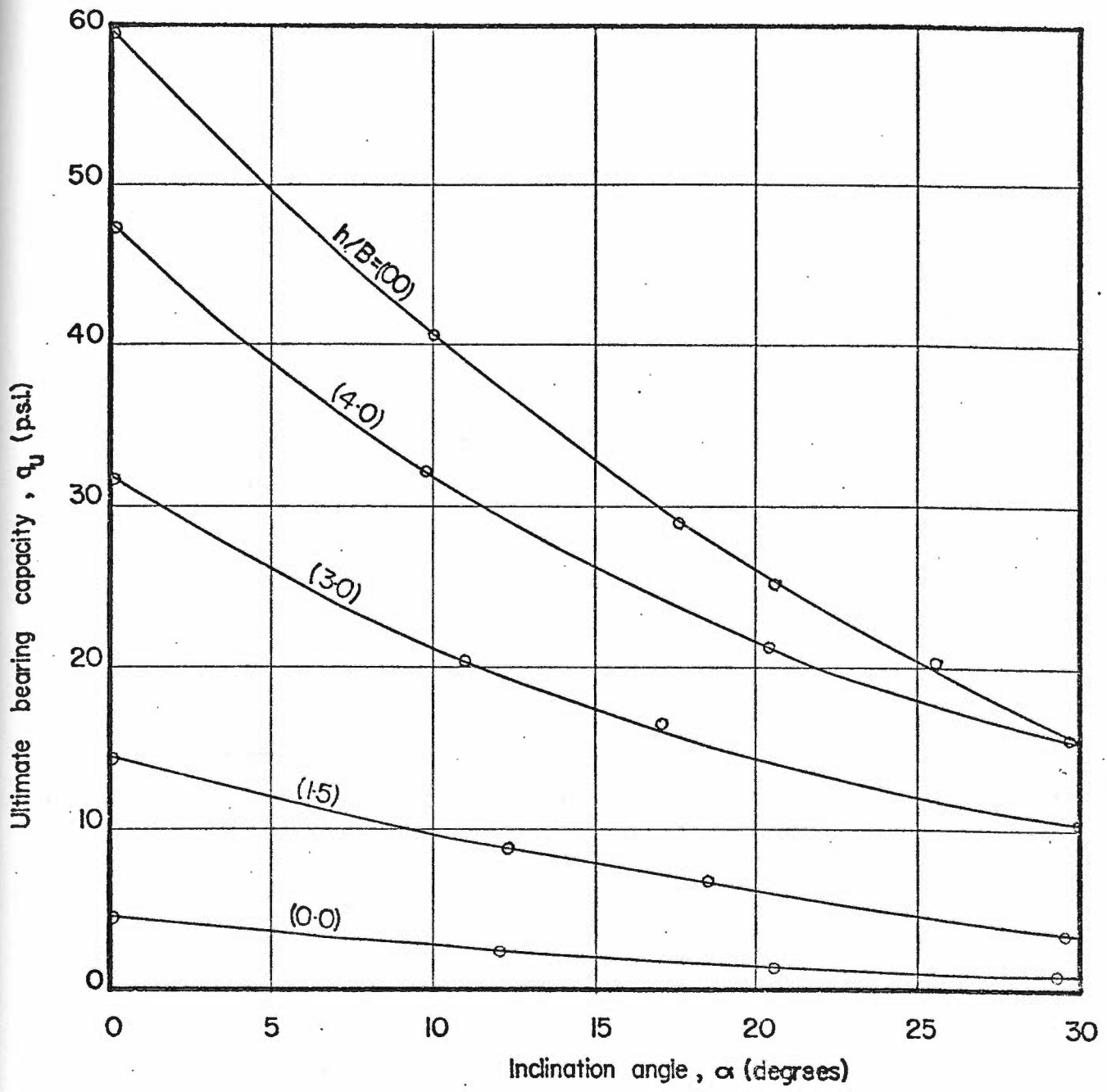

FIGURE 5·15 SUMMARY OF TEST RESULTS - BURIED STRIP FOOTING IN DENSE SAND OVERLYING LOOSE SAND (D/B = 1)

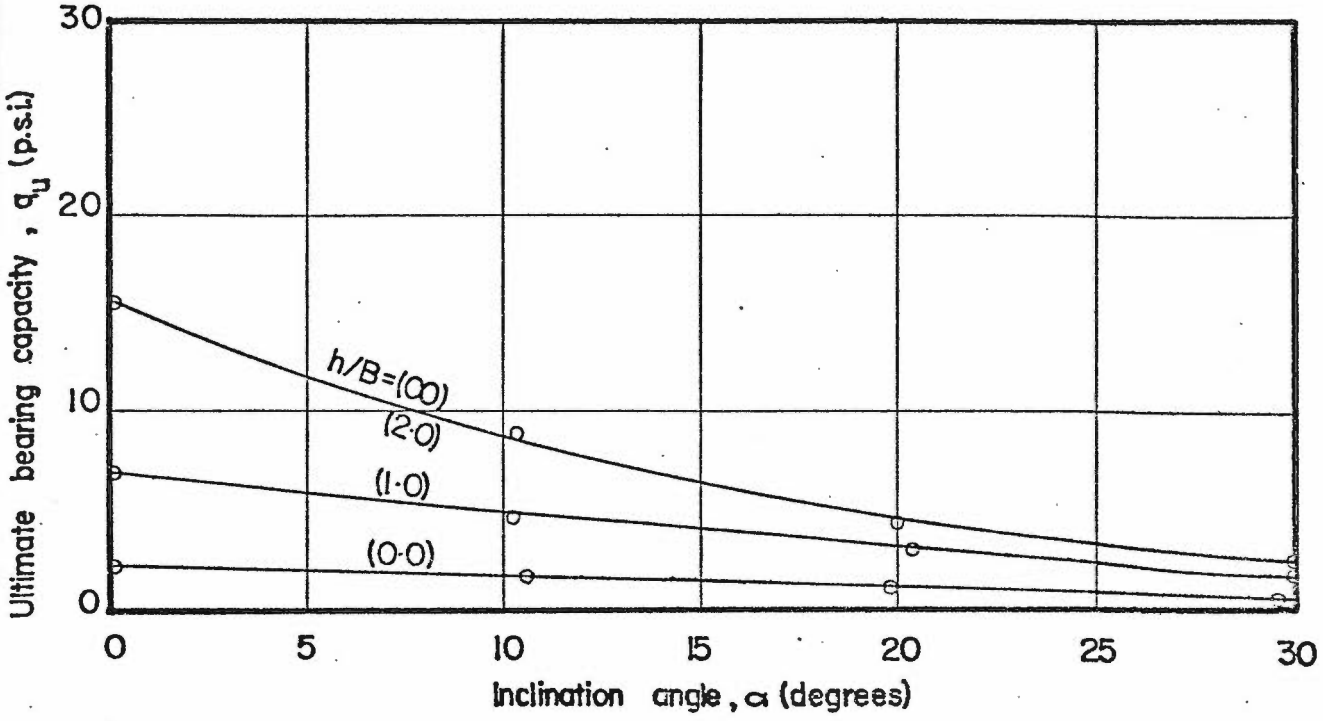

FIGURE 5·16 SUMMARY OF TEST RESULTS - SURFACE CIRCULAR FOOTING ON DENSE SAND OVERLYING LOOSE SAND (D/B = 0)

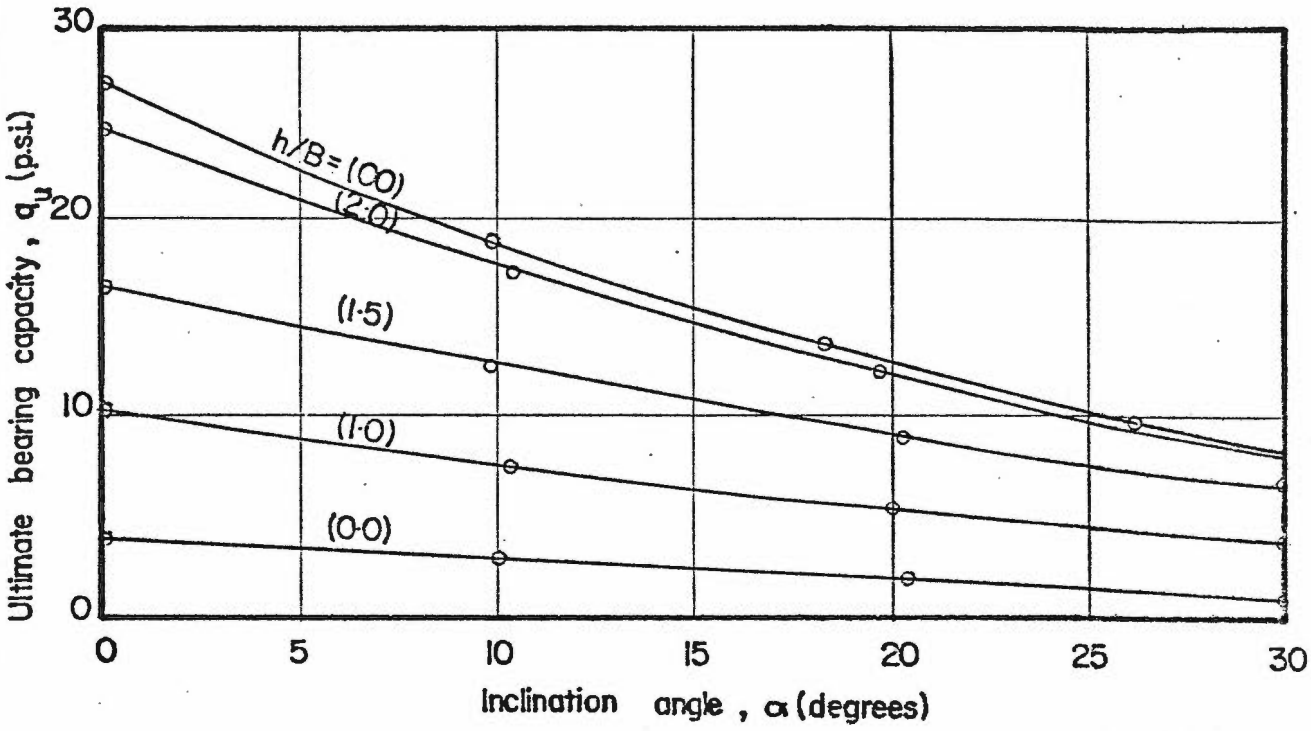

FIGURE 5·17 SUMMARY OF TEST RESULTS - BURIED CIRCULAR FOOTING IN DENSE SAND OVERLYING LOOSE SAND (D/B = 0·5)

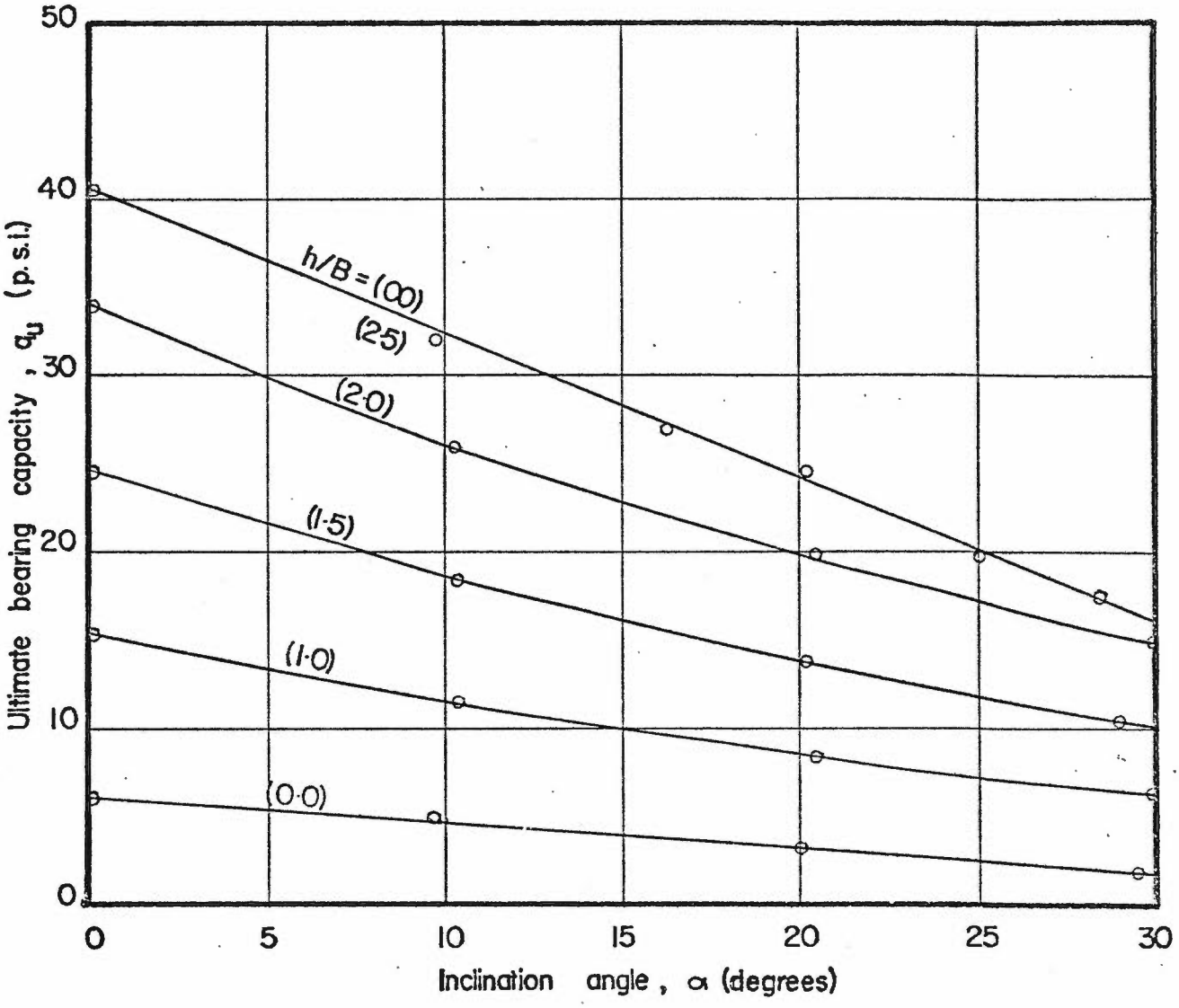

FIGURE 5·18 SUMMARY OF TEST RESULTS - BURIED CIRCULAR FOOTING IN DENSE SAND OVERLYING LOOSE SAND (D/B = 1)

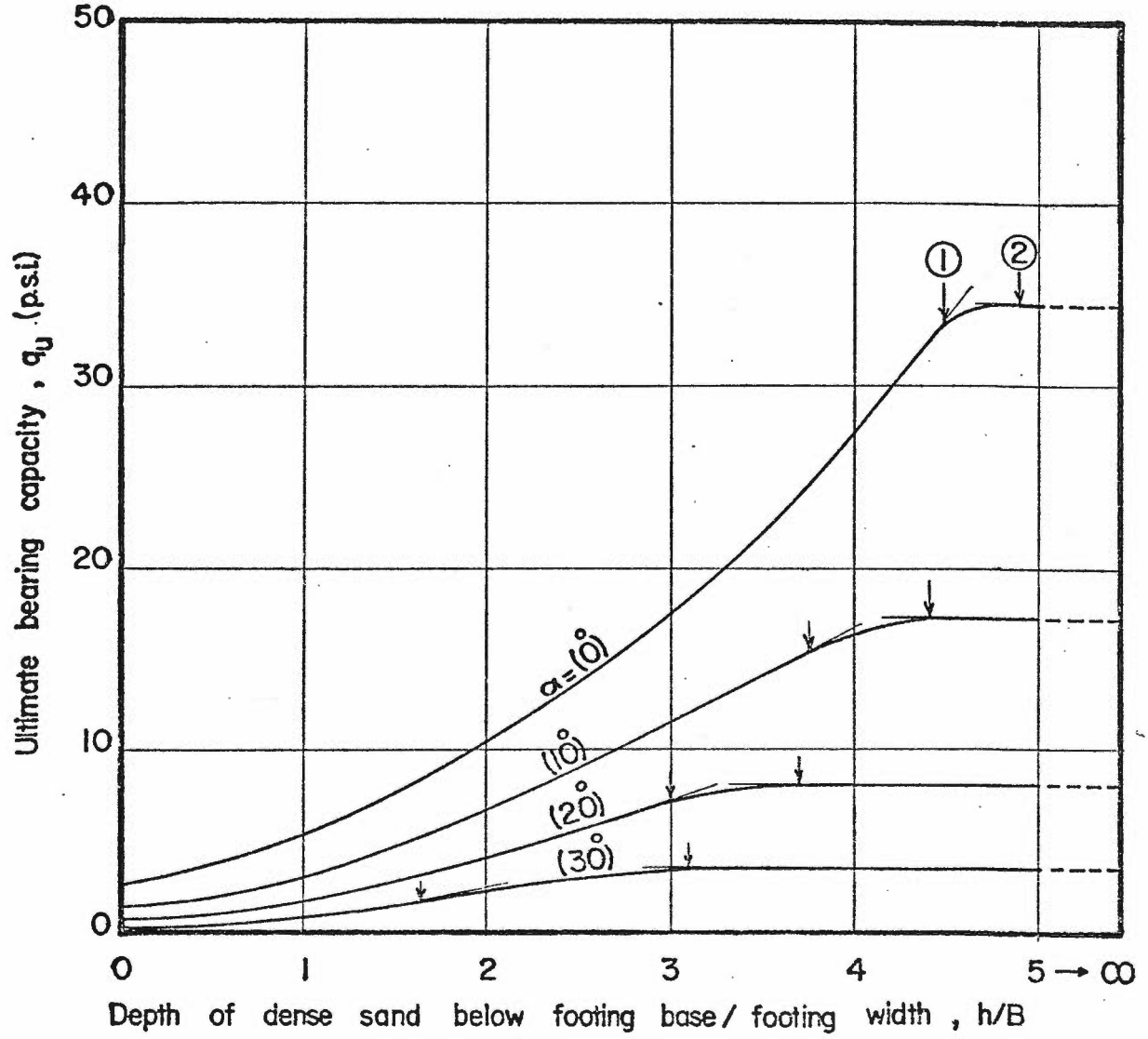

FIGURE 5·19 q_u VERSUS h/B RATIO FOR SURFACE STRIP FOOTING ON DENSE SAND OVERLYING LOOSE SAND (D/B = 0)

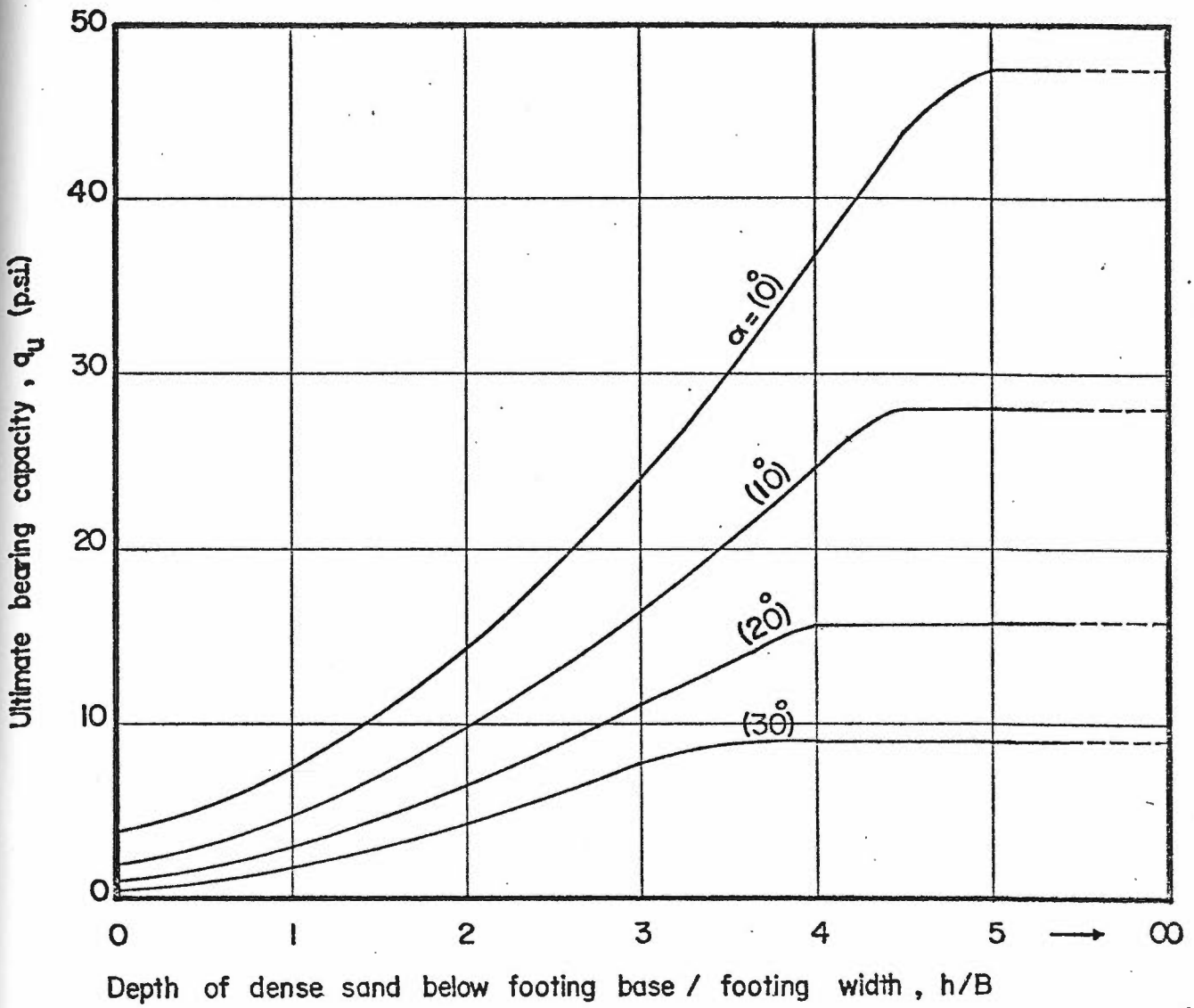

FIGURE 5·20 q_u VERSUS h/B RATIO FOR BURIED STRIP FOOTING IN DENSE SAND OVERLYING LOOSE SAND (D/B = 0·5)

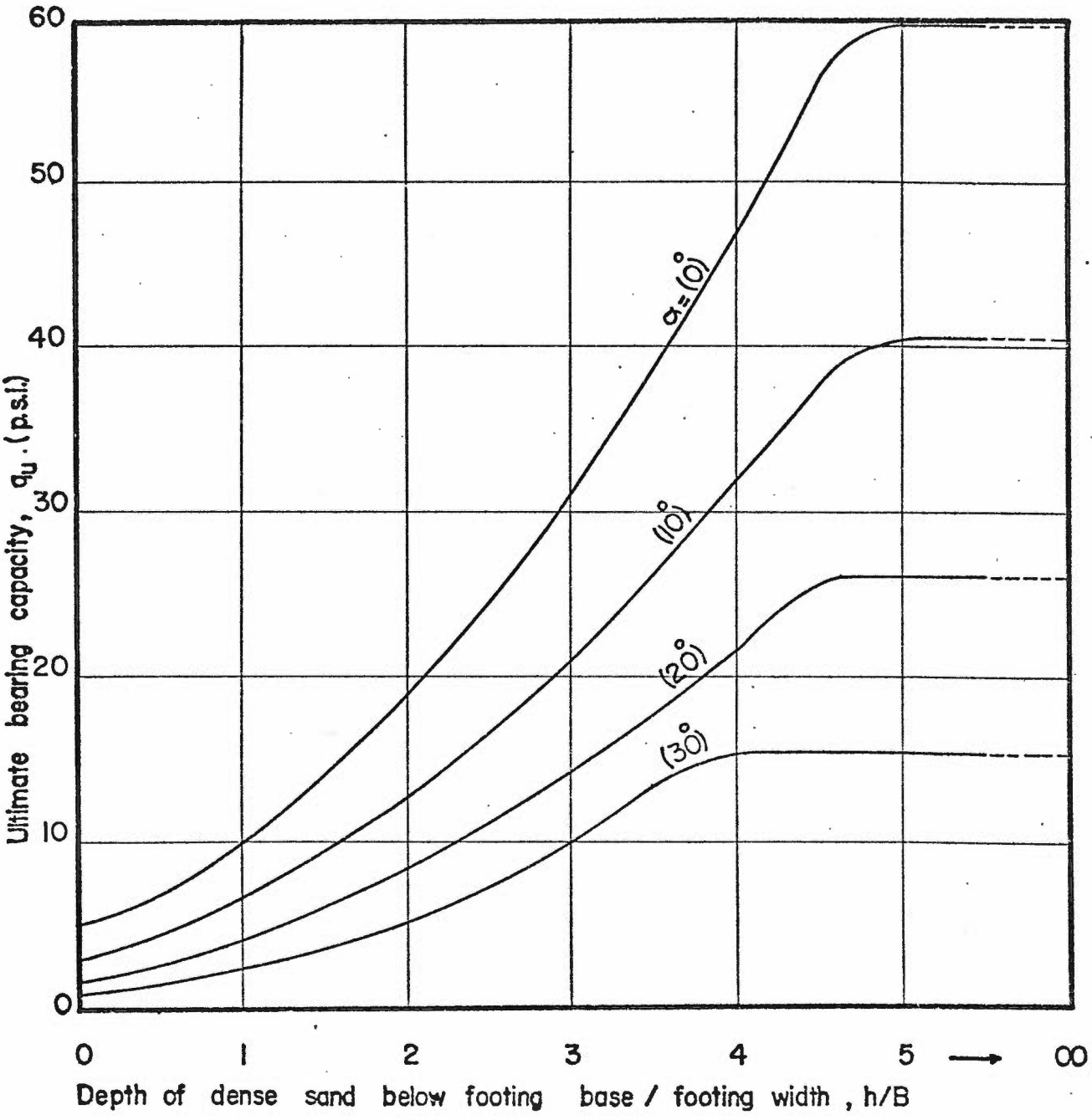

FIGURE 5·21 q_u VERSUS h/B RATIO FOR BURIED STRIP FOOTING IN DENSE SAND OVERLYING LOOSE SAND (D/B=1)

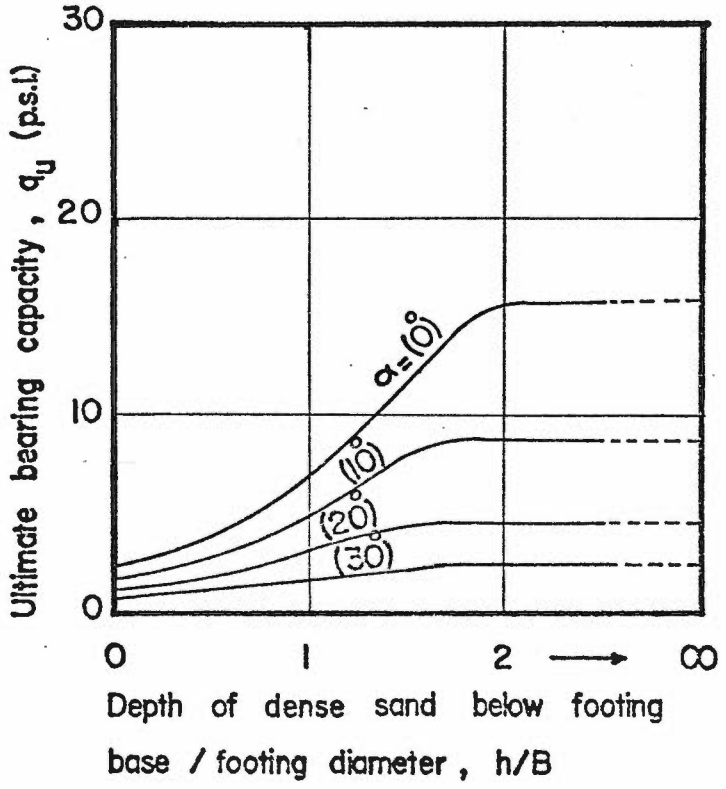

FIGURE 5·22 q_u VERSUS h/B RATIO FOR SURFACE CIRCULAR FOOTING ON DENSE SAND OVERLYING LOOSE SAND (D/B = 0)

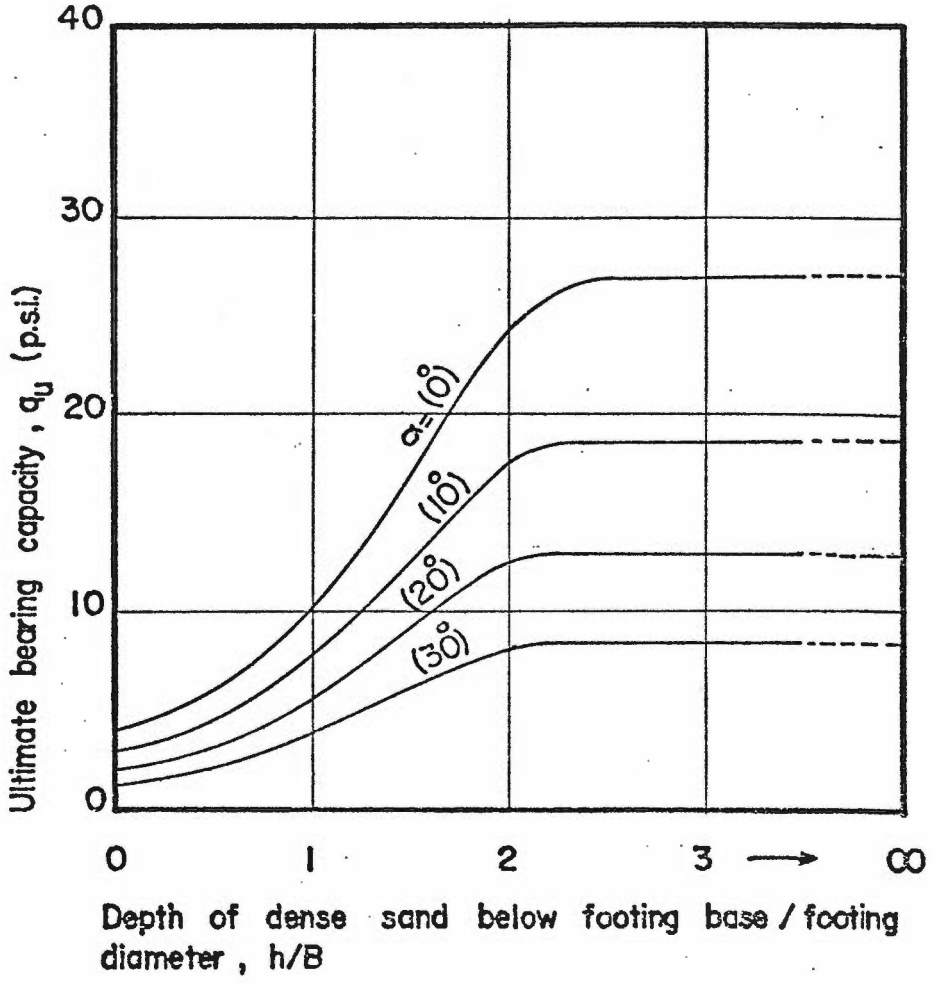

FIGURE 5·23 q_u VERSUS h/B RATIO FOR BURIED CIRCULAR FOOTING IN DENSE SAND OVERLYING LOOSE SAND (D/B = 0·5)

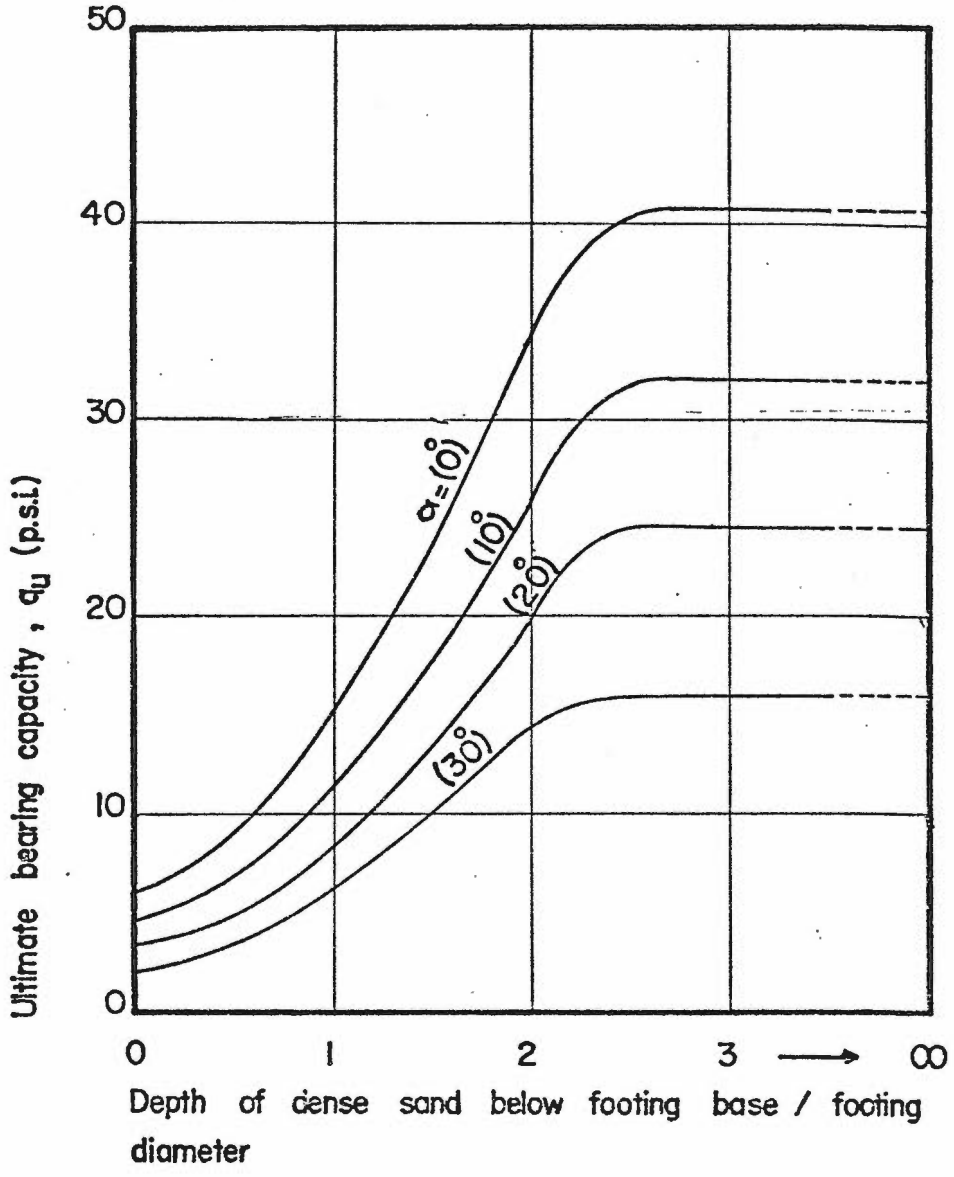

FIGURE 5·24 q_u VERSUS h/B RATIO FOR BURIED CIRCULAR FOOTING IN DENSE SAND OVERLYING LOOSE SAND (D/B= 1)

the variation of the ultimate bearing capacity with the h/B ratio for inclination angles of 0, 10, 20 and 30 degrees. It should be noted that the ultimate bearing capacities are expressed as the inclined load.

As would be expected, the observed ultimate bearing capacity increased rapidly with increasing thickness of the dense sand below the footing base up to a maximum value, and decreased with increasing angle of inclination, α. This maximum value was equal to the ultimate bearing capacity of the footing in homogeneous dense sand buried at the same depth and subjected to load having the same inclination angle, but with relatively higher settlement at failure. Meyerhof (1955), quoted that for a strip footing on homogeneous sand, the ratio of the maximum depth of the failure zones to the footing width varies with the angle of internal friction, ϕ. This ratio for the dense sand used in this investigation ($\phi = 47.7^{\circ}$) is equal to 1.7, which gave evidence that the ultimate bearing capacity was considerably affected by the weaker bottom layer. Thus, a greater h/B ratio, depending on the relative strength of the layered system, was necessary in order to achieve complete failure in the dense sand layer without exceeding a tolerable pressure at the interface with the weaker layer. In these series of tests the settlement at failure was found to increase with an increase in the buried depth, and decreased with increasing inclination angle, α, while the horizontal movement increased.

Test results of these series are analyzed in this section according to the punching theory. Punching phenomenon was observed by Brown (1967) for the case of stiff clay layer overlying soft clay, and by Meyerhof (1974) for the case of dense sand layer overlying clay. This

theory is discussed in Chapter 2. In this chapter the punching theory is extended to cover any combination of two-layered soils in which the strong layer is sand and overlies a deep weaker layer. The theory is also extended to footings subjected to inclined loads.

In the present investigation, observations of the upper layer deformation for the strip footing test series, as shown in Figures 5.25 to 5.28, indicated that the dense sand beneath the footing tends to move, with least resistance, in the direction of the applied load. In other words, failure took place by punching of a column, which consisted of the footing base and the underlying dense sand into the lower layer, developing shear failure in the upper and lower layers as if they were independent of each other. The column sides were approximately parallel to the direction of the applied load in the upper half of the dense sand layer and curving slightly outward in the lower half. However, the distribution of contact pressure at the soil interface was concentrated in the middle portion between two planes passing with the footing edges and parallel to the direction of the applied load.

Figure 5.29.a shows a strip footing of width, B, and buried to a depth, D, in the upper dense sand layer, subjected to axial vertical loads. Figure 5.29.b shows the same footing subjected to central inclined loads at an angle α with the vertical. As a simplifying assumption, ab and cd were assumed to be the failure planes in the upper dense sand layer, Figures 5.29.a and 5.29.b. Thus, the mobilized angle of shearing resistance along the assumed failure planes, δ, must be less than the angel of internal friction, ϕ, of the upper dense sand.

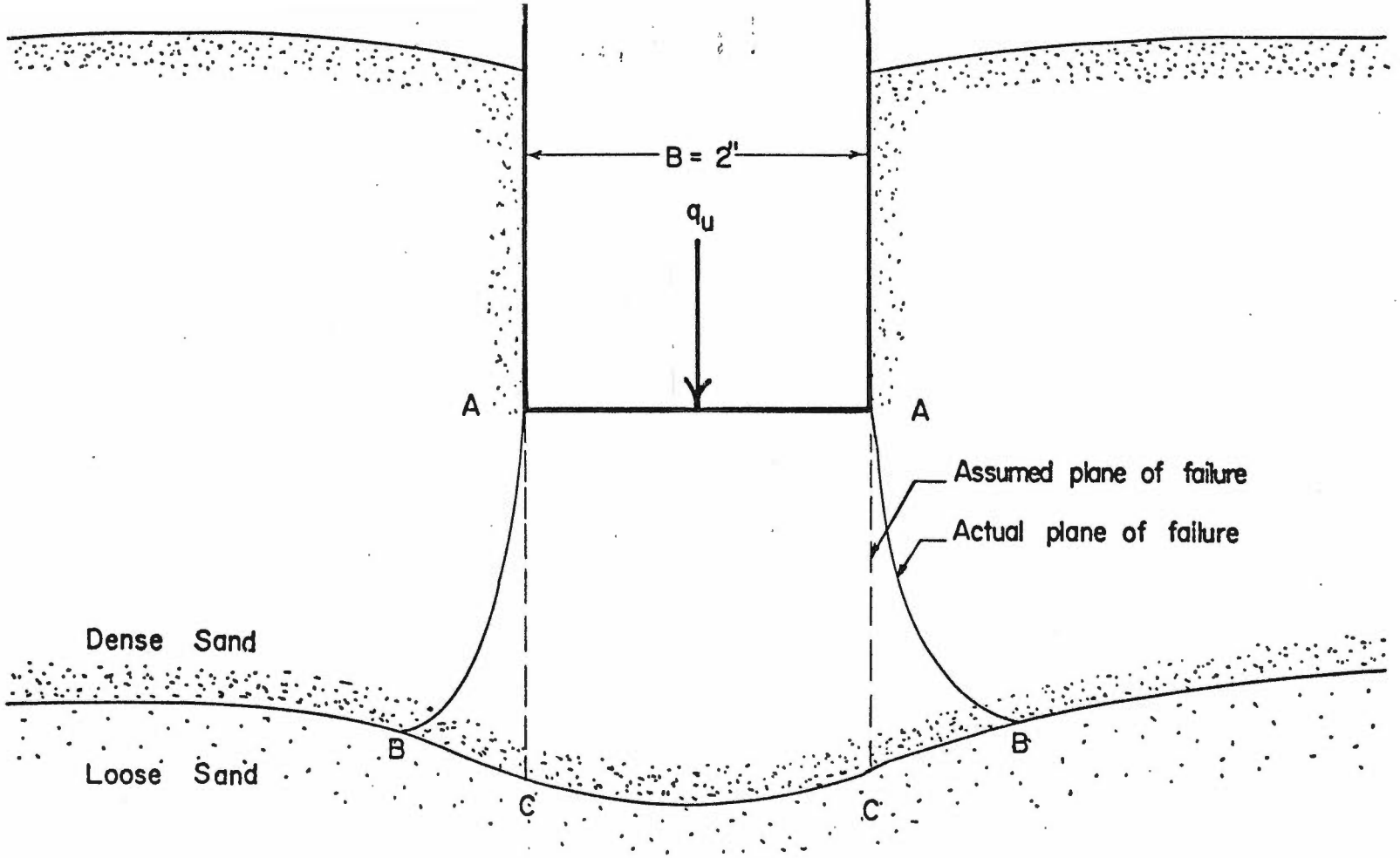

FIGURE 5·25 OBSERVED DEFORMATION OF THE INTERFACE LINE (BURIED STRIP FOOTING UNDER VERTICAL LOAD SCALE 1:1)

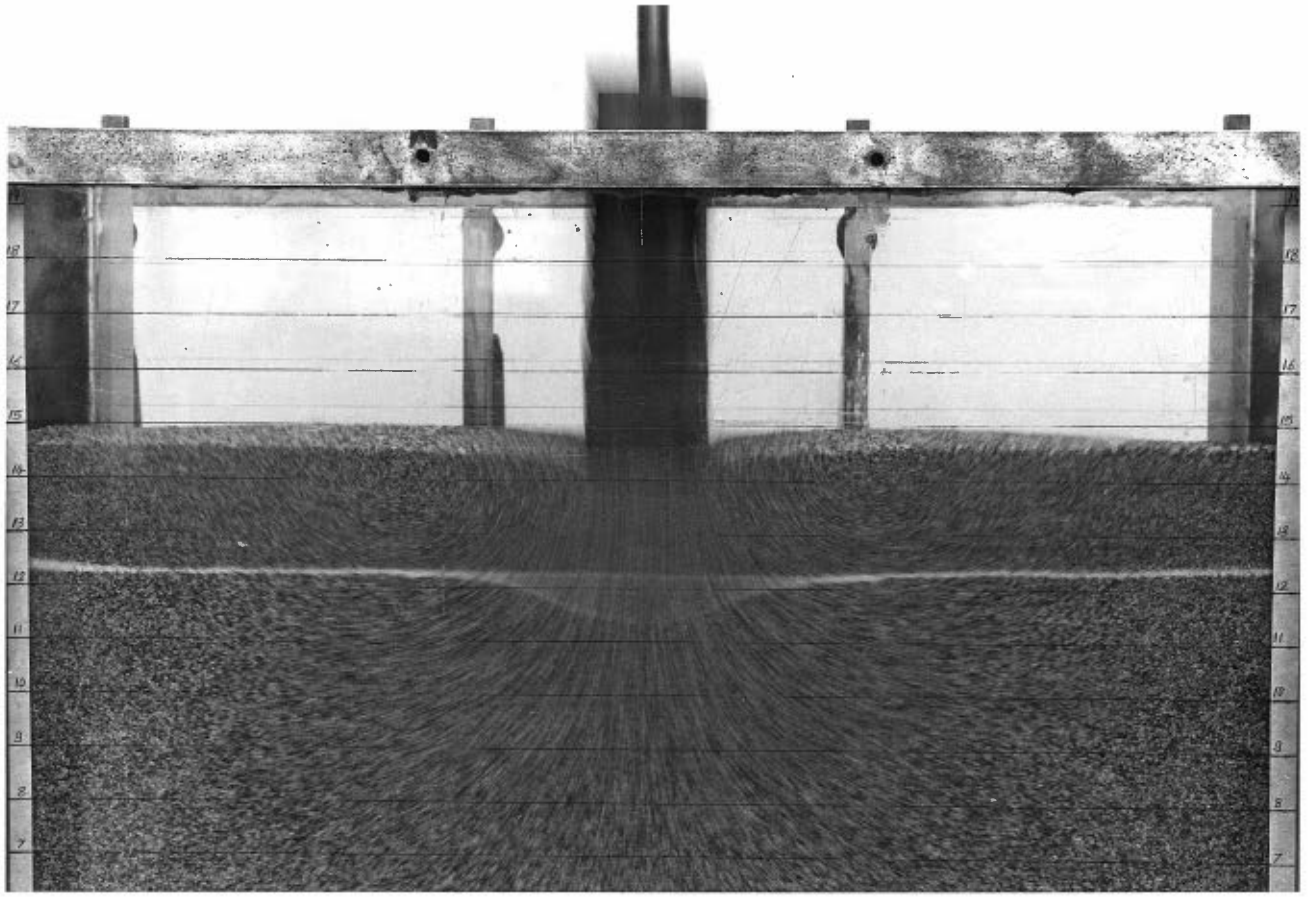

FIGURE 5.26 TIME EXPOSURE PICTURE - STRIP FOOTING UNDER VERTICAL LOAD IN DENSE SAND LAYER OVERLYING LOOSE SAND.

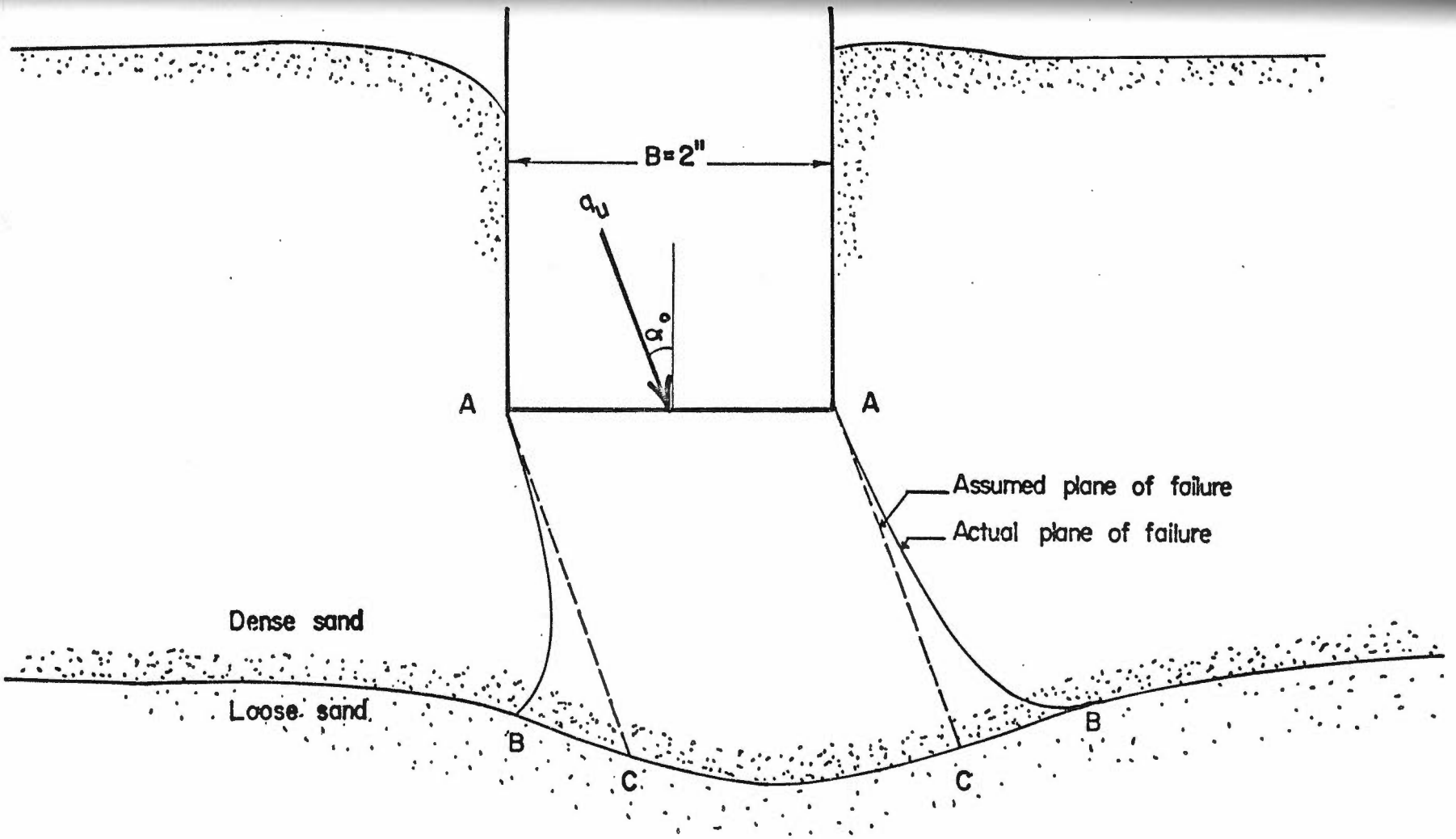

FIGURE 5·27 OBSERVED DEFORMATION OF THE INTERFACE LINE (BURIED STRIP FOOTING UNDER INCLINED LOAD - SCALE 1 : 1)

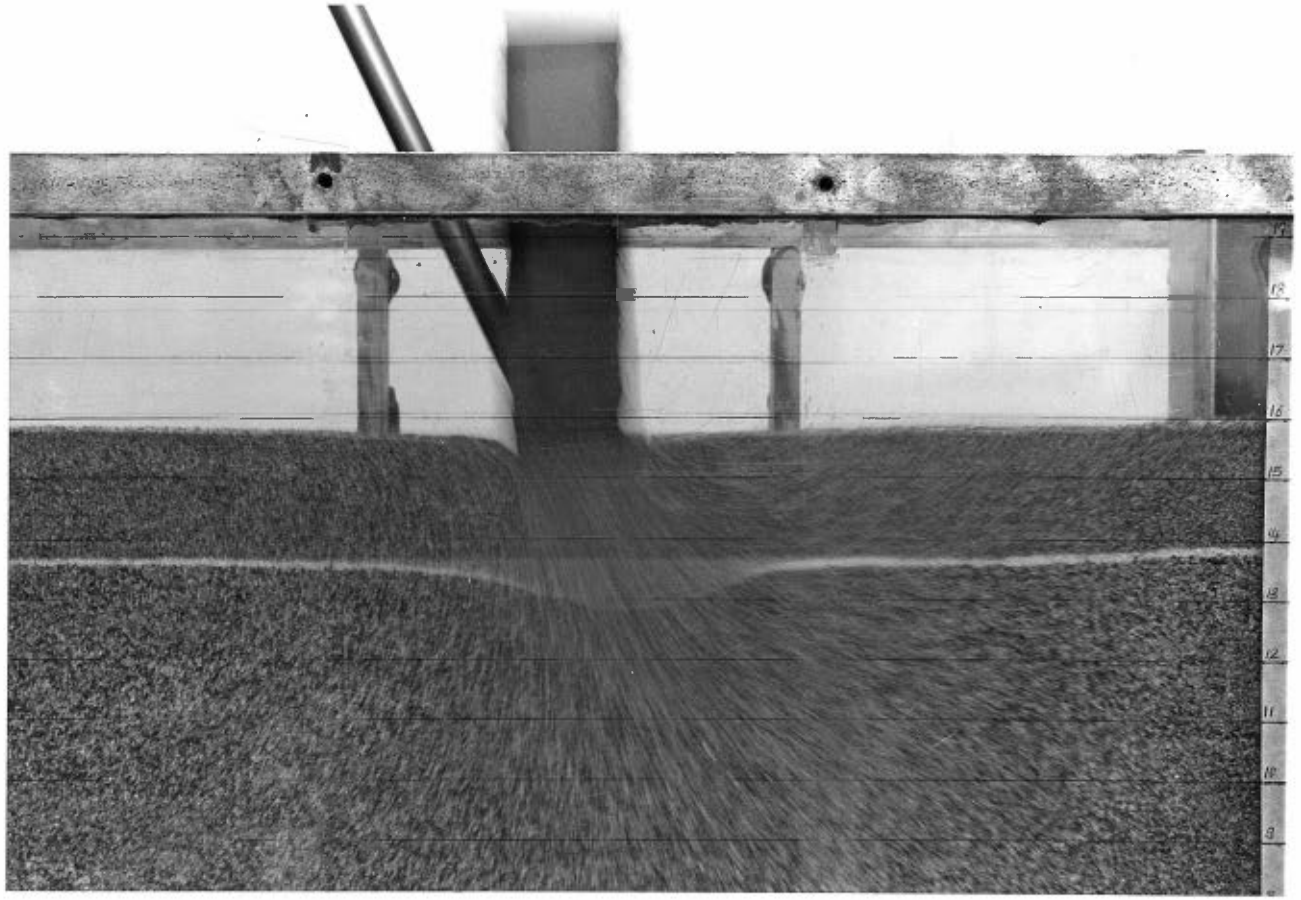

FIGURE 5.28 TIME EXPOSURE PICTURE - STRIP FOOTING UNDER INCLINED LOAD IN DENSE SAND LAYER OVERLYING LOOSE SAND.

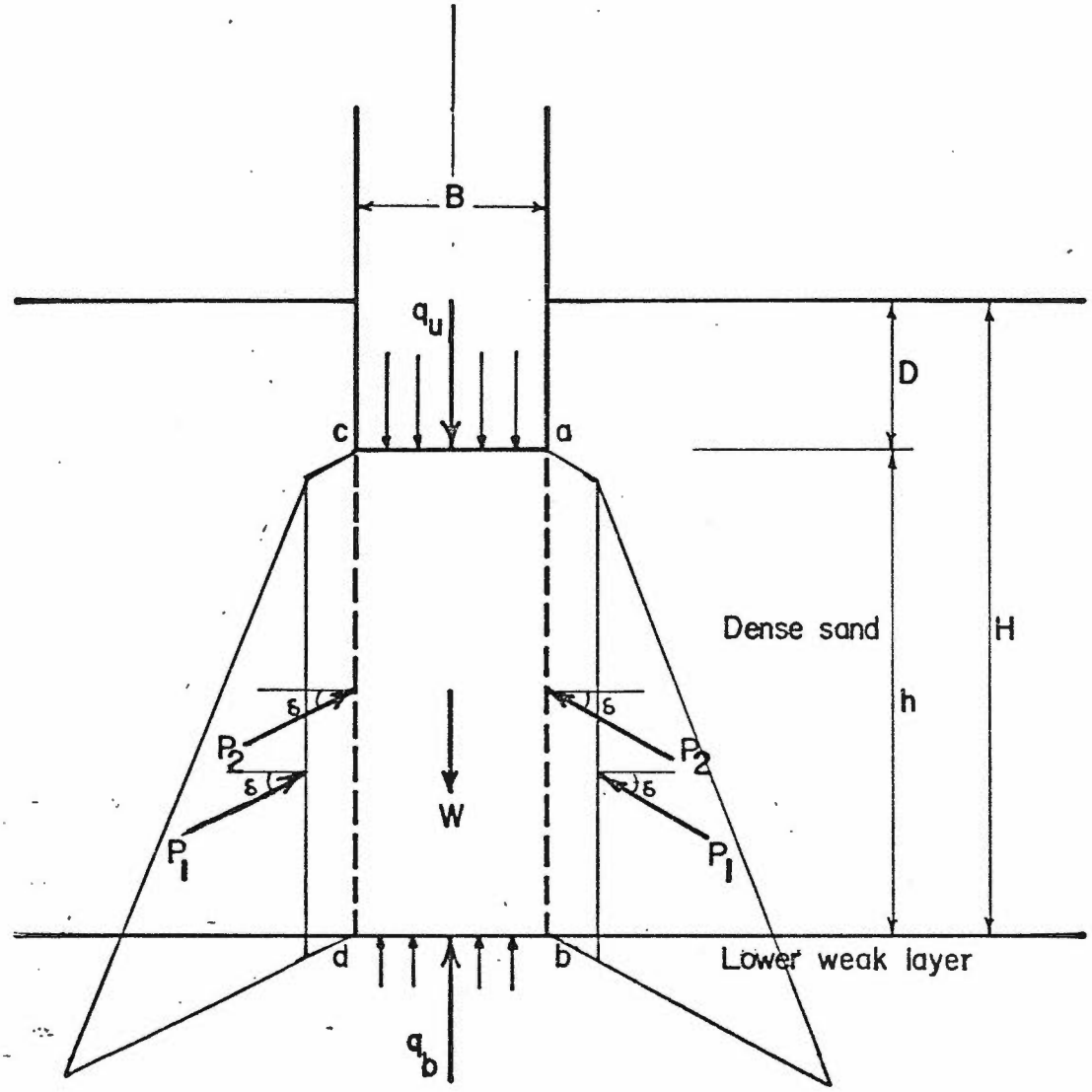

FIGURE 5·29a STRESS DIAGRAM — STRIP FOOTING UNDER VERTICAL LOAD

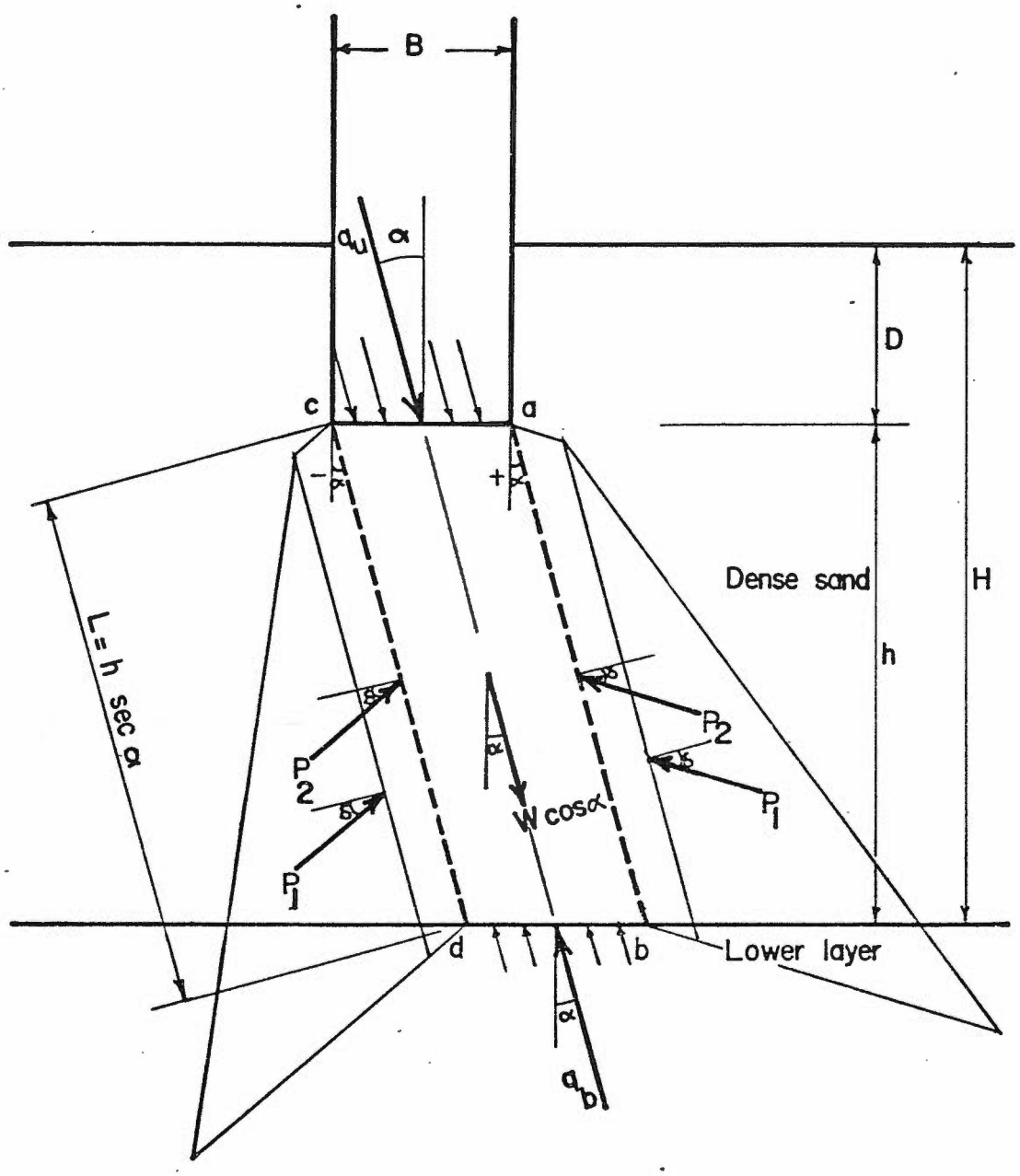

FIGURE 5·29b STRESS DIAGRAM — STRIP FOOTING UNDER INCLINED LOAD

According to Meyerhof (1974), the ultimate bearing capacity of footing in layered system, under vertical or inclined loads, would be the ultimate bearing capacity of the same footing located at the soil interface and subjected to a load having the same inclination angle (assuming the lower layer to be deep and homogeneous), plus the shearing forces developed on the assumed planes of failure in the upper layer as the footing driven into the lower layer. These shearing forces are obtained as the components of the total passive pressure along the assumed failure planes.

From earth pressure theories, the magnitude of the passive pressure and consequently, the shearing stress acting on the assumed failure planes will have a triangular distribution (P_1) due to weight component, and rectangular distribution (p_2) due to surcharge component, (Figure 5.28). Further, the passive pressure on a plane inclined at $-\alpha$ was greater than it was for one inclined at $+\alpha$. However, based on the observation during testing, failure takes place by punching in the load direction into the lower layer, the equilibrium conditions must be satisfied in a direction normal to the failure planes. This condition can be justified only if the mobilized passive pressures are the same on both sides of the assumed failure planes, so that the pressure on the plane inclined at $+\alpha$ governs. The passive earth pressure coefficients, $K_{p\gamma}$ and K_{pq}, due to weight and surcharge components respectively, are taken from Caquot and Kerisel (1948 and 1968) have been presented for positive values of α, in Figures 5.30 and 5.31 for the case of $\delta = \phi$. For the case of δ less than ϕ, reduction factors R_γ and R_q have been introduced by Caquot and Kerisel (1948 and 1968), as shown in Figures 5.32 and 5.33.

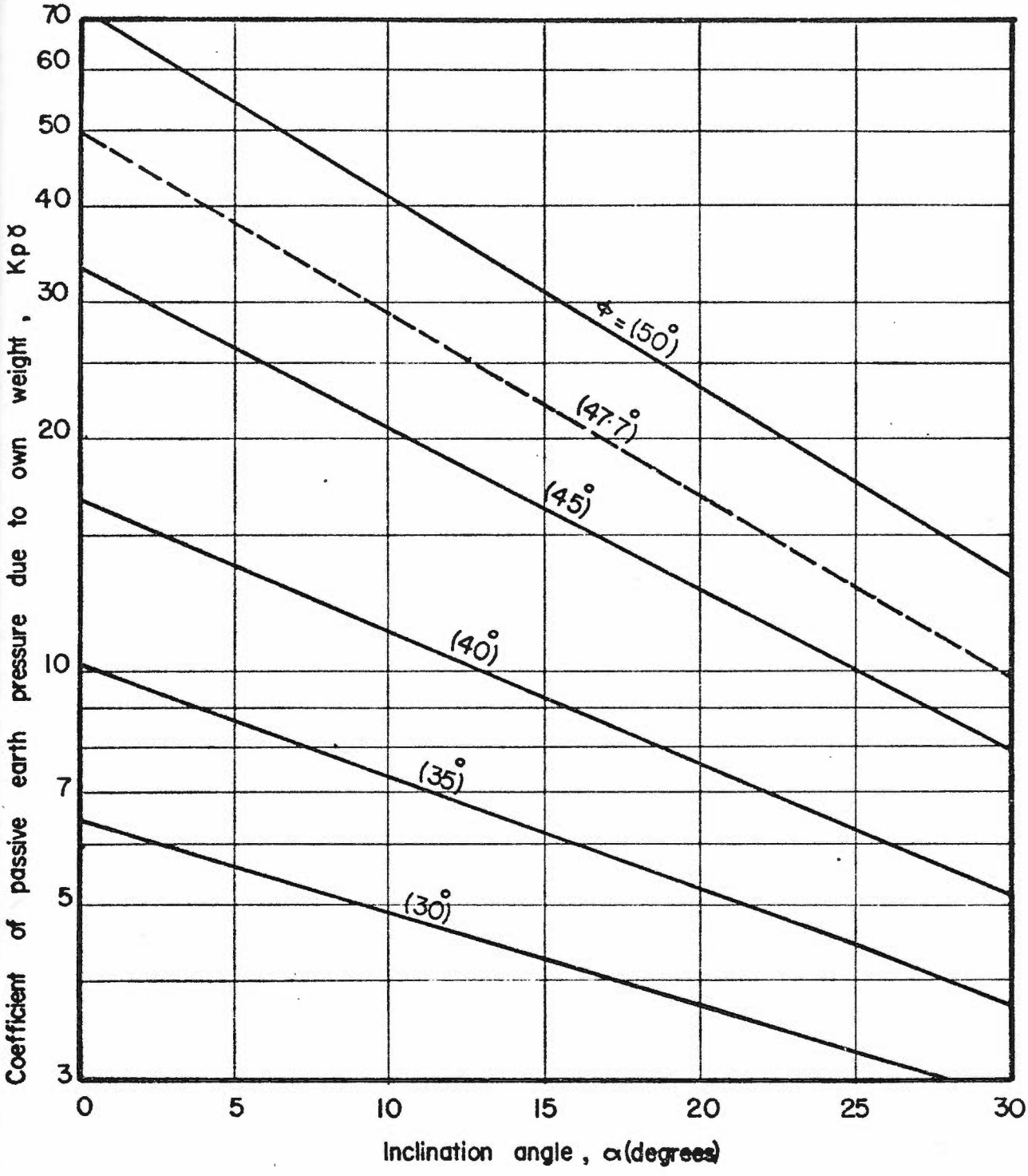

FIGURE 5·30 THEORETICAL PASSIVE EARTH PRESSURE COEFFICIENT — WEIGHT COMPONENT ($\delta/\Phi = 1$)
AFTER CAQUOT AND KERISEL , 1948

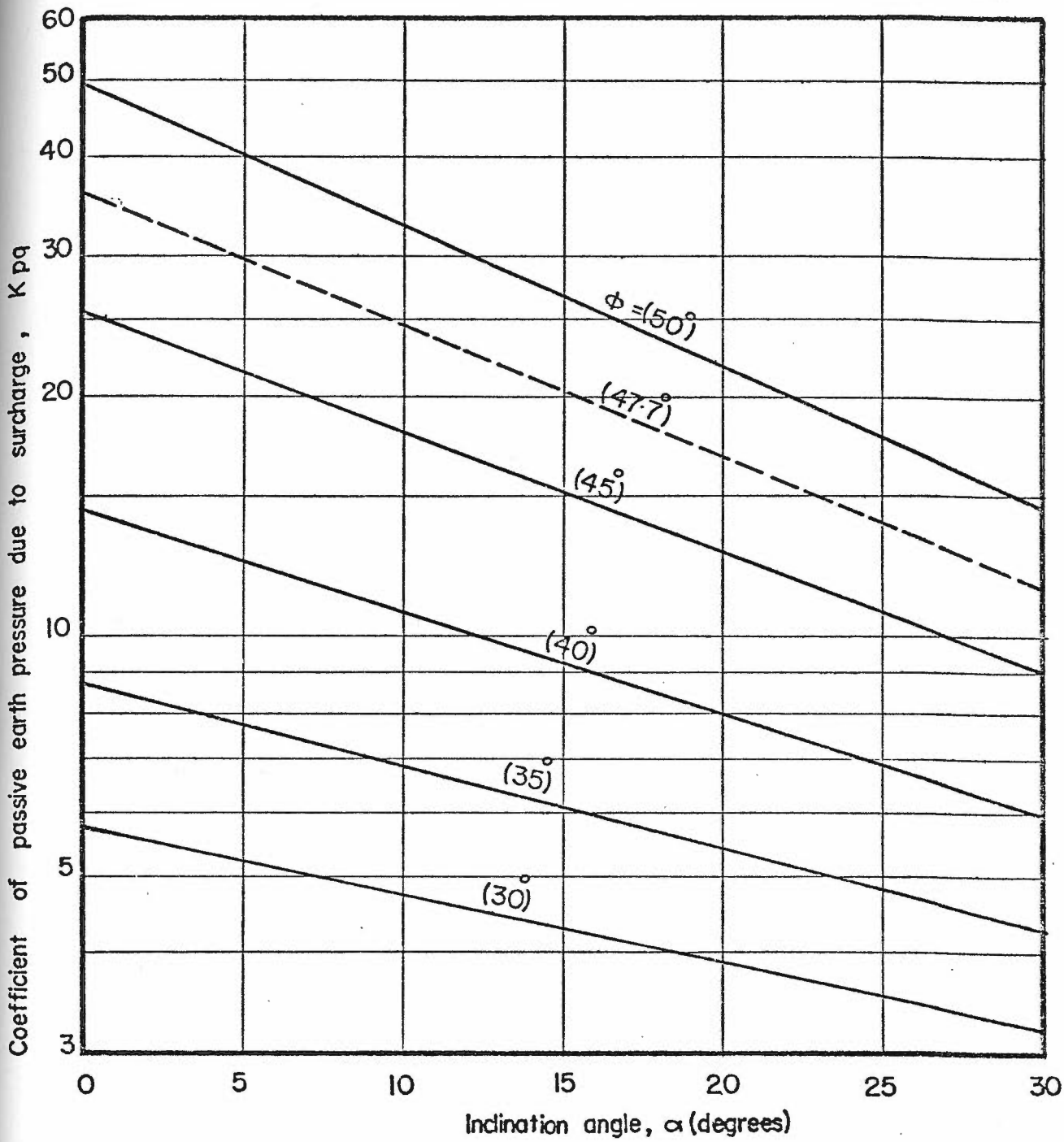

FIGURE 5·31 THEORETICAL PASSIVE EARTH PRESSURE COEFFICIENT — SURCHARGE COMPONENT ($\delta/\Phi = 1$) AFTER CAQUOT AND KERISEL, 1948

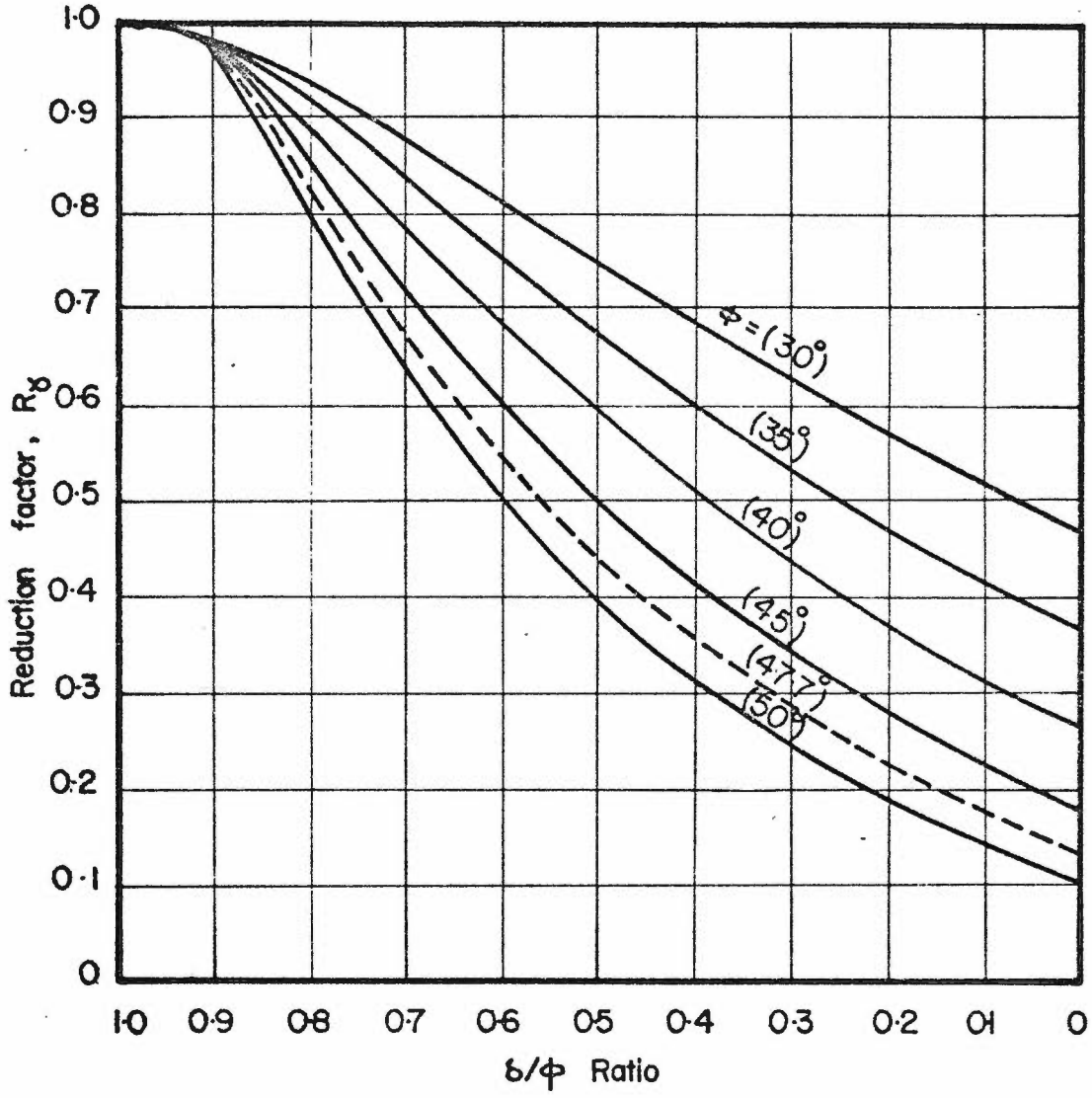

FIGURE 5·32 THEORETICAL REDUCTION FACTOR FOR THE WEIGHT COMPONENT OF PASSIVE EARTH PRESSURE - AFTER CAQUOT AND KERISEL, 1948

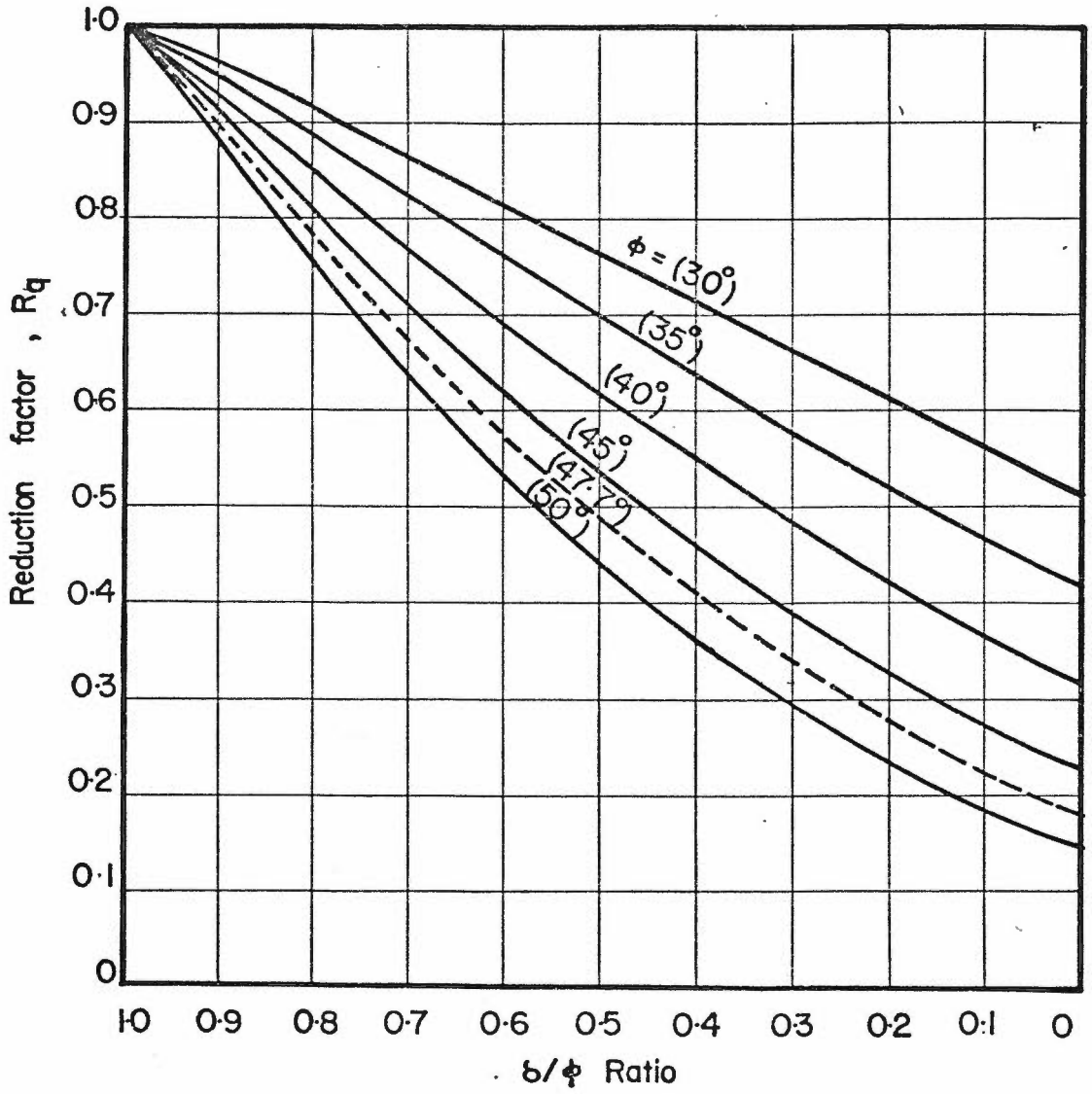

FIGURE 5·33 THEORETICAL REDUCTION FACTOR FOR THE SURCHARGE COMPONENT OF PASSIVE EARTH PRESSURE - AFTER CAQUOT AND KERISEL, 1948

Taking the block of the dense sand (a b c d) (Figure 5.29.b.) as a free body, the equilibrium equation of the external forces in the direction of the applied load is given below in sections 5.4.1 and 5.42 for the case of strip and circular footing, respectively. Two additional equilibrium equations are given in Appendix III.

5.4.1 Case of strip footing

$$q_u \cdot B = q_b \cdot B + 2(P_1 + P_2) \sin \delta - \gamma_1 B(h) \cos \alpha \quad (5.7)$$

$$\text{or} \quad q_u = q_b + \frac{2}{B}(P_1 + P_2) \sin \delta - \gamma_1 h \cos \alpha \leq q_t \quad (5.8)$$

where: q_u = ultimate bearing capacity of the layered system measured in the loading direction,

q_b = ultimate bearing capacity measured in the load direction of a footing with the same width at the soil interface,

q_t = ultimate bearing capacity of homogeneous upper layer soil, measured in the loading direction,

P_1 = total passive earth pressure on the assumed failure planes due to weight component:

$$\text{i.e. } P_1 = 1/2\ R_\gamma K_{p\gamma} \cdot \gamma_1 (h \sec \alpha)^2 \quad (5.9)$$

P_2 = total passive earth pressure on the assumed failure planes due to surcharge component:

$$\text{i.e. } P_2 = R_q K_{pq}\ \gamma_1 D \cdot h \sec \alpha \quad (5.10)$$

α = angle of the applied load with the vertical,

δ = the average mobilized angle of shearing resistance on the assumed failure planes,

and γ_1 = unit weight of dense sand.

Substituting with P_1 and P_2 from equations 5.9 and 5.10 in equation 5.8

$$q_u = q_b + \frac{2}{B}\{\tfrac{1}{2}R_\gamma K_{P\gamma}\gamma_1 h^2 \sec^2\alpha + R_q K_{pq}\,\gamma_1 D{\cdot}h \sec\alpha\}\sin\delta$$

$$- \gamma_1 h\cos\alpha \leq q_t \qquad (5.11)$$

$$\text{or } q_u = q_b + \frac{\gamma_1 h \sec\alpha}{B}(R_\gamma K_{P\gamma}.h\sec\alpha + 2R_q K_{Pq}.D)\sin\delta$$

$$- \gamma_1 h\cos\alpha \leq q_t \qquad (5.12)$$

Setting $K_{t\gamma} = R_\gamma K_{P\gamma}\sin\delta$

$$K_{tq} = R_q K_{Pq}\sin\delta$$

where $K_{t\gamma}$ and K_{tq} are the coefficients of punching resistance due to the weight and surcharge components respectively for strip footing, thus

$$q_u = q_b + \frac{\gamma_1 h\sec\alpha}{B}\{K_{t\gamma}.h\sec\alpha + 2K_{tq}.D\} - \gamma_1 h\cos\alpha \qquad (5.13)$$

$$\leq q_t$$

In the case of strip footing under vertical loads ($\alpha = 0$), equation 5.13 can be written as:

$$q_u = q_b + \frac{\gamma_1 h}{B}\{K_{t\gamma}.h + 2K_{tq}.D\} - \gamma_1 h \qquad (5.14)$$

$$\leq q_t$$

5.4.2 Case of circular footings

$$q_u{\cdot}A = q_b{\cdot}A + (P_1 = P_2)\,C{\cdot}\sin\delta - \gamma_1 (h){\cdot}A{\cdot}\cos\alpha \qquad (5.15)$$

or

$$q_u = q_b + \frac{C}{B}(P_1 + P_2)\sin\delta - \gamma_1 h\cos\alpha \qquad (5.16)$$

$$\leq q_t$$

where A = area of footing base $= \frac{\pi B^2}{4}$,

C = Circumference of footing $= \pi B$, and

other notations are the same as before. Substituting for P_1 and P_2 from equations 5.9 and 5.10 in equation 5.16

$$q_u = q_b + \frac{4}{B}\{\tfrac{1}{2}R_\gamma K_{P\gamma}.\gamma_1 . h^2 \sec^2\alpha + R_q K_{Pq}.\gamma_1 D.h \sec\alpha\}\sin\delta$$

$$- \gamma_1 h\cos\alpha \leq q_t \qquad (5.17)$$

or

$$q_u = q_b + \frac{2\gamma_1 h\cos\alpha}{B}(R_\gamma K_{P\gamma}.h\sec\alpha + 2R_q K_{Pq}.D)\sin\delta$$

$$- \gamma_1 h\cos\alpha \leq q_t \qquad (5.18)$$

Setting $s_\gamma K_{t\gamma} = R_\gamma K_{P\gamma}\sin\delta$

$$s_q K_{tq} = R_q K_{Pq}\sin\delta$$

where $s_\gamma K_{t\gamma}$ and $s_q K_{tq}$ are the coefficients of punching resistance due to the weight and surcharge components respectively for circular footing

s_γ and s_q being shape factors, thus

$$q_u = q_b + \frac{2\gamma_1 h\sec\alpha}{B}\{s_\gamma K_{t\gamma}.h\sec\alpha + 2s_q K_{tq}.D\}$$

$$- \gamma_1 h\cos\alpha \leq q_t \qquad (5.19)$$

Again, in the case of a circular footing under vertical loads ($\alpha = 0^{o}$) equation 5.19 can be written as:

$$q_u = q_b + \frac{2\gamma_1 h}{B}\{s_\gamma K_{t\gamma} \cdot h + 2s_q K_{tq} \cdot D\} - \gamma_1 h \qquad (5.20)$$

$$\leq q_t$$

Equations 5.14 and 5.20 for predicting the ultimate bearing capacity of strip and circular footings respectively, under vertical loads can be derived (Meyerhof, 1974) by equating the external forces acting on the vertical failure planes (Figure 5.29.a). However, equations 5.13 and 5.19 are general equations for the same footings respectively under vertical or inclined loads.

Solutions of equations 5.13, 5.14, 5.19 and 5.20 can be obtained as follows:

(i) For example, equation 5.13 can be written as:

$$\frac{q_u - q_b + \gamma_1 h \cos\alpha}{\frac{\gamma_1 h \sec\alpha}{B}} = \{K_{t\gamma} h \sec\alpha + 2K_{tq} \cdot D\} \qquad (5.21)$$

(ii) The left hand side of equation 5.21 can be evaluated from the test data.

(iii) On the right hand side of equation 5.21, $K_{t\gamma}$ and K_{tq} can be evaluated by assuming a value of δ/ϕ_1. Different values of δ/ϕ_1 were used until both sides of equation 5.21 are equal.

(14) Using the existing value of δ/ϕ_1 from step (iii), $K_{t\gamma}$ and K_{tq} can be evaluated.

In the present investigation q_b was calculated from the following equations:

(i) In the case where the bottom layer is sand:

$$q_b = \tfrac{1}{2} \gamma_2 B N_{\gamma 2} + \gamma_1 H N_{q2} \qquad (5.22)$$

where $N_{\gamma 2}$ and N_{q2} are the bearing capacity factors for the homogeneous lower sand layer (under the same inclination angle, α, as the layered system).

It should be noted that in determining q_b, only the weight of the upper layer was considered (Terzaghi, 1943).

(ii) In the case where the bottom layer is clay:

$$q_b = C_u N_c + \gamma_1 H \qquad (5.23)$$

Where C_u is the undrained shear strength of the lower clay layer, as determined from unconfined tests, and N_c is the surface bearing capacity factor for the homogeneous lower clay layer (under the same inclination angle, α, as the layered system).

Equations 5.13, 5.14, 5.19 and 5.20 have been modified to take into account the footing settlement at failure. The measured settlement, S, from footing test was divided into two components, S_1 and S_2, where:

account the footing settlement at failure. The measured settlement, S, from footing test was divided into two components, S_1 and S_2, where:

S_1 = settlement of the upper layer (added to the initial depth D - equation 5.21),

and S_2 = settlement of the lower layer (added to the thickness H - equations 5.22 and 5.23).

The method used in this investigation for calculating S_1 and S_2 values is explained in the following example:

Example:

From test No. 26 (Dense sand overlying loose sand)

D/B = 0.5

(S/B) at failure = 26%

i.e. S = 0.52" (B = 2")

From test No. 2 (Homogeneous dense sand)

D/B = 0.5

$(S/B)_f$ = 14%

From test No. 12 (Homogeneous loose sand)

D/B = 0.5

$(S/B)_f$ = 31%

$$S_1 = 0.26 \times \frac{0.14}{0.14 + 0.31} B = 0.16"$$

$$S_2 = 0.26 \times \frac{0.31}{0.14 + 0.31} B = 0.36"$$

5.5 Analysis of Surface Strip Footing Tests Under Vertical Loads and Values of Coefficients of Punching Resistance.

Employing equation 5.14 and data from Tables 4.3 to 4.5 the experimental δ/ϕ_1 ratios were computed from which the experimental coefficients of punching resistance, $K_{t\gamma}$ and K_{tq}, were calculated. These values are given in Tables 5.6 and 5.7 for the cases of dense sand over loose sand, dense sand over compact sand and dense sand over clay and are shown in Figure 5.34.

It is evident from Figure 5.34 that the ratio of δ/ϕ_1 and consequently the coefficients of punching resistance decreased rapidly for h/B values less than 0.5 (Dembicki, 1973 and Sastry, 1976) and tended to zero within the range of h/B values from zero to 0.5. This sudden decrease in δ/ϕ_1 ratio indicated the experimental lower limit of the punching theory and that for h/B values less than 0.5 failure may occur by bending of the upper layer. Also, beyond the limiting depth ratio of the upper layer, as indicated by an arrow (1) in Figures 5.10 and 5.11 the analysis showed a decrease in value of the coefficients of shearing resistance. This provided a method of determining the upper limit of the punching theory, when the bearing capacity of homogeneous dense sand governs the footing design. Within these two limits, the coefficients of punching resistance did not vary significantly with the h/B values (Figure 5.34). In Figures 5.10 and 5.11 the region between points (1) and (2) is a transition zone in which the failure mechanism changed from punching (point 1) to the classical bearing capacity failure of homogeneous soil (point 2). It should be noted that both punching and bearing capacity theories overestimate the ultimate load within this

Table 5.6

Analysis of Surface Strip Footing Tests Under Vertical loads on Two Sand Layers

Layer Combination	Test No.	h/B	q_u (psi) Observed	q_b (psi) Calculated	Deduced δ/ϕ_1	Experimental Punching Coefficients		q_2/q_1
						$K_{t\gamma}$	K_{tq}	
Dense over Loose Sand	17	0.25	2.93	2.94	0.00	---	---	0.076
	18	0.5	3.69	3.42	0.50	8.89	7.23	
	19	1.0	5.32	4.34	0.49	8.53	6.95	
	20	2.0	10.55	6.25	0.50	8.89	7.23	
	21	3.0	17.54	8.14	0.50	8.89	7.23	
	22	4.5	33.61	10.96	0.51	9.27	7.52	
	23	5.0	34.50	11.91	0.46	7.63	6.19	
Dense Over Compact Sand	36	0.5	16.12	15.54	0.69	18.26	13.19	0.325
	37	1.0	22.67	20.49	0.69	17.94	12.99	
	38	1.5	30.48	25.43	0.70	18.56	13.36	
	39	2.0	33.95	30.38	0.46	7.63	6.19	

Table 5.7

Analysis of Surface Strip Footing Tests Under

Vertical Loads on Dense Sand Overlying Clay

Test No.	h/B	q_u (psi) Observed	C_u (psi)	$q_2=C_u N_c$ (psi) Calculated	q_2/q_1	q_b (psi) Calculated	Deduced δ/ϕ_1	Experimental	
								$K_{t\gamma}$	K_{tq}
40	1	8.28	1.28	6.82	0.20	6.94	0.56	11.22	8.73
41	1	11.90	1.80	9.61	0.28	9.73	0.68	17.68	12.83
42	2	29.01	3.09	16.47	0.48	16.71	0.79	24.74	16.94

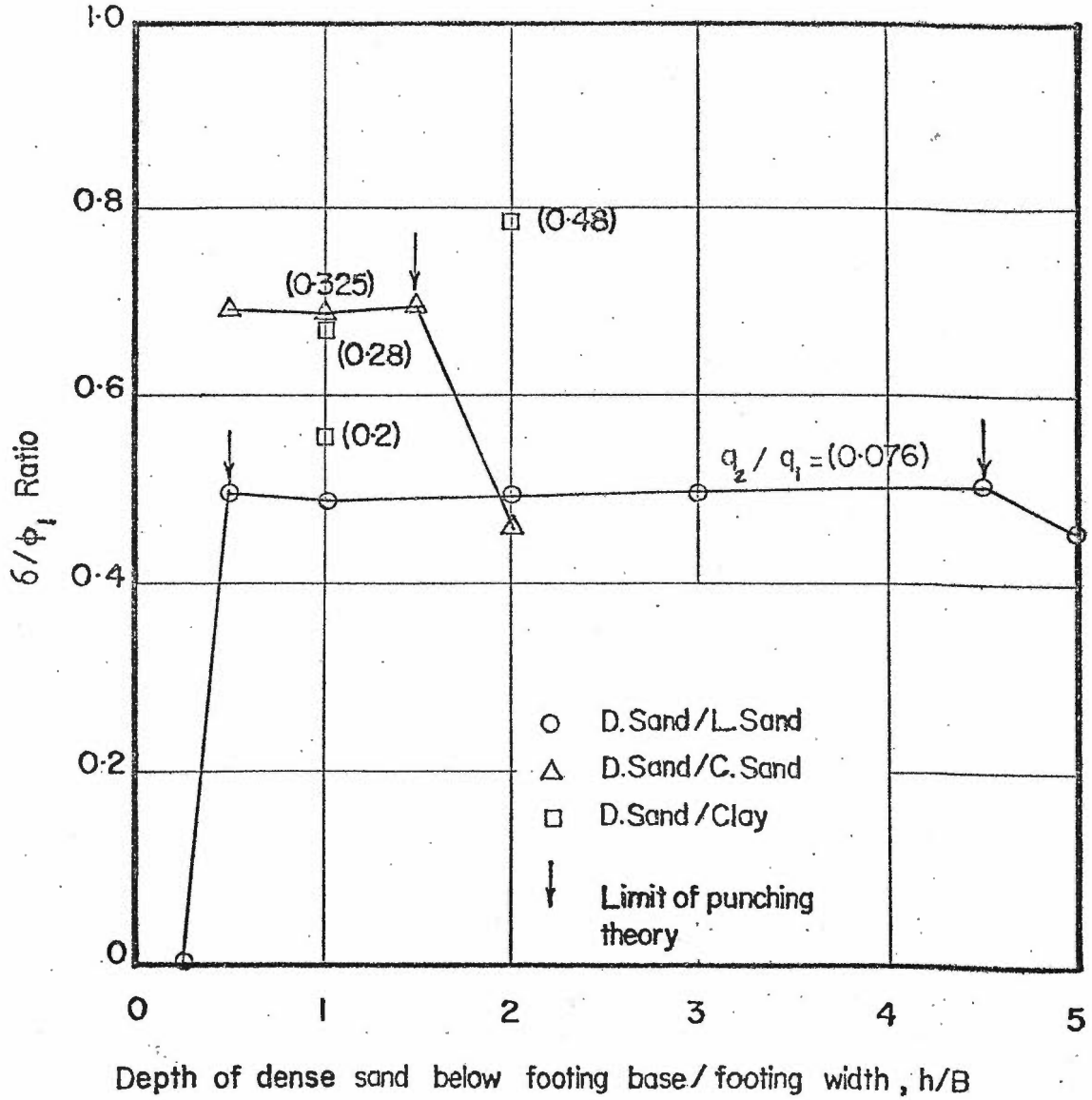

FIGURE 5·34 EXPERIMENTAL δ/ϕ_i RATIOS FOR SURFACE STRIP FOOTING ON A STRONG LAYER OVERLYING A WEAK LAYER — UNDER VERTICAL LOADS

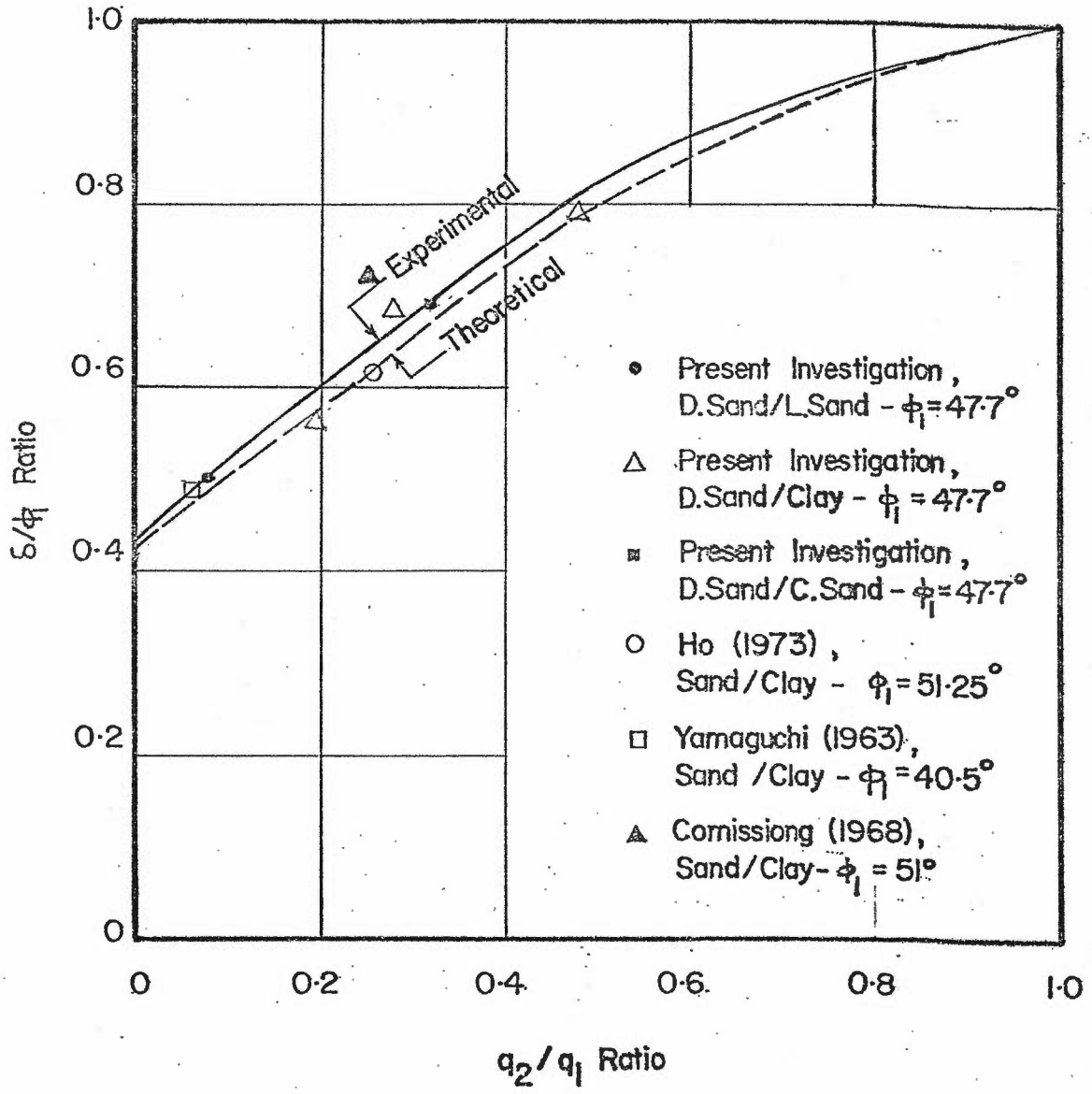

FIGURE 5·35 EXPERIMENTAL δ/ϕ_1 RATIO - FOR SURFACE STRIP FOOTING ON A STRONG LAYER OVERLYING A WEAK LAYER — UNDER VERTICAL LOADS

However, the bearing capacity theory for homogeneous soil gives theoretical results which are closer to the experimental values.

In practice, it is recommended that the foundation design be based on the homogeneous soil of the lower layer when the h/B ratio is less than the lower limit 0.5, regardless of the existence of a thin, dense sand layer. For h/B values beyond the upper limit, the design should be based on the homogeneous dense sand (upper layer), since the bottom layer theoretically, should have no influence on the ultimate bearing capacity of the layered system.

Experimental δ/ϕ_1 ratios obtained in this investigation and calculated from the data reported by other researchers are plotted against q_2/q_1 as shown in Figure 5.35. The quantity, q_2/q_1, is defined as the ratio of lower layer to upper layer ultimate bearing capacities of surface strip footings, each layer being considered to be separate and homogeneous. As shown in Figure 5.35, the initial q_2/q_1 ratio of the layered soil had a predominant influence on δ/ϕ_1 ratio.

From Figure 5.35 it is clear that the deduced δ/ϕ_1 ratio from the experimental work is usually less than unity. This ratio depends, to a large extent, on the q_2/q_1 ratio. This can be explained by the following arguments:

1. If the analysis is made on the real curved planes of failure, AB, (Figure 5.25), the angle of friction δ will be equal to ϕ_1. If, however, the analysis is made on the assumed vertical planes AC, the angle of friction δ

mobilized must be less than ϕ_1, as failure has not taken place on the assumed planes (Meyerhof, 1974).

2. The shear failure in the soil under a footing is a phenomenon of progressive rupture at variable stress levels (Muhs, 1963 and DeBeer, 1965 a, b, 1967). Thus, when the slip line AB (Figure 5.25) reached B, mobilizing the peak shear strength at that point, the soil strength at the beginning of the slip line (point A) must be less than that at B. In other words, the angle of shearing resistance at point A was less than that at point B. This behaviour is reflected in a decrease in the δ values.

3. Based on the fact that the failure strain of the upper dense sand was less than that of the lower weak layer, the simultaneous occurrence of shearing failure in both layers could not take place and more strain was required for the upper layer to reach the lower layer failure strain value. Thus, the mobilized angle of shearing resistance of the upper dense sand could be less than the peak value and higher than or equal to the residual value. However, rendering an interpretation of the ϕ_1 value would be rather difficult and questionable.

4. The mobilized passive earth pressure on the assumed failure planes decreased with a decrease in the lower layer strength. This can be explained by the fact that, with decreasing lower layer strength (represented by the

q_2 value), the vertical displacement of the dense sand column abcd (Figure 5.29.a) increased and the lateral movements decreased, resulting in a decrease in the passive pressure. This lateral movement may not be sufficient for the maximum mobilization of the passive pressure that would be generated by the full value of the angle of shearing resistance ϕ_1.

A mathematical verification for arguments 1 to 3 is difficult at best, if not impossible. Also, it is difficult to separate these effects in evaluating the average mobilized angle of shearing resistance (δ) and consequently, the mobilized passive pressure on the assumed failure planes. However, difficulties arising from these arguments may be overcome using the following assumptions. Firstly, if we allow that the average angle of shearing resistance (δ) must be less than the angle of shearing resistance (ϕ_1) and secondly, this angle δ is used in the form of a ratio of ϕ_1, then the effects of arguments 1, 2 and 3 are largely included in the analysis. These δ/ϕ_1 values can be determined experimentally for design purposes, as shown in Figure 5.35. It may be added that the δ/ϕ_1 values tend to unity as the q_2/q_1 values tended to unity. This may be explained by the fact that $q_2/q_1 = 1$ is the case of the homogeneous soil where the assumed vertical planes are real planes of failure in the radial shear zones (Meyerhof, 1951). Thus, the mobilized angle of shearing resistance (δ) on these vertical planes must be equal to the angle of shearing resistance (ϕ_1) of the soil (i.e. $\delta/\phi_1 = 1$). It is of interest to note that the relationship between δ/ϕ_1 and q_2/q_1 can be represented by the following equation:

$$\delta/\phi_1 = 0.43 + (q_2/q_1) - 0.45\ (q_2/q_1)^2 \qquad (5.24)$$

With respect to the fourth argument, unfortunately, no such general method of analysis has been developed for predicting the passive pressure in layered soils. However, in order to study the reduction in the passive pressure due to existence of the weak lower layer, a sliding surface was assumed, which consisted of a curved part (bd) and a straight part (de) behind a rough vertical wall (Figure 5.36). The curved portion (bd) of the sliding surface can either be an arc of a circle or a logarithmic spiral (Terzaghi, 1943 and Terzaghi and Peck, 1967). For the purpose of this study, both the friction circle method and the logarithmic spiral method were employed (Figures 5.36.a and 5.36.b respectively). The results of this analysis are given in Table 5.8. Table 5.8 and Figure 5.35 clearly show that the theoretical reduction factors R_γ and the relationship between q_2/q_1 and δ/ϕ_1 agreed well with the observed values.

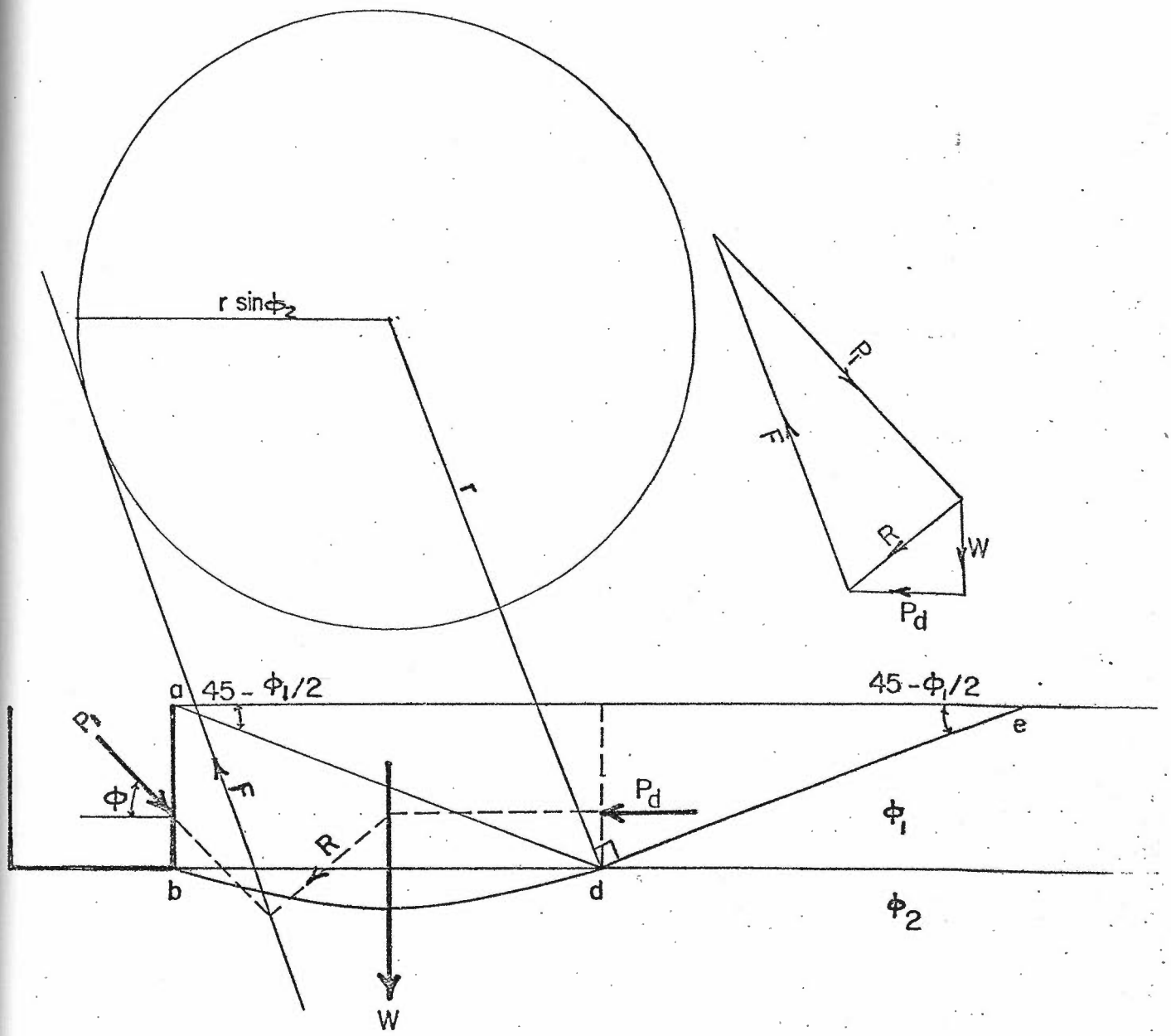

FIGURE 5·36·a FRICTION CIRCLE METHOD FOR DETERMINING PASSIVE EARTH PRESSURE ON THE ASSUMED PLANES OF FAILURES

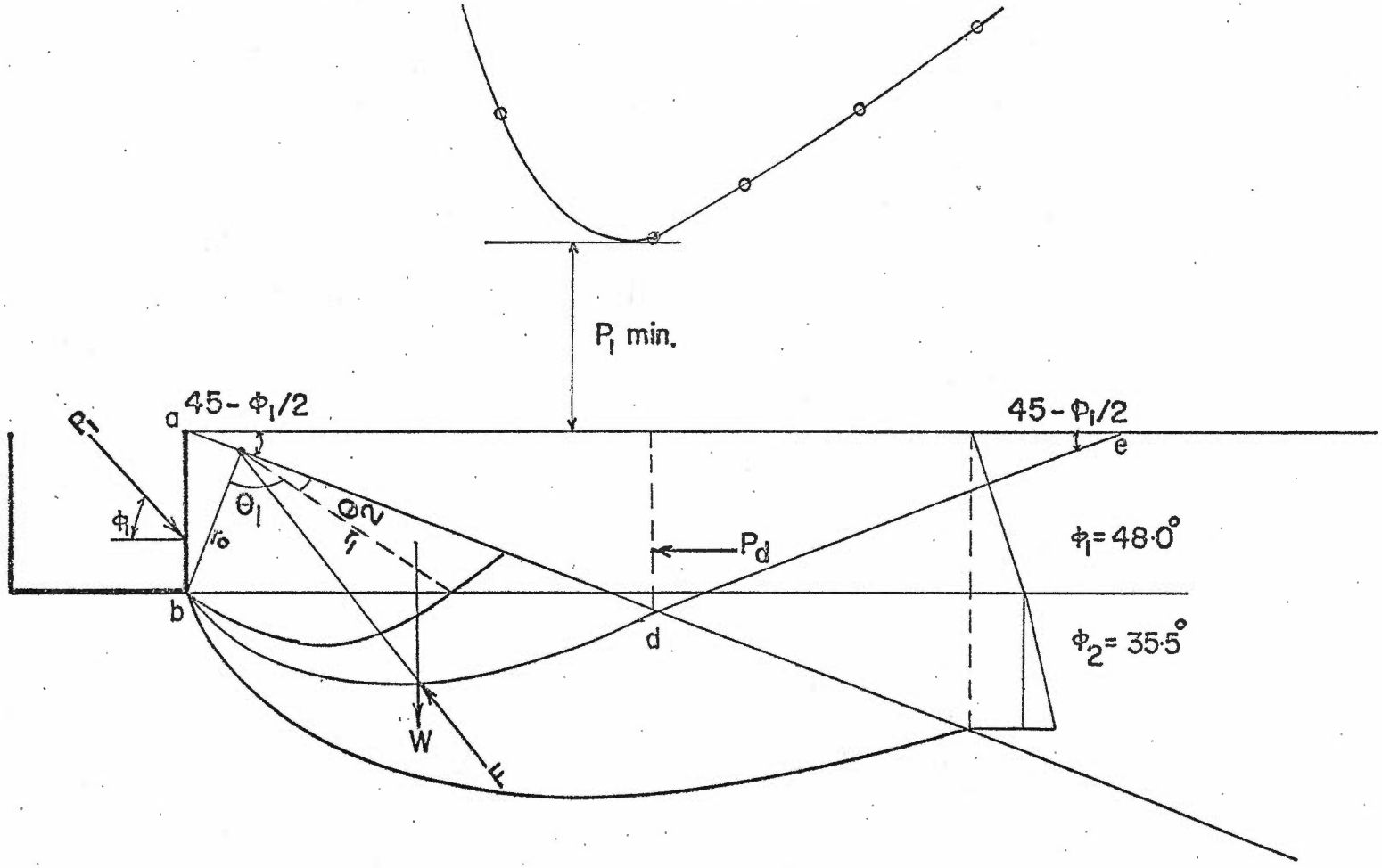

FIGURE 5·36·b LOGARITHMIC METHOD FOR DETERMINING PASSIVE EARTH PRESSURE ON THE ASSUMED PLANES OF FAILURES

Table 5.8

Comparison between the Experimental and Theoretical

Values of Reduction Factor R_γ

ϕ_1 (degrees)	ϕ_2 (degrees)	Experimental R_γ	Theoretical R_γ		Theoretical	
			Friction circle method	logarithmic spiral method	q_2/q_1	δ/ϕ_1
48	48	1.00	1.00	1.00	1.00	1.00
48	45	0.82	0.80	--	0.49	0.79
48	42.8	0.67	0.66	0.65	0.30	0.69
48	35.5	0.44	0.41	0.42	0.07	0.47
48	30	0.39	0.36	--	0.03	0.41

Based on the fact that the locally mobilized angle of shearing resistance (δ_z) on the assumed failure plane at point A (Figure 5.25) must be equal to the angle of shearing resistance of the upper layer (ϕ_1), since it is located on the assumed as well as on the real failure planes. Moving down from the point A to C on the assumed failure plane, the angle δ_z decreased with increasing the depth, z, (Figure 5.37.a) to a minimum value of $\lambda\phi_2$ at the point C at the soil interface. Bearing in mind that point C was not located on the real failure plane (point B), the value of λ must have been less than one. The value of λ does not depend only on the lower layer strength but also on the upper layer strength or on the relative strength of the two layers, since point C was located on the interface surface. The variation of the locally mobilized angle of shearing resistance (δ_z) with the depth (z) could be linear (Curve No. 1) or curved (Curve No. 2), (Figure 5.37.a).

Trial calculations using values of λ of 0, 0.1, 0.2, . . . , and unity showed that, the relationships represented in curve (1) (Figure 5.37.a) overestimated the average mobilized angle of shearing resistance δ along the assumed failure plane AC with respect to the deduced values from the present investigation. Similar calculations have been made with regard to curve (2) which could be part of a parabola or other curves. After several trials on different curve shapes with the factor λ varying from zero to one as mentioned above, the deduced average angles of shearing resistance (δ) could be calculated if:

(1) the factor λ was replaced with the ratio of q_2/q_1,

(2) the relationship represented by curve No. (2) was taken as a parabola with the following equation:

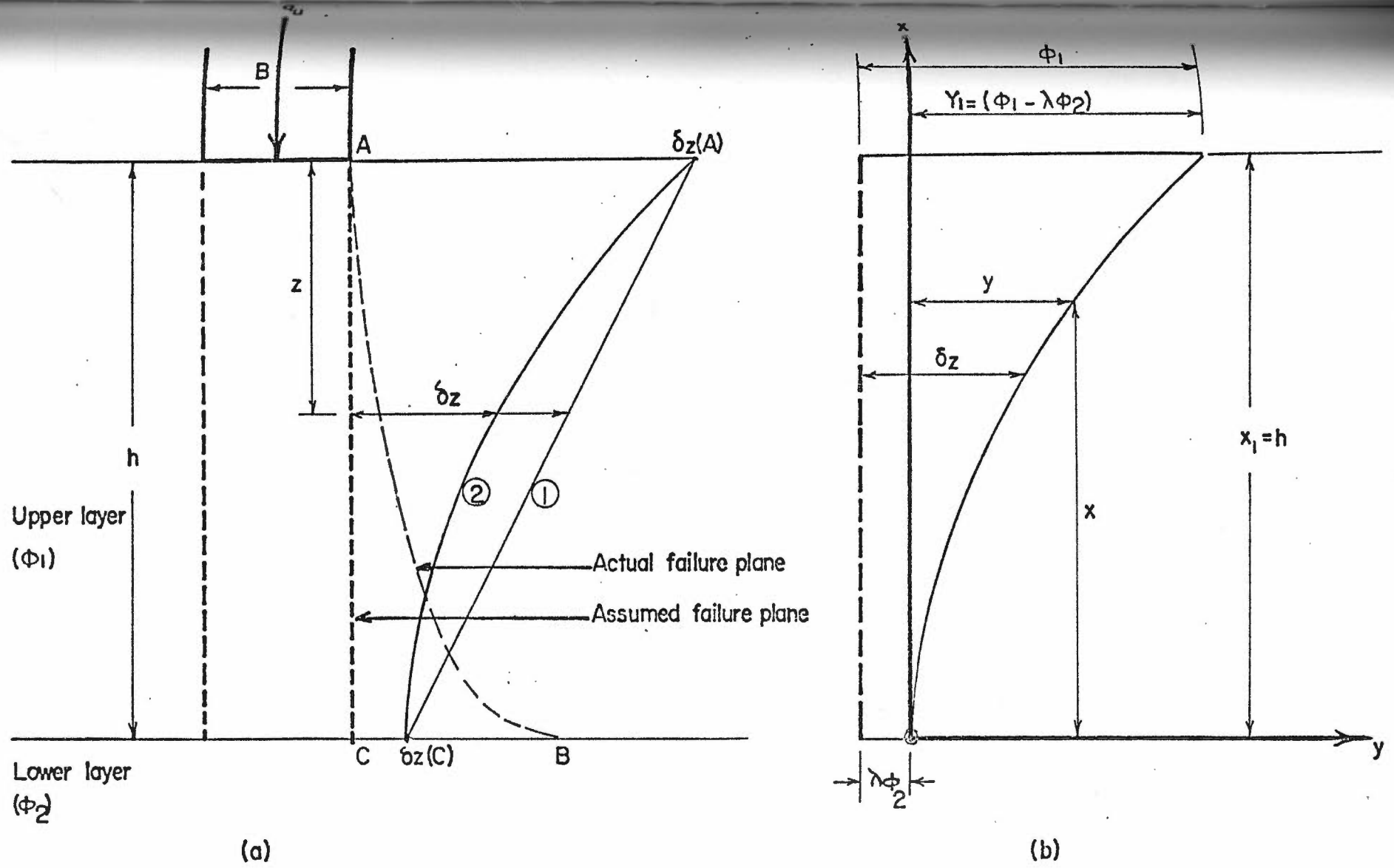

FIGURE 5·37 DISTRIBUTION OF THE LOCAL ANGLE OF SHEARING RESISTANCE ON THE ASSUMED FAILURE PLANE - STRIP FOOTING ON A STRONG LAYER OVERLYING A WEAK LAYER

$$y = ax^2 \qquad (5.25)$$

with the origin at the soil interface, the assumed failure plane and the interface plane between the two layers were assigned the "X" axis and "Y" axis respectively. Further "a" is a constant value of

$$a = \frac{Y_1}{(X_1)^2} \qquad (5.26)$$

where $X_1 = h$ = depth of the upper layer thickness below the footing base

and $Y_1 = \phi_1 - (q_2/q_1)\ \phi_2 \qquad (5.27)$

It should be noted here that the two assumptions mentioned above are reasonable assumptions and represent a reality since in item (1) the ratio q_2/q_1 expressed the relative strength of the two layers and in item (2) the proposed parabola reflected the difference between the assumed failure plane from the real one, which had a direct effect on the δ values. The analysis of the case of dense sand over loose sand and dense sand over compact sand are given in Table 5.9, and an example of the calculation is given in the following section.

Table 5.9

Comparison Between Theoretical and Experimental

Average δ/ϕ_1 Ratios

Case	ϕ_1 (degrees)	ϕ_2 (degrees)	q_2/q_1	Average δ/ϕ_1	
				Experimental	Theoretical
Dense/loose	47.7	35.5	0.076	0.50	0.57
Dense/Compact	47.7	42.8	0.325	0.69	0.66

Model Calculations

Case of Dense Sand overlying loose sand

$\phi_1 = 47.7^{\circ}$

$\phi_2 = 35.5^{\circ}$

$q_2/q_1 = 0.076 = \lambda$

$Y_1 = 47.7 - (0.076)\ 35.5 = 45.0$ (from equation 5.27)

Assume $h = 4 = X_1$, thus

$$a = \frac{Y_1}{(X_1)^2} = \frac{45}{(4)^2} = 2.81$$ (from equation 5.26)

Further $y = 2.81\ x^2$ (from equation 5.25)

and $\delta_z = \lambda\ \phi_2 + y = 2.70 + y$

Using these results, values of y and δ_z were calculated at different depths and consequently the δ_z/ϕ_1 ratios were calculated. As the values of δ_z/ϕ_1 were known and using $\phi = 47.7$, the values of the reduction factor, R_γ, were determined from Figure 5.32. The passive pressure coefficient, $K_{p\gamma(\delta)}$ at each depth were calculated from the follcwing equation

$$K_{p\gamma(\delta)} = R_{\gamma(\delta)} \cdot K_{p\gamma} \quad (\delta = \phi_1)$$

where

$$K_{p\gamma\ (\delta = \phi)} = 50.^0 \text{ for } \phi = 47.7^\circ \quad \text{(from Figure 5.29)}$$

$$\text{and } \alpha = 0^\circ$$

The values for $K_{p\gamma\ (\delta)}$ were calculated for values of x equal to 0, 1, . , and h and where an average value of $K_{p\gamma}$ for each unit depth was introduced. These values were calculated as following:

x	y	δ_z	δ_z/ϕ_1	R_γ	$K_{p\gamma(\delta)}$	Avergage $K_{p\gamma}$
0	0	2.70	0.06	0.16	7.75	
						8.40
1	2.81	5.51	0.12	0.18	9.00	
						11.40
2	11.24	13.94	0.29	0.28	13.75	
						20.12
3	25.29	28.00	0.59	0.53	26.50	
						38.25
4	44.96	47.70	1.00	1.00	50.00	

The integration of the total passive earth pressure along the depth h was 10.56 (psi) which gave an overall average passive pressure coefficient of 25.7. Thus

$$R_\gamma = \frac{K_{p\gamma\ (\text{overall})}}{K_{p\gamma\ (\delta = \phi)}} = \frac{25.7}{50.0} = 0.51$$

and from Figure 5.32 the corresponding δ/ϕ_1 value was 0.57. This value of δ/ϕ_1 compares reasonably well with that observed (Fig. 5.34).

In this analysis the depth ratio h/B was set at values of 2, 3, and 4 for each layer combinations, and it is of interest to note that the results yielded one average value for δ/ϕ_1 for each case which confirmed the results of the present investigation (Figure 5.34).

5.6 Analysis of Surface Strip Footing Tests Under Inclined Loads and Values of Coefficients of Punching Resistance

Employing equation 5.12 and data from Table 4.11, the experimental δ/ϕ_1 values were computed and plotted in Figure 5.38, from which the experimental coefficients of punching resistance, $K_{t\gamma}$ and K_{tq}, were calculated. These values are given in Table 5.11 and a model calculation is given below:

For h/B = 2, and $\alpha = 10^{\circ}$

From Figure 5.19, q_u = 6.7 psi and S = 0.26 inch

Calculation of Upper and Lower Layer Settlement S_1 and S_2

From Table 4.11, the settlements at failure for a surface strip footing, tested under $\alpha = 10^{\circ}$, on homogeneous dense and loose sand are 7% and 27% respectively. Thus

$$S_1 = 0.26 \times \frac{7}{(7 + 27)} = 0.05"$$

$$S_2 = 0.26 \times \frac{27}{(7 + 27)} = 0.21"$$

Calculation of q_b

From Table 5.3.a the bearing capacity factors, N_γ and N_q for

Table 5.10

Analysis of Surface Strip Footing Tests Under Inclined Loads

- Dense Sand Overlying Loose Sand

α (degrees)	$\frac{h}{B}$	q_u (psi) Observed	q_b (psi) Calculated	Deduced δ/ϕ_1	Experimental Punching Coefficients	
					$K_{t\gamma}$	K_{tq}
10	0.5	1.93	1.76	0.55	6.37	5.74
	1	3.15	2.43	0.55	6.37	5.74
	2	6.70	3.78	0.54	6.25	5.64
	3	11.70	5.15	0.54	6.14	5.54
	4	16.20	6.51	0.49	5.13	4.70
	4.5	17.25	7.19	0.45	4.30	3.95
20	0.5	0.90	0.79	0.60	4.51	4.65
	1	1.70	1.18	0.60	4.51	4.65
	2	4.20	1.97	0.59	4.43	4.57
	3	6.40	2.76	0.51	3.19	3.39
	3.3	7.00	2.99	0.49	2.92	3.16
	4	8.00	3.54	0.42	2.25	2.48

Table 5.10(continued)

Analysis of Surface Strip Footing Tests Under Inclined Loads

- Dense Sand Overlying Loose Sand

α (degrees)	$\frac{h}{B}$	q_u (psi) Observed	q_b (psi) Calculated	Deduced δ/ϕ_1	Experimental Punching Coefficients	
					$K_{t\gamma}$	K_{tq}
20	4.5	8.00	3.93	0.36	1.66	1.89
30	0.5	0.45	0.36	0.66	3.26	3.80
	1	1.00	0.60	0.65	3.14	3.70
	2	2.15	1.07	0.53	2.01	2.50
	2.5	2.85	1.31	0.49	1.78	2.25
	3	3.20	1.55	0.43	1.37	1.76

NOTE: q_u have been read from Figure 5.19.

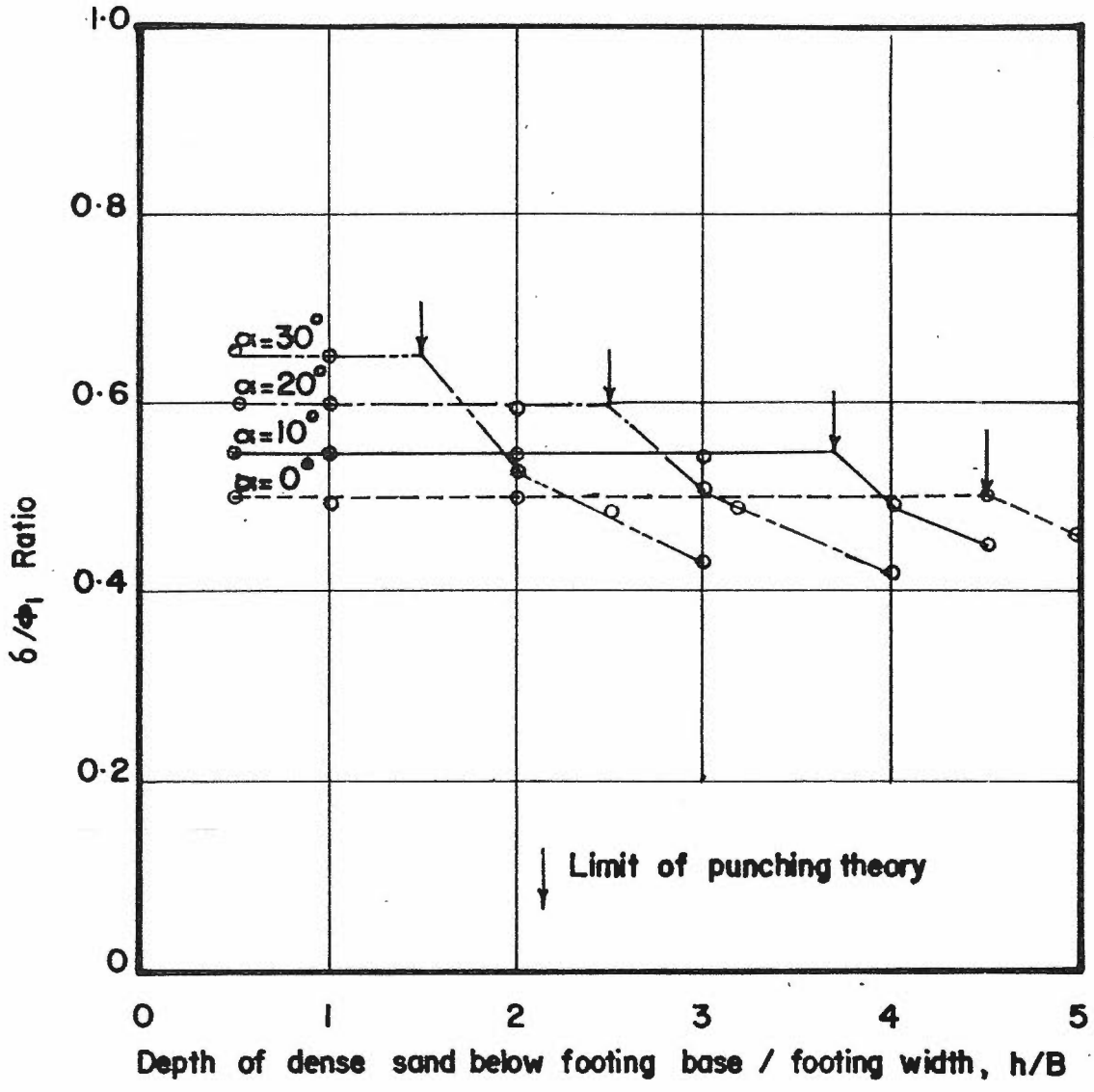

FIGURE 5·38 EXPERIMENTAL δ/Φ_1 RATIOS FOR STRIP FOOTING ON DENSE SAND OVERLYING LOOSE SAND - UNDER INCLINED LOADS

a strip footing under $\alpha = 10^{o}$, were 17.5 and 11.5, respectively. Thus

$$q_b = 0.5\ \gamma_2\ BN_\gamma + (\gamma_1 H + \gamma_2 S_2)\ N_q$$

where

$\gamma_1 = 0.06$ psi (Dense Sand)

$\gamma_2 = 0.05$ psi (Loose Sand)

$q_b = 0.5 \times 0.05 \times 2 \times 17.5 + (0.060 \times 4 + 0.05 \times 0.21)\ 11.5$

$= 3.78$ psi

From Equation 5.21

$$\text{left hand-side} = \frac{\dfrac{q_u - q_b + \gamma_1 h \cos\alpha}{\gamma_1 h \sec\alpha}}{B}$$

$$= \frac{\dfrac{6.7 - 3.87 + 0.06 \times 4 \times \cos 10}{0.06 \times 4 \times \sec 10}}{2} = 25.16$$

$$\text{right hand-side} = K_{t\gamma} \cdot h \cdot \sec\alpha + 2K_{tq}\ (D + S_1)$$

$$= (R_\gamma\ K_{p\gamma} \cdot h \cdot \sec\alpha + 2R_q K_{pq}\ S_1)\ \sin\delta$$

where $K_{p\gamma} = 29.4$ (Figure 5.30)

$K_{pq} = 24.6$ (Figure 5.31)

for $\phi = 47.7^{o}$

and $\alpha = 10^{o}$

After several trials, a ratio of $\delta/\phi_1 = 0.54$ was found to satisfy the left-hand side of equation 5.20.

Working back to evaluate the right-hand side of this equation for $\delta/\phi_1 = 0.54$, and $\phi_1 = 47.7^{o}$

$R_\gamma = 0.48$ (from Figure 5.33)

and $R_q = 0.52$ (from Figure 5.33)

also $\delta = 26.0^{\circ}$, and $\sin\delta = 0.44$

Thus right-hand side = $(0.48 \times 29.4 \times 4 \times \sec 10^{\circ} + 2 \times 0.52 \times 24.6 \times 0.05) \sin (0.54 \times 47.7) = 25.46$ in.

Then $K_{t\gamma} = K_{p\gamma} \cdot R_{\gamma} \cdot \sin\delta$

$= 29.4 \times 0.48 \times 0.44 = 6.25$

and $K_{tq} = K_{pq} \cdot R_q \cdot \sin\delta$

$= 24.0 \times 0.52 \times 0.44 = 5.64$

From Table 5.10, one can note that the deduced δ/ϕ_1 ratio remained approximately constant with increasing h/B ratios up to a point defined by an arrow (point 1, Figure 5.19). For greater h/B ratios there was a transition region, terminated by a second arrow (point 2) on q_u versus h/B curves, (Figure 5.19), where the failure mechanism changed from punching to the classical bearing capacity failure for homogeneous soils.

The average δ/ϕ_1 values deduced from this investigation with $q_2/q_1 = 0.076$ are plotted against the inclination angle, α, in Figure 5.39. As shown in Figure 5.39, the δ/ϕ_1 value increased linearly with increasing angles of inclination (α). This can be explained by the following arguments:

1. By increasing the inclination angle, α, the horizontal movement increased and thus the mobilized passive pressure increased and consequently the δ/ϕ_1 ratio increased.

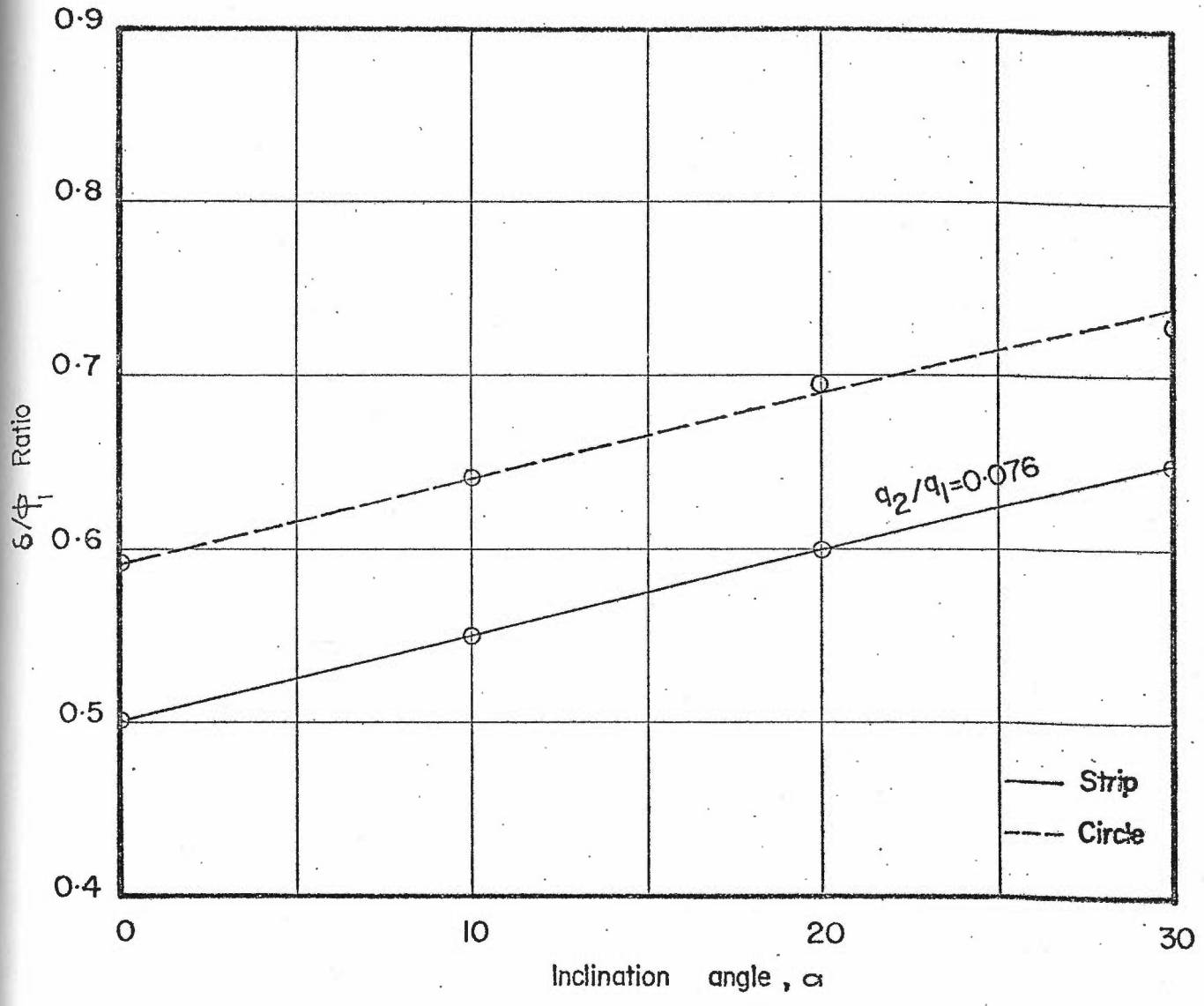

FIGURE 5·39 VARIATION OF THE AVERAGE MOBILIZED δ/ϕ_1 RATIOS WITH INCLINATION ANGLE, α - STRIP FOOTING ON DENSE SAND OVERLYING LOOSE SAND

2. By increasing the inclination angle (α) there was a possibility that the failure surface behind the dense sand column moved up and consequently, the effect of the weak lower layer decreased.

3. By increasing the inclination angle (α) the assumed failure plane was approaching the actual failure plane, and consequently the mobilized angle of shearing resistance (δ) on the assumed failure plane increased.

The rate of increase in the ratio δ/ϕ_1 with increasing inclination angle (α) may vary with the initial ratio of q_2/q_1 (calculated for surface strip footing under vertical load). However, it is recommended that the design of footings subjected to inclined loads be based on the δ/ϕ_1 values as determined for the same footing under vertical loads as shown in Figure 5.35. It is of interest to note that while the δ/ϕ_1 ratio increased with increasing inclination angle (α) the q_2/q_1 ratio determined at angle (α) decreased.

5.7 Analysis of Buried Strip Footing Tests Under Vertical And Inclined Loads and Values of Depth Factor

The increase in the ultimate bearing capacity, q_u, of a strip footing with depth in a layered system can be explained in terms of depth effects. Hence, Equation 5.13 can be modified to contain a depth factor, d_q, as follows:

$$q_u = q_b + \frac{\gamma_1 h \sec\alpha}{B} (K_{t\gamma} \cdot h \sec\alpha + 2d_q K_{tq} \cdot D) - \gamma_1 \cos\alpha \quad (5.28)$$

$$\leq q_t$$

In order to determine the values of the depth factor, d_q, to be introduced into the punching formula for the ultimate bearing capacity, the deduced coefficients of punching resistance $K_{t\gamma}$ and K_{tq} from the surface footing tests under the same load inclinations were used in Equation 5.28 and the data from Tables 4.3 and 4.11 for vertical and inclined loads respectively. The results are given in Tables 5.11 to 5.14 for footings under vertical and inclined loads, respectively, and presented in graphical form in Figure 5.40.

From Figure 5.40, it can be seen that the strength of the overburden contributed considerably more to the punching resistance of the layered system than was the case for ultimate bearing capacity of homogeneous dense sand for which $d_q = 1 + 0.26\ D/B$ (Meyerhof, 1963) for vertical load. This may be explained by the fact that the failure mechanism in the layered system was not the same as in the case of a homogeneous soil. However, the following empirical formula which is represented as full lines in Figure 5.40 may be suggested:

$$d_q = 1 + 0.15 \frac{D}{B} \tan\left(45 + \frac{\phi}{2}\right) (1 - \tan\alpha) \left\{1 + 0.28 \frac{h}{B} (1 - \tan\alpha)\right\} \qquad (5.29)$$

Table 5.11

Analysis of Buried Strip Footing Tests in Dense Sand Overlying Loose Sand - Under Vertical Loads ($\alpha = 0^{o}$)

Test No.	$\frac{h}{B}$	$\frac{D}{B}$	q_u (psi) Observed	q_b (psi) Calculated	Deduced Depth Factor d_q
25	0.5	0.5	5.26	4.34	1.37
--	1.0		7.70	5.29	1.43
26	2.0		14.71	7.19	1.73
27	3.0		24.66	9.10	2.11
--	4.0		37.00	10.98	2.38
28	4.5		44.01	11.93	2.49
31	0.5	1.0	7.02	5.34	1.55
32	1.5		14.48	7.21	1.77
33	3.0		31.85	10.09	2.21
--	4.0		47.80	11.98	2.56
34	4.5		56.82	12.92	2.70

Table 5.12

Analysis of Buried Strip Footing Tests in Dense Sand Overlying Loose Sand - Under Inclined Loads ($\alpha = 10^{o}$)

$\frac{h}{B}$	$\frac{D}{B}$	q_u (psi) Observed	q_b (psi) Calculated	Deduced Depth Factor d_q
0.5	0.5	3.10	2.46	1.25
1.0		4.80	3.13	1.30
2.0		9.70	4.49	1.51
3.0		16.30	5.85	1.64
4.0		24.85	7.20	1.85
4.5		28.00	7.88	1.40
0.5	1.0	4.40	3.16	1.45
1.0		6.75	3.84	1.51
2.0		13.00	5.22	1.65
3.0		21.40	6.58	1.83
4.0		31.75	7.95	1.99
4.5		37.80	8.62	2.09

Table 5.13

Analysis of Buried Strip Footing Tests in Dense Sand Overlying Loose Sand Under Inclined Loads ($\alpha = 20^{\circ}$)

$\frac{h}{B}$	$\frac{D}{B}$	q_u (psi) Observed	q_b (psi) Calculated	Deduced Depth Factor d_q
0.5	0.5	1.65	1.19	1.15
1.0		2.85	1.58	1.21
2.0		6.25	2.37	1.31
3.0		10.95	3.17	1.39
4.0		15.75	3.95	0.98
0.5	1.0	2.50	1.59	1.29
1.0		4.15	1.99	1.33
2.0		8.60	2.79	1.44
3.0		14.50	3.59	1.54
4.0		21.65	4.38	1.60
4.5		25.80	4.78	1.64

Table 5.14

Analysis of Buried Strip Footing Tests in Dense Sand Overlying Loose Sand - Under Inclined Loads ($\alpha = 30^{o}$)

$\frac{h}{B}$	$\frac{D}{B}$	q_u (psi) Observed	q_u (psi) Calculated	Deduced Depth Factor d_q
0.5	0.5	0.97	0.68	1.06
1.0		1.80	0.84	1.06
2.0		4.35	1.32	1.15
3.0		7.90	1.80	1.20
0.5	1.0	1.50	0.85	1.07
1.0		2.70	1.08	1.15
2.0		5.95	1.56	1.21
3.0		10.20	2.04	1.25
4.0		15.30	2.52	1.21

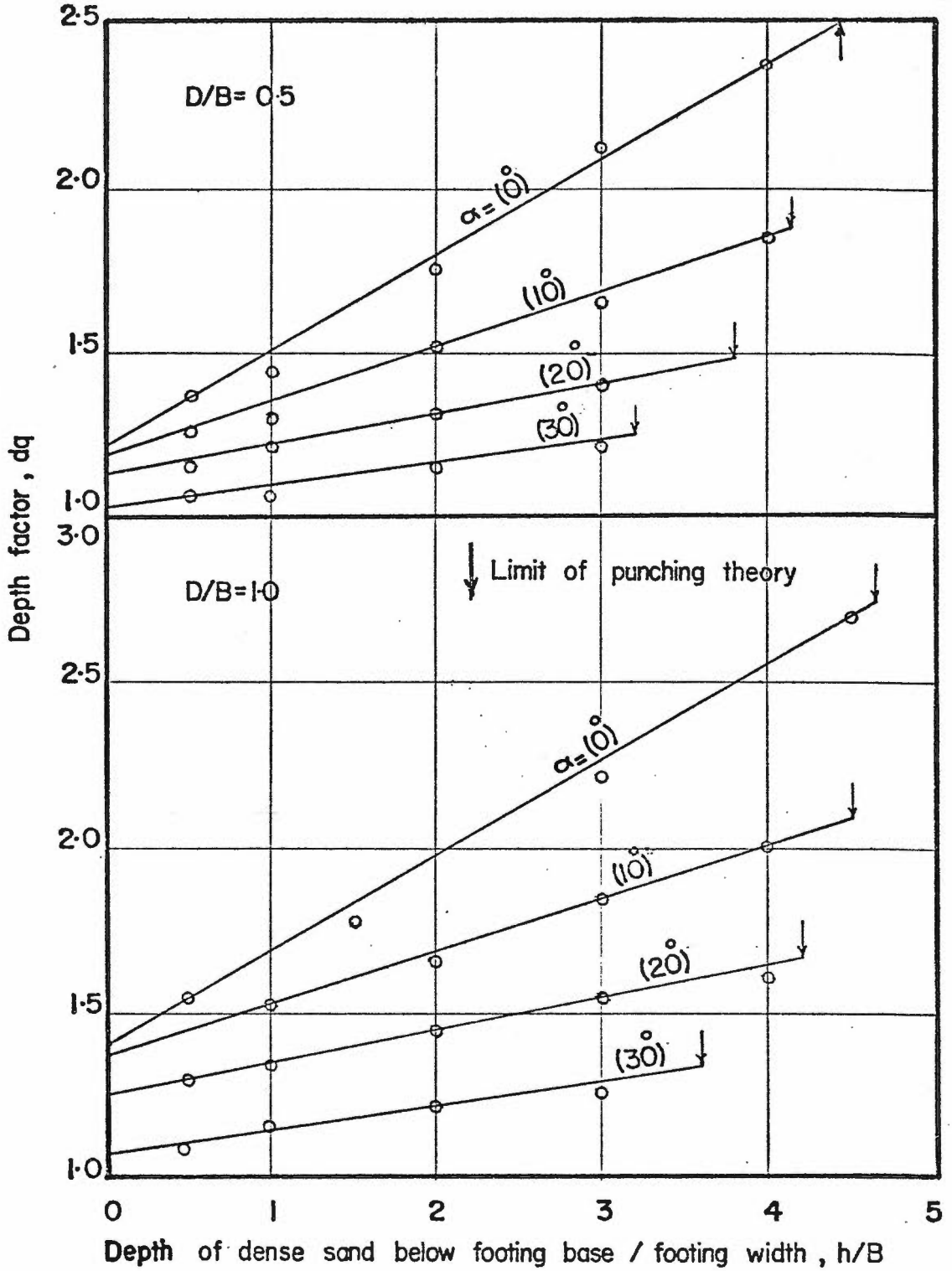

FIGURE 5·40 EXPERIMENTAL DEPTH FACTOR dq - STRIP FOOTING IN DENSE SAND OVERLYING LOOSE SAND

5.8 Analysis of Circular Footing Tests Under Vertical and Inclined Loads - and Values of Shape Factors

The relation between the coefficients of punching resistance of circular and strip footings can be expressed by means of shape factors defined as

$$s = \frac{\text{coefficient of punching resistance of circular footing}}{\text{coefficient of punching resistance of strip footing}}$$

(under the same load inclination, α)

Using Equation 5.18 and data from Tables 4.6 and 4.12 for surface footings under vertical and inclined loads respectively, the experimental δ/ϕ_1 values were computed from which the experimental values of the coefficients of punching resistance, $s_\gamma K_{t\gamma}$ and $s_q K_{tq}$ were computed. From the latter and the experimental values of coefficients of punching resistance for strip footing (Tables 5.6 and 5.10 for vertical and inclined loads, respectively) the shape factors, s_γ and s_q were calculated. These values are given in Tables 5.15 and 5.16 for vertical and inclined loads respectively, and presented in graphical form in Figures 5.41 and 5.42. From Figure 5.41 the experimental δ/ϕ_1 values and consequently the experimental coefficients of punching resistance $s_\gamma K_{p\gamma}$ and $s_p K_{pq}$ did not vary significantly with h/B ratio for the same inclination angle, α, up to a limiting depth ratio of the upper layer, at which the bearing capacity of homogeneous dense sand rules. In order to compare the experimental δ/ϕ_1 values for the case of dense sand overlying loose sand, deduced from circular footing tests under vertical and inclined loads to the values deduced from strip footing tests, it was decided to superimpose these ratios for circular footing

on Figure 5.39, from which it can be seen that the average mobilized δ/ϕ_1 ratios for circular footing are greater than those for strip footing. This was possibly due to higher passive pressures mobilized on the punching column in a circular footing as compared to a strip footing. As a result of greater δ/ϕ_1 values for circular than for strip footings, shape factors s_γ and s_q must be greater than one within the punching limits (Figure 5.42). Meyerhof (1974) suggested for conservative design the use of shape factors equal to unity for such footings under vertical loads, in other words to use the deduced δ/ϕ_1 ratio from a strip footing test (Figure 5.35) to predict the ultimate bearing capacity for a circular footing.

The buried circular footing tests were analyzed in order to bring out the depth effects. Thus, Equation 5.18 can be written as

$$q_u = q_b + \frac{2\gamma_1 \, h \sec \alpha}{B} (s_\gamma K_{t\gamma} \cdot h \sec \alpha + 2 \, d_q \, s_q K_{tq} \cdot D) - \gamma_1 h \cos \alpha \qquad (5.30)$$

Employing Equation 5.30, values of punching resistance $s_\gamma K_{t\gamma}$ and $s_q K_{tq}$ as deduced from surface footing tests (Tables 5.15 and 5.16), and data from Tables 4.6 and 4.12 for buried footings under vertical and inclined loads respectively, the experimental depth factors d_q were computed. These values which are given in Tables 5.17 to 5.20 and plotted in Figure 5.43 are generally smaller than the depth factors for strip footings. The following empirical formula for determining the factor d_q is suggested

$$d_q = 1 + \frac{0.15}{2} \frac{D}{B} \tan \left(45 + \frac{\phi}{2}\right) (1 - \tan \alpha) \left\{1 + 0.1 \frac{h}{B}\right\} \qquad (5.31)$$

Table 5.15

Analysis of Surface Circular Footing Tests on Dense Sand Overlying Loose Sand ($\alpha = 0$)

Test No.	$\frac{h}{B}$	q_u (psi) Observed	q_b (psi) Calculated	Deduced δ/ϕ_1	Experimental Punching Coefficients		Deduced Shape Factors	
					$s_\gamma K_{t\gamma}$	$s_q K_{tq}$	s_γ	s_q
43	0.5	3.77	2.94	0.59	12.88	9.94	1.44	1.37
44	1.0	6.90	3.85	0.59	12.67	9.78	1.42	1.35
45	1.75	14.30	5.26	0.58	12.42	9.17	1.39	1.26
46	2.0	15.86	5.74	0.54	10.44	8.25	1.17	1.14

Table 5.16

Analysis of Surface Circular Footing Tests Under Inclined Loads

- Dense Sand Overlying Loose Sand

α^o	$\frac{h}{B}$	q_u (psi) Observed	q_b (psi) Calculated	Deduced δ/ϕ_1	Experimental Punching Coefficient		Deduced Shape Factor	
					$s_\gamma K_{t}$	$s_q K_{tq}$	s_γ	s_q
10	0.5	2.60	2.01	0.64	8.96	7.65	1.40	1.33
	1.0	5.00	2.75	0.64	8.96	7.65	1.40	1.33
	1.5	8.00	3.50	0.61	8.18	7.08	1.29	1.24
	2.0	8.65	4.27	0.47	4.62	4.29	0.74	0.76
20	0.5	1.45	1.02	0.70	6.49	6.32	1.44	1.35
	1.0	3.20	1.52	0.69	6.27	6.14	1.39	1.32
	1.5	4.50	2.03	0.59	4.36	4.50	0.97	0.97
30	0.5	0.80	0.51	0.73	4.08	4.67	1.25	1.21
	1.0	1.70	0.87	0.63	2.94	3.48	0.93	0.94
	1.5	2.15	1.20	0.46	1.53	1.97	0.59	0.63

Note: q_u have been read from Figure 5.24.

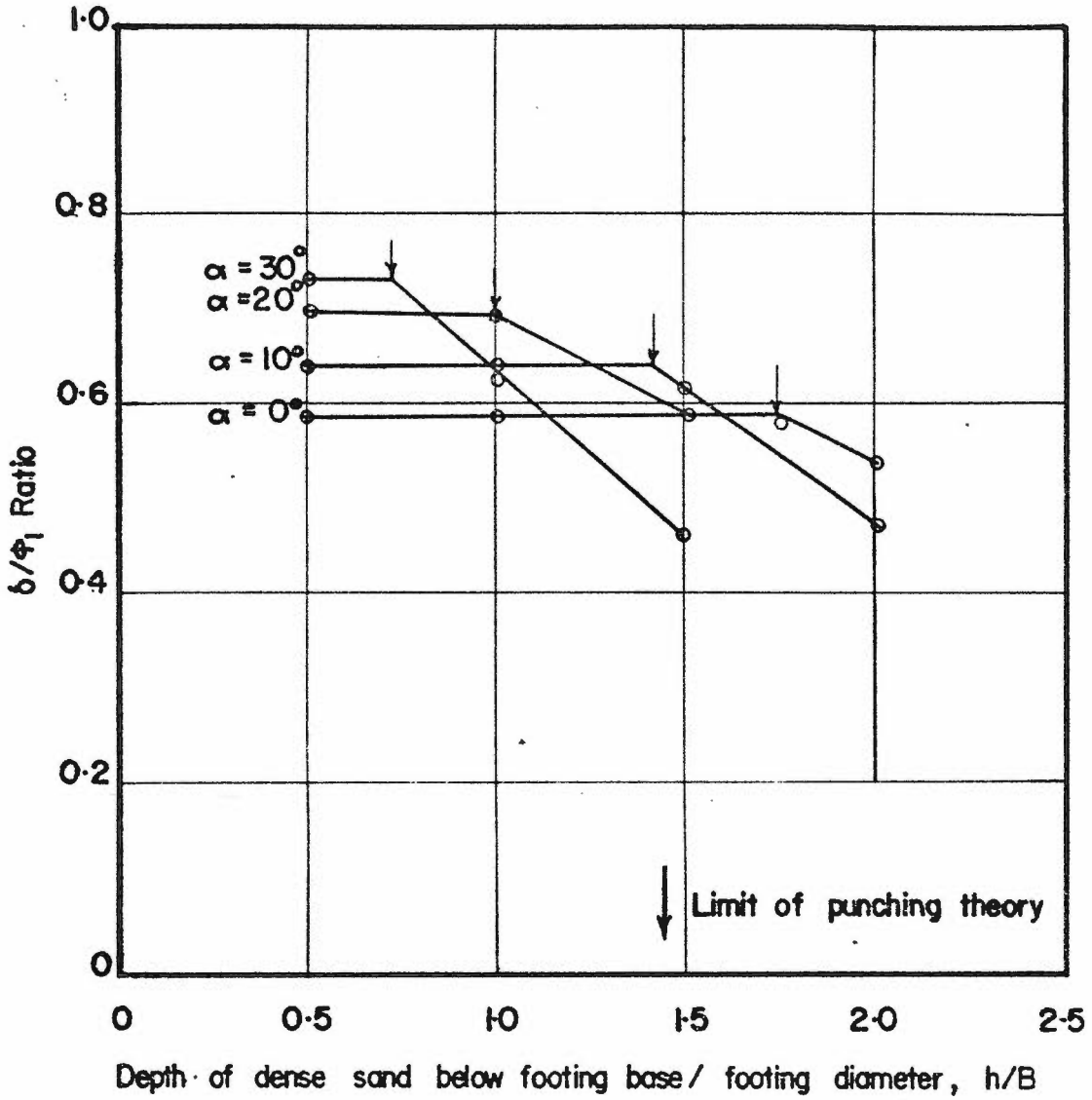

FIGURE 5·41 EXPERIMENTAL δ/ϕ_1 RATIOS FOR CIRCULAR FOOTING ON DENSE SAND OVERLYING LOOSE SAND - UNDER INCLINED LOADS

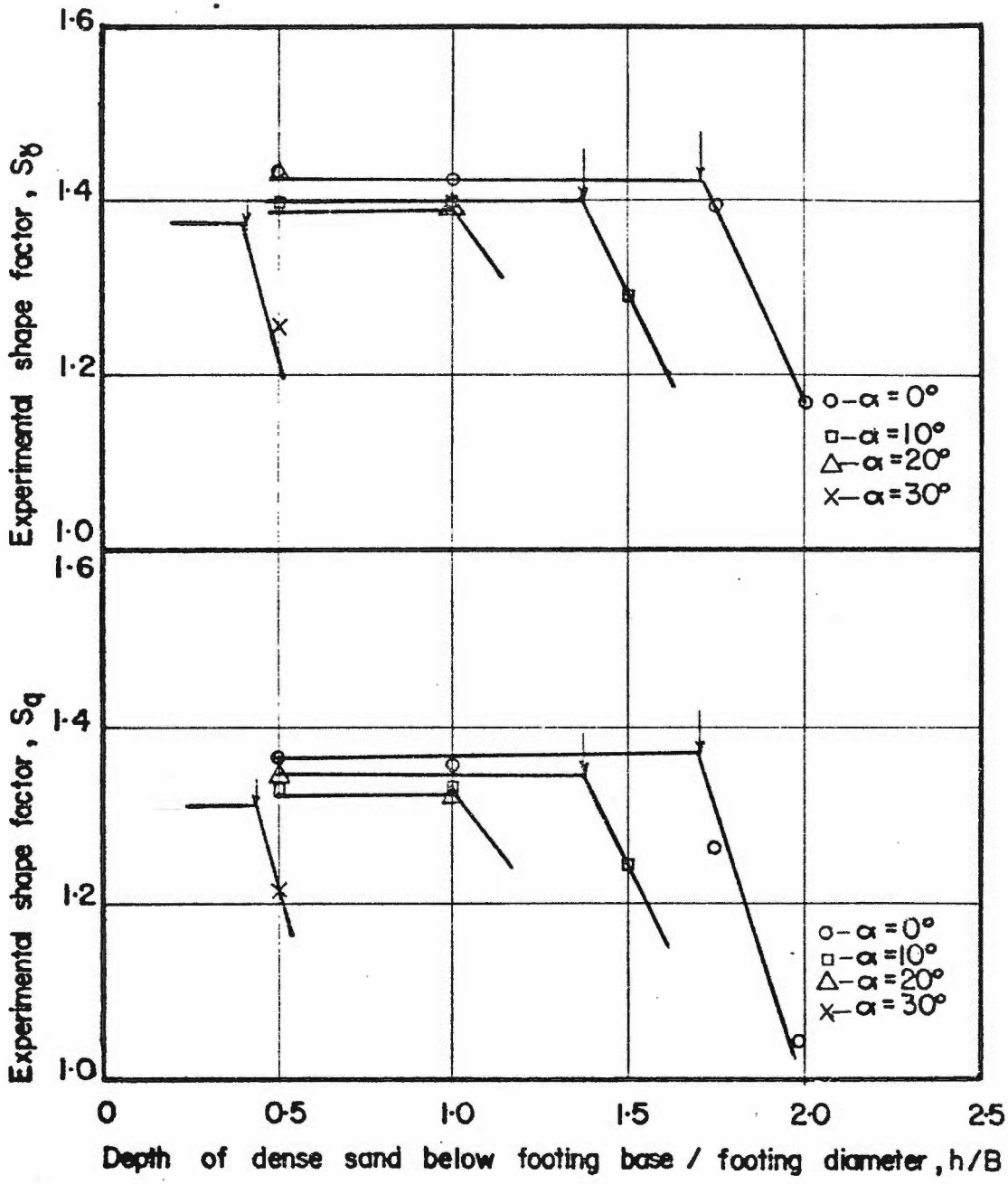

FIGURE 5·42 EXPERIMENTAL SHAPE FACTORS, S_γ AND S_q - CIRCULAR FOOTING ON DENSE SAND OVERLYING LOOSE SAND

Table 5.17

Analyses of Buried Circular Footing Tests in Dense Sand Overlying Loose Sand Under Vertical Loads ($\alpha = 0$)

Test No.	$\frac{h}{B}$	$\frac{D}{B}$	q_u (psi) Observed	q_b (psi) Calculated	Deduced Depth Factor d_q
48	0.5	0.5	6.13	3.92	1.15
49	1.5		17.49	5.77	1.23
50	2.0		25.18	6.72	1.27
53	1.0	1.0	15.24	5.84	1.29
54	1.5		23.95	6.78	1.39
55	2.0		34.16	7.73	1.45
56	2.5		40.64	8.65	1.07

Table 5.18

Analyses of Buried Circular Footing Tests in Dense Sand Overlying Loose Sand Under Inclined Loads ($\alpha = 10^{o}$)

$\frac{D}{B}$	$\frac{h}{B}$	q_u (psi) Observed	q_b (psi) Calculated	Deduced Depth Factor d_q
0.5	0.5	4.45	2.80	1.11
	1.0	8.00	3.56	1.14
	1.5	12.75	4.31	1.19
	2.0	17.70	5.07	1.00
1.0	0.5	6.55	3.59	1.23
	1.0	11.55	4.35	1.29
	1.5	18.10	5.11	1.39
	2.0	26.00	5.87	1.47

Table 5.19

Analyses of Buried Circular Footing Tests in Dense Sand Overlying Loose Sand - Under Inclined Loads ($\alpha = 20^{o}$)

$\frac{D}{B}$	$\frac{h}{B}$	q_u (psi) Observed	q_b (psi) Calculated	Deduced Depth Factor d_q
0.5	0.5	2.9	1.56	1.11
	1.0	5.6	2.08	1.12
	1.5	9.2	2.58	1.15
	2.0	12.5	3.10	0.81
1.0	0.5	4.5	2.09	1.21
	1.0	8.4	2.61	1.25
	1.5	13.4	3.13	1.31
	2.0	19.7	3.65	1.42

Table 5.20

Analyses of Buried Circular Footing Tests in Dense Sand Overlying Loose Sand - Under Inclined Loads ($\alpha = 30^{o}$)

$\frac{D}{B}$	$\frac{H}{B}$	q_u (psi) Observed	q_b (psi) Calculated	Deduced Depth Factor d_q
0.5	0.5	1.85	0.89	1.06
	1.0	3.90	1.23	1.10
	1.5	6.60	1.58	1.13
	2.0	9.15	1.93	0.84
1.0	0.5	3.00	1.25	1.13
	1.0	6.00	1.59	1.21
	1.5	9.75	1.94	1.27
	2.0	14.50	2.30	1.36

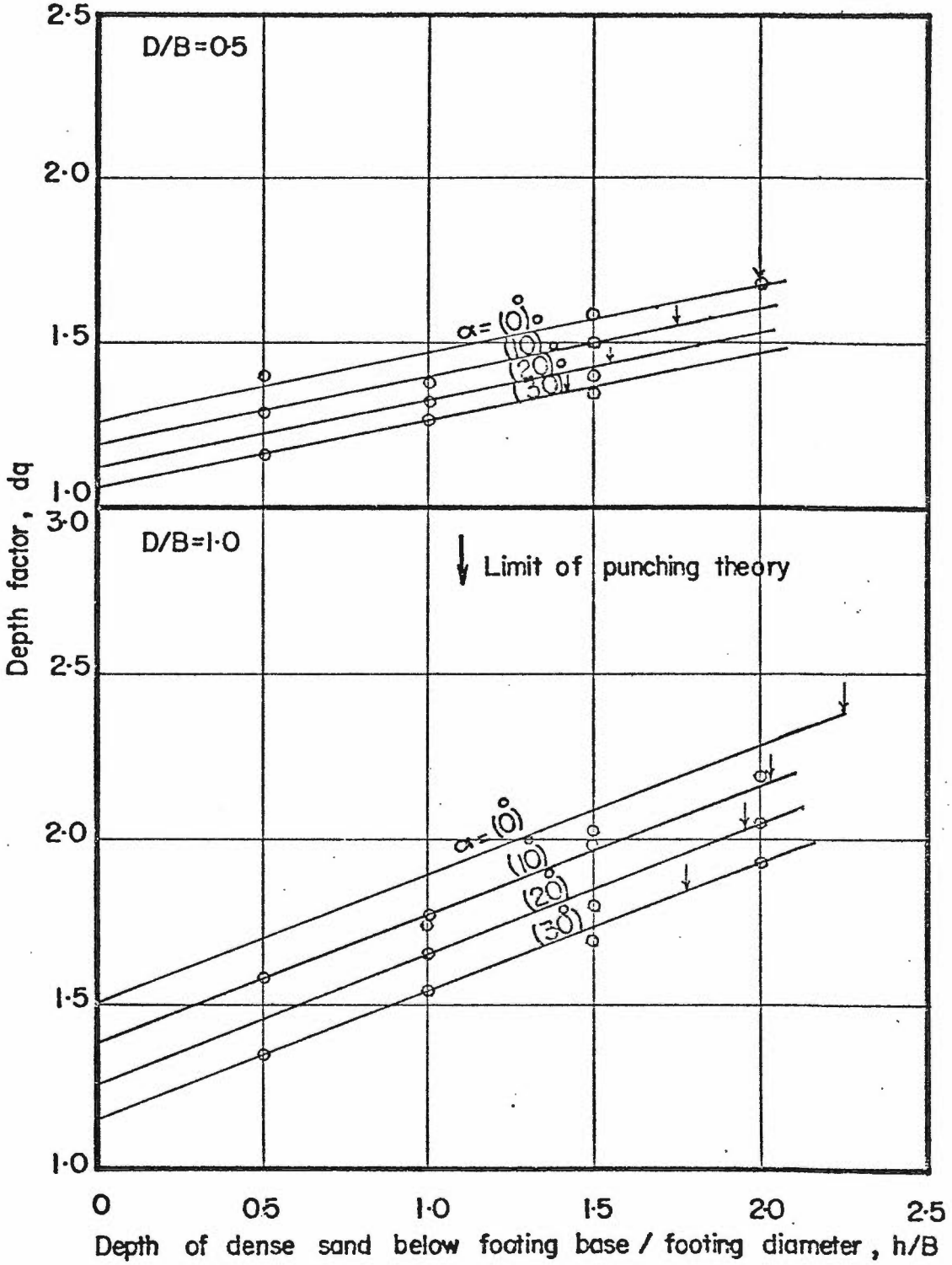

FIGURE 5·43 EXPERIMENTAL DEPTH FACTOR dq - CIRCULAR FOOTING IN DENSE SAND OVERLYING LOOSE SAND

5.9 Suggested Design Procedure for Footings in a Strong Layer Overlying a Weak Layer

The design method adopted currently and which was proposed by Meyerhof (1974) has the following limitations:

1. The theory was based on the weight component of the passive earth pressure coefficient, $K_{p\gamma}$, whereas the surcharge component, K_{pq}, becomes significant for buried footings.

2. The theory suggested an average value of $\delta/\phi_1 = 2/3$ to be used, which is in the middle of the engineering interest range. From Figure 5.34, a value of $\delta/\phi_1 = 2/3$ corresponds to a value of $q_2/q_1 = 0.35$. Thus, the theory will overestimate the punching resistance if $q_2/q_1 < 0.35$, and underestimate it if $q_2/q_1 > 0.35$.

The proposed design procedure on the basis of the present investigation has the following steps:

1. Based on the plane strain angles of shearing resistance of the upper and lower layers, ϕ_1 and ϕ_2, respectively or undrained shear strength, C_u, of the lower layer if it is clay, calculate q_1 and q_2 from the following equations

$$q_1 = \tfrac{1}{2} \gamma_1 B N_{\gamma 1}$$

$$q_2 = \tfrac{1}{2} \gamma_2 B N_{\gamma 2} \qquad \text{(for sand)}$$

$$= c_u N_c \qquad \text{(for clay)}$$

2. Using the ratio value of q_2/q_1, determine the δ/ϕ_1 ratio from Figure 5.35.

3. For a strip footing under vertical load, enter with this value of δ/ϕ_1 in Figure 5.44, to determine values of the punching coefficient $K_{t\gamma}$, K_{tq}. Use equation 5.14 to predict the ultimate bearing capacity.

4. For a circular footing under vertical load, use equation 5.20 with $s_\gamma = s_q = 1$.

5. For footings under inclined loads use equations 5.13 and 5.19 for strip and circular footings, respectively, with the values of K_p and R from Figures 5.30 to 5.33 with the above ratio of δ/ϕ_1 (conservative).

   As an alternative method for design footing under inclined loads, the designer may use the punching coefficient $K_{t\gamma}$ and K_{tq} for the same footing under vertical load, thus

$$K_{t\gamma(\alpha)} = i_{t\gamma} K_t \ (\alpha = 0)$$

and $$K_{tq(\alpha)} = i_{tq} K_{tq(\alpha = 0)}$$

   where $i_{t\gamma}$ and i_{tq} are inclination factors given in Figure 5.45. It is of interest to note that these factors are independent of δ/ϕ_1 ratios.

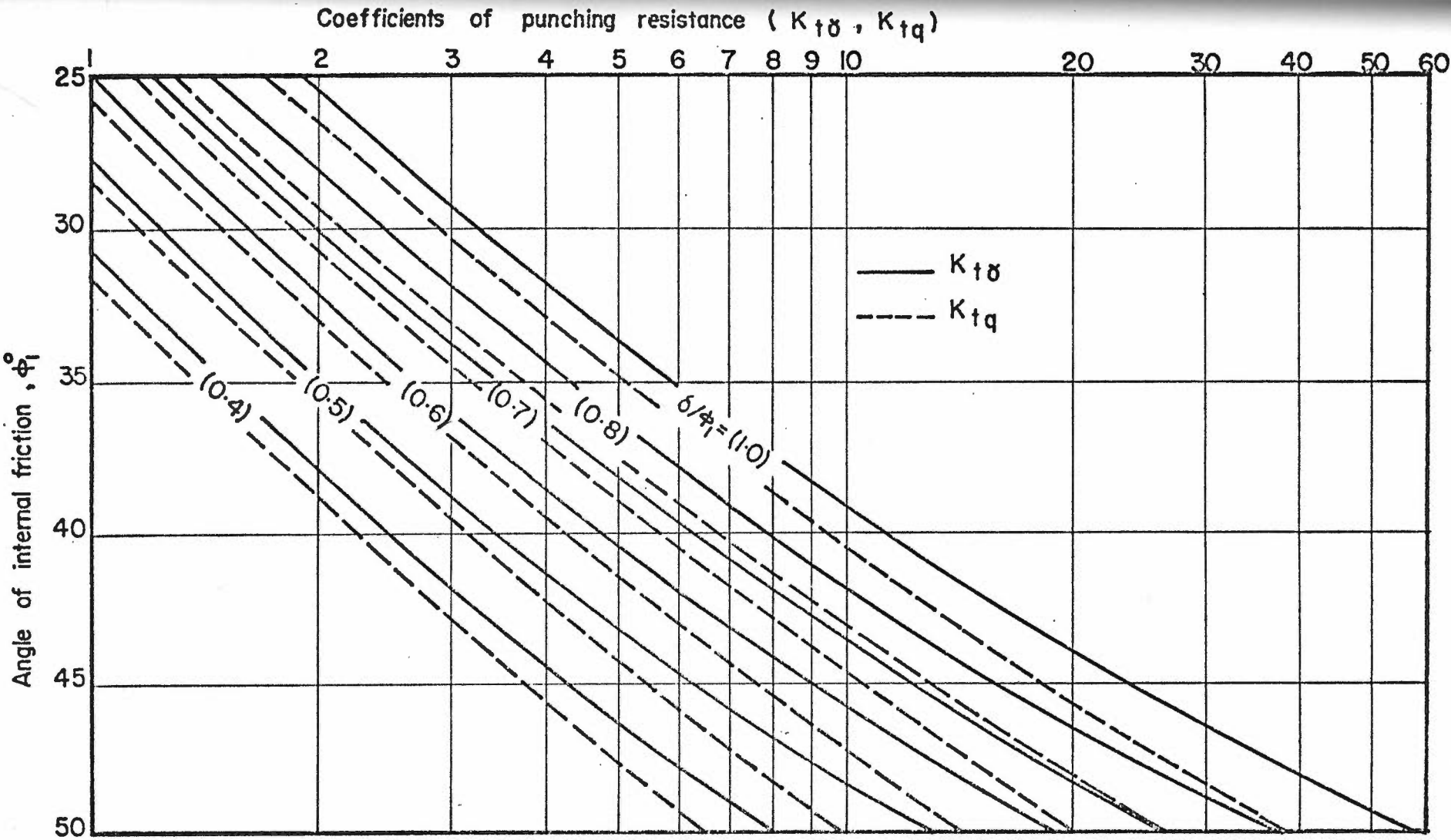

FIGURE 5·44 THEORETICAL COEFFICIENTS OF PUNCHING RESISTANCE FOR STRIP FOOTINGS - UNDER VERTICAL LOADS

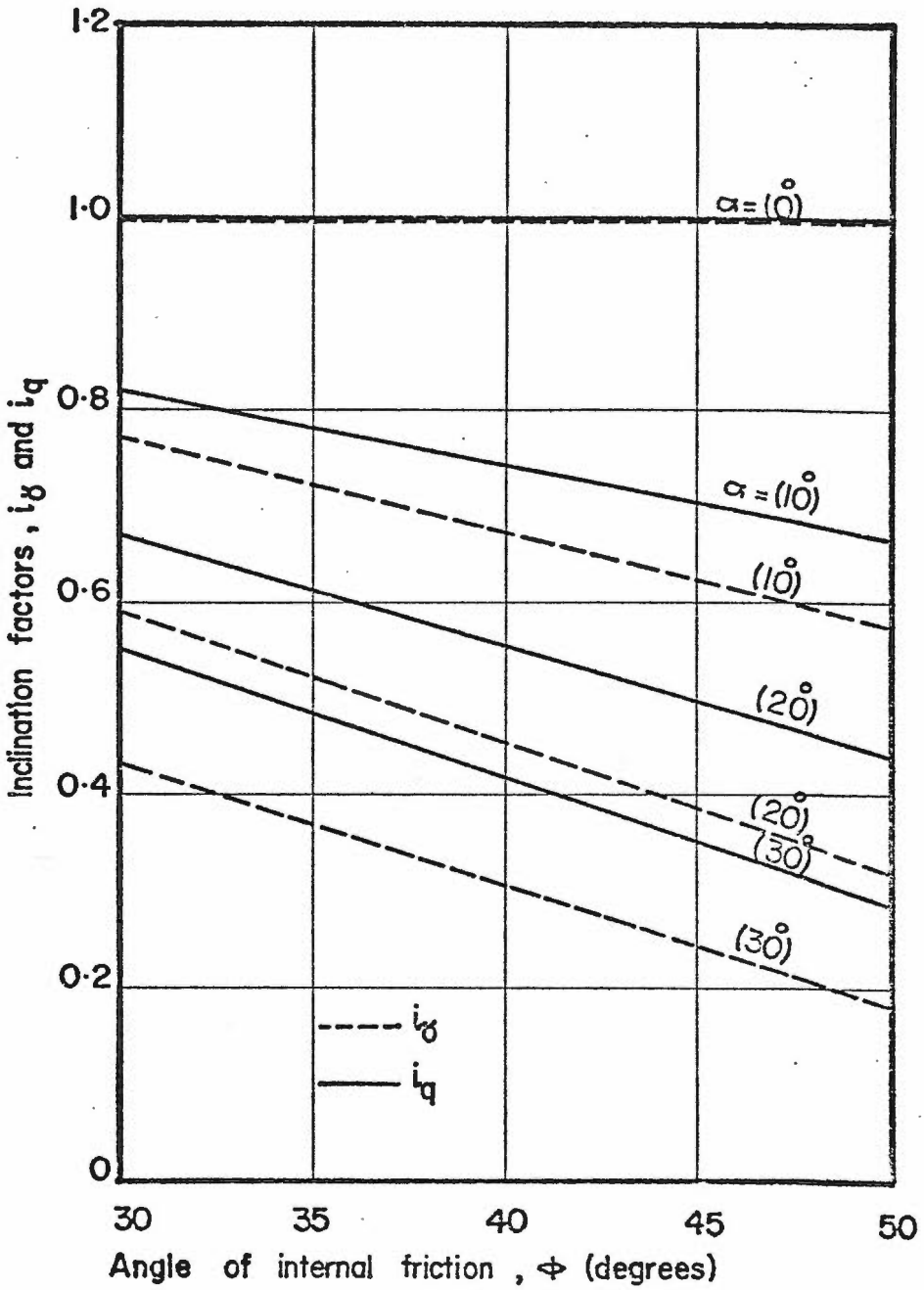

FIGURE 5·45 THEORETICAL INCLINATION FACTORS i_γ AND i_q - FOR STRIP FOOTINGS

Chapter 6

ANALYSIS AND DISCUSSION OF TEST RESULTS ON WEAK LAYER OVERLYING STRONG LAYER

6.1 General

The behaviour of footings in homogeneous weak soils has been investigated by various researchers and several design methods have been developed to determine their carrying load. However, the case of a weak layer resting on a strong layer is frequently encountered. The behaviour of footings in such soil combinations is a complex soil-structure interaction problem. Difficulties arise in defining the mode of failure of the soil in the footing vicinity and establishing an ultimate load criterion. The available literature provides very little information on this problem.

In this chapter an extension of the same method published by Meyerhof (1974) is made to analyze the present test results of footings on a loose sand layer overlying dense sand and on a compact sand layer overlying dense sand. The test results reported by previous researchers are also analyzed. The theory developed was further extended to apply to footings subjected to inclined loads. Test results of footings on homogeneous loose, compact and dense sand were given in Tables 4.2 and 4.10 for vertical and inclined loads, respectively, and have been discussed in Chapter 5. These results are used in the analysis of the test data on the two-layered soil systems.

6.2 Footing Tests on Two-Layered Systems

The test results of strip and circular footings under vertical loads (groups F through H) and under inclined loads (groups L and M) are summarized in Tables 4.7 to 4.9, and 4.13 and 4.14, respectively. In order to illustrate the influence of the lower dense sand layer on the footing capacity, as well as the load inclination angle, the test results are presented in this chapter in graphical form. For vertical load tests, Figures 6.1 through 6.3, show the variation of the ultimate bearing capacity, q_u, versus the ratio of the upper layer thickness below the footing base to the footing width or diameter, h/B, and for inclined load tests, Figures 6.4 through 6.9, show the variation of the ultimate bearing capacity, q_u, (inclined at angle α) versus the inclination angles α ranging 0 to 30°. Again, for convenience, the inclined load tests are represented in Figures 6.10 through 6.12 for comparison of the variation of the ultimate bearing capacity with h/B ratio for the various inclination angles.

The observed ultimate bearing capacity showed a rapid decrease with increased thickness of the upper weak layer below the footing base, from a maximum value for a footing at the interface to a minimum for a footing in the homogeneous upper soil layer. Also, the ultimate bearing capacity decreased rapidly with increasing load inclination angle (α). Observations of the layer deformation (in the strip footing series) Figures 6.13 and 6.14 for vertical and inclined load tests respectively, indicated that the rupture surface did not extend into the bottom dense sand layer, but was confined to the upper loose sand. In other words, the upper weak layer mass beneath the footing failed laterally by squeezing (Brown, 1967 and Meyerhof, 1974).

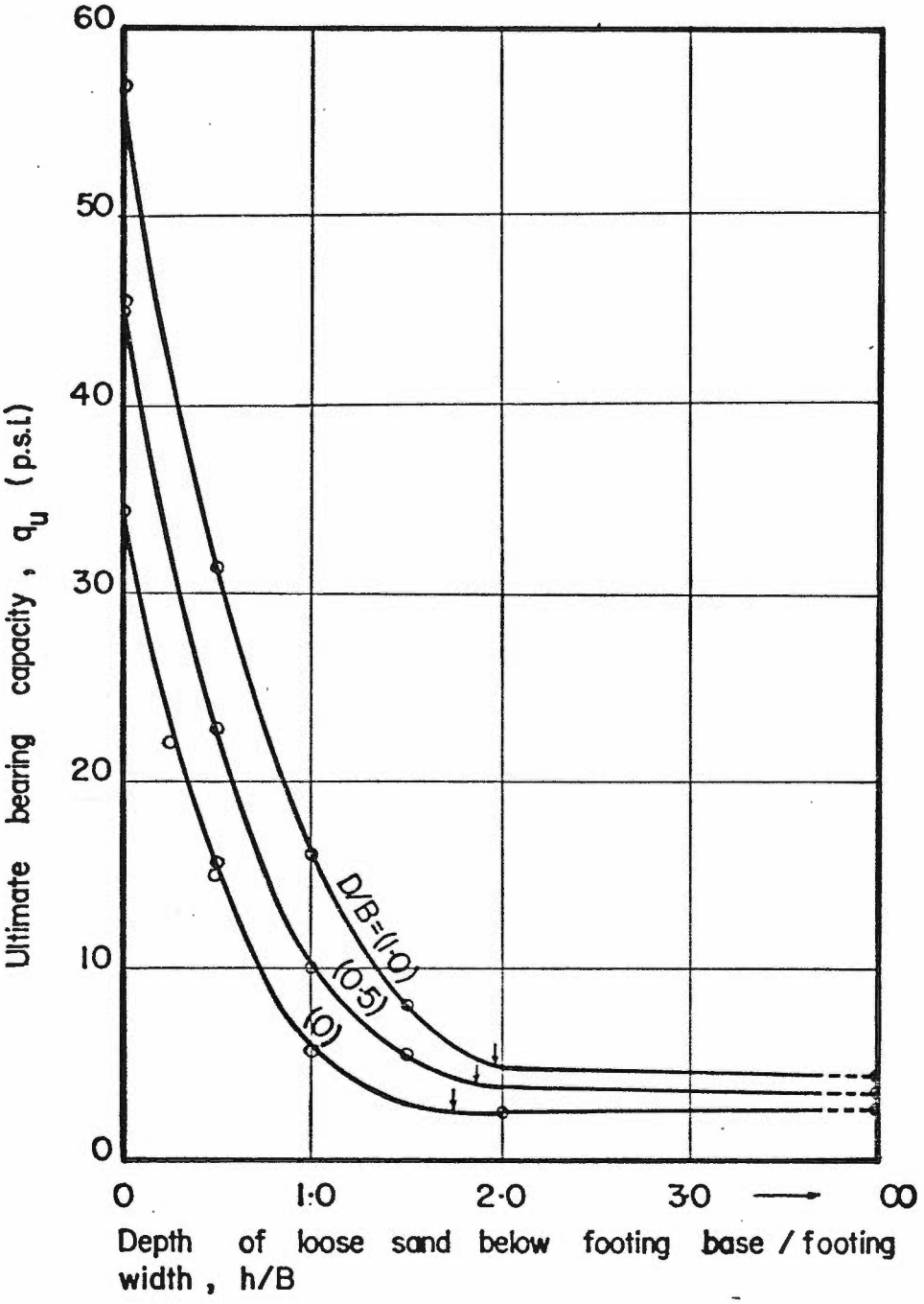

FIGURE 6·1 . SUMMARY OF TEST RESULTS - STRIP FOOTING IN LOOSE SAND LAYER OVERLYING DENSE SAND ($\alpha = 0°$)

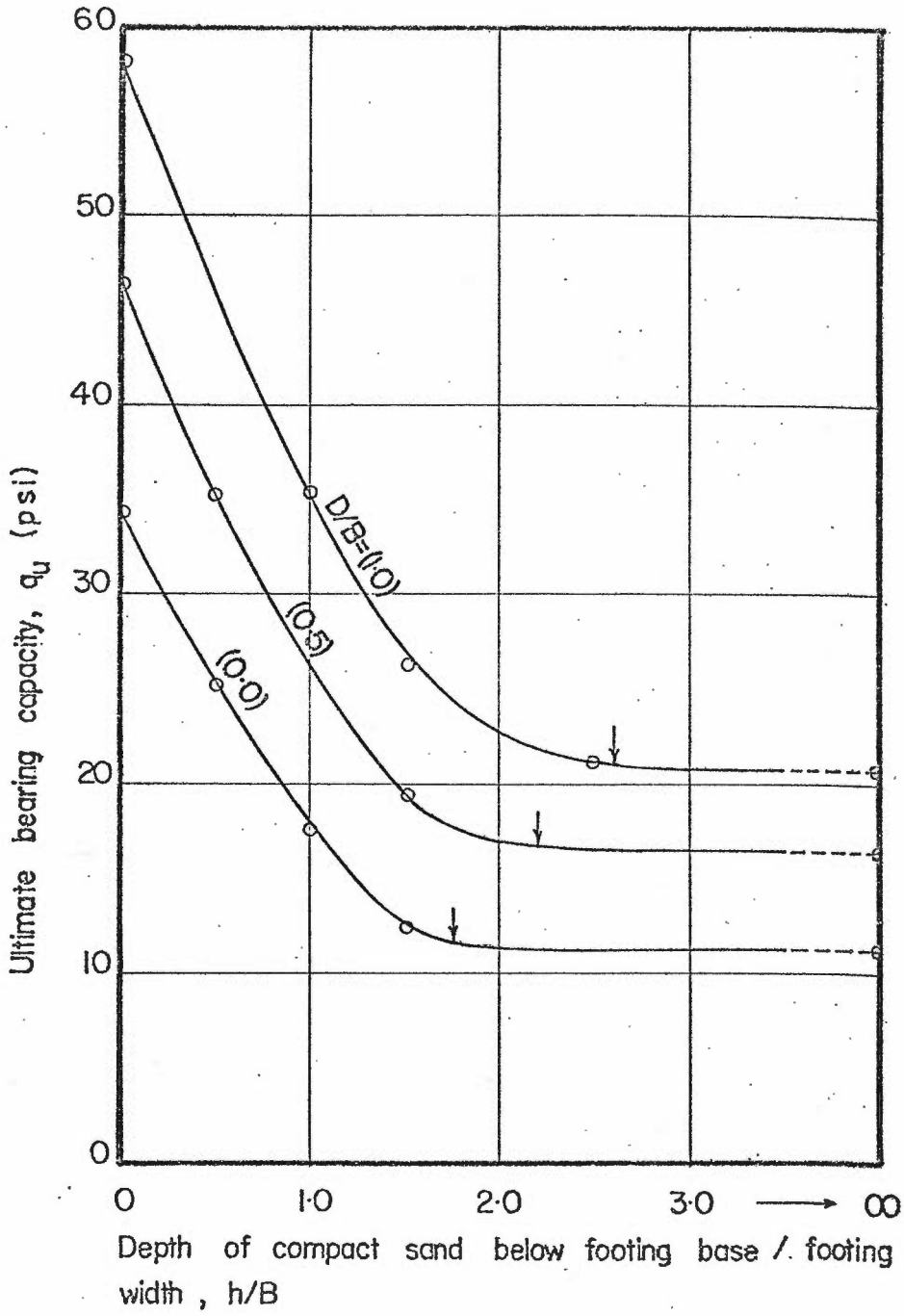

FIGURE 6·2 SUMMARY OF TEST RESULTS - STRIP FOOTING IN COMPACT SAND LAYER OVERLYING DENSE SAND ($\alpha = 0°$)

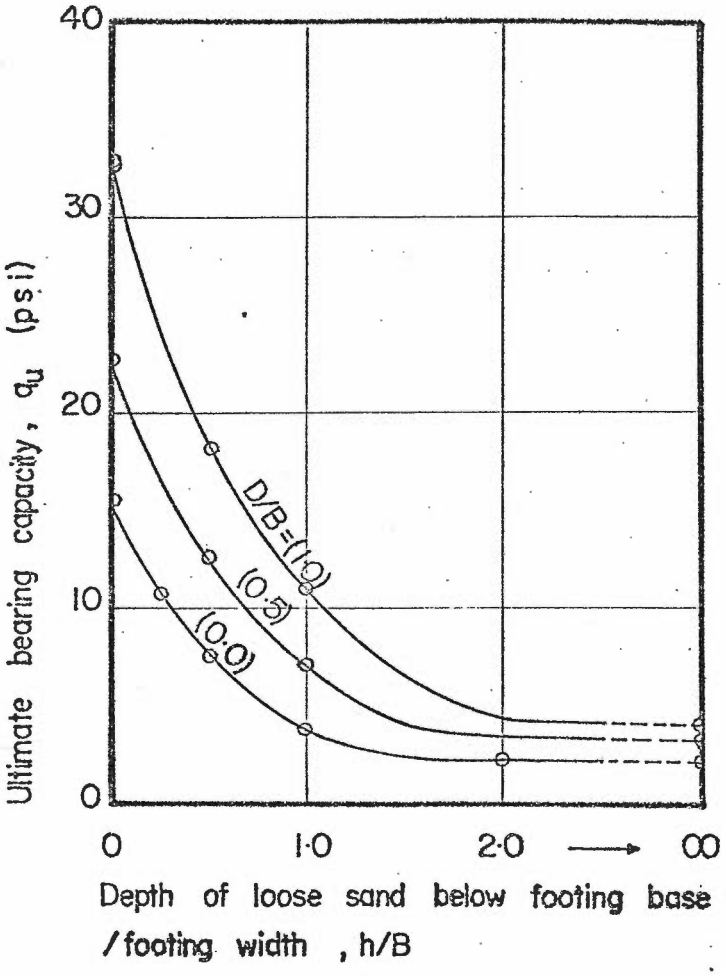

FIGURE 6·3 SUMMARY OF TEST RESULTS - CIRCULAR FOOTING IN LOOSE SAND LAYER OVERLYING DENSE SAND ($\alpha=0^{\circ}$)

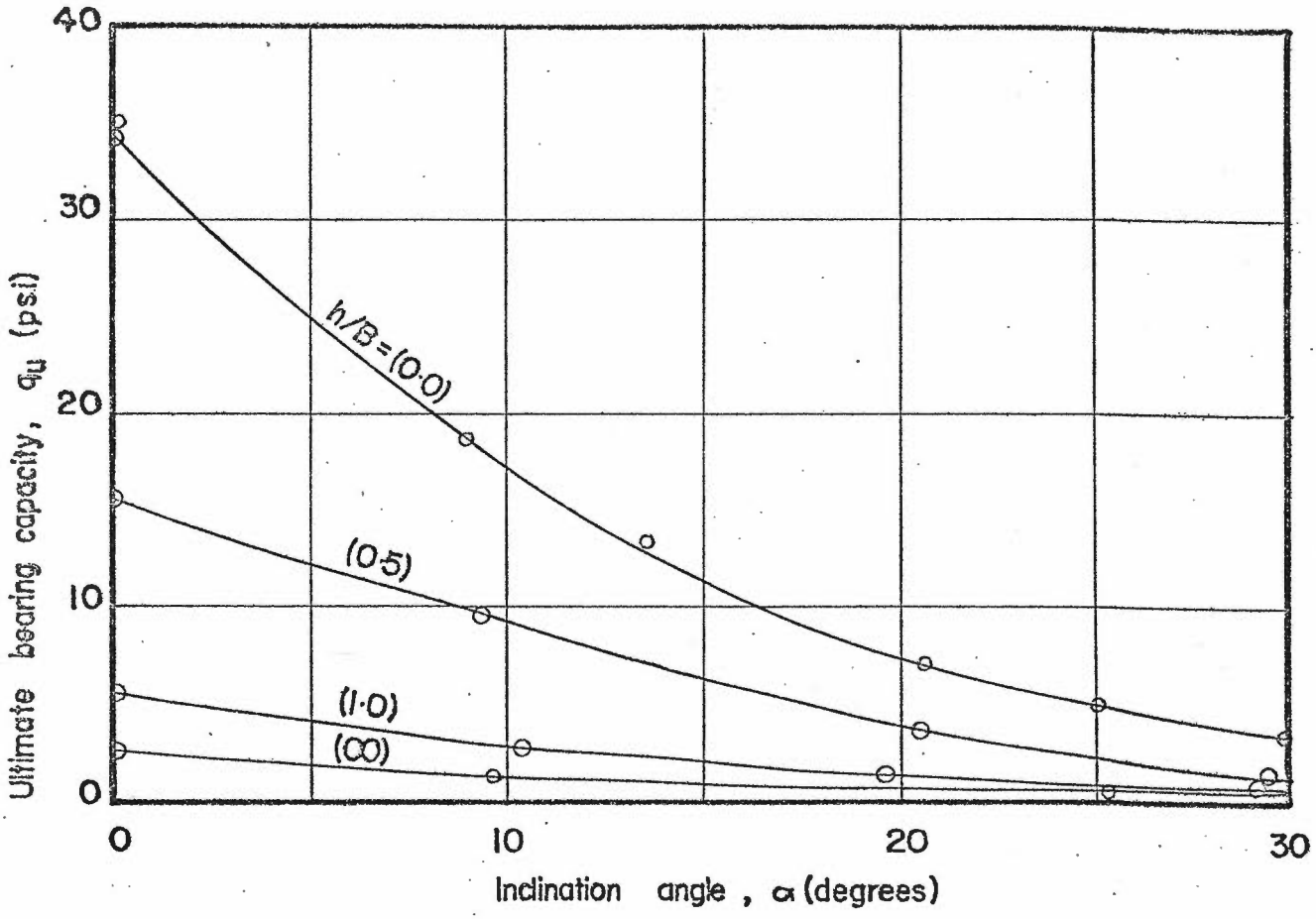

FIGURE 6·4 SUMMARY OF TEST RESULTS - STRIP FOOTING ON LOOSE SAND LAYER OVERLYING DENSE SAND (D/B = 0·0)

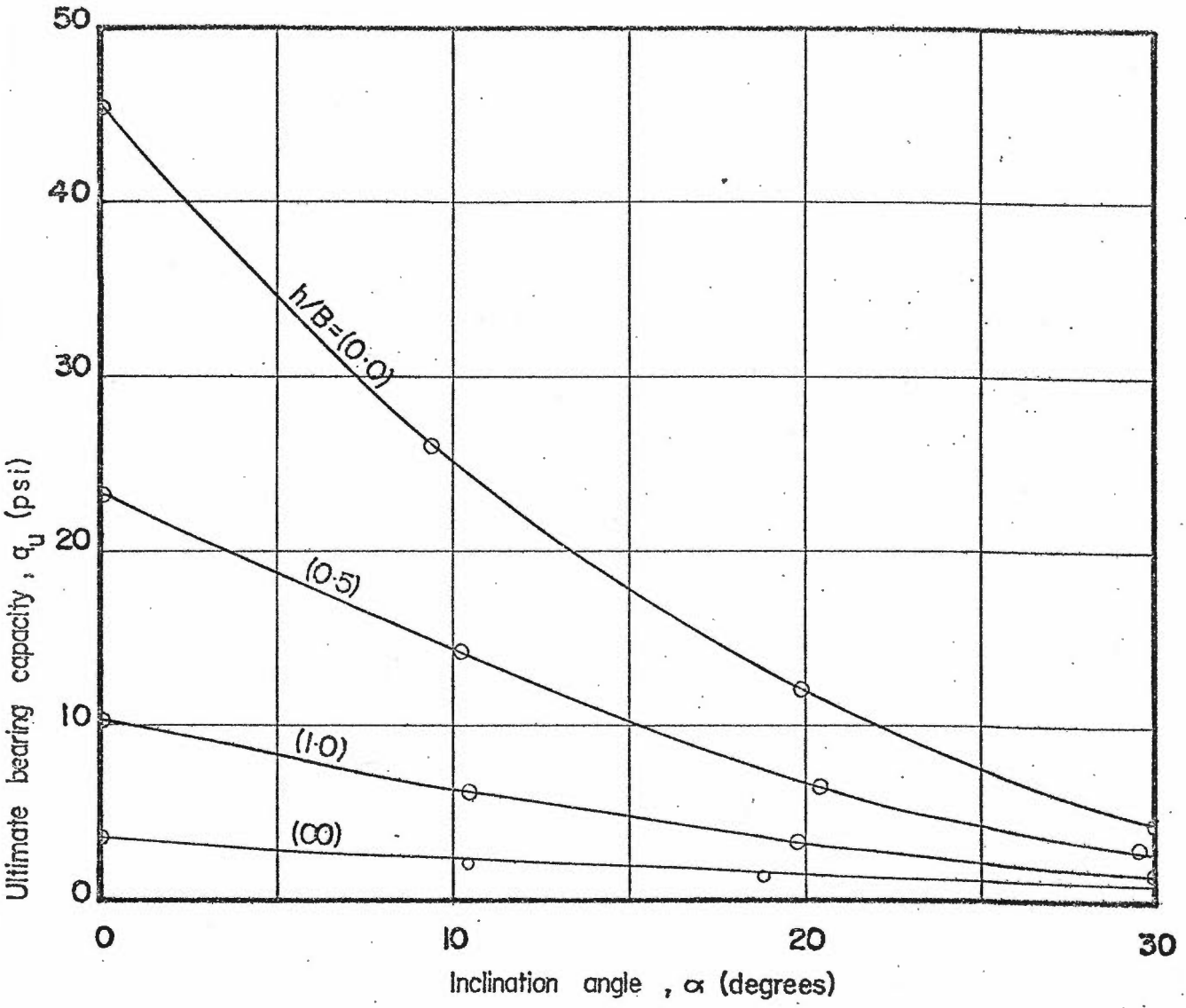

FIGURE 6·5 SUMMARY OF TEST RESULTS - STRIP FOOTING IN LOOSE SAND LAYER OVERLYING DENSE SAND (D/B = 0·5)

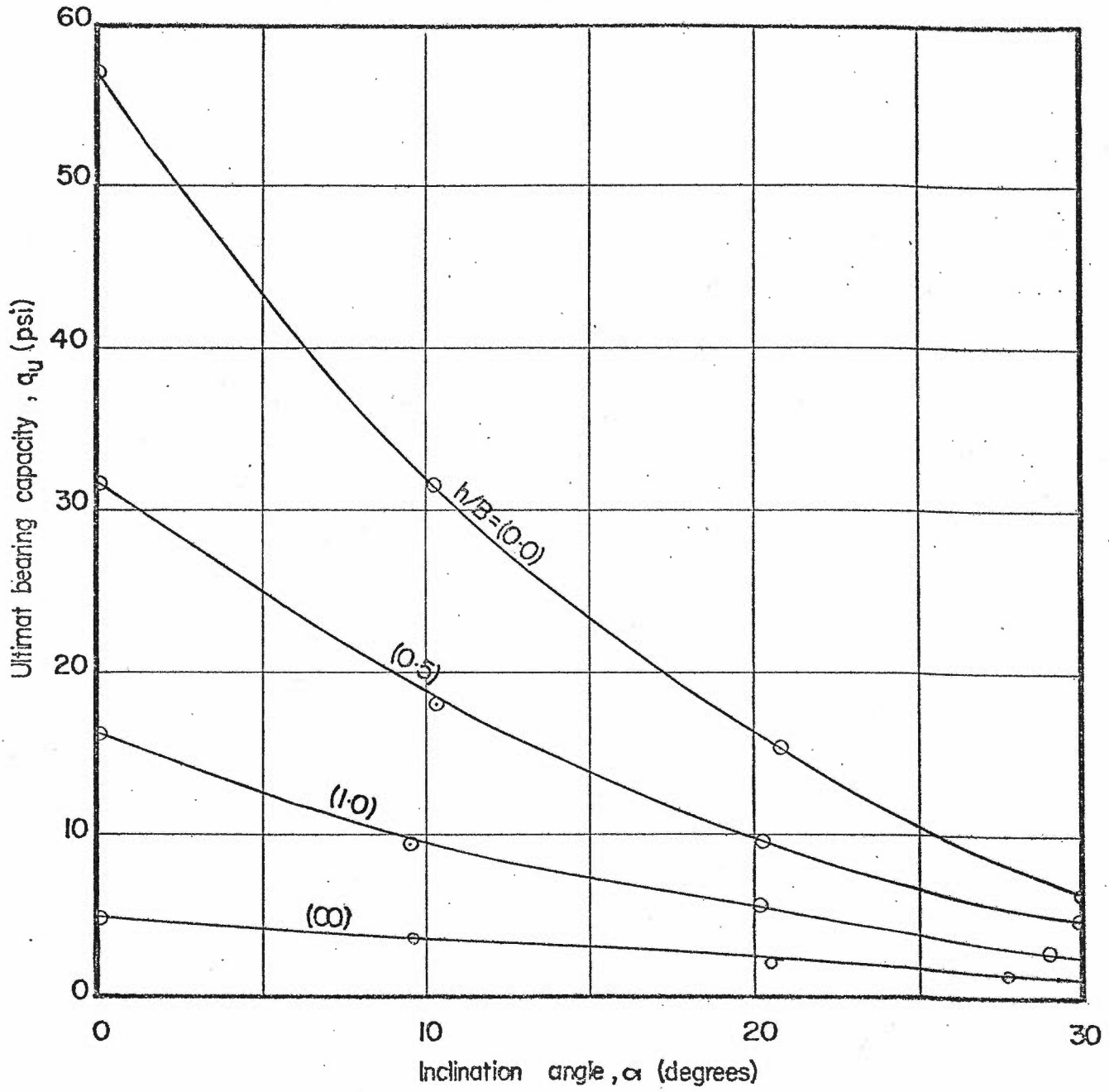

FIGURE 6-6 SUMMARY OF TEST RESULTS - STRIP FOOTING IN LOOSE SAND LAYER OVERLYING DENSE SAND (D/B = 1·0)

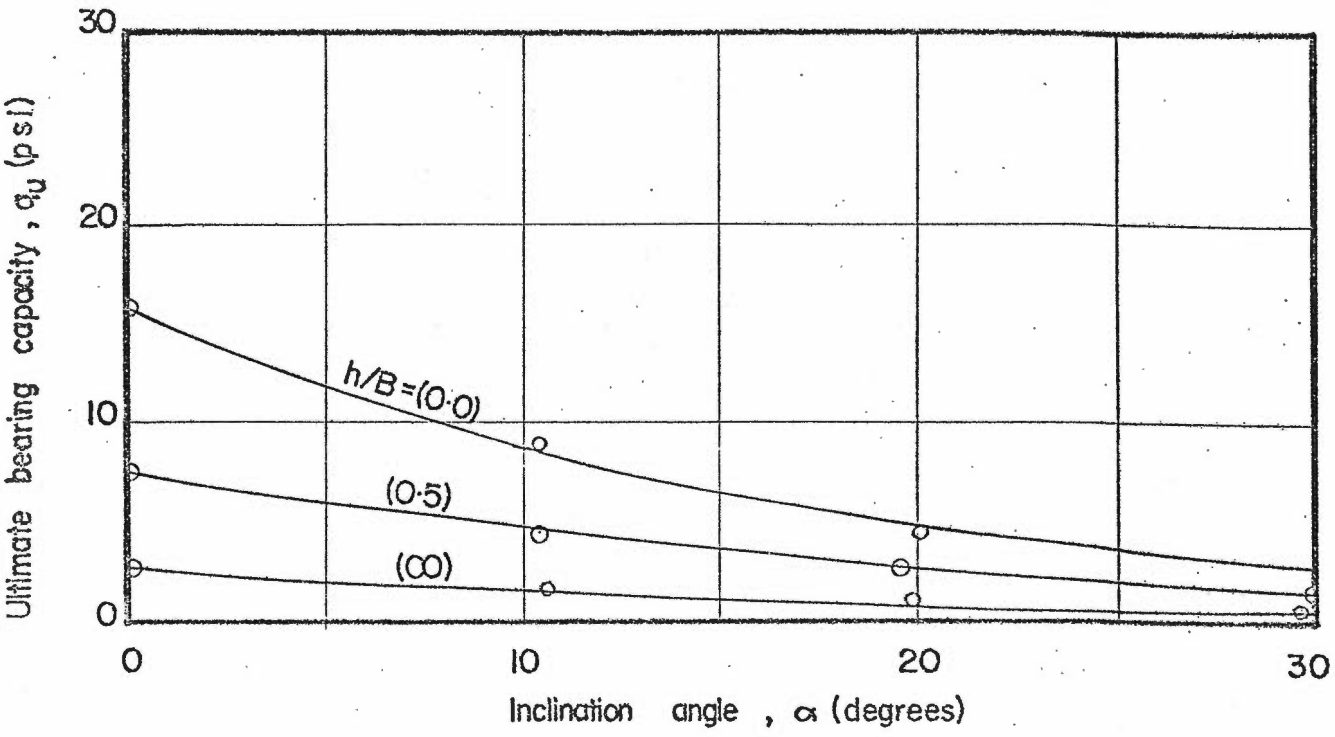

FIGURE 6-7 SUMMARY OF TEST RESULTS - CIRCULAR FOOTING ON LOOSE SAND LAYER OVERLYING DENSE SAND (D/B=0·0)

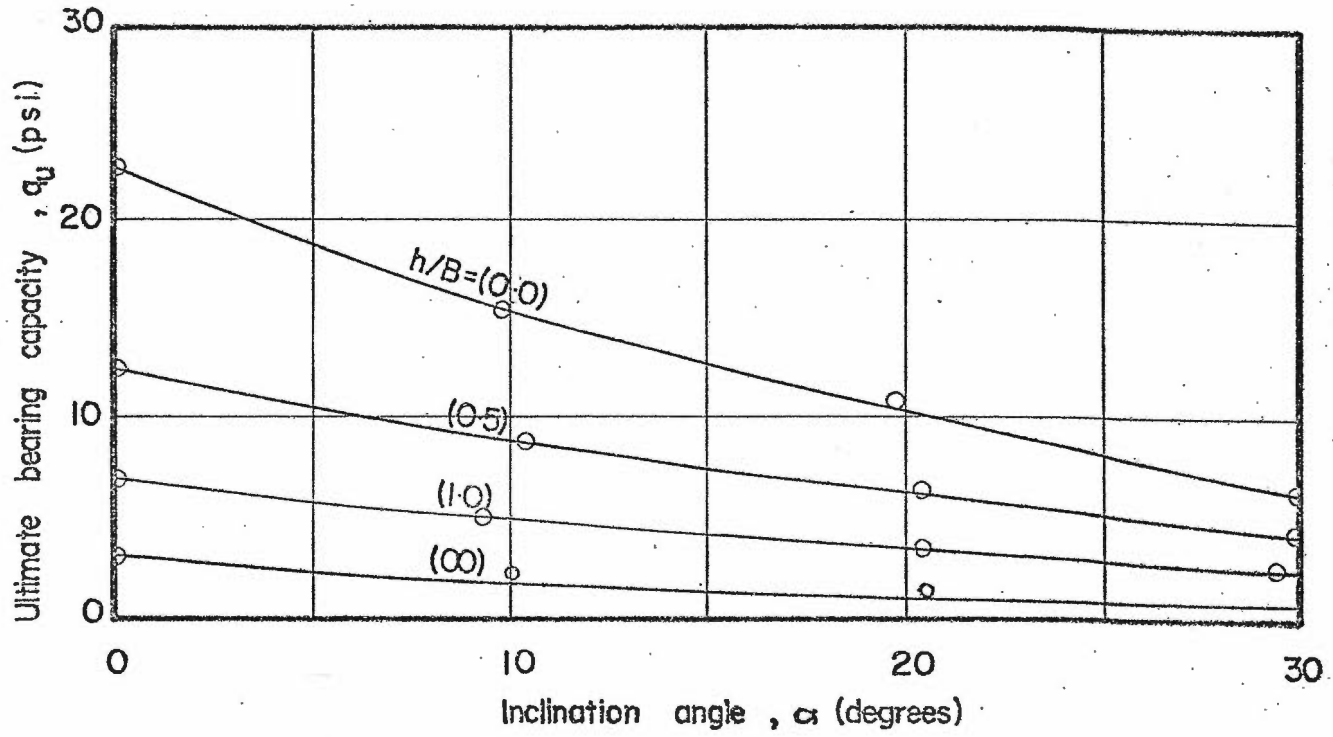

FIGURE 6·8 SUMMARY OF TEST RESULTS - CIRCULAR FOOTING IN LOOSE SAND LAYER OVERLYING DENSE SAND (D/B = 0·5)

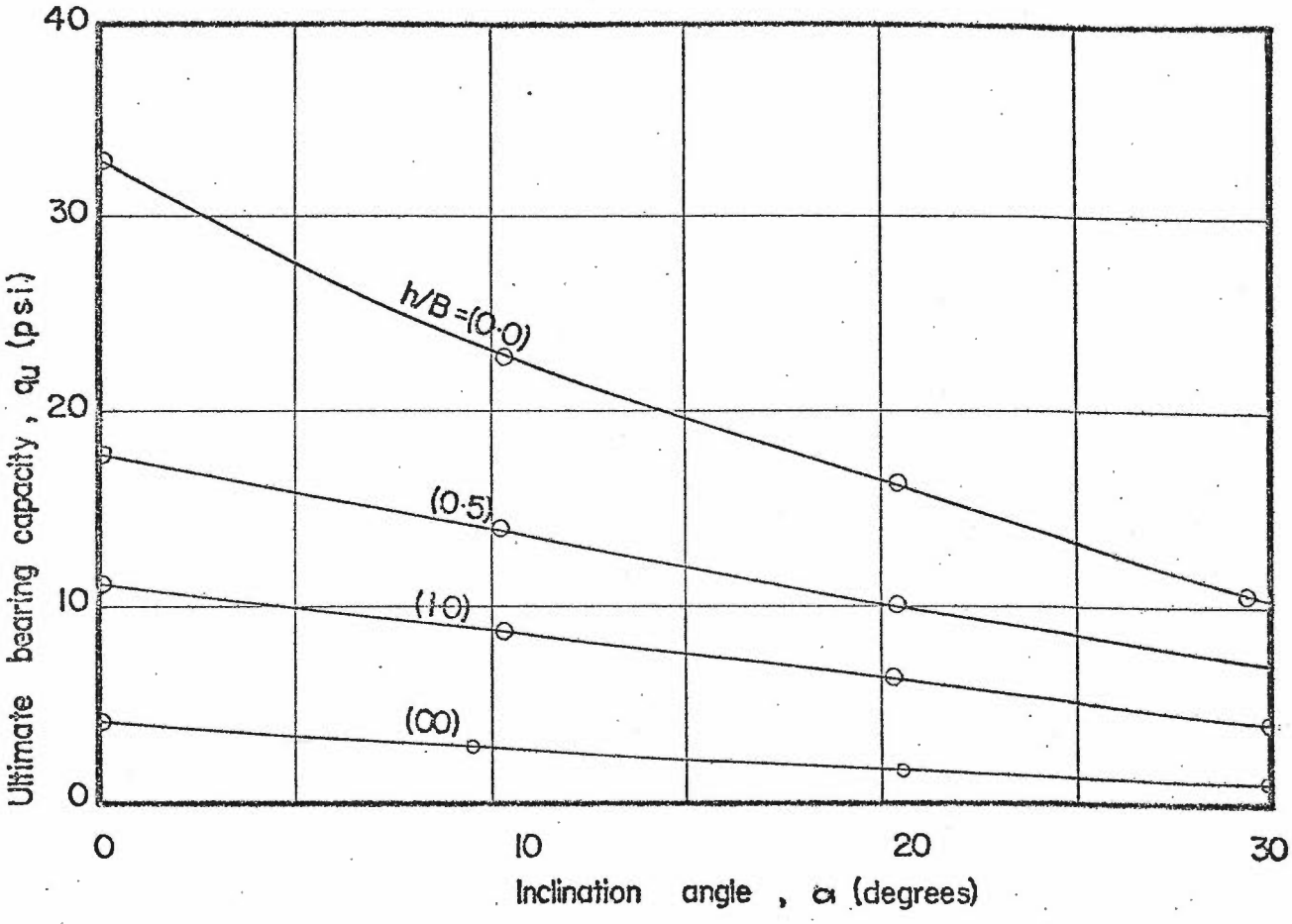

FIGURE 6·9 SUMMARY OF TEST RESULTS - CIRCULAR FOOTING IN LOOSE SAND LAYER OVERLYING DENSE SAND (D/B=1·0)

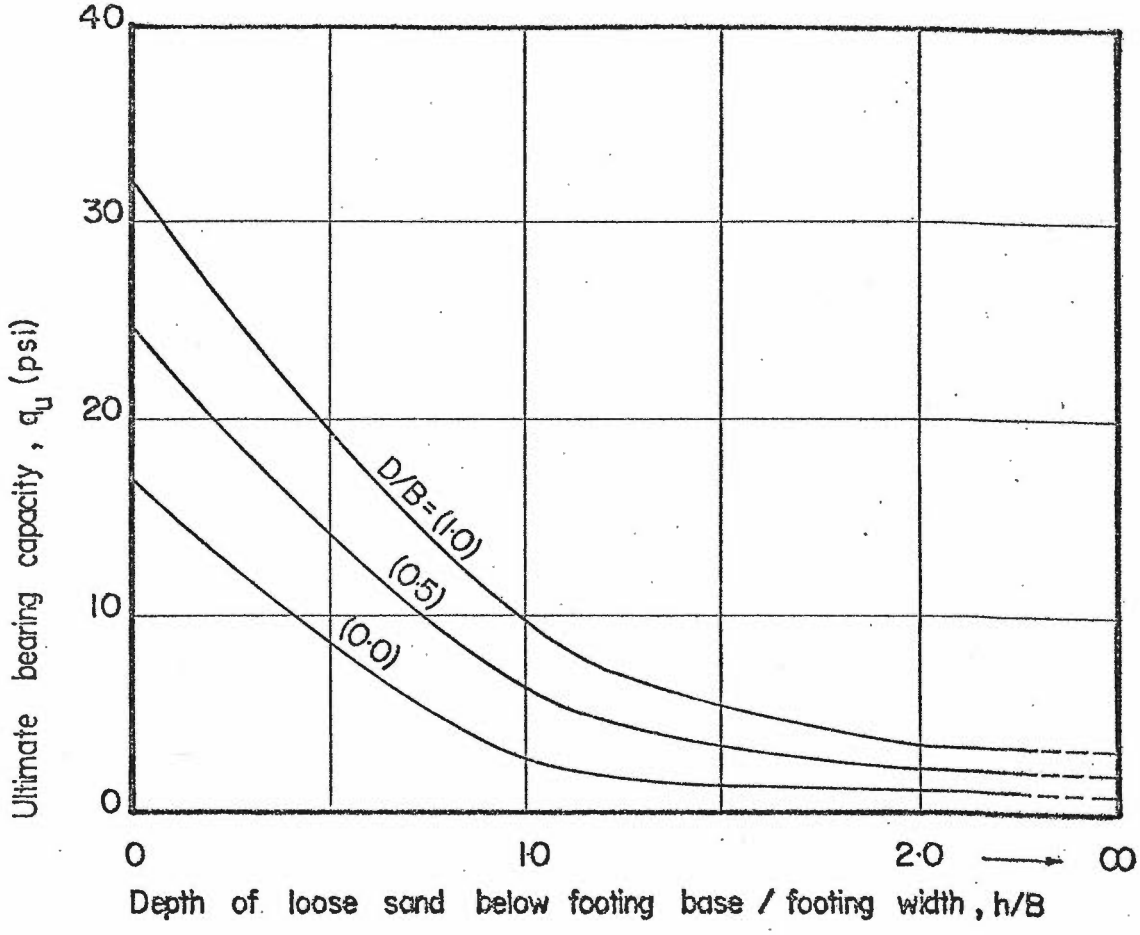

FIGURE 6·10 q_u VERSUS h/B RATIO - STRIP FOOTING IN LOOSE SAND OVERLYING DENSE SAND ($\alpha = 10^{\circ}$)

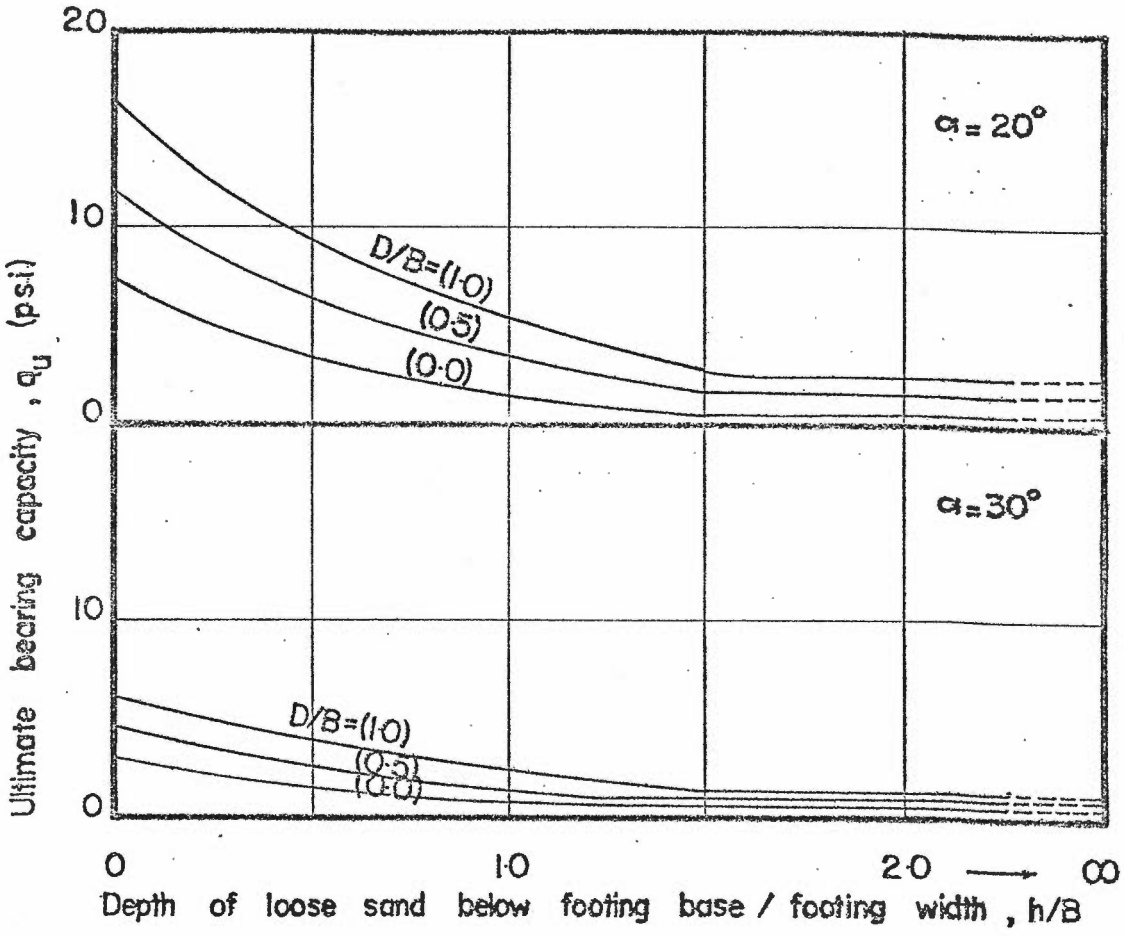

FIGURE 6·11 q_u VERSUS h/B RATIO - STRIP FOOTING IN LOOSE SAND OVERLYING DENSE SAND

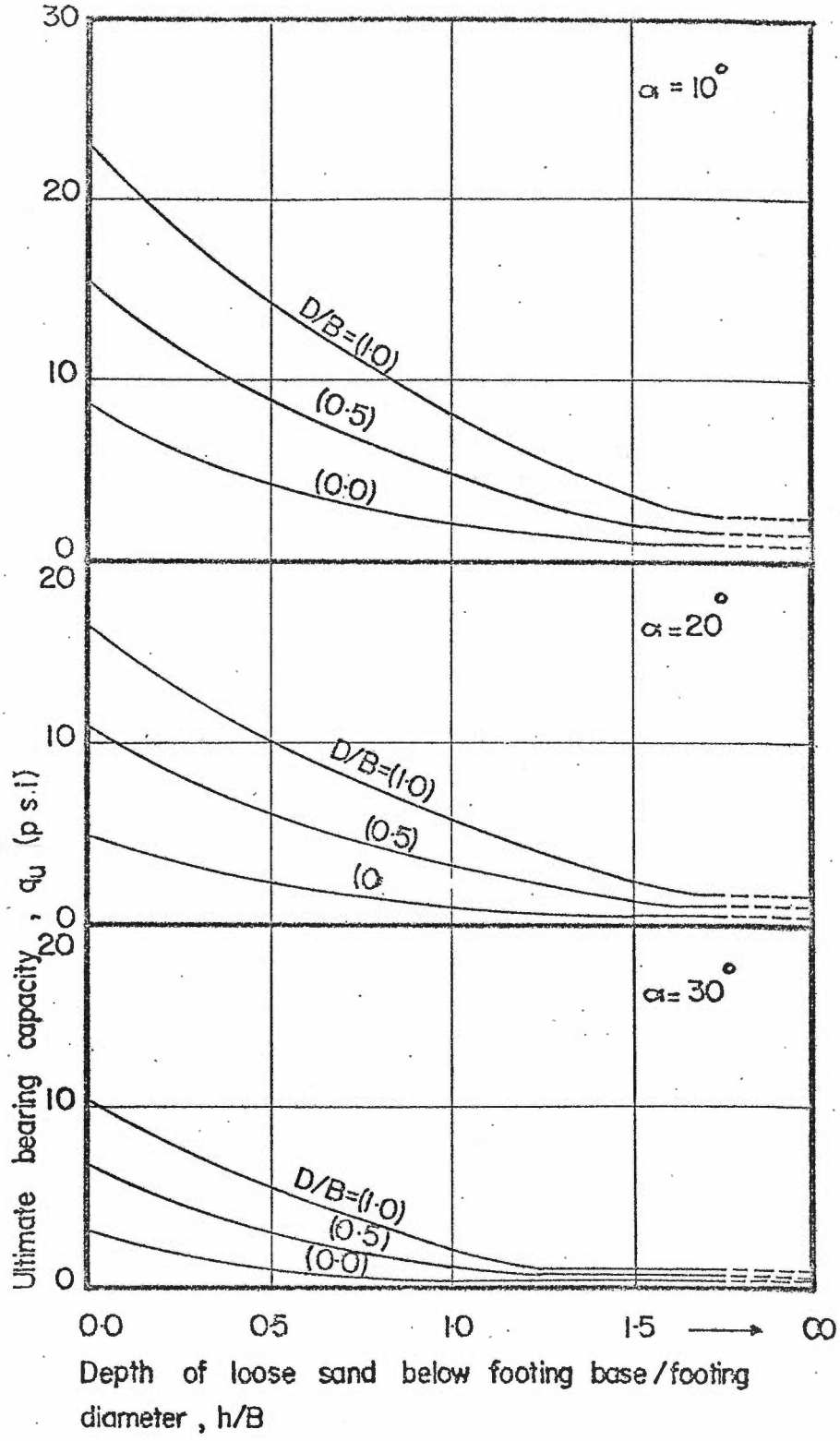

FIGUR 6·12 q_u VERSUS h/B RATIO - CIRCULAR FOOTING IN LOOSE SAND OVERLYING DENSE SAND

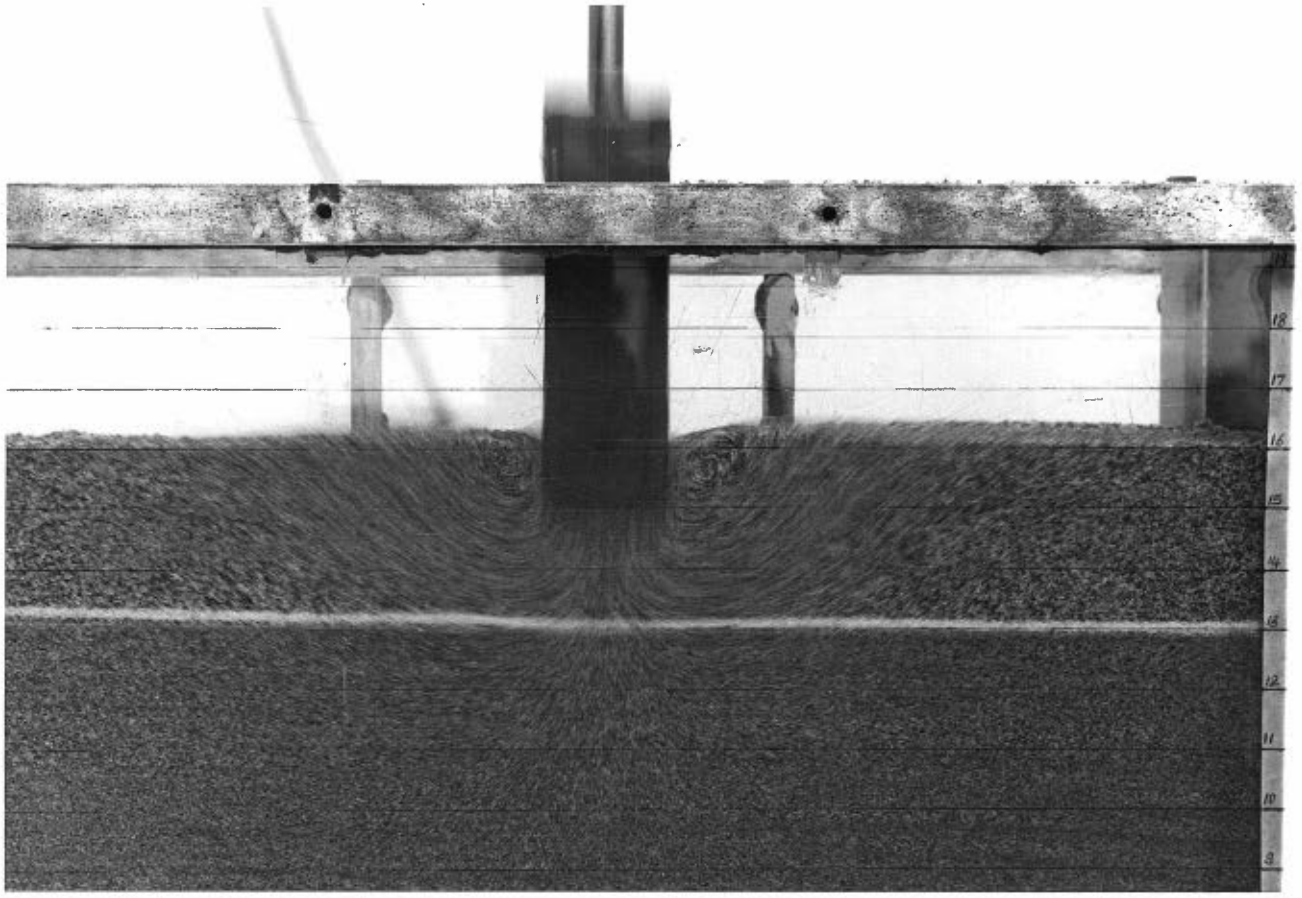

FIGURE 6.13 TIME EXPOSURE PICTURE - STRIP FOOTING UNDER VERTICAL LOAD IN LOOSE SAND LAYER OVERLYING DENSE SAND.

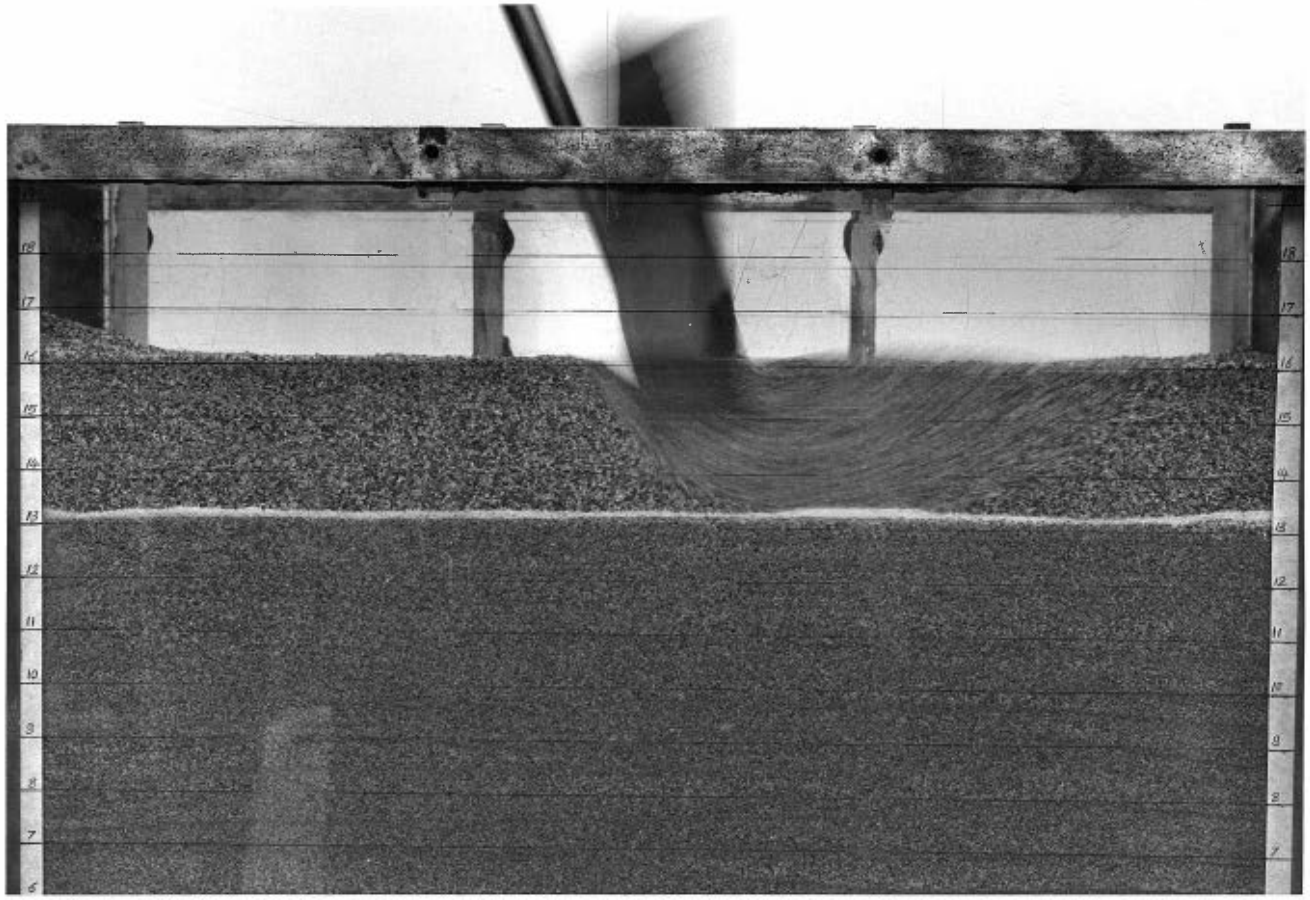

FIGURE 6.14 TIME EXPOSURE PICTURE - STRIP FOOTING UNDER INCLINED LOAD IN LOOSE SAND OVERLYING DENSE SAND.

6.3 Analysis of Strip Footing Tests Under Vertical Loads and Values of the Modified Bearing Capacity Factors

Meyerhof (1974) presented a solution for this problem by assuming that the lower layer acted as a rigid base and employed Mandel and Salencon's theory (1972) to determine the modified bearing capacity factors N'_γ and N'_q which depend on the angle of shearing resistance, ϕ of the upper sand, the ratio h/B and the footing roughness. Thus, the ultimate bearing capacity of the layered system can be calculated from the following equation:

$$q_u = 0.5\ \gamma_1\ B\ N'_\gamma + \gamma_1\ D\ N'_q \qquad (6.1)$$

$$\leq 0.5\gamma_2\ B\ N_{\gamma 2} + \gamma_1\ H\ N_{q2} \qquad \text{(for sand)}$$

or $$\leq C_u\ N_c \qquad \text{(for clay)}$$

Equation 6.1 can be considered as an extension of the conventional theory of bearing capacity to the case of a weak soil layer overlying a strong layer. Thus, it offers a simple solution to the problem stated. It should be mentioned that this theory considers the strength of the lower layer to provide the upper limits of N'_γ and N'_q equal to $N_{\gamma 2}$ and N_{q2}, respectively, for ϕ_2 for sand or N_c for clay.

From the present strip footing tests, trial calculations were made to determine the modified bearing capacity factors, N'_γ and N'_q employing equation 6.1. Thus the ultimate bearing capacity, q_u, was plotted against the buried depth (D) after adding the amount of footing settlement at failure, (Figures 6.15 and 6.16) for the cases of loose sand over dense sand and compact sand over dense sand, respectively. The deduced bearing capacity factors, N'_γ and N'_q and the theoretical

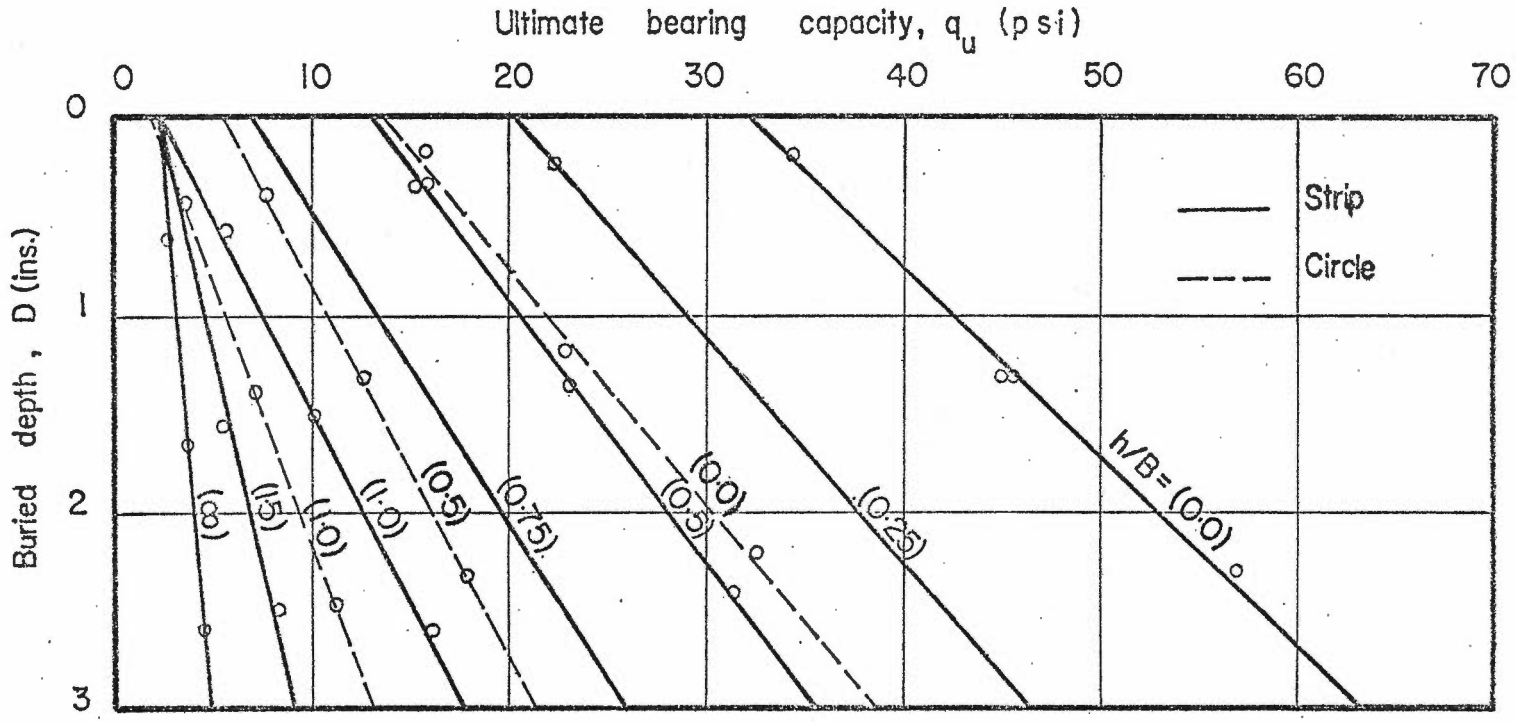

FIGURE 6·15 ULTIMATE BEARING CAPACITY VERSUS BURIED DEPTH — LOOSE SAND LAYER OVERLYING DENSE SAND

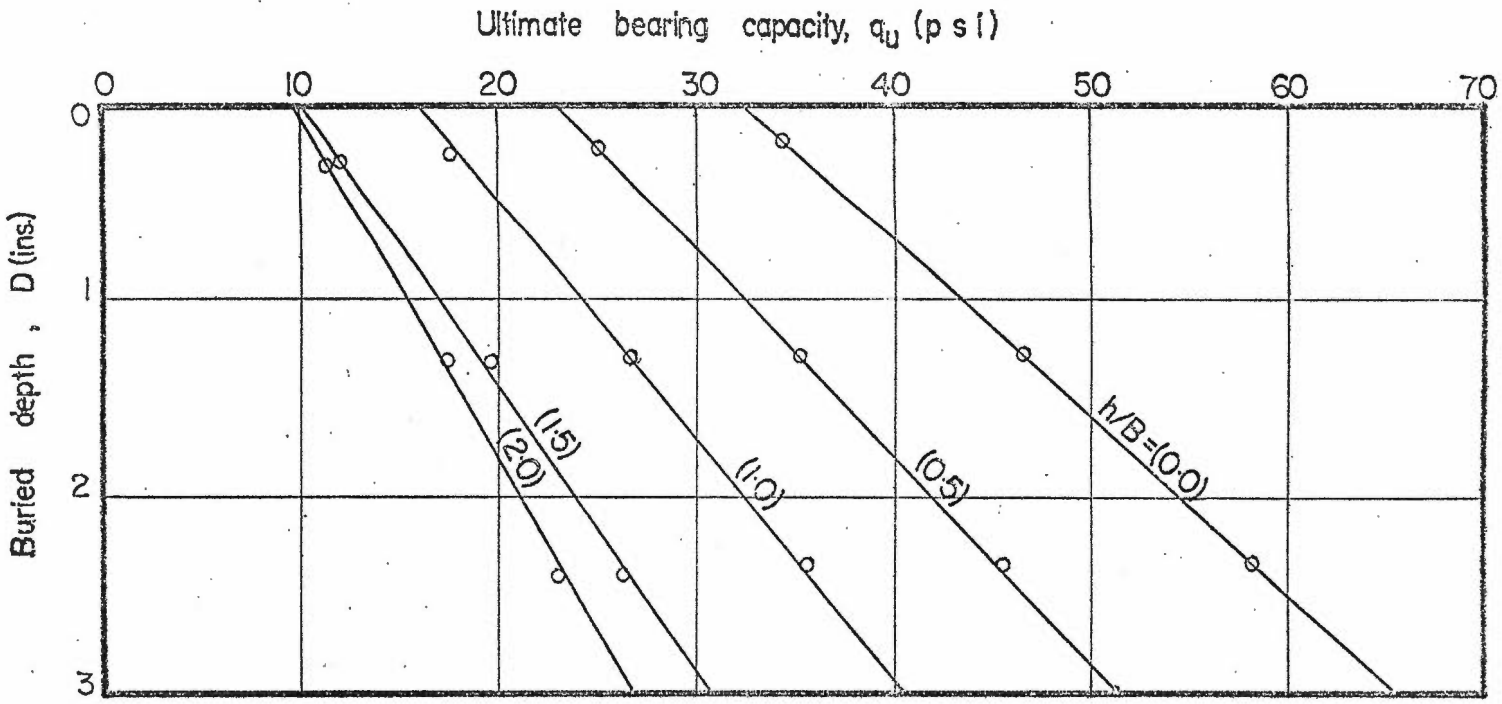

FIGURE 6·16 ULTIMATE BEARING CAPACITY VERSUS BURIED DEPTH - STRIP FOOTING IN COMPACT SAND OVERLYING DENSE SAND

values (Meyerhof, 1974) are given in Table 6.1.

Table 6.1

Analysis of Strip Footing Tests Under Vertical Loads

Weak Sand Layer Overlying Dense Sand

$\frac{h}{B}$	Loose Sand*/Dense Sand***				Compact Sand**/Dense Sand***			
	Experimental		Theoretical		Experimental		Theoretical	
	N'_γ	N'_q	N'_γ	N'_q	N'_γ	N'_q	N'_γ	N'_q
0.	523.0	199	523	199	535	199	535	199
0.25	403.0	167	523	199	--	--	535	199
0.50	256.0	150	80	50	418	171	535	199
0.75	138.0	122	48	35	--	--	300	199
1.00	44.0	98	42	25	291	151	165	170
1.50	41.5	44	42	20	182	127	140	135
2.00	41.5	16	42	16	173	107	140	100

Deduced

* $\phi_\gamma = 35.5^\circ$, $\phi_q = 30.0^\circ$ with weighted average $\phi_1 = 34.0^\circ$

** $\phi_\gamma = 42.8^\circ$, $\phi_q = 42.0^\circ$ with average $\phi_1 = 42.4^\circ$

*** $\phi_2 = 47.7^\circ$

A comparison between the experimental bearing capacity factors and the theoretical values as suggested by Meyerhof (1974), (Table 6.1) revealed that the theory did not quantitatively support the trend of decreasing values of N'_γ and N'_q with increasing h/B ratio as observed from the present experiments. Though it could be concluded that the theory was not truly valid, this may have been due to the assumption that the lower layer acted as a rigid base.

For the cases of loose sand over dense sand and compact sand over dense sand, the modified bearing capacity factors were plotted against h/B ratio values in Figures 6.17 and 6.18 respectively where the present experimental values are shown as points. An almost linear decrease of N'_γ and N'_q was noticed with increasing h/B ratio, as shown in these Figures. The maximum values of N'_γ and N'_q were equal to the bearing capacity factors for homogeneous dense sand, $N_{\gamma 2}$ and N_{q2}, respectively, for h/B equal to zero, and the minimum values were equal to the bearing capacity factors for homogeneous upper layer soil $N_{\gamma 1}$ and N_{q1} at h/B equal $(\frac{h_f}{B})_\gamma$ and $(\frac{h_f}{B})_q$ respectively, beyond which N'_γ and N'_q remained essentially constant. Thus

$$N'_\gamma = N_{\gamma 2} - \frac{h}{h_f}\,(N_{\gamma 2} - N_{\gamma 1}) \geq N_{\gamma 1} \qquad (6.2)$$

and

$$N'_q = N_{q2} - \frac{h}{h_{fq}}\,(N_{q2} - N_{q1}) \geq N_{q1} \qquad (6.3)$$

where $\frac{h_f}{B}$ is the depth ratio of the failure surface in a thick bed of sand. The theoretical values of $\frac{h_f}{B}$ were given by Meyerhof (1974) as a function of the angle of shearing resistance (ϕ) and for convenience,

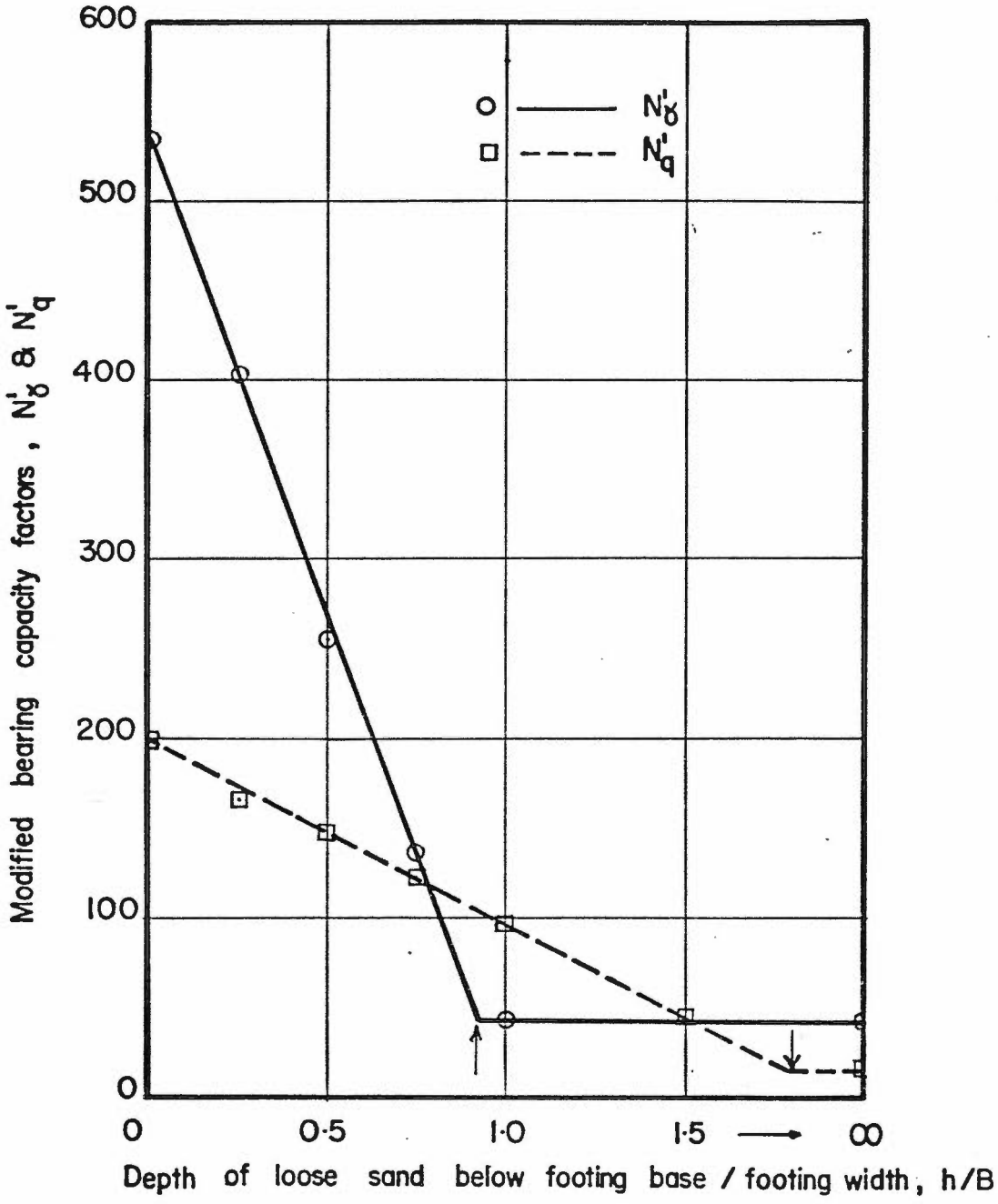

FIGURE 6·17 EXPERIMENTAL MODIFIED BEARING CAPACITY FACTORS - LOOSE SAND LAYER OVERLYING DENSE SAND

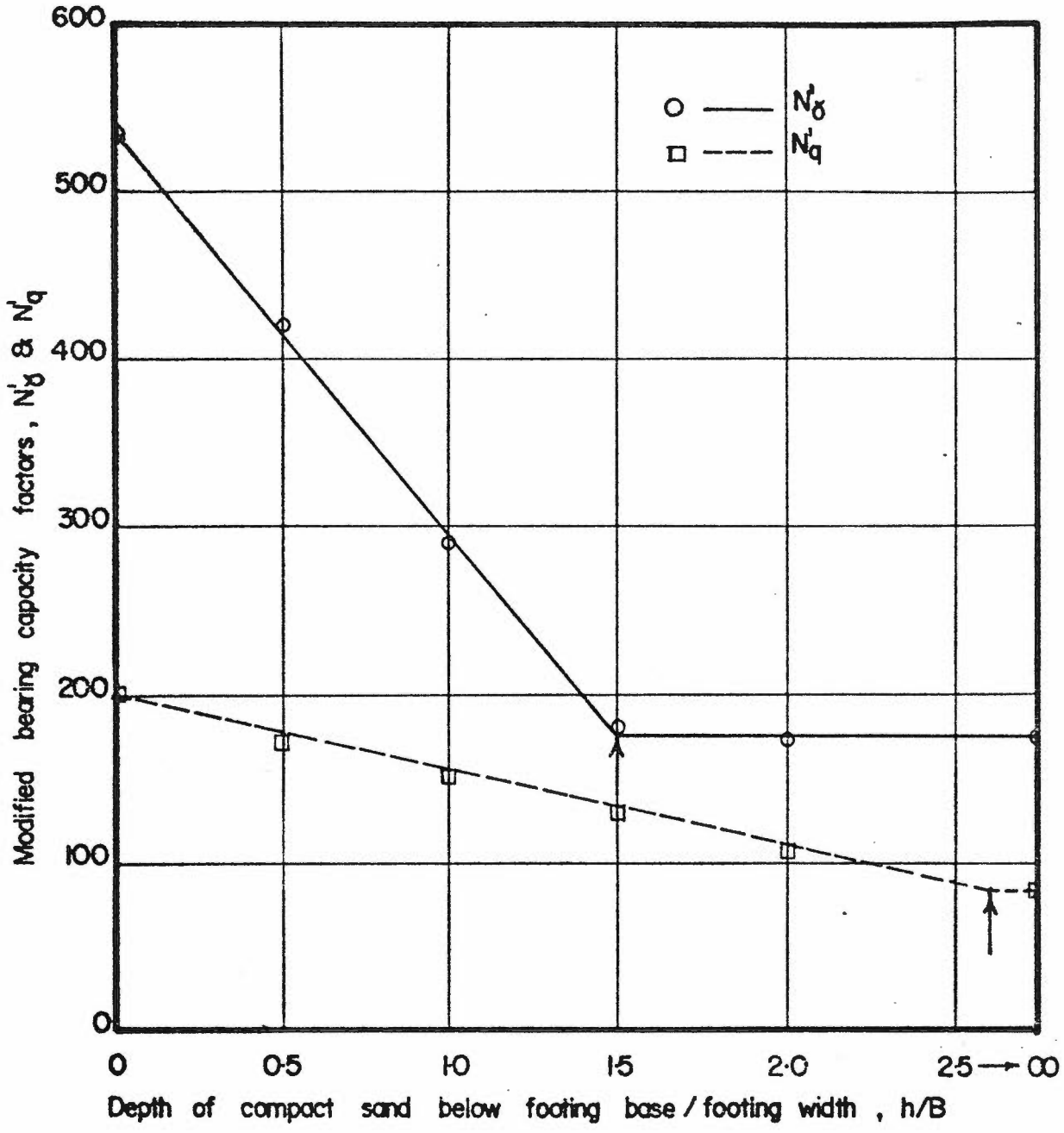

FIGURE 6·18 EXPERIMENTAL MODIFIED BEARING CAPACITY FACTORS - COMPACT SAND LAYER OVERLYING DENSE SAND

these values are shown in Figure 19. Comparison of the experimental and theoretical depth ratios $\frac{h_f}{B}$ is given in Table 6.2 and showed good agreement.

Table 6.2

Experimental and Theoretical Depth/Width Ratios at Failure

L. Sand/D. Sand				C. Sand/D. Sand			
Experimental		Theoretical		Experimental		Theoretical	
$(\frac{h_f}{B})_\gamma$	$(\frac{h_f}{B})_q$	$(\frac{h_f}{B})_\gamma$	$(\frac{h_f}{B})_q$	$(\frac{h_f}{B})_\gamma$	$(\frac{h_f}{B})_q$	$(\frac{h_f}{B})_\gamma$	$(\frac{h_f}{B})_q$
0.93	1.80	.97	1.82	1.50	2.60	1.35	2.65

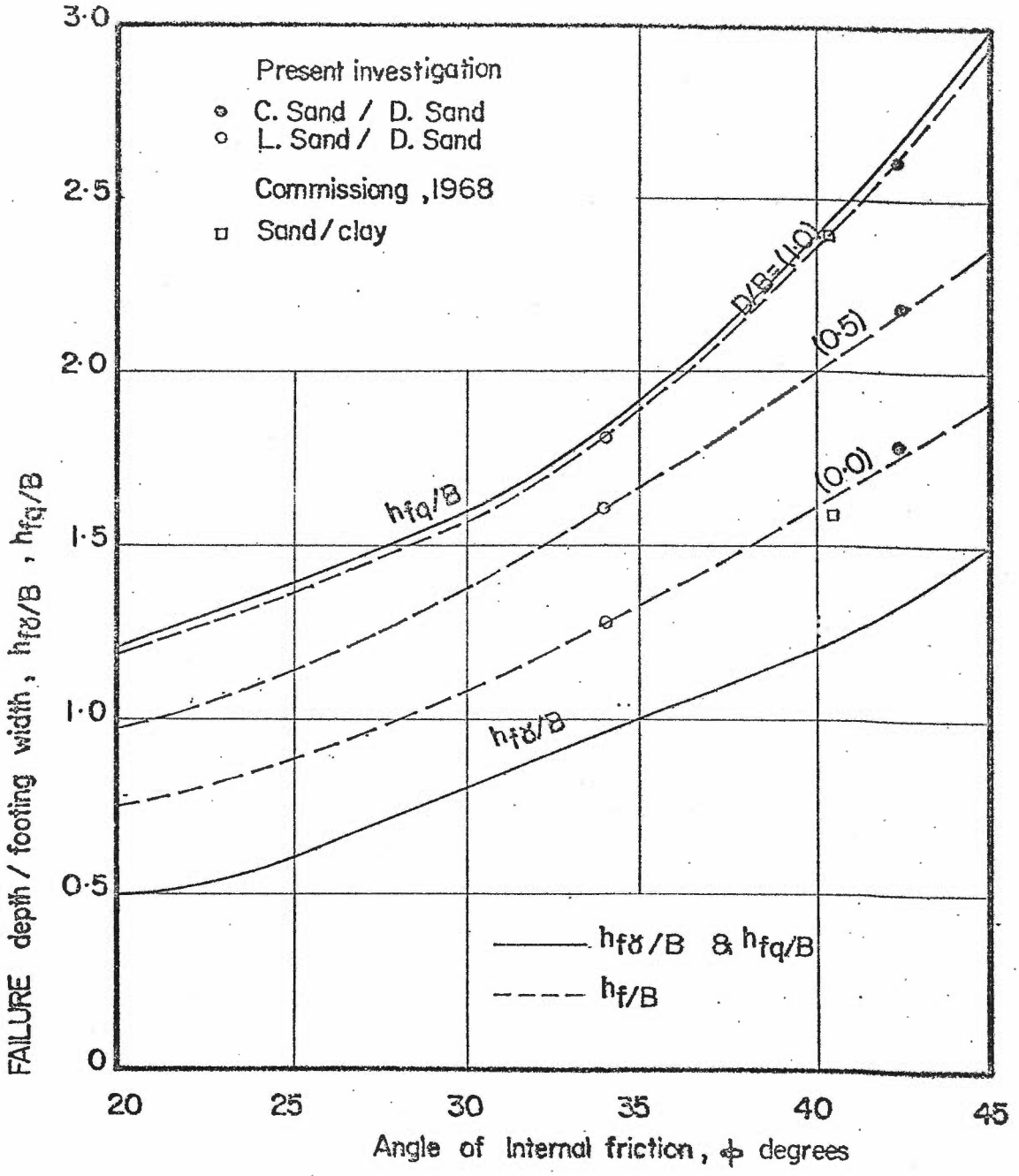

FIGURE 6·19 THEORETICAL FAILURE DEPTHS (AFTER MEYERHOF, 74)

It should be mentioned that if the analyses were carried out without adding the footing settlement at failure to the buried depth (D) the results would have shown a parabolic relationship for N'_γ versus h/B instead of a linear one while the linear N'_q relationship would have remained unchanged. In that case equation 6.2 should be replaced by

$$N'_\gamma = N_{\gamma 1} + (N_{\gamma 2} - N_{\gamma 1}) \left(1 - \frac{h}{h_{f\gamma}}\right)^2 \qquad (6.4)$$

$$\leq N_{\gamma 2}$$

This finding confirmed the parabolic relationship suggested by Meyerhof, (1974), to predict the ultimate bearing capacity for the case stated. According to the present test results, (Figures 6.1 to 6.5) the ultimate bearing capacity decreased rougly parabolically with increasing h/B ratio values (concave downwards) until a ratio of $\frac{h}{B}$ equals $\frac{h_f}{B}$, beyond which q_u remained constant and equal to q_u for homogeneous loose sand. This relationship is

$$q_u = q_1 + (q_2 - q_1) \left(1 - \frac{h}{h_f}\right)^2 \leq q_2 \qquad (6.5)$$

Where h_f is the weighted average of $h_{f\gamma}$ and h_{fq} for a given $\frac{D}{B}$ as shown in Figure 6.19 and q_1 and q_2 are the ultimate bearing capacities of strip footing in homogeneous upper and lower soil layers respectively, at the buried depth $(\frac{D}{B})$ at which q_u was calculated. It is of interest to note that this relationship has been compared with the test results of the present investigation, where good agreement was found. The deduced ratios of $\frac{h_f}{B}$ for $\frac{D}{B}$ values of 0, 0.5, and 1.0 from the present investigation and from previous researchers were plotted in Figure 6.19.

The test results of surface strip footings on compact sand over stiff clay (Commissiong, 1968) are analyzed in the following section and similar conclusions were drawn by comparing experimental modified bearing capacity factor N'_γ deduced from the test results with the theoretical values given by equation 6.4. These values are given in Table 6.3. Tests on a strip footing on homogeneous compact sand yielded an average bearing capacity factor of $N_\gamma = 112.0$, which was equal to the $N_{\gamma 1}$ in the layered system. The corresponding angle of internal friction was $\phi = 40.5^\circ$. Thus for $\phi_1 = 40.5^\circ$ and from Figure 6.19 $\frac{h_{f\gamma}}{B} = 1.24$. Equivalent $N_{\gamma 2}$ values were calculated for each test from

$$N_{\gamma 2} = \frac{C_u N_c}{\frac{1}{2} \gamma B}$$

Table 6.3

Analysis of Commissiong's Test Results

Strip Footing on Sand Overlying Clay

$\frac{h}{B}$	Ultimate Load q_u (psi)	C_u (psi)	$N_{\gamma 2}$	Modified Bearing Capacity Factor N'_γ	
				Experimental	Theoretical
0.25	18.8	4.0	245	204.7	196.8
0.50	14.5	3.9	238	157.9	156.9
1.00	10.8	4.2	261	117.6	117.6
1.50*	9.8	4.1	253	106.7	118.2*

* $\frac{h}{B} > \frac{h_{f\gamma}}{B}$

6.4 Analysis of Circular Footing Tests under Vertical Loads and Values of Shape Factors

Equation 6.1 can be conventionally extended to predict the ultimate bearing capacity of a circular footing by introducing shape factors s_γ and s_q (Meyerhof, 1974). Thus

$$q_u = 0.5\ \gamma_1\ B\ s'_\gamma\ N'_\gamma + \gamma_1\ D\ s'_q\ N'_q$$

$$\leq 0.5\ \gamma_2\ B\ s_{\gamma 2}\ N_{\gamma 2} + \gamma_1\ H\ s_{q2}\ N_{q2} \qquad (6.6)$$

The test results of circular footing in loose sand overlying dense sand (Table 4.9) were plotted against the buried depth after adding the settlement at failure (Figure 6.16). From this Figure the modified bearing capacity factors $s'_\gamma\ N'_\gamma$ and $s'_q\ N'_q$ were computed and the corresponding shape factors s'_γ and s'_q were calculated, which are given in Table 6.4. From Table 6.4, reasonable agreement was found between the experimental shape factor as deduced from the present test results and the theoretical values proposed by Meyerhof (1974) except at $\frac{h}{B}$ equal infinity, where for homogeneous loose sand the shape factors, s_γ and s_q were equal to 0.82 and 1.00 respectively for the sand used in this investigation (see Chapter 5.2).

Table 6.4

Analysis of Circular Footing Tests Under Vertical Loads - Loose Sand* Overlying Dense Sand**

$\frac{h}{B}$	Experimental Bearing Capacity Factors		Shape Factors			
			Experimental		Theoretical	
	$S'_\gamma N'_\gamma$	$S'_q N'_q$	S'_γ	S'_q	S'_γ	S'_q
0.0	224.3	162.3	0.43	0.77	-	-
0.5	108.2	102.3	0.42	0.68	0.46	0.68
1.0	33.4	80.6	0.76	0.82	0.60	0.95
∞	34.0	16.0	0.82	1.00	0.60	1.20

Deduced

* $\phi_\gamma = 35.5^\circ$, $\phi_q = 30.0^\circ$

** $\phi_2 = 47.7^\circ$

6.5 Analysis of Footing Tests Under Inclined Loads and Values of Inclination Factors

Equation 6.1 can be generalized by multiplying each of its terms with a set of shape and inclination factors. Thus equation 6.1 can be written as:

$$q_u = 0.5\ \gamma_1\ B\ s'_\gamma\ i'_\gamma N'_\gamma + \gamma_1\ D\ s'_q\ i'_q\ N'_q$$

$$\leq 0.5\ \gamma_2\ B\ s_{\gamma 2}\ i_{\gamma 2}\ N_{\gamma 2} + \gamma_1\ H\ s_{q2}\ i_{q2}\ N_{q2} \qquad (6.7)$$

where: q_u is defined as the bearing capacity in the direction of the load,

s'_γ and s'_q are shape factors,

i'_γ and i'_q are inclination factors,

N'_γ and N'_q are the modified bearing capacity factors, determined from equations 6.2 and 6.3 respectively.

Employing equation 6.6 and data from Tables 4.13 and 4.14 for strip and circular footings, respectively, in loose sand layer overlying dense sand, after being represented in Figures 6.20 and 6.21, the values of inclination factors, i'_γ and i'_q, and shape factors s'_γ and s'_q were computed. These values are given in Tables 6.5 and 6.6 respectively.

From Table 6.3, and as would be expected, the experimental inclination factors i'_γ and i'_q decreased rapidly with increasing the inclination angle α, and did not vary significantly with h/B value. It was noted that these deduced values (i'_γ, i'_q) from the present investigation were close to the theoretical values suggested by Brinch Hansen (1961), which are given for the vertical component of the load. These values

as given by Brinch Hansen are:

$$i_\gamma = (1 - \tan \alpha)^2 \qquad (6.8)$$

and $$i_q = i_\gamma^2 = (1 - \tan \alpha)^4 \qquad (6.9)$$

thus $$i'_\gamma = \frac{i_\gamma}{\cos\alpha} \quad \text{and} \quad i'_q = \frac{i_q}{\cos\alpha}$$

The theoretical values of the inclination factors, i'_γ and i'_q are also given in Table 6.5.

From Table 6.6 it can be seen that the experimental shape factor s'_γ and s'_q varied with h/B ratio (Meyerhof, 1974), from the case of homogeneous dense sand at h/B = 0 to the case of loose sand at h/B = ∞. Also these values (s'_γ, s'_q) increased significantly with increasing the inclination angle, α. This can be explained by the fact that, by increasing the inclination angle, α, the horizontal movement increased and thus the mobilized passive pressure on the circular footing will be higher than for the strip. The experimental shape factors s'_γ and s'_q were close to the theoretical values suggested by Meyerhof 1974 being divided by cos α. The theoretical values are also given in Table 6.6.

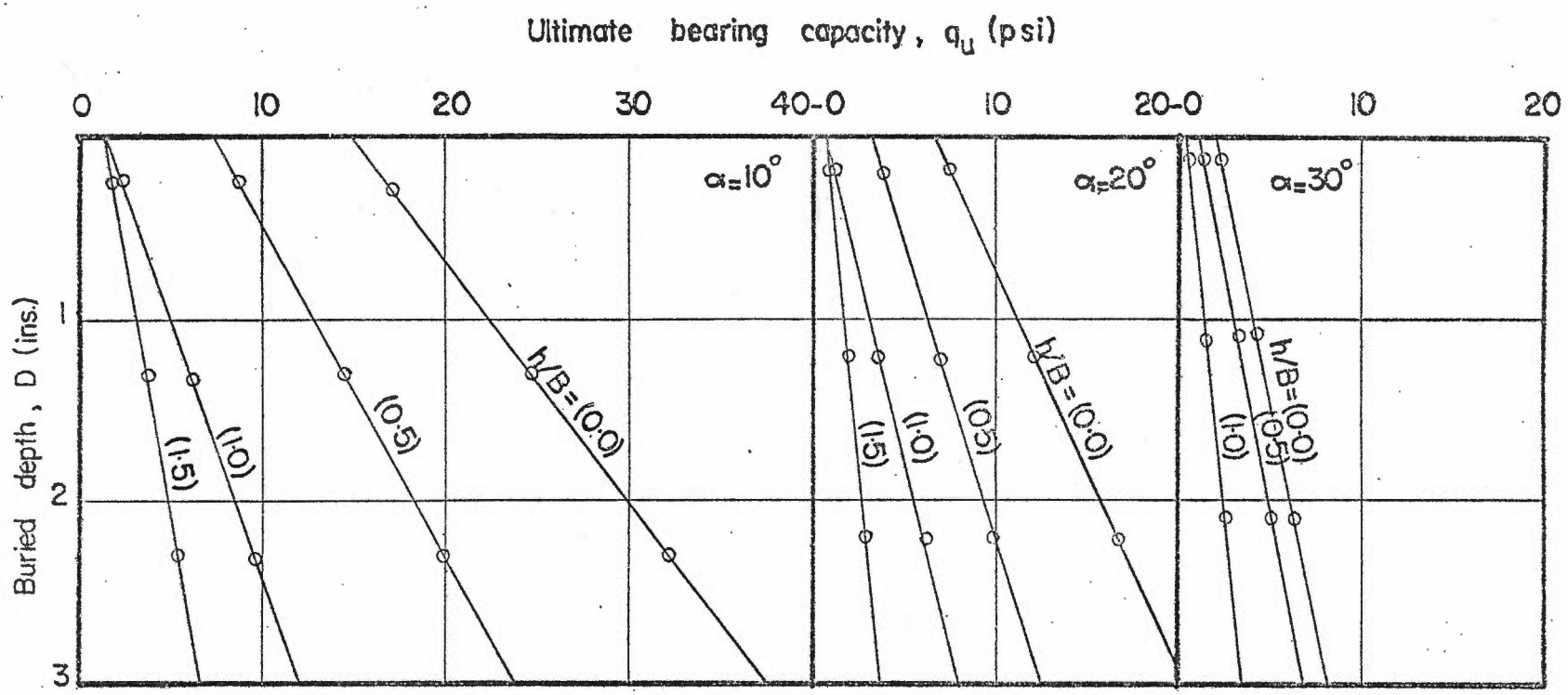

FIGURE 6·20 ULTIMATE BEARING CAPACITY VERSUS DEPTH - STRIP FOOTING IN LOOSE SAND LAYER OVERLYING DENSE SAND

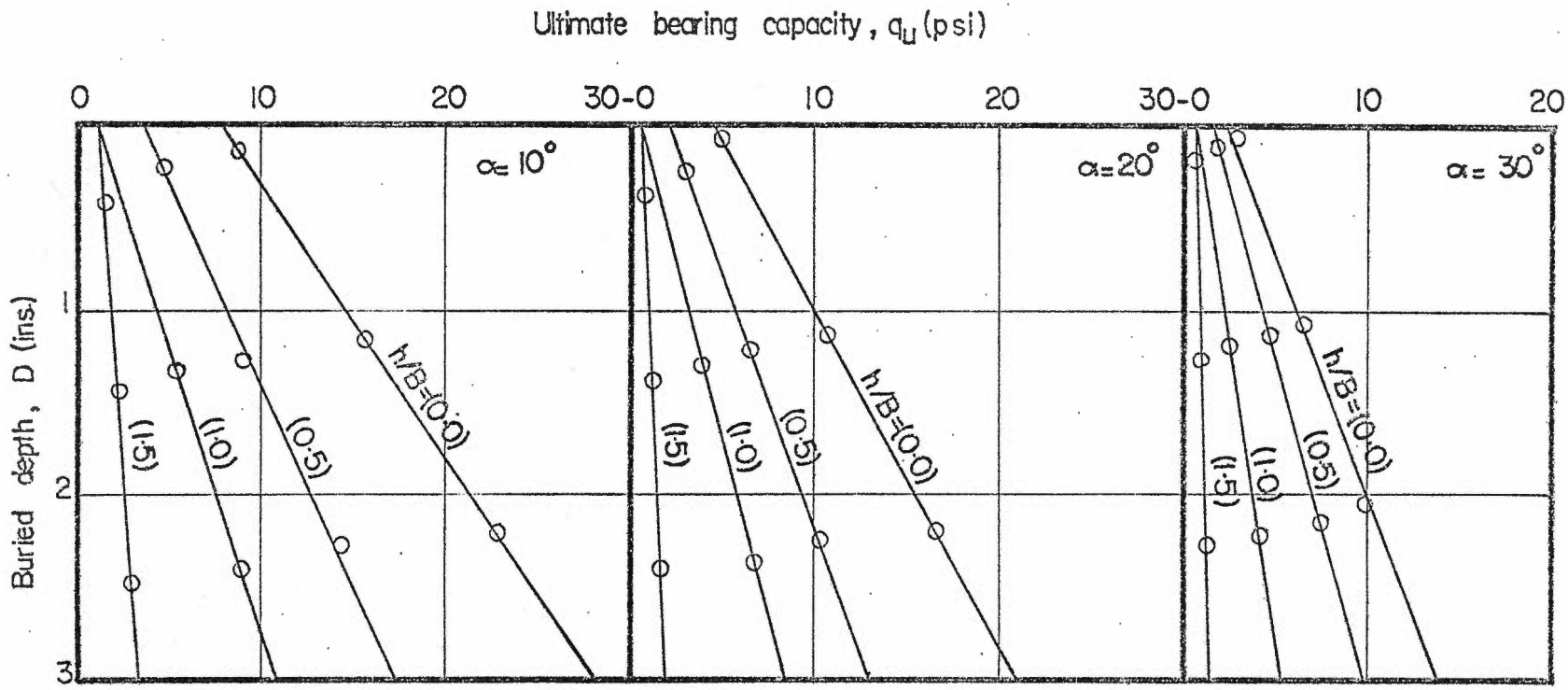

FIGURE 6·21 ULTIMATE BEARING CAPACITY VERSUS DEPTH - CIRCULAR FOOTING IN LOOSE SAND LAYER OVERLYING DENSE SAND

Table 6.5

Analysis of Strip Footing Tests Under Inclined Loads

Loose Sand Layer Overlying Dense Sand

Inclination angle α (degrees)	$\frac{h}{B}$	Bearing Capacity Factors		Inclination Factors			
				Experimental		Theoretical	
		$i'_\gamma N'_\gamma$	$i'_q N'_q$	i'_γ	i'_q	i'_γ	i'_q
10	0.0	246	148	0.47	0.74	0.47	0.69
	0.5	142	108	0.55	0.72	0.47	0.69
	1.0	24	69	0.54	0.70	0.47	0.69
	1.5	24	29	0.58	0.67	0.47	0.69
20	0.0	108	89	0.21	0.44	0.17	0.44
	0.5	59	63	0.23	0.42	0.17	0.44
	1.0	10	45	0.22	0.46	0.17	0.44
	1.5	10	20	0.24	0.44	0.17	0.44
30	0.0	33.2	39.4	0.06	0.20	0.04	0.21
	0.5	21.6	37.4	0.09	0.24	0.04	0.21
	1.0	3.9	21.6	0.09	0.22	0.04	0.21

Table 6.6

Analysis of Circular Footing Tests Under Inclined Loads

Loose Sand Layer Overlying Dense Sand

Inclination Angle α^{o} degrees	$\frac{h}{B}$	Bearing Capacity Factors		Shape Factors			
				Experimental		Theoretical	
		$S'_\gamma\ i'_\gamma\ N'_\gamma$	$S'_q\ i'_q\ N'_q$	S'_γ	S'_q	S'_γ	S'_q
10	0.0	124.62	137.76	0.50	0.93	--	--
	0.5	68.88	88.57	0.48	0.82	0.46	0.69
	1.0	19.68	64.95	0.82	0.94	0.61	0.97
	∞	19.68	15.74	0.82	0.54	--	--
20	0.0	84.63	110.21	0.78	1.23	--	--
	0.5	39.36	73.82	0.66	1.17	0.49	0.72
	1.0	8.85	54.12	0.88	1.20	0.64	1.01
	∞	8.85	12.79	0.88	0.64	--	--
30	0.0	39.36	73.80	1.18	1.87	--	--
	0.5	26.57	58.06	1.23	1.55	0.53	0.79
	1.0	4.92	34.44	1.26	1.59	0.69	1.10
	∞	4.92	15.75	1.26	0.72	--	--

6.6 Suggested Design Procedure for Footing in a Weak Layer Overlying a Strong Layer

The proposed design procedure on the basis of the present investigation has the following steps.

1. Based on the plane strain angle of shearing resistance of the upper and lower layers, ϕ_1 and ϕ_2 respectively. Determine the bearing capacity factors $N_{\gamma 1}$, N_{q1} and $N_{\gamma 2}$, N_{q2}.

2. For strip footing under vertical load, use equations 6.2 and 6.3 to predict the modified bearing capacity factors N'_{γ} and N'_{q}. The ultimate bearing capacity for this footing can be calculated by substituting these values in equation 6.1.

3. As an alternative method for predicting the ultimate bearing capacity of strip footing under vertical load, use the parabolic relationship (equation 6.5) proposed by Meyerhof (1974) where values of the h_f/B ratio are shown in Figure 6.19 for D/B values of 0, 0.5, and 1.0.

4. For circular footing under vertical load, use equation 6.6 and values of the shape factors given by Meyerhof, (1974).

5. For strip or circular footings under inclined load, use equation 6.7, with the inclination factor values given by Meyerhof (1953) or Brinch Hansen (1961), and the shape factors given by Meyerhof (1974) after dividing them by cos α.

Chapter 7

CONCLUSIONS AND RECOMMENDATIONS

7.1 General

The salient observations and important conclusions drawn from the analyses of the test results of the present and previous investigations, are summarized in this concluding chapter which includes suggestions for further work.

7.2 Strong Layer Overlying Weak Layer

A generalized design theory for the ultimate bearing capacity of strip and circular footings under vertical or inclined loads in a strong sand layer overlying a weak layer has been developed based on the assumption of punching the upper strong layer into the lower weak layer. Design procedure and design charts have been proposed for design use (see Chapter 5.9).

Analyses of the experimental results of the present investigation and other researchers revealed that the factors that determine the ultimate bearing capacity of footings in a strong layer overlying a weak layer. These factors are:

1. The shear strength of the upper and lower layers.
2. The relative strength of the upper and lower layers, which was represented in this thesis by the ratio of q_2/q_1.
3. Thickness of the upper layer below footing base, h.
4. Depth of the footing in the upper layer, D.

5. Inclination angle, α.
6. Shape of footing.
7. Compressibilities of component layers.

Additional research in the subject is suggested. It should include:

1. Extending the punching theory for the case where the upper layer is clay, and the lower layer could be sand or clay, for footings subjected to vertical or inclined loads. Such a study could aim to determine the relationship q_2/q_1 versus C_a/C_u (see Figure 5.35) where C_a is the mobilized shear strength on the assumed failure planes, and C_u is the undrained shear strength of the upper layer.
2. Study of the scale effect in the punching theory, by conducting tests using a wide range of footing sizes.
3. Study the effect of the upper layer strength by conducting tests using a wide range of angles for the internal friction of the upper sand layer, or the undrained shear strength if the upper layer is clay. This study could confirm if δ/ϕ_1 values or C_a/C_u in case of the upper layer is sand or clay respectively, vary with upper layer strength. Also this study could be extended to find a relationship between the depth factor d_q, the upper layer strength, and the q_2/q_1 ratio.
4. Study the shape factors for different footing shapes by conducting tests on circular, square, rectangular, and strip footings. This study should attempt to introduce values

for the shape factors to be recommended for the punching theory.

5. Instrumented strip footing with width not less than one foot (see Figures 3.7 and 3.8) could provide useful qualitative and quantitative data which may be of help in understanding the punching phenomena.

6. The study of the ultimate bearing capacity of footings in strong layer overlying weak layer could be extended to investigate the footing settlement associated with failure and the settlement at any working load.

7.3 Weak Layer Overlying Strong Layer

Empirical equations have been proposed for predicting the ultimate bearing capacity of strip or circular footings in a weak sand layer overlying a strong layer under vertical or inclined load. These equations hold promise for estimating the ultimate bearing capacities of such footings, since the experimental results of the present and other investigations have proved their feasibility. Design procedure has been given (see Chapter 6.6).

Analyses of footing tests under vertical loads based on the principles suggested by Meyerhof (1974) showed good agreement between computed and observed values of ultimate bearing capacity (calculated from the parabolic relationship) and shape factors for circular footings. In the meantime values of the modified bearing capacity factors given by him did not agree well with the deduced values.

Additional research in the subject should include:

1. Scale effect could be significant on the observed ultimate bearing capacity of footings having wide range of sizes. This may be because the footing failure occurs by squeezing the weak layer soil below the footing base.

2. Checks on the validity of equations 6.2 and 6.3 are required by conducting tests using a wide range of angles of internal friction for the upper and lower layers, keeping in mind that upper layer packing could be loose or compact and the lower layer packing must be dense (see Table 3.1).

3. Studies of the inclination factors and shape factors for footings under inclined loads.

4. Studies of the footing settlement at any working load. This work should attempt to establish methods for predicting settlement of footings under working load, which could be the criterion for foundation design.

REFERENCES

Bazan, I., 1971, "Bearing Capacity of Footings at the Interface of Two-Layered Soils", M. Eng. Thesis, Nova Scotia Technical College, Halifax, N. S.

Brown, J. D., 1967, "The Ultimate Bearing Capacity of Layered Clay Foundations", Ph. D. Thesis, Nova Scotia Technical College, Halifax, N. S.

Button, S. J., 1953, "The Bearing Capacity of Footings on a Two-Layered Cohesive Sub-Soil", Proc. 3rd Int. Conf. Soil Mech. and Found. Eng. Zurich, Switz. 1, p. 356.

Caquot, A. and Kerisel, J., 1948, "Tables de Pousseé et Butee", Bauthier-Villars, Paris.

Caquot, A. and Kerisel, J., 1966, "Traite de Mecanique des Sols", Gauthier-Villars, Paris.

Commissiong, D. M., 1968, "The Ultimate Bearing Capacity of Surface Footings on Dry Sand Overlying Saturated Clay", M. Eng. Thesis, Nova Scotia Technical College, Halifax, N. S.

DeBeer, E. E., 1965, "Bearing Capacity and Settlement of Shallow Foundations on Sand", Proceedings of a Symposium at Duke University, Durham, N. C., p. 15.

DeBeer, E. E., 1970, "Experimental Determination of the Shape Factors and the Bearing Capacity Factor of Sand", Geotechnique, 20 (4): p. 387.

DeBeer, E. E., and Vesić, A. B., 1958, "Etude Expérimentale de la Capacite Portate du Sable sous des Fondations Directes Établies en

Surface", Annales des Travaux Publics de Belgique, Vol. 59, p. 5.

Desai, C. S., and Reese, L. C., 1970a, "Ultimate Capacity of Circular Footings on Layered Soils", J. Indian Nat. Soc. Soil Mech. Found. Eng. 96 (1), p. 41.

Graham, J., 1971, "Calculation of Passive Pressure in Sand", Canadian Geotechnical Jnl. 8, p. 566.

Hansen, J. Brinch, 1961, "A General Formula for Bearing Capacity", Bulletin No. 11, Danish Technical Institute, Copenhagen, Denmark, p. 38.

Hansen, J. Brinch, 1970, "A Revised and Extended Formula for Bearing Capacity", Bulletin No. 28, Danish Geotechnical Institute, Copenhagen, Denmark.

Ho, K. C., 1973, "The Ultimate Bearing Capacity of Shallow Footings on Sand Overlying Clay", M. Eng. Thesis, Nova Scotia Technical College, Halifax, N. S.

Ko, H. Y. and Davidson, L. W., 1973, "Bearing Capacity of Footings in Plane Strain", ASCE, Vol. 99, No. SM1, p. 45.

Kwaku, S. F., 1964, "Laboratory Study of Lime Stabilized Clay Sub-Grade Under Static and Repeated Loads", M. Eng. Thesis, Nova Scotia Technical College, Halifax, N. S.

Mandel J. et Salencon, J., 1972, "Force Portante d'un Sol sur une Assise Rigide (Etude Theorique)", Geotechnique 22, No. 1, p. 77.

Meyerhof, G. G., 1950, "The Bearing Capacity of Sand", Ph. D. (Eng.), Thesis, University of London, England.

Meyerhof, G. G., 1951, "The Ultimate Bearing Capacity of Foundations", Geotechnique, Vol. 2, p. 301.

Meyerhof, G. G., 1956, "Discussion on Rupture Surface in Sand Under Oblique Loads", Proc. ASCE, Vol. 82, No. SM8.

Meyerhof, G. G., 1963, "Some Recent Research on the Bearing Capacity of Foundations", Can. Geot. J., 1 (1), p. 16.

Meyerhof, G. G., 1965, "Shallow Foundations", Jl. Soil Mech. Found. Eng., ASCE, Vol. 95, No. SM2, p. 21.

Meyerhof, G. G., 1974, "Ultimate Bearing Capacity of Footings on Sand Layer Overlying Clay", 26th Annual Geot. Conf., pp. 219-225.

Meyerhof, G. G. and Ranjan, G., 1972, "The Bearing Capacity of Rigid Piles Under Inclined Loads in Sand", Canadian Geotechnical Jnl., Vol. 9, p. 430.

Meyerhof, G. G. and Valsangkar, A. J., 1977, "Bearing Capacity of Piles in Layered Soils", Proc. 9th Int. Conf. on Soil Mech., Vol. 2, Tokyo, Japan.

Muhs, H., 1963, "On the Phenomenon of Progressive Rupture in Connection with the Failure Behaviour of Footings in Sand", Discussion, Proc. 6th Int. Conf. Soil Mech. and Found. Eng., Montreal, Canada, 3, pp. 419-421.

Myslivec, A., 1971, "Bearing Capacity of Layered Subsoil", Proc. 4th Budapest Conference on Soil Mechanics and Foundation Engineering, p. 677.

Nagaoka, H., 1971, "Some Problems on Mechanical Behaviours of Foundations", (Japanese), pp. 5-56.

Prandtl, L., 1920, "Ueber die Harte Plastischer Körper", Hachr. Kgl. Ges. Wiss Göttingen, Math-Phys. Kl, p. 74.

Purushothamraj, P. et al, 1974, "Bearing Capacity of Strip Footings in

Two-Layered Cohesive Friction Soils", Can. Geo. Jour., Vol. II, No. 1, p. 32.

Rowe, P. W. and Peaker, K., 1965, "Passive Earth Pressure Measurements", Geotechnique, Vol. 15, p. 57.

Sastry, V. V., 1976, "Bearing Capacity of Piles in Layered Soil", Ph. D. Thesis, Nova Scotia Technical College, Halifax, N. S.

Siva Reddy, A. and Ramanathan J. Srinivasan, 1970, "Bearing Capacity of Footings on Anisotropic Soil", Jour. Soil Mech. and Div. Proc. ASCE, Nov., No. SM6.

Skempton, A. W., 1948, "The $\phi = 0$ Analysis of Stability and its Theoretical Basis", Proc. 2nd Int. Conf. Soil Mech., Vol. 1, p. 72.

Taylor, D. W., 1948, "Fundamentals of Soil Mechanics", John Wiley and Sons, New York.

Tcheng, Y., 1957, "Fondations Superficielles en Milieu Stratifié", Proc. 4th Int. Conf. Soil Mech. and Found. Eng., 1, p. 449.

Terzaghi, K., 1943, "Theoretical Soil Mechanics", John Wiley and Sons, New York.

Terzaghi, K. and Peck, R. B., 1967, "Soil Mechanics in Engineering Practice", 2nd ed., John Wiley and Sons, New York.

Vesić, A. S., 1963, "Bearing Capacity of Deep Foundations in Sand", Highway Research Board Record, No. 39.

Vesić, A. S., 1973, "Analysis of Ultimate Loads of Shallow Foundations", ASCE, 99, No. SM1, p. 45.

Vyalov, S. S., 1967, "Bearing Capacity of Weak Soil Layer with Underlying Rigid Base", Proc. 3rd Asian Reg. Conf. Soil Mech. Found. Eng., Haifa, Vol. 1, p. 245.

Yamaguchi, H., 1963, "Practical Formula for Bearing Value of Two Layer Ground", Proc. 2nd Asian Reg. Conf. Soil Mech., p. 176.

APPENDICES

Appendix I

(1) Triaxial Test Results

Standard triaxial test apparatus with a volume measuring device was utilized (Sastry, 1976) to determine the shear strength properties of the sand used in the present investigation. The following ranges of porosities η and cell pressures $\sigma 3$ were employed:

Packing	Range of η%	$\sigma 3$psi	No. of Tests
Dense	36-38	4-10-40-57	10
Compact	38.40	4-10-75	11
Loose	40-44	1-4-10	8

The angle of internal friction was determined for each test from

$$\sin \phi = \frac{\sigma 1 - \sigma 3}{\sigma 1 + \sigma 3}$$

The results of these tests are presented in Figure I.1. Typical stress-strain and volume change curves are given in Figures I.2 and I.3 for dense samples tested at different cell pressures while the effect of porosity on peak stress ($\sigma 1 - \sigma 3$) and volumetric strain ε_v is shown in Figures I.4 and I.5. The Mohr Coulomb envelope for a typical dense sand test is plotted in Figure I.6.

(ii) Direct Shear Test Results

The results of these tests are given in Table I.1 and presented in Figure I.7.

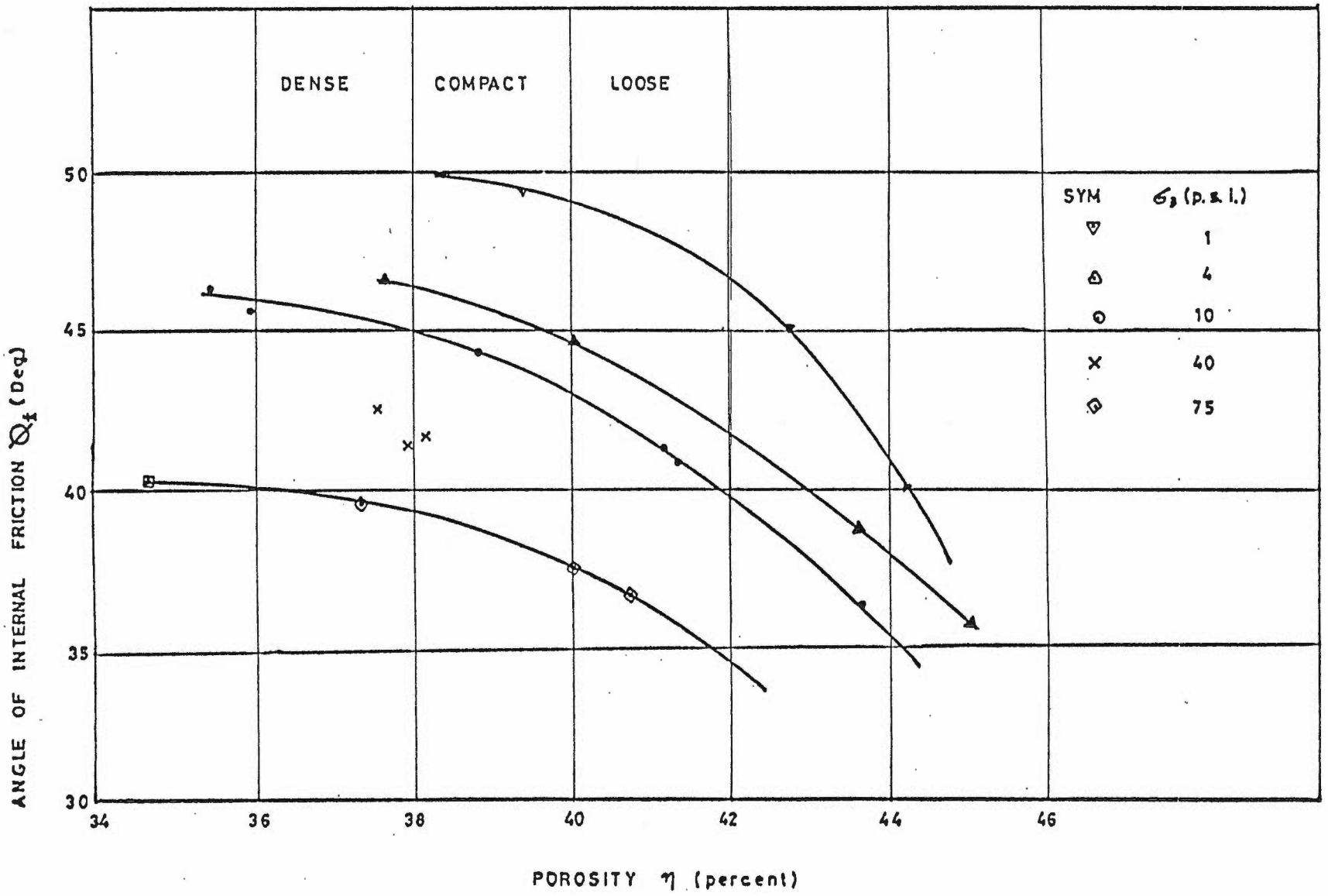

FIGURE I·1 RESULTS OF TRIAXIAL TESTS ON DRY SAND (AFTER SASTRY, 1977)

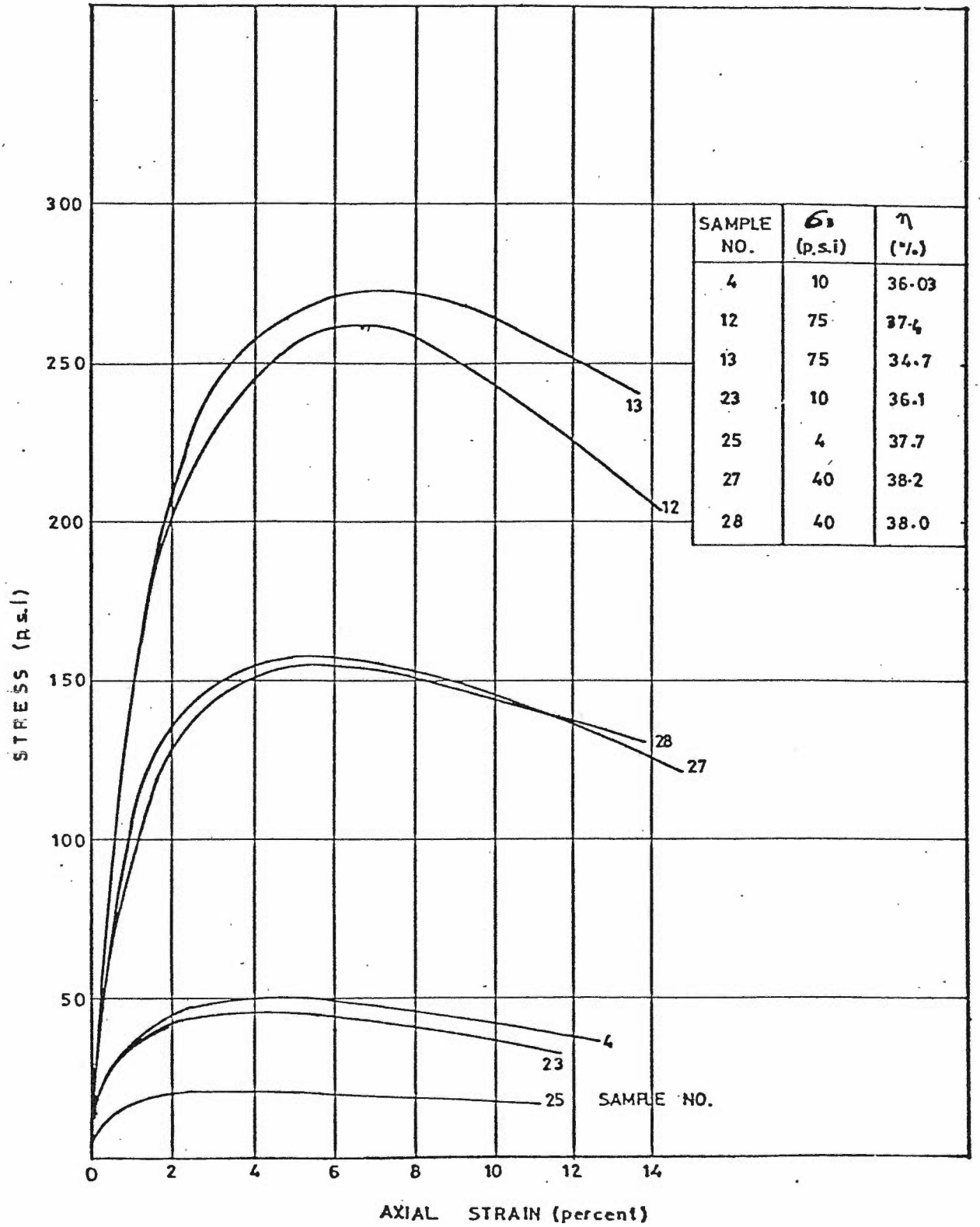

FIGURE I·2 EFFECT OF CELL PRESSURE ON STRESS STRAIN BEHAVIOUR OF DENSE SAND

(AFTER SASTRY, 1977)

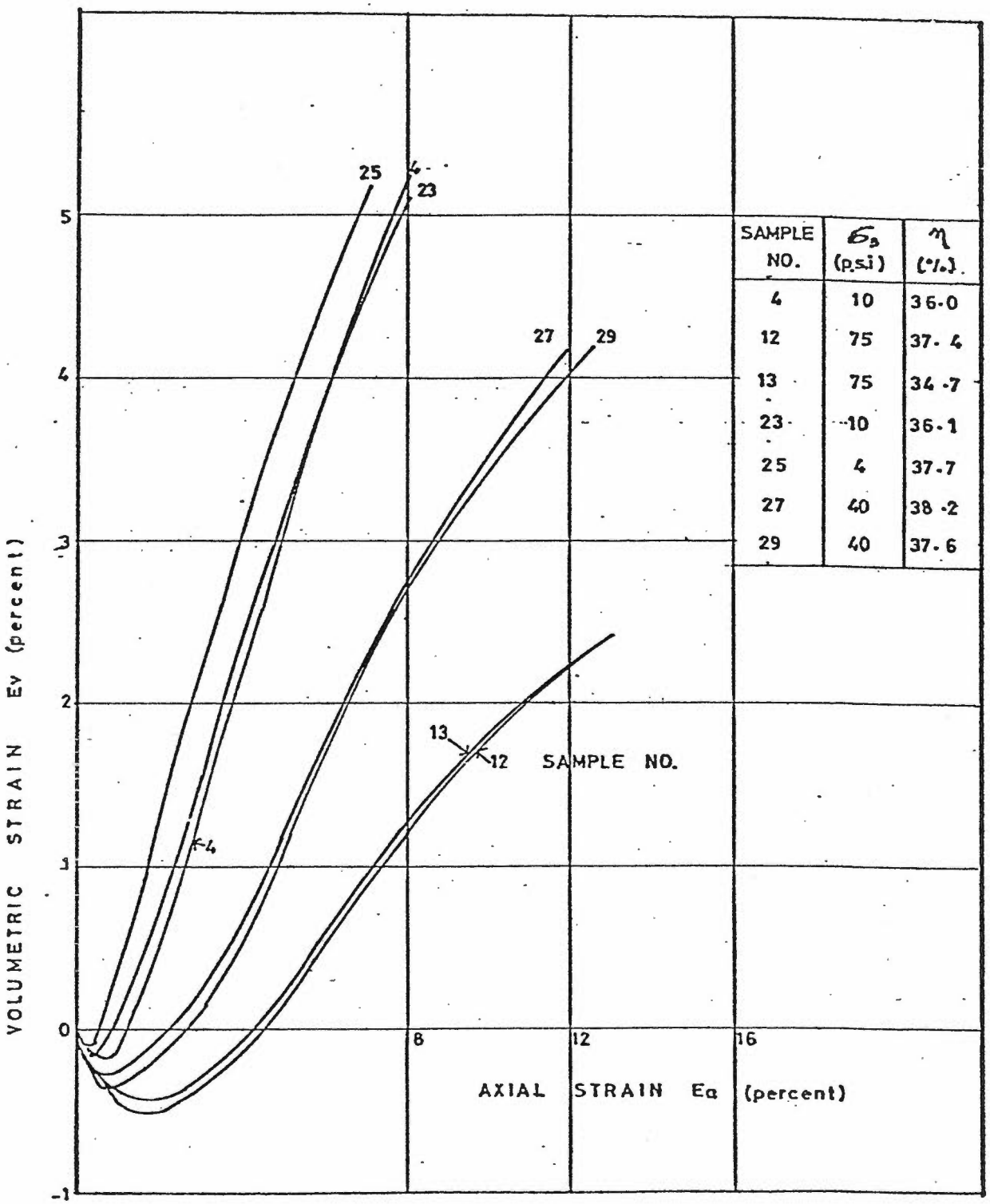

FIGURE I·3 EFFECT OF CELL PRESSURE ON VOLUMETRIC STRAIN OF DENSE SAND (AFTER SASTRY, 1977)

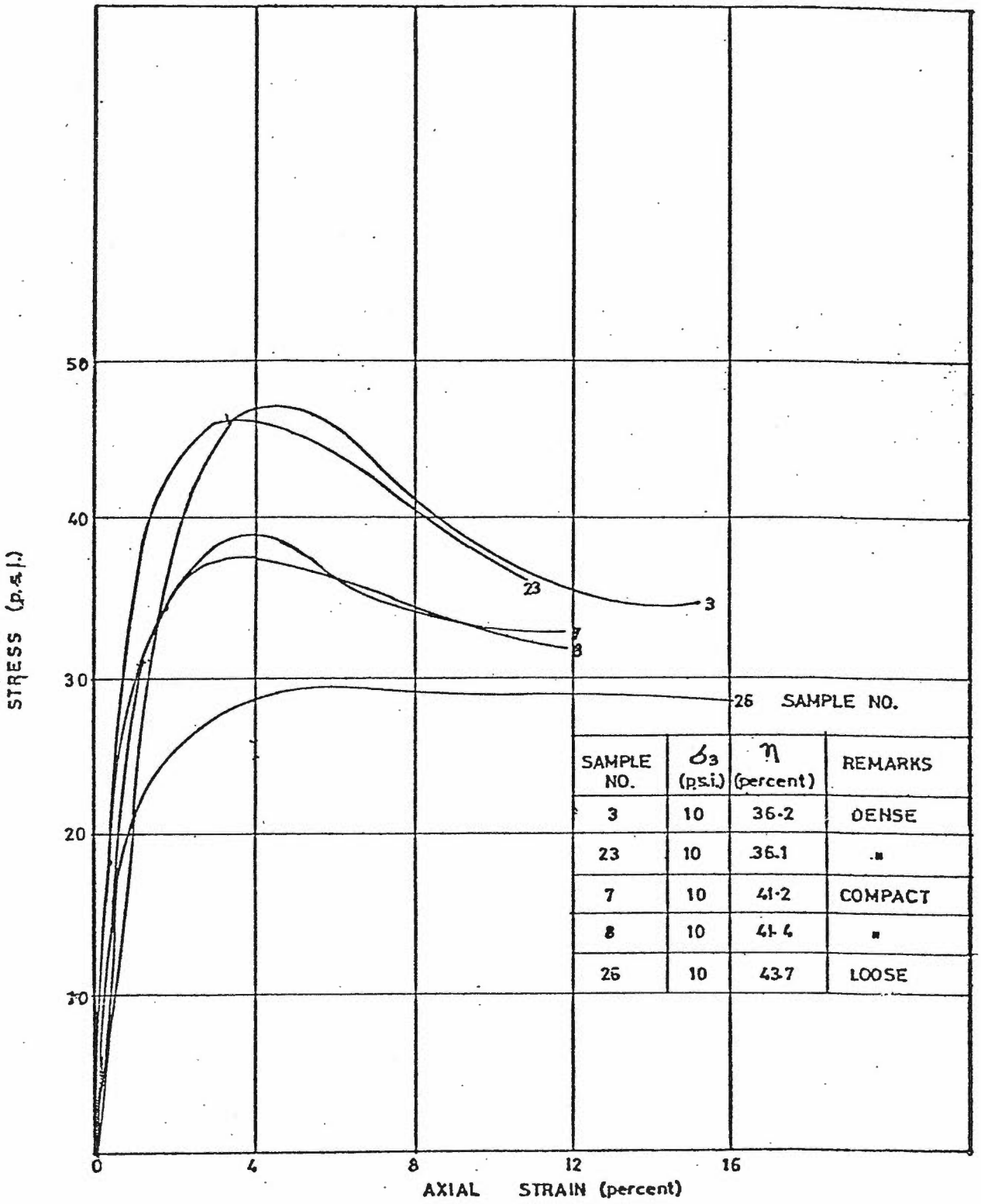

FIGURE I·4 EFFECT OF POROSITY ON STRESS STRAIN BEHAVIOUR OF SAND
(AFTER SASTRY, 1977)

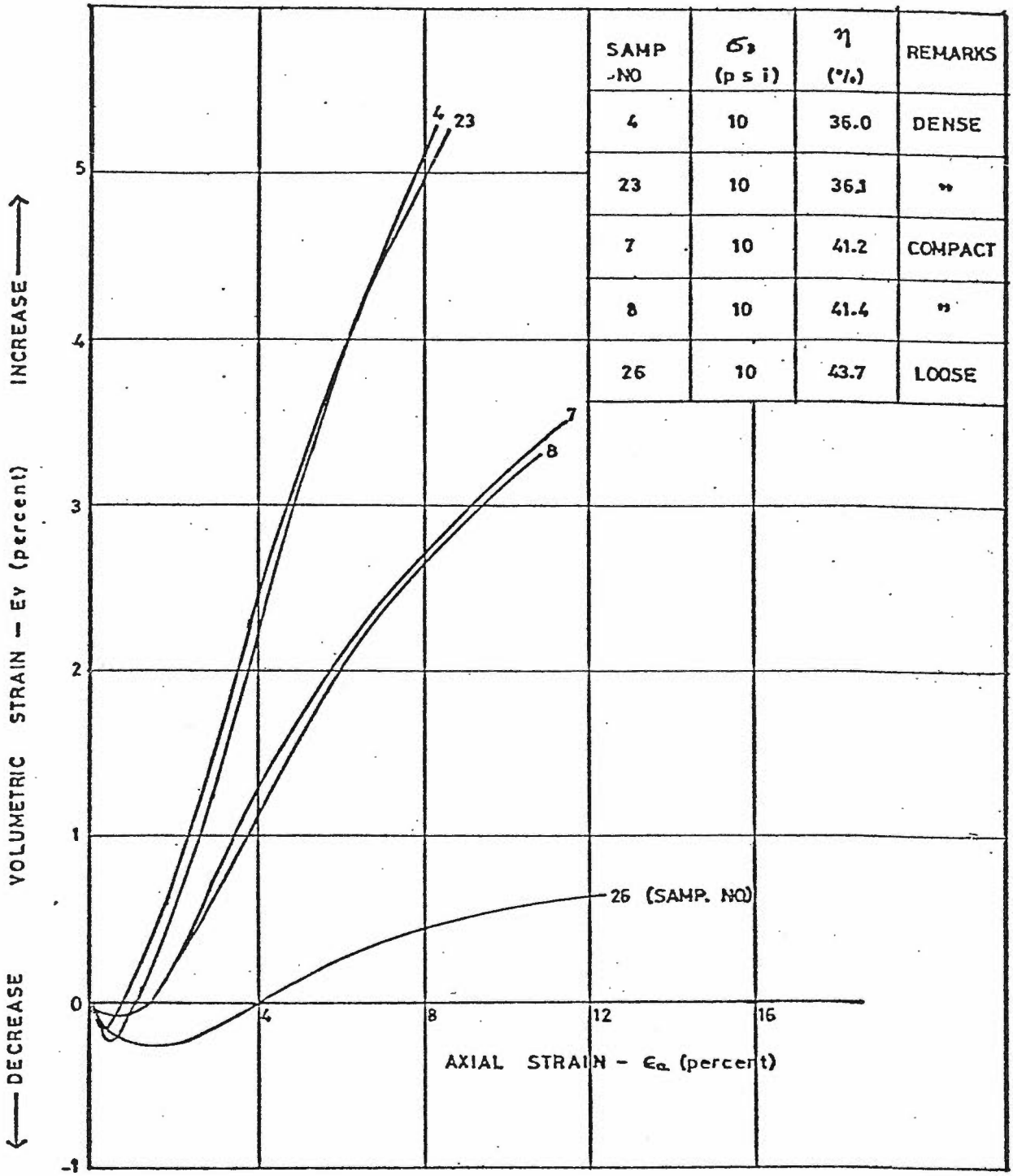

FIGURE I·5 EFFECT OF POROSITY ON VOLUMETRIC STRAIN OF SAND
(AFTER SASTRY, 1977)

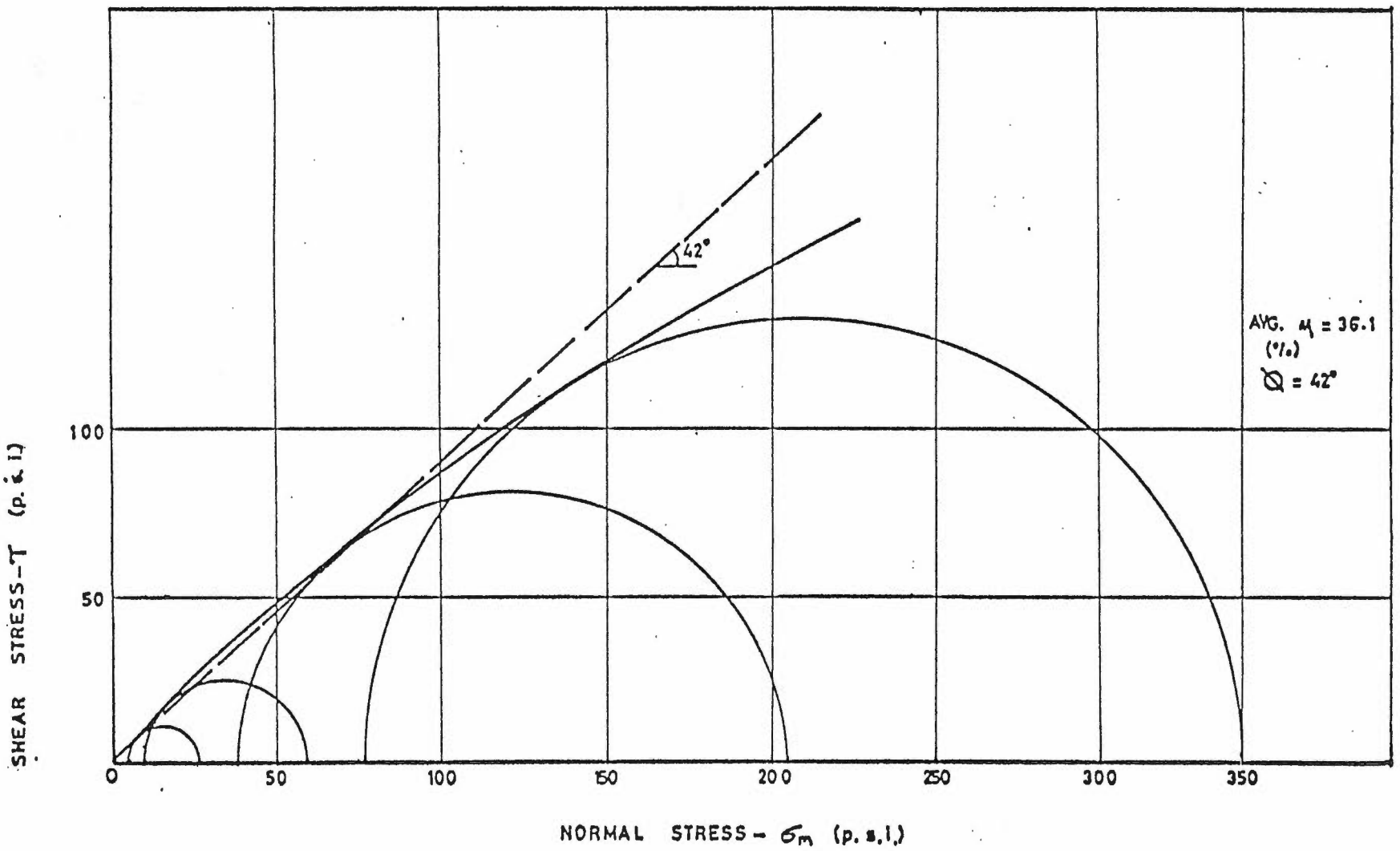

FIGURE I·6 MOHR COULOMB ENVELOPE FOR DENSE SAND (AFTER SASTRY, 1977)

TABLE I·1

DIRECT SHEAR TEST RESULTS

Test No.	Bulk Density of Sand γ_s (lb/ft^3)	Normal Stress σ (psi)	Peak Shear Stress (τ_{peak}) (psi)	Residual Shear Stress (τ_{res}) (psi)	$\tan\phi_{peak} = \frac{\tau_{peak}}{\sigma}$	Peak Friction Angle (ϕ_{peak}) (deg.)	$\tan\phi_{res} = \frac{\tau_{res}}{\sigma}$	Residual Friction Angle (ϕ_{res}) (deg.)	Remarks
1	104.1	14.22	14.48	9.63	1.018	45.5	0.677	34.1	Dense sand
2	104.1	14.22	14.48	9.63	1.018	45.5	0.677	34.1	"
3	104.8	14.22	14.57	9.70	1.025	45.7	0.682	34.3	"
4	106.5	10.62	11.24	7.24	1.058	46.6	0.682	34.3	"
5	103.2	10.62	11.40	7.77	1.073	47.0	0.732	36.2	"
6	104.1	10.62	11.08	7.33	1.043	46.2	0.690	34.6	"
7	104.2	7.15	7.82	5.22	1.093	47.5	0.730	36.1	"
8	103.1	7.15	8.15	5.22	1.140	48.7	0.730	36.1	"
9	105.3	7.15	7.98	5.22	1.116	48.0	0.730	36.1	"
10	105.3	5.25	5.70	3.86	1.085	47.3	0.736	36.4	"
11	106.3	5.25	6.03	3.91	1.149	49.0	0.745	36.7	"
12	103.8	5.25	5.86	3.91	1.116	48.0	0.745	36.7	"

Table I.1 (continued)

Test No.	Bulk Density of Sand γ_s (lb/ft^3)	Normal Stress σ (psi)	Peak Shear Stress (τ_{peak}) (psi)	Residual Shear Stress (τ_{res}) (psi)	$\tan\phi_{peak} = \frac{\tau_{peak}}{\sigma}$	Peak Friction Angle (ϕ_{peak}) (deg.)	$\tan\phi_{res} = \frac{\tau_{res}}{\sigma}$	Residual Friction Angle (ϕ_{res}) (deg.)	Remarks
13	103.8	3.42	3.99	2.77	1.116	49.4	0.810	39.0	Dense sand
14	106.8	3.42	4.15	3.15	1.213	50.5	0.921	42.6	"
15	104.8	3.42	4.07	2.97	1.190	44.9	0.868	41.0	"
	104.67					47.6		36.6	average
16	91.3	2.52	2.24	-	0.893	41.7	-	-	Loose sand
17	92.4	2.52	2.34	-	0.928	42.8	-	-	"
18	90.9	2.52	2.24	-	0.893	41.7	-	-	"
	91.5					42.0			average

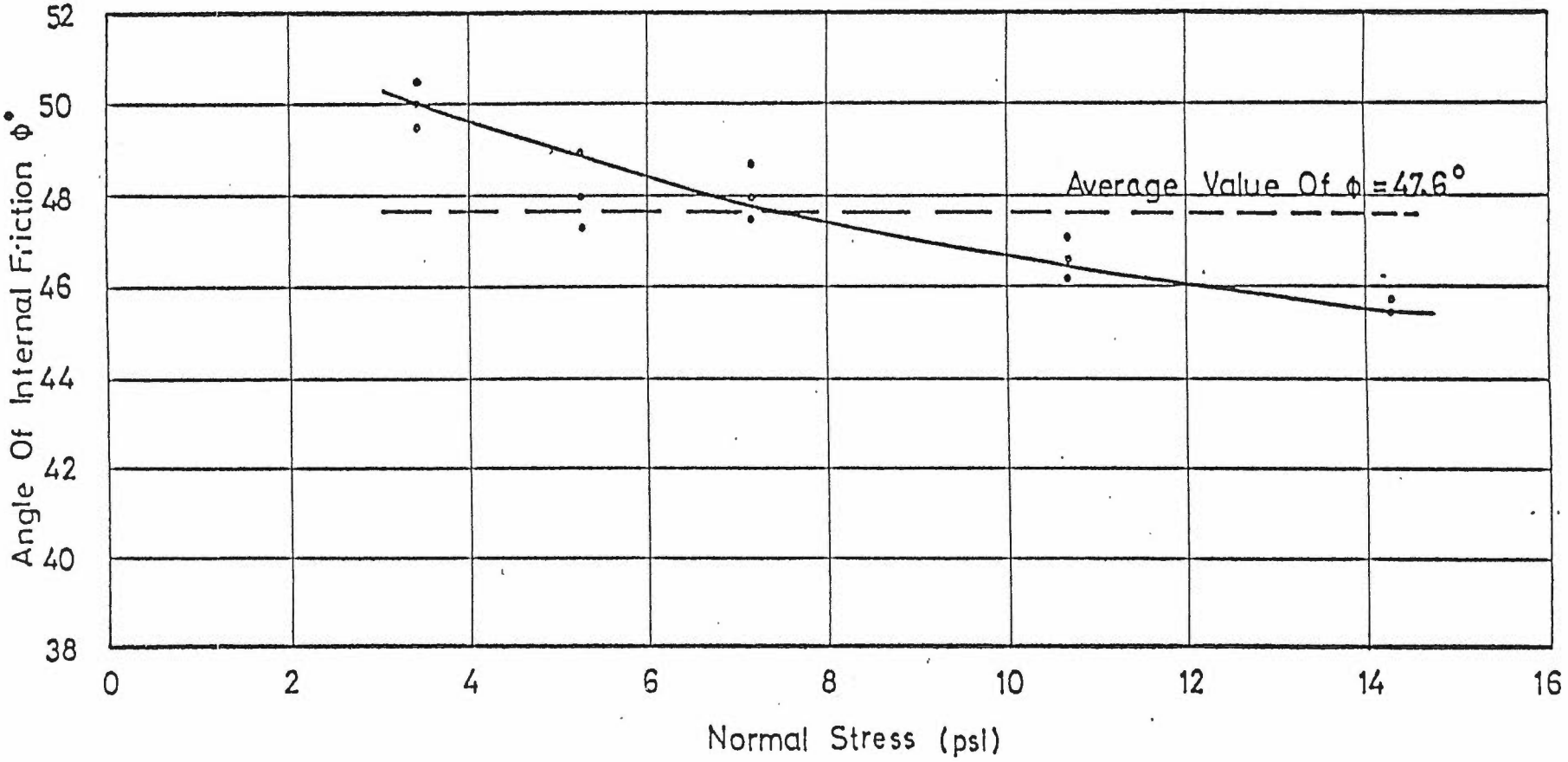

FIG. I·7 RELATION BETWEEN ANGLE OF INTERNAL FRICTION ϕ AND NORMAL STRESS FOR DENSE SAND.
(AFTER BAZAN, 1976)

APPENDIX II

Three Piece Footing Calibration

Load cells were calibrated using an Instron Universal Testing Machine for the range of 0 to 150 pounds. The load cells were numbered according to the following sketch.

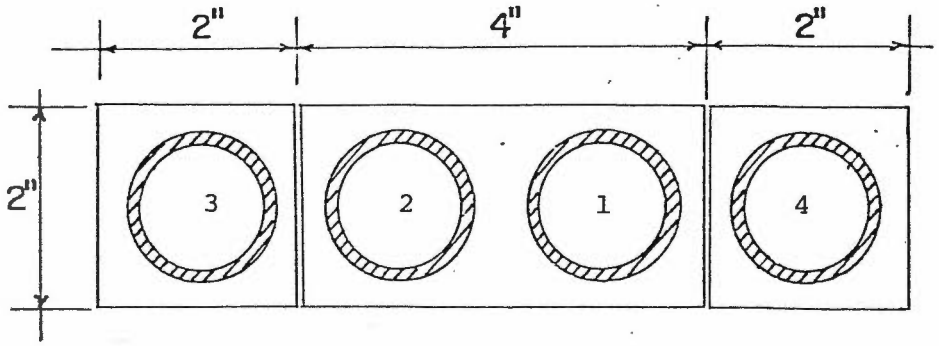

Load Cell No.	Division/lb.
1	2.40
2	2.72
3	3.56
4	3.56

APPENDIX III

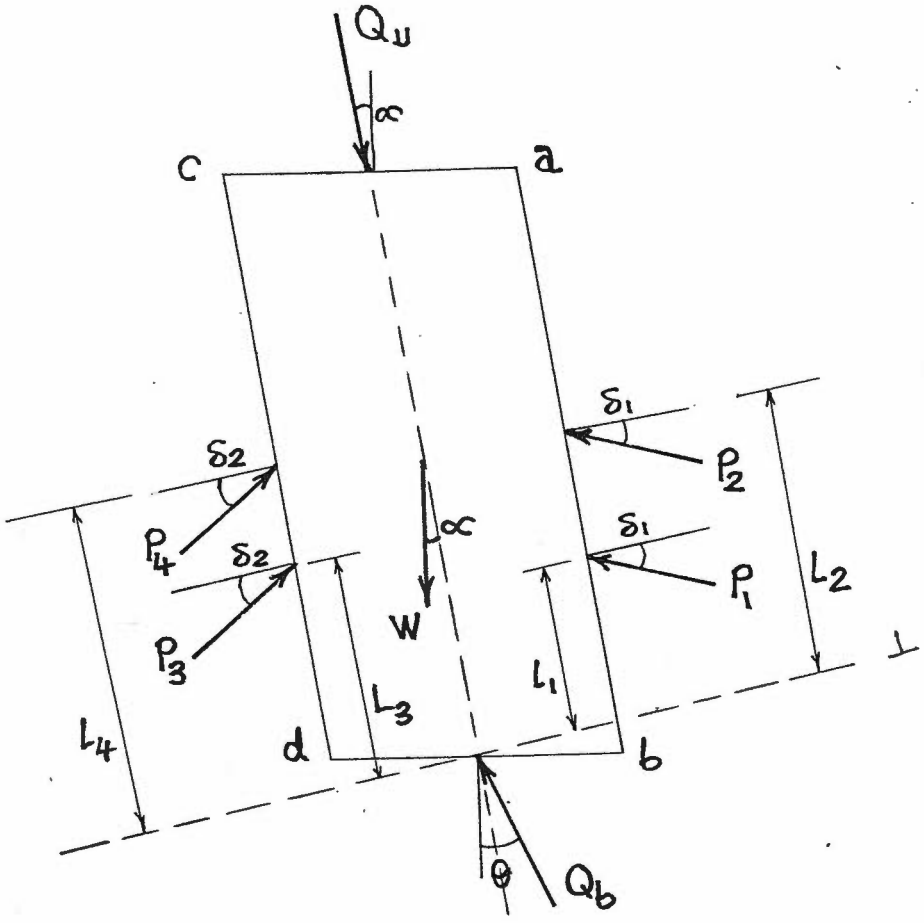

The free body taken from the upper layer and bounded by the assumed failure planes (a b c d) (see the above sketch) is acted upon the following forces:

P_1 & P_3 = total passive earth pressure on the assumed planes (ab, cd) due to the weight component

P_2 & P_4 = total passive earth pressure on the assumed failure planes (ab, cd) due to the surcharge component

Q_u = the ultimate load which can be carried by the layered system and measured in the loading direction

Q_b = reaction from the lower layer

W = weight of the column (abcd)

In addition,

δ_1 = is the mobilized angle of friction on the assumed failure plane ab

δ_2 = is the mobilized angle of friction on the assumed failure plane cd

θ = is the inclination angle of the line of action of Q_b with the vertical.

The equilibrium equation can be written as:

(i) Summation of the external forces in the load direction must be equal to zero. Thus

$$Q_u + W \cos \alpha - (P_1 + P_2) \sin \delta_1 - (P_3 + P_4) \sin \delta_2 - Q_b \cos (\theta-\alpha) = 0 \qquad \text{(III.1)}$$

(ii) Summation of the external forces perpendicular to the load direction must be equal to zero. Thus

$$(P_1 + P_2) \cos \delta_1 + W \sin \alpha + Q_b \sin (\theta-\alpha) - (P_3 + P_4) \cos \delta_2 = 0 \qquad \text{(III.2)}$$

(iii) Summation of the moments about a point must be equal to zero. Taking moments about point O yields

$$P_1 \cos \delta_1 L_1 + P_2 \cos \delta_1 L_2 + W \cdot \frac{h}{2} \tan \alpha - P_3 \cos \delta_2 L_3 - P_4 \cos \delta_2 L_4 = 0 \qquad \text{(III.3)}$$

It can be seen from Equations III.1 to III.3 that the problem is highly statically indeterminate due to the large number of unknown parameters. In order to simplify the problem and obtain a solution for the ultimate bearing capacity of layered system a number of assumptions were made to decrease the number of unknown parameters. These assumptions are as follows:

$$P_1 = P_3$$

$$P_2 = P_4$$

$$\delta_1 = \delta_2 = \delta, \text{ and } \theta = \alpha$$

As a result of these above mentioned assumptions, equation III.1 can be written as given in Chapter 5 (equation 5.7). The other two equilibrium equations can be simplified and written as:

$$W \sin \alpha = 0 + P \qquad \text{(III.2)'}$$

$$P_1 \cos \delta(l_1 - L_2) + P_2 \cos \delta(L_3 - L_4) - W \cdot \frac{h}{2} \tan \alpha = 0 \qquad \text{(III.3)'}$$

In equation (III.2)' since both W and sin α are greater than zero the value of W sin α cannot be equal to zero. However, the magnitudes of W and sin δ are both quite small and consequently the product of W and

sin δ will be small enough to be considered approximately equal to zero. Therefore, the sum of forces perpendicular to the failure planes can be assumed equal to zero.

Equation (III.3)' cannot be solved directly due to the number of unknowns. However, the experimental observation that equilibrium does exist leads to the conclusion that the values of the unknown parameters must be adjusted internally in order to satisfy equation (III.3)'.